

CRISPR Genome-editing Studies Reveal Potential Vulnerabilities in Targeting Tumor-suppressors and Oncogenes of Aggressive Cancers.

Division of Experimental Surgery

Department of Medicine

McGill University

Montreal, Canada

2024

A thesis submitted to McGill University in partial fulfillment of the requirements of the degree of Doctor of Philosophy

©Julien Boudreault 2024

Contents

Lists of abbreviations	9
Abstract (English)	12
Résumé (Français)	14
Contribution of the author	16
Contribution to the original knowledge	18
Acknowledgments	20
Dedications	21
Epigraph	22
Chapter One: Introduction	23
1.1 Cancer research	24
1.2 Melanoma Cancer	24
1.2.1 Melanogenesis	24
1.2.2 Melanoma genesis	25
1.2.3 Key genetic alterations associated with melanoma progression	26
1.2.3.1 BRAF and NRAS	26
1.2.3.2 Tumor suppressors inactivation (CDKN2A and PTEN)	27
1.2.3.3 MITF	27
1.2.4 Metastasis and melanoma	28
1.3 Transforming Growth Factor β	29
1.3.1 TGFβ signaling pathway	29
1.3.1.1 SMAD-dependent pathway	30
1.3.1.2 SMAD-independent pathway	31
1.3.2 Dual role of TGFβ	33
1.3.3 TGFβ as a tumor suppressor	33

1.3.3.1 Cell cycle inhibition	33
1.3.3.2 Apoptosis	33
1.3.4 TGFβ as a tumor promoter	34
1.3.4.1 EMT	34
1.3.4.2 Angiogenesis	35
1.3.4.3 Immunologic surveillance escape	35
1.3.5 TGFβ and melanoma	35
1.3.5.1 TGFβ isoforms in melanoma	35
1.3.5.2 TGFβ and growth inhibition in melanoma	36
1.6 Stemness and melanoma	38
1.6.1 Melanoma stem cell concept	38
1.6.2 Melanoma stem cell markers	39
1.6.2.1 CD133	39
1.6.2.2 CD271	40
1.6.2.3 ALDH	40
1.6.2.4 ABCB5 and ABCG2	41
1.6.2.5 CD20	41
1.6.3 Melanoma stem cell expansion	41
1.6.4 Role of TGFβ in stemness	41
1.7 MEN1: Multiple endocrine neoplasia-type 1	43
1.7.1 MEN1 genome-wide interactome	43
1.7.2 Cellular functions of MEN1	43
1.7.3 MEN1 in TGFβ signaling	44
1.7.4 MEN1 in melanoma	46
1.8.1 Pancreatic Cancer	48

1.8.2 Pancreatic Cancer driver mutations	49
1.8.2.1 KRAS	50
1.8.2.2 Other mutations in PDAC	52
1.9 Discovery of CRISPR: The rise of CRISPR as the genome-editing technology	53
1.9.1 The diversity of the CRISPR system	54
1.9.2 Genome editing with CRISPR, a biotechnology tool	55
1.9.3 DNA repair mechanisms of Cas cleavage	56
1.9.4 CRISPR off-target effects	57
1.9.5 Design of sgRNA for genome-editing	58
1.9.6 Alternative CRISPR technologies	58
1.9.7 CRISPR/Cas editing strategy	60
1.9.8 CRISPR in cancer research	61
1.9.9 CRISPR screening in cancer research	62
1.9.9.1 Pooled and arrayed CRISPR screens	62
1.9.9.2 Arrayed CRISPR screens	63
1.9.9.3 High content CRISPR screens	63
1.10 Heat shock proteins, Heat Shock response, Heat Shock factors and HSPE1 (Hsp10) . 67	
1.10.1 HSPs classification	68
1.10.2 HSFs and HSPs in cancer	68
1.10.3 HSP60 and HSP10	68
1.11 Rationale and objectives	69
Chapter 2	71
2.1 Preface:	72
2.2 Abstract:	72
2.3 Introduction:	73

2.4 Material and methods Introduction:	74
2.5 Results:	79
2.6 Discussion:	83
2.7 Aknowledgements :	85
2.8 Figures of chapter 2	86
Chapter 3:	95
3.1 Preface:	96
3.1 Abstract:	96
3.2 Introduction	96
3.3 Material and methods	98
3.4 Results	102
3.5 Discussion	108
3.6 Aknowledgements	109
3.7 Figures of chapter 3	110
Chapter 4	121
4.1 Preface:	122
4.2 Abstract:	122
4.3 Introduction	123
4.4 Material and methods	124
4.5 Results	128
4.6 Discussion	135
4.7 Acknowledgements	137
4.7 Figures of chapter 4	137
Chapter 5: Integrative discussion	154
Discussion of the experimental work	155

Stemness and melanoma.....	155
Addressing the dual role of TGFβ.....	157
SMAD2, SMAD3 and SMAD4 differential signaling in oncogenesis.....	159
Discussion of MEN1 and melanoma.....	160
Discussion of PDAC and CRISPR screening.....	162
Conclusion and perspectives	167
References.....	167

List of figures

Figure 1.1: Clark Model Illustration of Melanoma Progression Stages and Histopathological Features.....	26
Figure 1.2: Schematic illustration of the signal transduction mediated by members of the Transforming Growth Factor- β (TGF β) superfamily.....	30
Figure 1.3: Schematic representation of non-canonical TGF β signaling and its crosstalk with various other signaling pathways.....	32
Figure 1.4: Schematic representation of two models reflecting the development and progression of cancer.....	39
Figure 1.5: Menin and TGF β /Activin signaling pathway.....	46
Figure 1.6: Physiology of the pancreas and histology of pancreatic cancer.	48
Figure 1.7: Histology of pancreatic cancer different subtypes.....	49
Figure 1.8: Pathways and respective genes mutation burden in pancreatic cancer.....	50
Figure 1.9: Pancreatic cancer progression in human and mouse.....	52
Figure 1.10: CRISPR/Cas9 genome editing mechanism.....	56
Figure 1.11: DNA repair upon CRISPR/Cas9 cleavage.....	57
Figure 1.12: Schematic representation of genome editing strategies and agents for CRISPR-based genome editing.....	60
Figure 1.13: Strategies for CRISPR/Cas delivery.....	61
Figure 1.14: Parameters of CRISPR screening.....	64
Figure 1.15 Schematic illustration of three distinct modes of CRISPR screening.	66
Figure 2.1. TGF β inhibits tumorsphere formation and self-renewal capacity in melanoma.....	86
Figure 2.2. Transcriptional downregulation of stemness markers by TGF β in Melanoma.....	88
Figure 2.3. The Smad3/4 pathway is required for TGF β -mediated inhibition of melanoma cancer stemness.....	90
Figure 2.4. Blocking TGF β /Smad signaling promotes melanoma tumor growth in vivo.....	92
Figure 2.5. The TGF β /Smad pathway inhibits melanoma lung metastasis in vivo.....	94
Figure 3.1. TGF β induces MEN1 gene expression in melanoma cells through Smad3.....	110
Figure 3.2. The TGF β /Smad3/MEN1 axis is essential for inhibiting melanoma tumor formation in vivo.....	111

Figure 3.3. The TGFβ/Smad3/MEN1 axis is essential for inducing cell cycle arrest in human melanoma cells.....	113
Figure 3.4. Expression of Menin mutants in HEK293 cells and generation of stable Men1 knock out melanoma cell lines.....	115
Figure 3.5. Expression and activity of menin missense mutants can be rescued by the proteasome inhibitor PS-341.....	117
Figure 3.6. Expression and activity of menin missense mutants can be rescued by RNAi targeting of the ubiquitin ligase CHIP.....	119
Figure. 4.1: In vivo genome-wide CRISPR screening in PDAC.....	138
Figure 4.2: Validation of depleted genes from CRISPR screen.....	140
Figure 4.3: HSPE1 promotes cell proliferation, tumorigenesis and increases higher tumor-initiating capacity in PDAC.....	142
Figure 4.4: Depletion of HSPE1 induces cell cycle arrest and increase apoptosis.....	144
Figure 4.5: KHS101 small-molecule curtails PDAC tumor formation.....	145
Figure 4.6: Role of OPA1 antiapoptotic protein in HSPE1-Induced oncogenic activities.....	147
Supplemental Fig.4.1: Mageck bioinformatic analysis of read counts of lof10 of missed gRNAs.....	148
Supplemental Fig.4.2: SURVEYOR Assay.....	149
Supplemental Fig.4.3: Colony formation assay of CRISPR-KO SCR, HSPE1 or HSPD1 HPAF-II cell line.....	149

Lists of abbreviations

ALDH: Aldehyde dehydrogenase

ALK : Activin-like kinase

ADP : Adenosine diphosphate

ATP : Adenosine triphosphate

bFGF: Basic fibroblast growth factor

BMP: Bone morphogenetic protein

Cas: CRISPR-associated protein

CASTs: CRISPR-associated transposons

CD133: Cluster of differentiation 133

CDK: Cyclin-dependent kinase

CDKI: Cyclin-dependent kinase inhibitor

ChIP: chromatin immunoprecipitation

Co-Smads: Common partner Smads

CRISPR: Clustered regularly interspaced short palindromic repeats

CRISPR_{ko}: CRISPR-Cas9 knock-out

CRISPR_{act}: CRISPR activation

CRISPR_i: CRISPR interference

dCas9: dead Cas9 (catalytically inactive)

dCas13: dead Cas13 (catalytically inactive)

DSBs: Double-Stranded breaks

DMEM: Dulbecco's modified Eagle medium

DMSO: Dimethyl sulfoxide

DNA: Deoxyribonucleic acid

DTT: Dithiothreitol

EDTA: Ethylenediaminetetraacetic acid

EGF: Epidermal growth factor

EGFR: Epidermal growth factor receptor

EMU: Epidermal melanin unit

ERAD: Endoplasmic reticulum-associated protein degradation

FACS: Fluorescence-activated cell sorting

FBS: Fetal bovine serum
FTS: Farnesyl thiosalicylic acid
Fz: Fanzor
G1: Gap 1 phase
G2: Gap 2 phase
GAPDH: Glyceraldehyde-3-phosphate dehydrogenase
hESCs: Human embryonic stem cells
HSPE1: Heat-Shock protein E member 1
HSPD1: Heat-Shock protein D member 1
HDR: Homologous recombination (or Homology-directed repair)
I-Smads: Inhibitory Smads
Indels: Insertion-deletion (of nucleotide bases in human genome)
LAP: Latency-associated peptide
LOH: Loss-of-heterozygosity
LTBP: Latent-binding protein
L-DOPA: L-dihydroxyphenylalanine
M phase: Mitosis phase
MEN1: Multiple endocrine neoplasia 1
MMEJ: Microhomology-mediated end joining
NHEJ: Non-Homologous end-joining
nt : nucleotide
PAM: Protospacer adjacent motif
PAR : Parental
PDAC: Pancreatic ductal adenocarcinoma
pegRNA: Prime editing guide-RNA
PI3K: Phosphatidylinositol 3-kinase
P-NET: Pancreatic neuroendocrine tumor
R-Smads): Receptor-regulated Smads
RNA: Ribonucleic acid
RNAi: RNA interference
RPMI: Rosewell park memorial institute medium

SCR: Scramble

SDS-PAGE : Sodium dodecyl sulfate–polyacrylamide gel electrophoresis

siRNA : Small-interfering RNA

sgRNA: Single-guide RNA

shRNA : Short-hairpin RNA

sp: Streptococcus pyogenes

TALE: Transcription activator-like effector

TALENs: Transcription activator-like effector nucleases

TAMs: Tumor-associated macrophages

tracrRNA: Trans-activating crispr RNA

T β RI: Type-I TGF β receptor

T β RII: Type-II TGF β receptor

TGF β : Transforming growth factor β

RNF43: Ubiquitin E3 ligase ring finger 43

VEGF: Vascular endothelial growth factor

WT: Wild type

ZFN: Zing-finger nucleases

Abstract (English)

Despite significant advancements in cancer detection and treatment, aggressive malignancies such as metastatic melanoma and pancreatic ductal adenocarcinoma (PDAC) continue to exact a heavy toll in terms of cancer-related mortality rates. Uncovering novel implications of oncogenes and tumor-suppressors in challenging-to-treat cancers has the potential to increase overall survival of patients through optimized and personalized therapies. We previously demonstrated that Transforming Growth Factor-beta (TGF β) acts as a potent tumor suppressor in melanoma by inhibiting cell cycle and inducing apoptosis. Therefore, we investigated the behavior of TGF β in melanoma cancer stem cells, which possess the capacity of self-renewal and produce a variety of tumor cell phenotypes by contributing to tumor-initiation, metastasis and therapy resistance. Our discovery revealed that TGF β /SMAD signaling suppresses stemness maintenance by disrupting tumorsphere formation and reducing CD133+ subpopulation in a SMAD3/4-dependent fashion. We observed that the mRNA level of several melanoma stemness markers was reduced when stimulated with TGF β . Moreover, our findings demonstrated that CRISPR-Cas9 knock-out (CRISPR_{ko}) of SMAD3 or SMAD4, effectively blocking TGF β /SMAD signaling, promoted both tumorigenesis and lung metastasis. With a focus on the common scientific aim related to TGF β , our investigations revealed that the SMAD3 interacting protein Menin, encoded by Multiple endocrine neoplasia type 1 (MEN1) gene, has a tumor suppressive role in melanoma. By using melanoma preclinical xenograft models, we found that CRISPR-KO of *MEN1* in several melanoma cancer cell types exhibited enhanced tumors growth when compared to the control group. We also discovered that the downregulation of Menin increases resistance to TGF β -mediated cell cycle inhibition and apoptosis. We further identified missense mutations resulting in the proteasomal degradation of the *MEN1* gene product and the subsequent loss of TGF β signaling. Our results define new molecular functions for the TGF β /SMAD/MEN1 signaling axis in melanoma.

Following our investigation of the TGF β pathway and the implication of the *MEN1* gene, we undertook a genome-wide approach to uncover potential novel oncogenes, tumor suppressors and pathways relevant to PDAC tumorigenesis. We conducted a genome wide loss-of-function CRISPR screen in a preclinical mouse model and identified heat-shock protein HSPE1 as our primary candidate. Indeed, HSPE1 downregulation in PDAC cancer cells results in a profound decrease of both cellular growth and tumorigenesis. We next investigated the impact of KHS101,

a validated HSPD1-HSPE1 complex inhibitor, and established its cytotoxic nature in relation to PDAC cancer cells both *in vitro* and *in vivo*. Moreover, we discovered that HSPE1 inhibition disrupts cell cycle through G₂/M arrest in PDAC cells and modifies critical cell cycle regulators expression, including PLK1. We observed that inhibiting HSPE1 leads to a reduction in OPA1 proteolytic cleavage. We exploited this vulnerability by administering MYLS22, an OPA1 inhibitor, to mice harboring pre-existing PDAC tumors, revealing that this treatment significantly reduced tumor size. In conclusion, our findings highlight a new role underlying PDAC tumorigenesis for HSPE1 and could unlock a new area of research towards precision medicine.

Résumé (Français)

Malgré les avancées scientifiques dans la détection et le traitement du cancer, les taux de mortalités sont toujours élevés dans les cancers agressifs tels que le mélanome métastatique et l'adénocarcinome pancréatique (AP). Plus d'information sur les gènes suppresseurs de tumeurs et d'oncogènes pourrait avoir le potentiel d'optimiser les thérapies de ces cancers résistants. Précédemment, nous avons démontré que le Facteur de Croissance Transformant Bêta (TGF β) agit comme un puissant suppresseur de tumeurs dans le mélanome par l'inhibition du cycle cellulaire et de l'induction de l'apoptose. Par conséquent, nous avons étudié l'effet de TGF β dans les cellules souches cancéreuses du mélanome, ayant la capacité de s'auto-renouveler, d'initier la tumorigenèse et la dissémination métastatique en plus de résister aux chimiothérapies. Notre découverte a révélé que la signalisation TGF β /SMAD inhibe le maintien de la pluripotence en perturbant la formation de sphères tumorales de cellules souches cancéreuse, en diminuant le niveau d'ARNm de plusieurs marqueurs de pluripotence mélanotique et en réduisant les sous-population cellulaire exprimant la protéine de surface CD133+. De plus, nos résultats ont montré que la suppression de l'expression de SMAD3 ou SMAD4 à l'aide de la technologie CRISPR, favorise à la fois la formation de tumeurs ainsi que de métastases dans les poumons. La suite de nos recherches scientifiques a révélé que Menin, encodée par le gène Néoplasie Endocrinienne Multiple de type 1 (MEN1), joue un rôle suppresseur de tumeurs dans le mélanome. En utilisant un modèle de xénotransplantation préclinique du mélanome, nous avons constaté qu'une réduction de l'expression de Menin via CRISPR augmente la croissance tumorale des cellules du mélanome. Nous avons également découvert que la diminution de l'expression de Menin accroît la résistance à l'inhibition du cycle cellulaire et à l'apoptose normalement induites par le TGF β . De plus, nous avons identifié des mutations faux-sens entraînant la dégradation protéasomale du produit génique de *MEN1* et la perte subséquente de la signalisation TGF β . Nos résultats définissent de nouvelles fonctions moléculaires pour l'axe de signalisation TGF β /SMAD/MEN1 dans le mélanome.

Par la suite, nous avons entrepris une approche génomique à grande échelle pour découvrir de nouveaux oncogènes, suppresseurs de tumeurs et voies de signalisation cellulaire pouvant potentiellement être impliqués dans la tumorigenèse de l'AP. Nous avons réalisé un criblage CRISPR à l'échelle du génome en utilisant un modèle murin préclinique et avons identifié la protéine de choc thermique 1 (HSPE1) comme notre principal candidat. En effet, la réduction de HSPE1 dans les cellules cancéreuses du PDAC entraîne une diminution significative à la fois de

la croissance cellulaire et de la tumorigenèse. Nous avons ensuite étudié l'impact de KHS101, un inhibiteur validé du complexe HSPD1-HSPE1, et confirmé sa nature cytotoxique en ce qui concerne les cellules cancéreuses du PDAC, à la fois *in vitro* et *in vivo*. De plus, nous avons découvert que l'inhibition de HSPE1 perturbe le cycle cellulaire en provoquant un blocage dans la phase G2/M dans les cellules du PDAC, et en modifiant l'expression génique de régulateurs cellulaires critiques, notamment PLK1. Également, nous avons observé que l'inhibition de HSPE1 entraîne une réduction du clivage protéolytique de OPA1. Nous avons exploité cette vulnérabilité en injectant le médicament MYLS22 dans des souris ayant des tumeurs préformées de PDAC et avons observé une réduction significative de la croissance tumorale par rapport aux groupes non-traités. En conclusion, les découvertes de nos recherches scientifiques mettent en évidence l'implication de HSPE1 dans la formation de tumeurs pancréatiques et pourraient ouvrir de nouvelles perspectives de recherche en médecine personnalisée.

Contribution of the author

This thesis is presented in manuscript-based format. I wrote the entirety of the thesis. The thesis consists of five chapters: Chapter 1 (literature review), Chapter 2-4 (scientific manuscripts) and chapter 5 (general discussion).

Chapter 2 was submitted to *Cancers* (MDPI) and is currently accepted. I designed and performed all the experiments and wrote the manuscript under my supervisor's guidance. Ni Wang performed all the *in vivo* experiments. Jean-Jacques Lebrun is involved in the supervision and manuscript editing.

Chapter 3 was recently submitted to *Molecular Cancer Research*. Mustafa Ghozlan, Lucie Canaff and I contributed equally to the experiments and manuscript writing. Ni Wang performed the *in vivo* experiments. Jean-Jacques Lebrun is involved in the project design, supervision and manuscript editing.

Chapter 4 is under preparation and is expected to be submitted. Gang Yan and Meiou Dai were involved in the CRISPR screening. Girija and Sophie assisted in some experiments. Ni Wang performed all the *in vivo* experiments. Jean-Jacques Lebrun is involved in the project design, supervision and manuscript editing.

I have contributed through scientific collaboration, helping with experimental design, bench work and manuscript editing in eight of these following articles as co-author in the course of my PhD studies:

Poulet S, Dai M, Wang N, Yan G, **Boudreault J**, Daliah G, Ali S, Lebrun JJ. Genome-wide *in vivo* CRISPR/Cas9 loss of function screen identifies TGF β 3 as an actionable biomarker of palbociclib resistance in TNBC. *Molecular Cancer* (Submitted in October 2023, in revision process)

Laham AJ, El- Awady R, Ayad MS, Wang N, **Boudreault J**, Ali S, Lebrun JJ. Targeting the DYRK1A kinase prevents tumorigenesis and metastasis and promotes G1/S targeting chemotherapy drug responses in breast and colon cancer. *Nature Precision Oncology* (Submitted in September 2023, in revision process)

Yan G, Dai M, Poulet S, Wang N, **Boudreault J**, Daliah G, Ali S, Lebrun JJ. Combined in vitro/in vivo genome-wide CRISPR screens in triple negative breast cancer identify cancer stemness regulators in paclitaxel resistance. *Oncogenesis*. 2023 Nov 6;12(1):51. doi: 10.1038/s41389-023-00497-9. PMID: 37932309; PMCID: PMC10628277.

Dai M, Yan G, Wang N, Daliah G, Edick AM, Poulet S, **Boudreault J**, Ali S, Burgos SA, Lebrun JJ. In vivo genome-wide CRISPR screen reveals breast cancer vulnerabilities and synergistic mTOR/Hippo targeted combination therapy. *Nat Commun*. 2021 May 24;12(1):3055. doi: 10.1038/s41467-021-23316-4. PMID: 34031411; PMCID: PMC8144221.

Yan G, Dai M, Zhang C, Poulet S, Moamer A, Wang N, **Boudreault J**, Ali S, Lebrun JJ. TGF β /cyclin D1/Smad-mediated inhibition of BMP4 promotes breast cancer stem cell self-renewal activity. *Oncogenesis*. 2021 Mar 1;10(3):21. doi: 10.1038/s41389-021-00310-5. PMID: 33649296; PMCID: PMC7921419.

Dai M, **Boudreault J**, Wang N, Poulet S, Daliah G, Yan G, Moamer A, Burgos SA, Sabri S, Ali S, Lebrun JJ. Differential Regulation of Cancer Progression by CDK4/6 Plays a Central Role in DNA Replication and Repair Pathways. *Cancer Res*. 2021 Mar 1;81(5):1332-1346. doi: 10.1158/0008-5472.CAN-20-2121. Epub 2020 Dec 28. PMID: 33372040.

Tian J, Wang V, Wang N, Khadang B, **Boudreault J**, Bakdounes K, Ali S, Lebrun JJ. Identification of MFGE8 and KLK5/7 as mediators of breast tumorigenesis and resistance to COX-2 inhibition. *Breast Cancer Res*. 2021 Feb 15;23(1):23. doi: 10.1186/s13058-021-01401-2. PMID: 33588911; PMCID: PMC7885389.

Shams A, Binothman N, **Boudreault J**, Wang N, Shams F, Hamam D, Tian J, Moamer A, Dai M, Lebrun JJ, Ali S. Prolactin receptor-driven combined luminal and epithelial differentiation in breast cancer restricts plasticity, stemness, tumorigenesis and metastasis. *Oncogenesis*. 2021 Jan 14;10(1):10. doi: 10.1038/s41389-020-00297-5. PMID: 33446633; PMCID: PMC7809050.

Contribution to the original knowledge

In the second chapter of this thesis, I demonstrated for the first time that TGF β has a negative role in stemness maintenance of melanoma. By using several melanoma cell lines, I showed that TGF β inhibits melanosphere formation. In that same direction, I showed that TGF β diminishes several well-known stem cell markers by using different methods including qPCR and flow cytometry in both 3D and monolayer cultured cells. Moreover, I showed that blocking SMAD3 and SMAD4 increased the tumor-initiating capacity through tumorsphere formation, tumorigenesis and metastasis dissemination to the lungs in preclinical models of melanoma. Together, these findings provide novel molecular insights on the negative role of TGF β toward self-renewal. Our mechanism could implicate a new therapeutic approach to target cancer stem cells, known to be responsible for relapse and chemoresistance in cancer patients, by mimicking the TGF β tumor-suppressive pathway.

In the third chapter of this thesis, I demonstrated role of MEN1 as a tumor suppressor in melanoma. Blocking MEN1 expression through CRISPR in various melanoma cell lines resulted in increased tumorigenesis. Furthermore, the tumor suppressive function of MEN1 was shown to operate through cell cycle inhibition, both *in vitro* and *in vivo*. A novel mutation in MEN1 kindreds affected by melanoma was identified, indicating heightened degradation of MEN1 gene products and a loss of TGF β signaling. By using pharmacological inhibitors and RNA interference targeting the proteasome, the induced rescue of MEN1 expression restored TGF β signaling. Our research suggests that employing FDA-approved drugs targeting proteasomal degradation, restoring the tumor-suppressive function of MEN1 and TGF β signaling, would be of great benefit to melanoma patients. As such, primary tumor formation and metastasis could be prevented.

In the fourth chapter of this thesis, by using a CRISPR screening based approach, I discovered a novel oncogene (HSPE1) in PDAC. I showed that repressing HSPE1 expression by means of CRISPR drastically slowed the growth of several PDAC cancer cell lines. Moreover, silencing HSPE1 inhibited cell cycle progression and increased apoptosis. I demonstrated that the HSPD1/HSPE1 protein complex could be targeted with the small molecule inhibitor KHS101, resulting in the effective slowing of tumor growth in two distinct PDAC cell lines. I further characterized the role of HSPE1 and showed that it induces the cleavage of OPA1 mitochondrial protein. Heading in that way, I showed that treating PDAC cells to OPA1 small molecule inhibitor displayed cytotoxicity in both *in vitro* and *in vivo* manner.

All those elements of the manuscript are considered original scholarship and distinct contributions to knowledge.

Acknowledgments

During my doctorate studies, I learned a lot about scientific methodology such as guessing the good hypotheses and asking the right questions to find better answers. I also learned a lot about defining what is good science and criticize my own findings. I would never have achieved all this work alone and that is why I would like to thank all the people who helped me along the way.

I would like to thank my supervisor, Dr. Jean-Jacques Lebrun, who believed in my capacities and offered my guidance throughout all the time I was in his lab. Back then, he offered me a research assistant position in his lab, where I worked from 2017 until the end of 2018. My passion led me to start a PhD at the beginning of 2019 to start my own projects. I would like to thank my committee meeting members, Dr. David Labbé (Chairperson), Dr. Suhad Ali and Dr. Sergio Burgos and external members for my doctoral comprehensive examination, Dr. Julia Valdemarin Burnier and Dr. Alexander Gregorieff, for their essential suggestions and commentaries during all the academic meetings.

I would also like to express my appreciation for internal and external and all the members who assisted to my oral defence.

I am grateful for all the past and current members of the laboratory with special thanks to Meiou Dai for all the time she spent on me for experimental design, explanations, troubleshooting and mentoring of experiments. I would like to thank Sophie Poulet, Girija Deliah, Gang Yan, Ni Wang, Karine Pasturaud, Jun Tian, Mustafa Ghozlan, Nadège Fils-Aimé and Lucie Canaff as valuable and indispensable members in the lab. I would like to thank other people from other labs: Dana Hamam, Anwars Shams, Hachim Ibrahim and Najat Binothman (Dr. Suhad Ali's lab), Philippe Duquette (Dr. Nathalie Lamarche's lab) and Matthew Leibovitch (Dr. Pnina Brodt's lab). I would like to thank all my friends that supported me outside the lab.

Finally, I would like to thank my family: my father André Groleau, my mother Annick Boudreault and my two brothers Pier-Olivier and Mathieu Boudreault. I would like to express my gratitude toward my fiancé Laïa Julio for her love and unfaltering support and for giving life to our child in February 2022, Ella Julio and eventually for the next little one still in her belly (due December 2023-January 2024).

Dedications

I would like to dedicate this thesis to my beloved father André Groleau who passed away on September 14th of 2023. You gave me the necessary strength and motivation to complete the final steps of this long academic journey. If resiliency would have a face, it would be yours. Without complaining or crying once, you fought your non-small cell lung cancer and enjoyed every day like it would be the last. You kept your kindness for your family and friends until the end.

I am glad that we had borrowed time together since the ALK+ mutation targeted therapy greatly extended your life expectancy. The doctors said back in 2014 that you had 6 months to live but you fought it like a warrior for a total of 9 years! We had the chance to do more mountain climbing in our beautiful wild backyard, snowboarding at Mont Grand-Fonds, kayaking in the St-Lawrence River alongside the playful white whales and swimming/scuba diving sessions in the La Malbaie river.

You are the reason why I chose cancer as my main research subject. May you rest peacefully and live eternally in our hearts. Je t'aime papa ♡.

De ton fiston,

Julien

Epigraph

Learn from yesterday, live for today, hope for tomorrow. The important thing is not to stop questioning. *-Albert Einstein*

Chapter One: Introduction

1.1 Cancer research

Several milestones have outlined the evolution of cancer research¹. Back in 1944, Oswald Avery found how DNA participated in the transmission of information in cells². These findings led to the discovery of the structure of DNA by Watson and Crick in 1953³. Later in the 70's, bacterial restriction enzymes cleaving DNA induced a revolution in molecular biology and led to serious advances in sequencing genomes⁴. Systemic research accompanied by later large-scale genomics helped to find mutations in genes driving or suppressing cancer growth. Indeed, by pharmacologically targeting those specific mutations in individual cancer patients brought a new concept, precision medicine, which goal is to personalize treatments for maximal efficacy⁵. In cancer, a better chance of prognostic is largely determined by an optimized treatment for an individual patient⁵. More research is needed on aggressive cancers relying on low-efficacy therapy, such as melanoma and pancreatic cancers, the two models investigated in this thesis.

1.2 Melanoma Cancer

1.2.1 Melanogenesis

Cutaneous melanoma is a disease that originated from melanocytes, a specialized pigment cell type giving its coloration to hair, skin and nails. The primary function of melanocytes is to produce a light-absorbing indole biopolymer, melanin. This molecule is secreted to neighboring keratinocytes through specialized organelles called melanosomes, covering nuclear DNA and granting protection by absorbing UV radiation.⁶ Melanin synthesis is a product of several enzymatic chemical reactions: hydroxylation of phenylalanine and conversion of tyrosine by tyrosinase forming black-brown eumelanin or yellow-red pheomelanin in the presence of cysteine or glutathione⁷. The melanogenesis is triggered by a series of signals including the rate-limiting oxidation of L-tyrosine L-dihydroxyphenylalanine (L-DOPA), catalyzed by tyrosinase, where both can act as hormone-like regulators of other cellular functions⁷. The action of α -melanocyte-stimulating hormone (α -MSH) or adrenocorticotrophic hormone (ACTH) on its receptor MC1R triggers the increase of intracellular cyclic adenosine monophosphate (cAMP) which activates the response element-binding protein (CREB)-signaling pathway in melanocytes. This event activates the transcription of a variety of downstream targets, including microphthalmia-associated transcription factor (MITF), playing a crucial role in the cascade of enzymes implicated in

melanogenesis, including the melanosome matrix protein PMEL from the tyrosinase enzyme family^{6,8}.

1.2.2 Melanoma genesis

A key event in the formation of melanoma is the loss of epidermal melanin unit (EMU) integrity. The EMU consists of melanocytes acting as sentinels, protecting keratinocytes, which in return regulate melanocytes division⁷. Disruption of this well-balanced homeostasis leads to uncontrolled melanocyte division and results in cellular malignancy⁷. The Clark model⁹, defining the key biological events in melanoma progression (Fig.1). The progression of melanoma consists in these steps: A benign nevus appears on the skin where BRAF or NRAS is mutated. The nevus has hyperplasia and aberrant differentiation where CDKN2A or PTEN are inactivated. The radial-growth phase of primary melanoma has increased MITF expression with decreased differentiation. Vertical growth phase is associated with E-cadherin and N-cadherin loss. In metastatic melanoma, cells dissociate from the primary tumor site and interact with dermal fibroblasts and endothelial cells and colony distant sites.

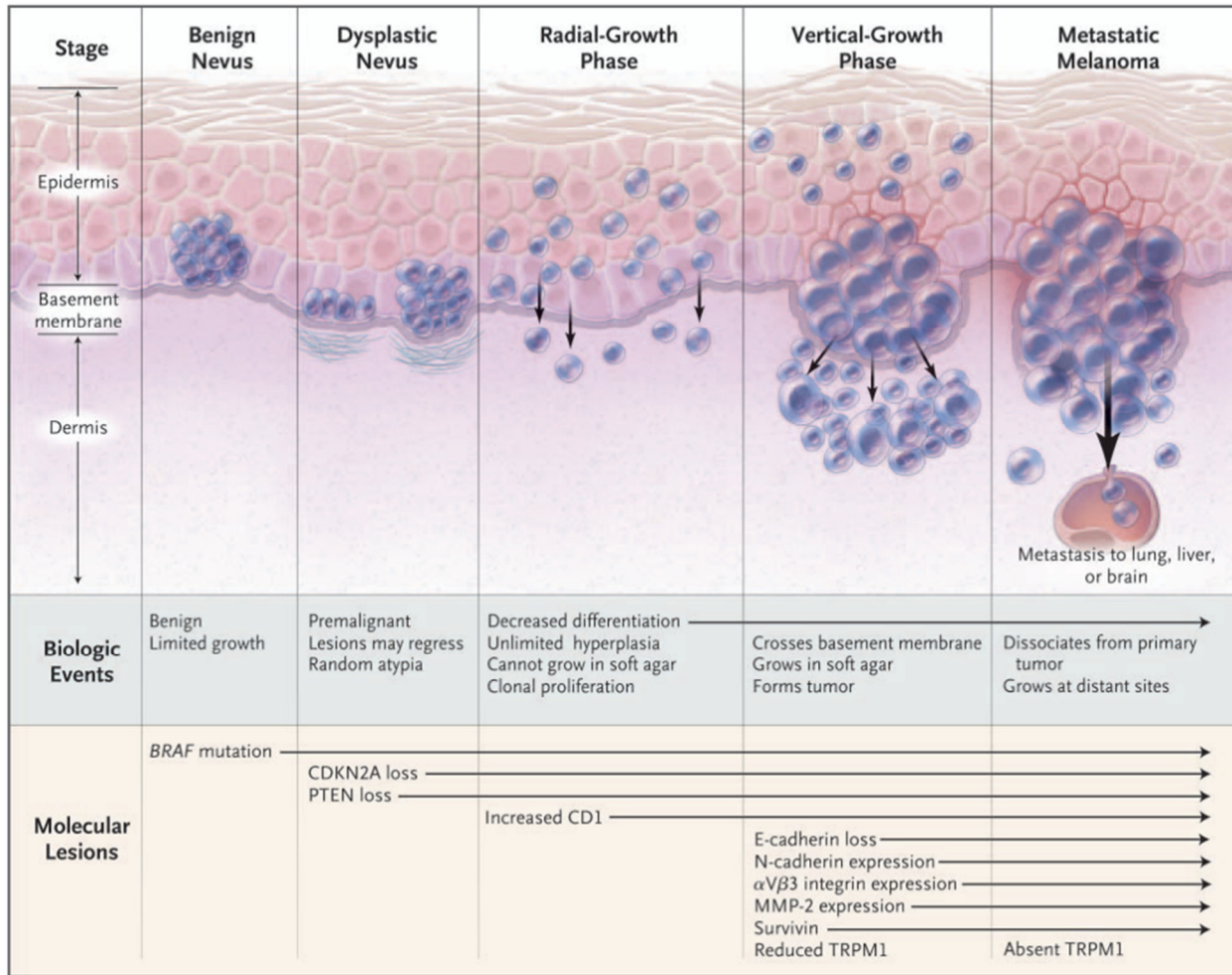


Figure 1.1: Clark Model Illustration of Melanoma Progression Stages and Histopathological Features. (Adapted from Miller *et al.* 2006)¹⁰

1.2.3 Key genetic alterations associated with melanoma progression

1.2.3.1 BRAF and NRAS

Several oncogenic pathways are known to be activated during melanoma progression. The most prominent mutation in melanoma is BRAF, an activating serine/threonine protein kinase in the mitogen-activated protein kinase (MAPK) signaling pathway. Around 80% benign nevi harbors a BRAF mutation in sequenced tumors of melanoma patients¹¹ (Fig 1.1). NRAS, another member of the MAPK pathway, is mutated in melanoma and are found in 15-20% of tumors^{12,13}. The most common BRAF mutation is the single-nucleotide substitution V600E, counting for 80% of all BRAF mutations. Several BRAF kinase inhibitors, including vemurafenib, dabrafenib and encorafenib, were developed to target this occurring oncogenic driver in melanoma which greatly

improved patients' response rate and overall survival when compared to chemotherapy¹⁴. However, therapy resistance was observed in relapsing patients treated with BRAF kinase inhibitors. The combinatorial therapy of both BRAF and MEK inhibition in melanoma BRAF V600E mutations greatly improved the survival rate of relapsing patients¹⁵. Still, the V600E mutation alone when introduced in normal melanocytes cannot induce oncogenic transformation, outlining the importance of all other mutations such as oncogene activation and inactivation of tumor suppressors happening in different stages of melanoma¹⁶.

1.2.3.2 Tumor suppressors inactivation (CDKN2A and PTEN)

Inactivation of the tumor suppressor p53, when combined with BRAF mutation, can lead to melanoma formation in zebrafish model¹⁷. This study emphasizes the fact that combination of both activation of oncogene and inactivation of tumor suppressor are common events in melanoma progression. However, in humans, there are two different tumor suppressors that are commonly mutated. First, CDKN2A, a gene encoding the two tumor suppressors p16^{INK4A} and p19^{ARF}, counts for 20-40% of germline mutation in familial melanoma. For example, an inactivated p16^{INK4A} is unable to perform its usual function where it blocks the cell cycle progression at G1/S phase by inhibiting cyclin dependent kinase 4 (CDK4). As a result, the cell cycle progresses abnormally leading to increased proliferation of melanoma cells. In nonfamilial melanoma, an occurrence of ~35% of PTEN inactivation is found in tumors. PTEN normal function is to attenuate a variety of growth factors such as phosphatidylinositol phosphate (PIP3), an intracellular signal molecule¹⁸. Indeed, its negative regulation on PI3K-AKT pathway is through dephosphorylation of PI3P in the cytoplasm, leading to high levels of oncogenic AKT¹⁹. Activated AKT inhibits the pro-apoptotic protein BAD and activates G1 cell cycle protein cyclin D1, activating the radial-growth phase and decreases differentiation in melanoma cancer cells. Finally, PTEN or CDKN2A-deficiency in cooperation with BRAF activation creates pre-malignant lesions which can lead to melanoma progression²⁰.

1.2.3.3 MITF

Another important gene in melanoma is Microphthalmia-associated transcription factor (MITF), playing a crucial role in melanocytes pigment synthesis, differentiation and lineage survival²¹. Indeed, when MITF mutates, several defects in melanocytes occur, including pigmentation

deficiency²². MITF is also a prototype lineage-survival oncogene and can promote malignant behavior of melanoma cancer cells in specific context. For example, MITF can increase the expression of the anti-apoptotic protein BCL2 by binding to its promoter²³ or increase the melanoma cancer cell proliferation by sustaining CKD2 kinase activity²⁴. MITF exhibits oncogenic activity in the context of activated MAPK pathway through BRAFV600E co-expression and cell-cycle deregulation, which is mediated through p16–CDK4–RB pathway inactivation²⁵. MITF can mediate the plasticity of melanoma cells by altering their transcriptomic profile according to whether MITF expression is high or low²⁶. Melanoma cells having high MITF expression are drug-resistant and proliferative whereas melanoma cells having low MITF expression and AP-1 high are more invasive²⁷. The loss of TRPM1, also known as metastatin, has been found to be transcriptionally controlled by MITF and has been correlated with metastasis potential in melanoma^{28,29}.

1.2.4 Metastasis and melanoma

Melanoma is notorious for its propensity to metastasize rapidly to secondary organ, which increases drug-resistance³⁰. Melanoma patients are usually cured after excision of their primary tumors, but high metastatic potential of melanoma cells participate in low-survival rate of metastatic melanoma patients. During metastasis progression, cells dissociate from the primary lesion of the organ of origin, the skin in the case of melanoma. Metastatic melanoma cells migrate in the surrounding matrix and then invade blood vessels and the lymphatic system to form metastatic lesions at a distant secondary site³¹. Alterations in genes that play a role in cell adhesion, such as cadherins—a group of proteins that maintain cell-to-cell contacts by forming connections with the actin cytoskeleton—and integrins—which mediate cell contacts with fibronectin, collagens, and laminin, are crucial components of the extracellular matrix¹⁰. However, targeting metastasis in melanoma is still challenging as many treated patients relapse, leading to poor prognosis. Understanding the complex patterns of genetic alterations and molecular mechanisms in melanoma metastasis is crucial, as preventing dissemination of cells in distant organs could be beneficial for relapsing cancer patients.

1.3 Transforming Growth Factor β

The transforming growth factor β (TGF β) comprises three different isoforms (TGF β 1-2-3), each encoded by a unique gene. The three TGF β isoforms share 70% homology and TGF β 1, which is often referred TGF β , is found to be most expressed isoform as well as the most studied³². TGF β molecules are activated through homodimerization and are stabilized by hydrophobic interactions and strengthened by a disulfide bond. Each monomer contains β strands interlocked by disulfide bonds that form the cysteine knot³³. To be active, TGF β needs to be processed from a large inactive precursor molecule called latent TGF β (Fig. 1.2). This precursor consists of a TGF β dimer in a non-covalent complex with two segments linked to two latent TGF β -binding proteins. First, the latency-associated peptide (LAP) that remains bound to TGF β after secretion, retaining TGF β in an inactive form. The second binding protein is the latent-binding protein (LTBP), which is linked to LAP by a disulfide bond. This precursor complex is release and stored in the extracellular matrix (ECM) and acts as a reservoir³². The activation of TGF β is controlled by several complex processes including integrin-mediated activation, where LAP interacts with integrin binding sequence in the ECM. Other mechanisms includes proteolytic enzymatic by furins, plasmin and calpain and acid, alkali or heat-induced proteolysis³⁴. An illustrative example demonstrates how an ECM metalloprotease, BMP-1, initiates the cleavage of LTBP1, resulting in the liberation of the latent complex. This liberation then activates MMP2-mediated cleavage of LAP, ultimately culminating in the release of the fully mature TGF- β 1 polypeptide.

1.3.1 TGF β signaling pathway

TGF β exerts multiple biological functions through activation of two distinct pathways, the canonic SMAD-dependent (Fig 1.2) and SMAD-independent pathway (fig 1.3).

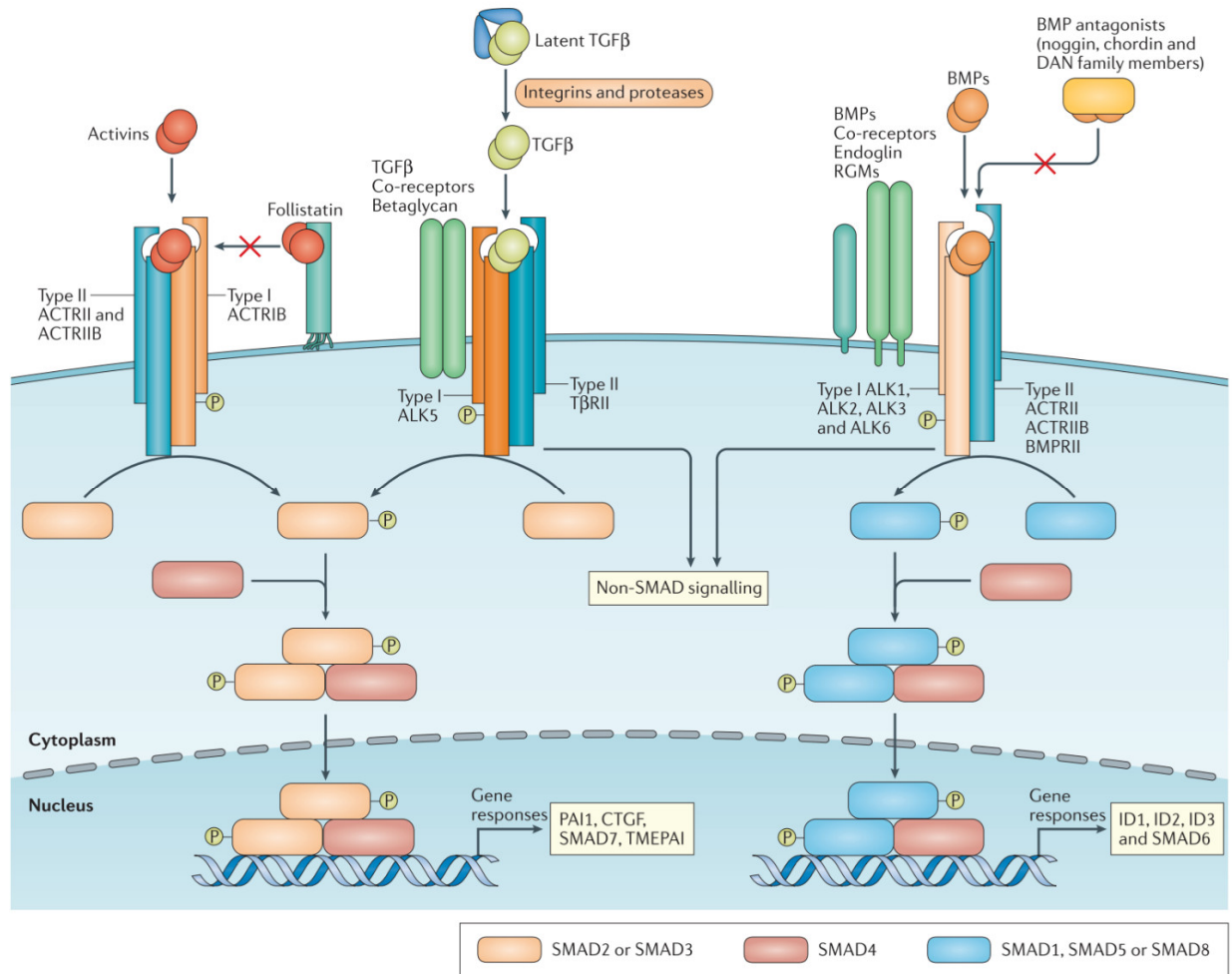


Figure 1.2: Schematic illustration of the signal transduction mediated by members of the Transforming Growth Factor- β (TGF β) superfamily. (Adapted from Chen *et al.*, 2016)³⁵

1.3.1.1 SMAD-dependent pathway

For the SMAD-dependent classical pathway (Fig. 1.2), there are two transmembrane Ser/Thr kinase receptors in the cell membrane that are activated upon TGF β ligand binding: TGF β receptor I (T β RI) and a specific TGF β receptor II (T β RII), also known as ALK5 (Fig. 1.2 middle). On the other side, activin-binding triggers activin signaling through receptor type II (ACTRII and ACTRIIB) and receptor type I ACTRIB (also known as ALK4) (Fig. 1.2 left). BMPs signal via BMP type II receptor (BMPRII) and several type I receptors including ACTRII, BMPRI, ALK1, ALK2, ALK3 and ALK6 (Fig. 1.2 right). Some co-receptor, TGF β receptor III (T β RIII) regulates the access of TGF β superfamily members³⁶. For example, betaglycan can increase the specificity of the different TGF β s isoforms³⁶. The activity of both TGF β and T β RII activate the kinase activity

and phosphorylation of T β RI. Subsequently, the activated T β RI can recruit and phosphorylate downstream receptor-regulated SMAD (R-SMAD) proteins, SMAD2 and SMAD3. Phosphorylated SMAD2 and SMAD3 can bind to the co-SMAD chaperone protein SMAD4. The SMAD complex is translocated to the nucleus and act as a transcription factor as they can activate the expression of many TGF β target genes³⁷.

TGF β , activins, and bone morphogenetic proteins (BMPs) interact with distinct heteromeric complexes formed by single transmembrane-spanning Type I receptors, also known as Activin Receptor-Like Kinases (ALKs), and Type II receptors, which possess serine/threonine kinase activity³⁸. SMADs serve as the specific transcriptional effectors for members of the TGF β superfamily. The activation of TGF β and activin receptors triggers the phosphorylation of receptor regulated SMAD2 and SMAD3, while BMP stimulation results in the phosphorylation of SMAD1, SMAD5, and SMAD8. SMADs form complexes with the common mediator, SMAD4. In addition to signaling through the canonical SMAD-dependent pathway, members of the TGF β superfamily also engage in non-SMAD signaling pathways, thereby having many crosslinks with numerous pathways. Each stage of the pathway, starting from ligand binding to the receptor, and extending to the regulation of activity, subcellular localization, and stability of intracellular effectors, is meticulously controlled. Notable components of the TGF β include CTGF (Connective-Tissue Growth Factor), DAN (Differential Screening-Selected Gene Aberrative in Neuroblastoma), ID (Inhibitor of DNA Binding), PAI1 (Plasminogen Activator-Inhibitor 1), PI3K (Phosphatidylinositol 3-Kinase), RGM (Repulsive Guidance Molecules), and TMEPAI (Transmembrane Prostate Androgen-Induced Protein). Inhibitory Smads (I-Smads), can play a crucial role in controlling TGF β signaling by repressing SMAD-mediated signaling responses: SMAD6 inhibits SMAD1 and SMAD5³⁹ while SMAD7 inhibits SMAD2 and SMAD3⁴⁰. Indeed, the expression of SMAD6/7 inhibitors is activated by their respective R-Smad/co-SMAD DNA-binding activity as they induce a negative feedback loop.

1.3.1.2 SMAD-independent pathway

Many signaling cascades can be activated in response to TGF β ^{41,42} (Fig 1.3). Indeed, TGF β signaling exhibits susceptibility to influence from pathways that extend beyond the canonical and non-canonical TGF β signaling routes. A pathway known to be activated downstream of TGF β signaling is the ERK/MAPK pathway. However, activation of ERK is context-dependent,

influenced by factors like growth factors in the cell culture medium, cell-cell contacts, interactions with the extracellular matrix, or specific oncogenic activation in the cancer model⁴². Other pathways known to be activated downstream of TGF β are the c-Jun amino terminal kinase (JNK), p38 MAPK, the I κ B kinase (IKK), phosphatidylinositol-3 kinase (PI3K), AKT and Rho family GTPases. Crosstalk between TGF β and many other pathways including WNT, Hedgehog, Notch, interferon (IFN), tumor necrosis factor (TNF) and RAS pathways, are also known to occur. Moreover, the effectors SMADs proteins can participate in microRNAs (miRNA) processing in response of TGF β stimulation^{43,44}. The dynamic interplay between TGF β and these interconnected pathways defines the multifaceted actions of TGF β , thereby orchestrating context-specific and temporally regulated signals.

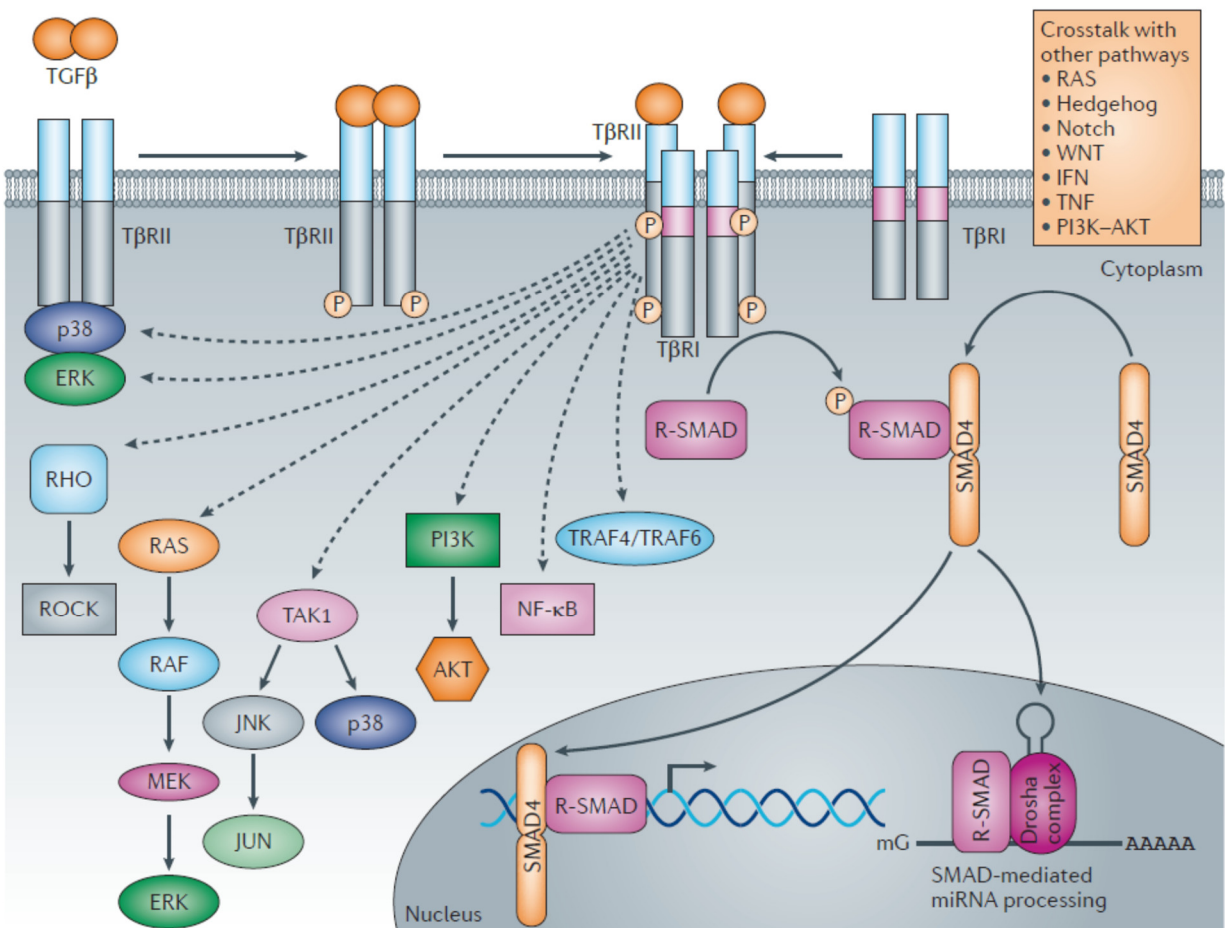


Figure 1.3: Schematic representation of non-canonical TGF β signaling and its crosstalk with various other signaling pathways. (Adapted from Akhurst et al. 2012)⁴⁵

1.3.2 Dual role of TGF β

TGF β has been shown to have a dual role during cancer progression. Tumor suppressive effects of TGF β , including inhibition of cell proliferation, induction of apoptosis, and inhibition of cell immortalization, are observed in normal epithelial cells and early carcinomas. In contrast, tumor promoting effects, including induction of epithelial-mesenchymal transition (EMT), cell adhesion, migration, invasion, chemoattraction, and tumor metastasis, are more specifically observed in more advanced stages of cancer.³²

1.3.3 TGF β as a tumor suppressor

1.3.3.1 Cell cycle inhibition

TGF β inhibits the G1 phase of the cell cycle progression through induction of expression of CDK inhibitors and the downregulation of c-Myc expression and cell differentiation inhibitors ID1, 2, and 3. Stimulation by TGF β induces the expression of the CDK inhibitor p15, whose role is to inhibit the formation of the complex between cyclin D with CDK4 or CDK6, implicated in G1 phase and S phase entry. Furthermore, TGF β increases the expression of p21, disrupting the formation of cyclin E or cyclin A complexes with CDK2, another important factor of G1/S phase. TGF β -associated transcription of p15 and p21 is mediated by binding of FoxO transcription factors to target their respective gene promoters. CDKN2B, encodes for p15 and CDKN1A encodes p21. The downregulation of c-Myc by TGF β is mediated through transcriptional repression by SMAD3, SMAD4 and CDK regulatory signals proteins p107 and E2F4/5⁴⁶. PP2A, a phosphatase, interfere with TGF β signaling and can inhibit p70^{S6}, a serine/threonine kinase that regulates translation of specific mRNAs and is essential for G1/S progression⁴⁷. In short, TGF β inhibits G1 phase progression, establishing a crucial role in disrupting key cell cycle events and preventing entry into the S phase.

1.3.3.2 Apoptosis

TGF β has been reported to promote pro-apoptotic effect in most cases including epithelium, liver and immune system³². A vast number of apoptotic target genes are known to be controlled by SMAD transcriptional complexes. TGF β -inducible early response gene 1 (TIEG1), a zinc-finger transcription factor, decreases the protein levels of the pro-apoptotic protein BCL2⁴⁸. Another protein, DAPK, also downregulates BCL2 expression through the action of SMAD2, SMAD3 and

SMAD4⁴⁹. In hepatocytes, GADD45B, BMF and BIM have been shown to be a mediator of TGF β -induced apoptosis through p38 activation^{50,51}. In gastric epithelial cells, BIM triggers apoptosis through the SMAD and Caspase-9 activation⁵². In hepatocellular carcinoma cells, TGF β increases PDCD4 expression, leading to apoptosis. This effect was demonstrated to be reversible through ectopic activation SMAD7, an inhibitor of the TGF β signaling pathway⁵³. In pancreatic cancer, TGF β has been shown to induce apoptosis in cells carrying a wild-type SMAD4 by inducing epithelial-to-mesenchymal transition (EMT) transcription factor Snail along with Sox4 expression⁵⁴. Of note, in pancreatic cancer, inactivation of the tumor suppressor SMAD4 is a common mutation. Indeed, in a SMAD4-deficient context, TGF β fails to induce apoptosis, highlighting the necessity of intact TGF β signaling for apoptosis induction. Therefore, SMAD4 inactivation can switch the role of TGF β from a tumor suppressor to a tumor promoter. Some proteins are not direct targets downstream TGF β but act as an apoptosis facilitator. An example is ARTS, which is released from mitochondria upon TGF β treatment and increases caspase-3 activity, leading to increased apoptosis⁵⁵. Our group previously found a crosstalk between TGF β and PI3K-AKT pathways as TGF β induces SMAD-dependent transcriptional regulation of SHIP which reduces AKT levels⁵⁶. Briefly, TGF β induces apoptotic effects by regulating a network of genes and pathways and highlights the importance of the crucial role of the SMADs in these tumor suppressive effects.

1.3.4 TGF β as a tumor promoter

1.3.4.1 EMT

Epithelial–mesenchymal transition (EMT) is a biological process where epithelial cells undergo cellular organization to mesenchymal phenotype. Transformed cells lose their polarity, adhesion and gain the ability to migrate and invade the surrounding area⁵⁷. EMT occurs in many different cellular contexts, including cancer, and can be induced by many types of inducing signals such as TGF β ⁵⁸. In later stage of cancer, cells become resistant to tumor suppressive effect of TGF β and undergo EMT. For example, the SMADs mediate EMT by inducing the expression of E-cadherin transcriptional repressors SNAIL, ZEB and TWIST⁵⁹. A study showed that SMAD3 and SMAD4 associate with SNAIL and that this complex represses an important set of proteins implicated in cell-cell junctions (CAR, occluding, claudin-3 and E-cadherin)⁶⁰. Another study using skin cancer as a model showed that SNAIL transcription by SMAD3/SMAD4 promoted to EMT and that

repression of SMAD2 enhanced this phenotype⁶¹. SMAD7 repression, through the action of micro-RNA182, over activates TGF β signaling and increases EMT⁶². These molecular mechanisms emphasize the pivotal role that TGF β acts in inducing an invasive cellular phenotype.

1.3.4.2 Angiogenesis

As tumor grows during cancer progression, the need for oxygen and nutrients is constantly increasing. To this end, cancer cells can secrete factors, such as TGF β , to increase endothelial cells growth to create new blood vessels. A study showed that activation of TGF β receptor contributes to maturation of blood vessels and activation of the endothelium⁶³. TGF β was previously shown to be a potent inducer of vascular endothelial growth factor (VEGF) in Ras-transformed cancer cells, leading to a pro-angiogenic response⁶⁴. The TGF β /T β RII/Smad3 axis was shown to be implicated in VEGF upregulation in oral squamous cell carcinoma tumor-associated macrophages (TAMs)⁶⁵. This study highlights the correlation between macrophages density and cancer progression by TGF β .

1.3.4.3 Immunologic surveillance escape

Important cells from the immune system, such as T lymphocytes and natural killer cells, can play an essential role in protecting the body against fast-dividing cells that could potentially form tumors³⁵. However, immune surveillance is bypassed by tumor cells through TGF β -induced immune evasion. However, how TGF β causes T cell dysfunction remains unclear⁵⁸. Targeted mutation of TGF β in mouse T-cell led to increased auto-immune response, highlighting its negative role in immune homeostasis⁶⁶. Similarly, a study showed that blockade of TGF β in T-cell can participate in the eradication of pre-formed tumors in mice⁶⁷. TGF β inhibition induces a cytotoxic T-cell response against colon tumor cells that prevented metastasis and restored sensitivity to anti-PD1-PDL1 therapy⁶⁸. A second paper showed that impaired TGF β /SMAD signaling participated in the regulation of tumor metastasis in urothelial cancer⁶⁹.

1.3.5 TGF β and melanoma

1.3.5.1 TGF β isoforms in melanoma

Expression and secretion of the three TGF β isoforms, in different immortalized melanoma cell lines issued from patient and normal melanocytes, has been extensively studied by several

research teams over the last two decades^{70,71,72,73}. TGF β 1 expression was found in normal melanocytes, in addition to primary and metastatic melanomas. TGF β 2 and TGF β 3 isoforms are not found in melanocytes but are expressed at heterogeneous levels in melanocytic neoplasia. TGF β 2 was revealed to be expressed at lower level, compared to all different isoforms, and displayed the lowest effect on cell growth inhibition. Also, TGF β 2 was expressed at heterogeneous levels, in advanced primary and metastatic melanomas, while TGF β 3 was consistently and highly expressed in these lesions⁷⁴. Expression of TGF β 2 and TGF β 3 isoforms are correlated with tumor progression, appearing in early melanoma and increasing with more aggressive stage^{75,74}. However, further studies are needed to understand the specific downstream signaling of the different isoforms of TGF β .

1.5.3.2 TGF β and growth inhibition in melanoma

Melanocytes are sensitive to the growth inhibition of TGF β but melanoma cells display various degrees of responsiveness/resistance to TGF β ^{76,77}. Several studies showed that melanoma cells *in vitro* are responsive to TGF β stimulation, have intact SMAD signaling and that it induces growth inhibition^{71,77-79}. Data of our own group⁸⁰ and others⁸¹, showed that TGF β prevent cell migration and invasion through the regulation of the plasminogen system. In that same direction, data of our own study showed that TGF β mediates growth inhibitory effects through the action of p21 and leukemia inhibitory factor (LIF)⁸². We also showed that TGF β induces a strong G1 cell cycle arrest and potent inducer of caspase-mediated cell death in many melanoma cell lines⁸². In a375 human melanoma cell line, integrin β 1 activates TGF β which increases the number of CD8+ tumor-infiltrating lymphocytes and produce tumor suppression⁸³. A recent study showed that introduction of a chimeric receptor comprising both T β RI and T β RII, able to trap all TGF β isoforms (TGF β 1-2-3) can slow melanoma progression⁸⁴. Indeed, the research group proposed that it could be possible to maintain the tumor-suppressive level concentration of TGF β without unwanted pro-tumorigenic responses. FIST, a chimeric protein of the fusion of IL-2 and the soluble extracellular domain of TGF β R II, inhibits TGF β by overexpressing SMAD7 which generated STAT1 hyperactivation via IL-2R on immune cells, producing an effective antitumor response⁸⁵. TGF β antagonizes IL-2 signaling primarily in the nucleus through the inhibitory activity of SMAD3 on a subset of IL-2 target genes. Additionally, using a dominant-negative version of SMAD3 blocked the ability of TGF β to inhibit individual IL-2 target genes, including c-myc, c-

fos, Cyclin D2, and cyclin E and IL-2-induced T cell proliferation⁸⁶. Finally, these studies highlight the protective role of TGF β in melanoma.

1.5.3.3 Phenotype switching and TGF β in melanoma

Phenotype switching, another term for explaining the transcriptomic switch from proliferative/invasive conferring plasticity to cancer cells^{87,88}. A group showed that one of these signatures involves the up-regulation of melanocytic genes including MITF, TYR, DCT and MLANA and other neural crest-related factors such as SOX10, TFAP1A and EDNRB⁸⁹. This transcriptomic signature is correlated with increased proliferation, low motility and sensitivity to growth inhibition by TGF β . Another signature implicates a lower expression of these mentioned genes and higher expression of other secreted products including INHBA, COL5A1, and SERPINE1⁸⁹. These factors participate in modifying the extracellular environment, therefore associating this specific transcriptomic profile with high motility and resistance to growth inhibition by TGF β ⁸⁹.

Phenotype switching has also been identified as an escape route for resistance to therapy such as BRAF and MEK pharmacologic targeting⁹⁰. For example, downregulation of SOX10 in melanoma activates TGF β signaling and leads to the upregulation of EGFR and PDGFRB, contributing to the resistance of MEK and ERK inhibitors through an oncogene senescence phenotype⁹¹. A recent study show that conditional deletion of SMAD4 has no effect on normal melanocytes growth but inhibited tumor growth and metastasis in melanoma independently of phenotype switching⁹². Same study also shows that conditional deletion of SMAD7, an antagonist of TGF β 1 receptor, enhanced both invasiveness and proliferation, highlighting the compatibility of invasion with a high proliferative state⁹². However, this result suggests that the mechanism is independent of phenotype switching, where cells can be both proliferative and invasive at the same time. A decrease in E-cadherin expression and upregulated expression of EMT-related transcription factors, Snail, Slug, Twist, and Zeb1 have been revealed to be correlated with the enhanced invasion and acquisition of stem cell-like properties⁹³. MSX1 induces a neural crest precursor-like state in melanocytes and melanoma cells, leading to a phenotypic transition in melanoma towards a highly invasive state, and depletion of MSX1 inhibits melanoma metastasis, suggesting that neural crest-like reprogramming is crucial for melanoma progression⁹⁴. Finally, these findings

highlight the importance of the expression of a subset of genes balancing a more proliferative type or invasive type, which is dependent on the cellular context.

1.6 Stemness and melanoma

Stem cells have self-renewal capacities, a mechanism where cells are able to replicate into identical and undifferentiated cells⁹⁵. Indeed, self-renewal involves the proliferation of cells with maintenance of multipotency and tissue regeneration⁹⁵. Several lines of evidences showed that cancer stem cells subpopulation could be the origin of metastasis and tumor heterogeneity in melanoma⁹⁶.

1.6.1 Melanoma stem cell concept

There are two models that were proposed to explain the heterogeneity in tumors; the stochastic clonal evolution model⁹⁷ and the hierarchical model⁹⁸ (Fig. 1.4). The first being characterized by similarity of all tumor cells where sub-clonal differences comes from genetic and epigenetic changes during carcinogenesis. The second is defined by a small and slow-cycling progression of subpopulation of undifferentiated cells, the stem cells, sustaining tumor growth^{99,100}. In melanoma, conflicting studies debate these cancer stem cell concepts. A group showed that melanoma cells issued from different patients have increased plasticity and can be reversed from differentiated to undifferentiated status¹⁰⁰. The same group showed that modification of xenotransplantation assay, by using severe immunodeficient mice, increased the detection of tumorigenic cells in melanoma patients samples by several degrees of magnitude¹⁰¹.

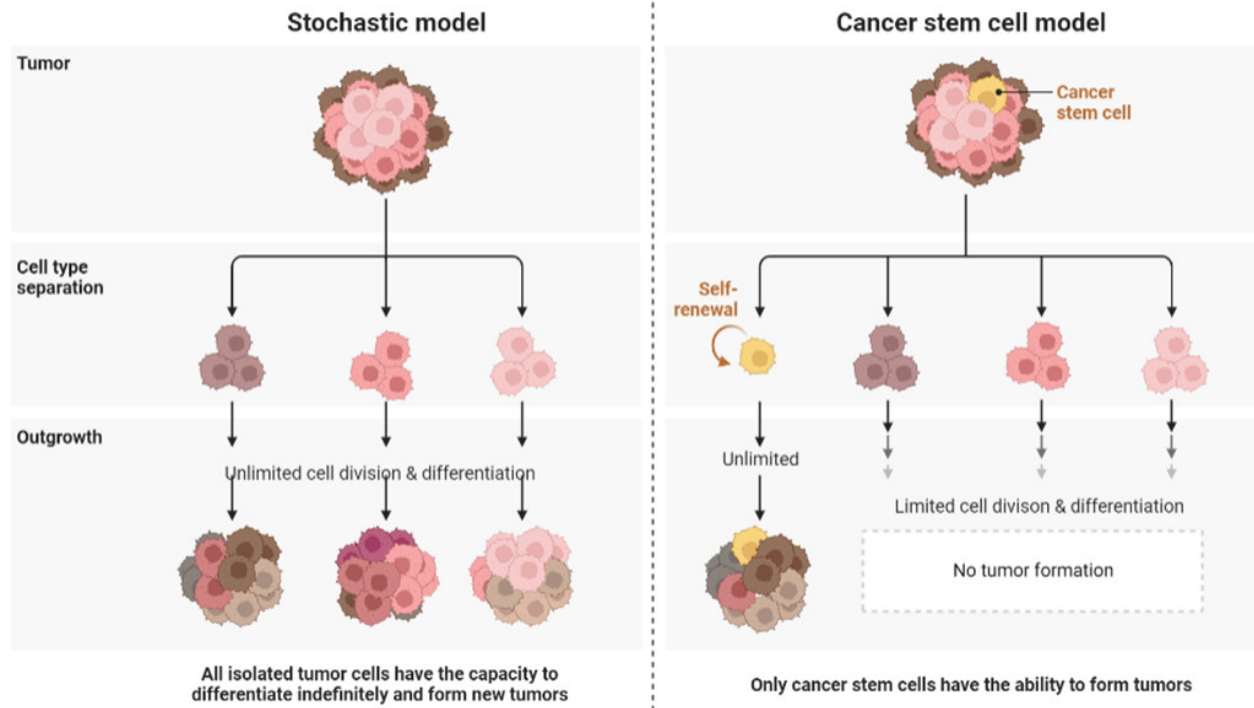


Figure 1.4: Schematic representation of two models reflecting the development and progression of cancer

1.6.2 Melanoma stem cell markers

Over the last decades, several biomarkers were discovered and linked with self-renewal capacity and stemness in melanoma.

1.6.2.1 CD133

A pentaspan transmembrane glycoprotein, CD133, also called Prominin1, has been linked with increased tumor potential and cancer stem cells properties in various tumor types including melanoma. However, the accuracy of CD133 as a stem cell biomarker has been debated by several studies¹⁰². CD133 was found to be overexpressed in several melanoma biopsy tissues¹⁰³ and sentinel lymph nodes of melanoma patients¹⁰⁴. Moreover, isolation of cells expressing only CD133 (referred as CD133+) by flow cytometry displayed increased tumor formation potential¹⁰³. CD133 expression was shown to be regulated in a cell-cycle dependence manner: CD133 antibody reactivity was reduced in arrested in G0/G1 phase but not in dividing cells in the G2/M phase¹⁰⁵. A study showed that CD133+ cells displayed a proliferative phenotype as opposed to CD133- with an invasive phenotype¹⁰⁶. A recent study showed that knockdown of CD133 reduced matrix

metalloproteinases MMP2/MMP9, which resulted in reduced invasion and melanoma metastatic burden¹⁰⁷.

1.6.2.2 CD271

Melanoma cell populations enriched in neutrophin receptor (CD271) have higher tumorigenic potential and were capable of metastasize to distant organs when transplanted *in vivo*¹⁰⁸. CD271 was also shown to play a role in phenotype switching, where it decreases proliferation and promoting invasiveness at the same time¹⁰⁹. Another study showed that elevated levels of CD271 can serve as a switch between proliferation/survival and differentiation/cell death¹¹⁰. A study showed that CD271 expression is linked with melanoma progression and that brain metastases had the highest expression¹¹¹.

1.6.2.3 ALDH

Melanoma and melanocytes have similar ALDHA1 and ALDHA6 mRNA expression as well as ALDH enzymatic activity¹¹². ALDHA1 and ALDHA3 are the two main isoenzymes conferring aldehyde dehydrogenase (ALDH) activity¹¹³. A study showed that ALDH1A1 is most expressed isoform in human melanomas samples and that ALDH1A3 expression is higher in melanoma cell line¹¹⁴. By using limiting-dilution transplantation assay to determine the minimum number of cells to form a tumor, a research group showed that 0.005% of ALDH+ melanoma cell is able to initiate a tumor in NOD/SCID mouse¹¹⁵. Indeed, the number of ALDH+ melanoma initiating cells (MIC) is 100-fold higher than the whole pool of unselected cells. Melanoma having increased ALDH enzymatic activity are prone to proliferate and metastasize more than the lacking ones¹¹³. The mutational status of BRAF was shown to be an important variable to assess the correlation between the expression status of ALDH and overall survival. The expression of ALDH1A3 is correlated with better prognosis in metastatic BRAF-mutant melanoma and ALDH1A1 correlated with better prognosis in BRAF wild-type melanoma¹¹⁶. ALDH was also found to be correlated with multidrug resistance in melanoma and was also linked with increase of CD271 expression¹¹⁷. ALDH+ melanoma stem cell population was found to be sensitive to nifuroxazide, an antidiarrheal agent identified as a STAT3 inhibitor, and that mutation in ALDHA3 isoform led to increased drug-resistance^{118,119}. Phenformin, an anti-diabetic drug, was shown to reduce the viability and

proliferation of cells with higher expression of ALDH¹²⁰. These results highlight the importance of ALDH in tumor-initiation and may be a potential target to help eradicate melanoma.

1.6.2.4 ABCB5 and ABCG2

Melanoma cells expressing higher amounts of the chemoresistance mediator ABCB5 were more tumorigenic than their ABCB5 negative counterpart¹²¹. ABCB5, by inducing the secretion of IL-1 β , maintain an IL-1 β /IL8/CXCR1 cytokine signaling axis and is correlated with increased tumor-initiating capacity and aggressiveness of melanoma¹²². A study showed that ABCB5 could be linked with BRAF-inhibitor drug resistance in two melanoma cell lines and that p-ERK is associated with this phenotype¹²³. Exome-sequencing of ABCB5 helped the identification of several mutations in melanoma samples and that ABCB5 mutation is correlated with CDKN2A and NRAS mutation¹²⁴.

1.6.2.5 CD20

The first study demonstrating the evidence of melanoma stem-cell revealed that a subpopulation of cells capable of propagating as nonadherent spheres, expressed high levels of CD20¹²⁵. Targeting a small fraction of melanoma cells expressing CD20 by CAR engineered cytotoxic T cells managed to eradicate melanoma tumor¹²⁶. This finding highlights the importance of targeting melanoma stem cells as a potential therapeutic approach to prevent tumor formation in melanoma.

1.6.3 Melanoma stem cell expansion

Currently, cells cultured under low-attachment surface is one of the most common techniques to expand cells possessing stem-cell like properties. They reflect the self-renewal capacity and multipotency of melanoma CSCs *in vitro*. These types of cells were shown to engraft immunodeficient mouse tissues at better efficiency than regular mono-layered cultured cells¹²⁵. This finding establishes a connection between stem cell properties and tumor-initiating capacities

1.6.4 Role of TGF β in stemness

Under normal physiologic conditions and during body growth, TGF β and its numerous family members exert whether alone or in partnership with various external cues to regulate somatic stem cells and participates in self-renewal ability and differentiation. Large-scale transcriptomic

characterization of ES cells and somatic stem cells elucidated signaling networks such as TGF β family signaling, prone to play important roles in the maintenance of the characteristics of ES cells¹²⁷. Secretory proteins Activin A and Nodal, stimulating TGF β signaling pathway, has been shown to be essential for maintenance of human embryonic stem cells (hESCs) into an undifferentiated state where it functions through SMAD2/3 activation and its downstream targets implicated in stemness such as Nanog^{128,129}. Mouse embryos with defective SMAD4 gene displayed proliferative defect and delayed growth in inner cell mass¹³⁰. In hESCs, the activated TGF β /activin/nodal axis contributes to the maintenance of human embryonic stem cell identity. For maintenance of an undifferentiated state, the signaling through phosphorylation of SMAD2/3 is increased directly downstream of Wnt in hESCs. The stemness-related transcriptional factor NANOG, SOX2, and OCT4 form a cooperative network inducing pluripotency in stem cells through this specific Wnt/TGF β partnership¹³¹. For stem cell studies, hair follicles have been widely used as a model for studying stem cells and early studies have showed that skin stem cells are involved in tumor formation¹³². A research group showed the implication of TGF β in promotion of melanocyte immaturity and quiescence¹³³. This effect is mediated by the downregulation of MITF and was correlated with SMAD2 phosphorylation in melanocytes. Several factors and signaling pathways, among TGF β , are modulated in many cancer stem cell models. Increased phosphorylation of STAT3 and activation of AKT pathway was detected in CSCs subpopulations of several melanoma cell lines¹³⁴. A signaling cross talk between the different SMADs factors and other pathways such as Nodal/Activin/pSMAD2/3, ERK/MAPK and canonical Wnt/GSK3 β / β -catenin also have an important role in dictating the stem cell homeostasis. The complex cross talk between s204 phosphorylation site in the SMAD3 linker region provided a paradigm for cell fate decisions during early embryonic development¹³⁵. In B16 mouse cells, the inhibition of MITF, a differentiation regulator in melanoma, increases the tumorigenic potential and upregulates Oc4 and Nanog stem cell markers. The CDK inhibitor p27, a known downstream target of TGF β ¹³⁶, participates in this molecular switch controlling the transition between undifferentiated/differentiated melanoma cell progeny¹³⁷. Newer concepts are arising to explain the biological factors that induces stemness, such as genetic modification¹³⁸ or epigenetic factors¹³⁹.

1.7 MEN1: Multiple endocrine neoplasia-type 1

Multiple endocrine neoplasia-type 1 (MEN1) as an autosomal dominant familial disorder characterized by varying combination of tumors in parathyroids, neuroendocrine pancreatic tumors (P-NET) and the anterior pituitary¹⁴⁰. The MEN1 gene has 10 exons and encodes a 2.8 kilobases transcript¹⁴¹. Menin is the 610 amino-acid nuclear protein (67kDa) expressed by the locus of MEN1¹⁴¹. Tumors affected by MEN1 inactivation can create many clinical effects which are caused by over secretion of endocrine substances including gastrin, insulin, parathyroid hormone, prolactin, growth hormone, glucagon or adrenocorticotrophic hormone. Indeed, over 500 germline and somatic mutations located in the protein-coding region of MEN1 have been identified¹⁴². Around 80% of mutations are nonsense or result in a frameshift predicting an inactive truncated product and 20% are missense mutations, which are degraded via the ubiquitin-proteasome pathway¹⁴². Allelic deletions resulting in MEN1 loss were discovered in patients with MEN1 disease, granting MEN1 as a tumor suppressor¹⁴³. Mice having an homozygous mutation in the MEN1 gene die *in utero* at day 12¹⁴⁴. However, heterozygous MEN1 mice were viable and fertile and can develop parathyroid, pancreatic, pituitary and adrenal tumours with hypercalcaemia, hypophosphataemia and hypercorticozonaemia¹⁴⁴.

1.7.1 MEN1 genome-wide interactome

The protein menin was shown to interact in the nucleus with several transcription factors, epigenetic regulators or proteins involved in DNA synthesis or repair¹⁴⁵. A genome-wide analysis, consisting of a chromatin-immunoprecipitation coupled with microarray analysis, was used to map MEN1 genomic binding sites and enable the finding of 20 000 novel MEN1-interacting promoter sites¹⁴⁶. Proteomic analysis of a P-NET cell line revealed 457 significantly altered proteins implicated in posttranslational modification and cell death/survival¹⁴⁷.

1.7.2 Cellular functions of MEN1

Menin was shown to act as a tumor suppressor in the nucleus by playing a role in cell cycle progression, DNA repair, DNA replication and transcription regulation¹⁴⁸. Menin was previously shown to interact with many transcription factors such as JunD, a functional component of the AP1 complex and that missense mutations of MEN1 disrupted this interaction^{149,150}. Menin binding induces the repression of the transcriptional activity of JunD by the recruitment of histone

deacetylase. Menin was also shown to interfere with Jun kinase (JNK) phosphorylation of JunD and c-Jun, interfering Ras signaling¹⁵¹. Moreover, the crystal structure of menin complexed with JunD gave insight about the mechanistic explanation in how this interaction blocks JNK-mediated phosphorylation, which inhibits JunD activity¹⁵². Menin was also shown to interact with MLL1¹⁵³ and MLL2¹⁵⁴ by interacting with their SET-domain possessing H3K4 methyltransferase, which can regulate the expression of cyclin-dependent inhibitors (CDKI) and homeobox domain genes. The MLL/Menin complex, a major influencer in leukemia carcinogenesis, is currently under investigation for its tumor suppressive role and is targeted by many small molecule inhibitors¹⁵⁵. The crystal structure gave insights about the binding of the deep pocket of menin complexed with either MLL1 or JunD in the same manner. However, a differential transcriptional outcome occurs as the interaction between menin and JunD prevent its activation through inhibition of JNK-mediated phosphorylation and MLL1 through the peptide-pocket yet interacting with LEDGF at a distinct surface. Menin was also shown to interact with c-Myc, a transcription factor activating several genes implicated in proliferation through binding of enhancer box and recruiting histones acetyltransferase, and SKI-interacting protein coactivator¹⁵⁶. The N-terminus of menin was shown to interact with the NF- κ B transcription factors p50, p52 and p65, which have a crucial role in cell survival and stress response¹⁵⁷. Menin was reported to interact with AKT in both *in vitro* and *in vivo* settings and downregulate its kinase activity resulting in decreased proliferation and increased apoptosis¹⁵⁸. In PNET cell line BON-1, menin was shown to be implicated in the regulatory mechanism of mTOR pathway, which has different roles in proliferation, autophagy and apoptosis¹⁵⁹. More specifically, prolonged rapamycin treatment on pancreatic neuroendocrine tumors potentiate mTORC2-AKT activation in menin-deficient context¹⁵⁹. Several nuclear receptors were shown to induce tumor-suppressive phenotype by interacting with menin, including the estrogen receptor- α ¹⁶⁰, vitamin D receptor¹⁶⁰, the retinoid X receptor¹⁶¹, the two specific peroxisome proliferator-activated receptors (alpha¹⁶² and gamma¹⁶¹), the liver X receptor alpha¹⁶³ and the androgen receptor¹⁶⁴. These molecular mechanisms highlight the tumor-suppressive role of MEN1 in many cellular contexts which implicate a variety of signaling pathways.

1.7.3 MEN1 in TGF β signaling

Data of our own group showed that menin interacts with SMAD3 by coimmunoprecipitation, which is the first evidence of menin involvement in TGF β pathway (Fig. 1.5). Moreover, we

showed that the menin inactivation through antisense RNA suppresses SMAD3-mediated transcriptional activity by preventing SMAD3/4 DNA association at regulatory sites, such as PAI-1 promoter¹⁶⁵. Moreover, we demonstrated that activin has a negative regulatory influence on PRL transcriptional expression through both SMADs and menin activity. The resulting PRL downregulation inhibits cell proliferation in somatolactotrope cells¹⁶⁶. A donor splice site mutation in the exon 3 of MEN1 gene leads to the production of an aberrant menin protein that is defective in mediating TGF β stimulated SMAD3 action, resulting in reduced cell proliferation control. Interestingly, this mutation has no significant impact on the normal function of menin in inhibiting the activity of transcriptional regulators JunD and NF-kB, highlighting the importance of the 35 lacking amino acid in the MEN1 mutant¹⁵³. These studies highlight the tumor suppressive role of menin in TGF β pathway related with the SMAD3 action. By immunoprecipitation, menin was also found to interact with SMAD1/5, which is activated by BMP, an important bone and cartilage factor in extraskeletal tissues¹⁶⁷. Therefore, this study links MEN1 with the differentiation of mesenchymal stem cells into the osteoblastic lineage and highlights the tumor-suppressive role of menin in the TGF β inhibitory actions by BMP-related SMAD proteins. A study that investigated the roles of TGF β and menin in parathyroid cell proliferation and PTH production. This study suggests that menin is essential for the inhibitory effects of TGF β on parathyroid cell proliferation and PTH secretion. Loss of TGF β signaling due to menin inactivation contributes to parathyroid tumorigenesis¹⁶⁸. In leukemia cells, TGF β stimulation inhibited proliferation and upregulated menin expression and this effect was hindered in MEN1-null cells. Moreover, excision of T β RII down-regulated menin in MLL-AF9 transformed bone marrow cells. These results highlight the cross-talk between TGF β and menin as their tumor-suppressive properties could be exploited in leukemia¹⁶⁹. A study revealed that the role of menin in cancer is context-dependent, functioning both as a promoter of epithelial-mesenchymal transition (EMT) linked to cell migration and as a modest inhibitor of cell growth. Menin suppresses the expression of CCAAT/enhancer-binding protein beta (CEBPB) and epithelial-specific genes through histone deacetylation, enhancing the EMT process driven by TGF β signaling. The findings also demonstrate that C/EBPb, downstream of Menin and TGF β signaling, plays a key role in balancing growth inhibition and EMT and can restore Menin's anticancer functions in pancreatic cancer by activating CDKN2A/B genes and opposing EMT processes¹⁷⁰.

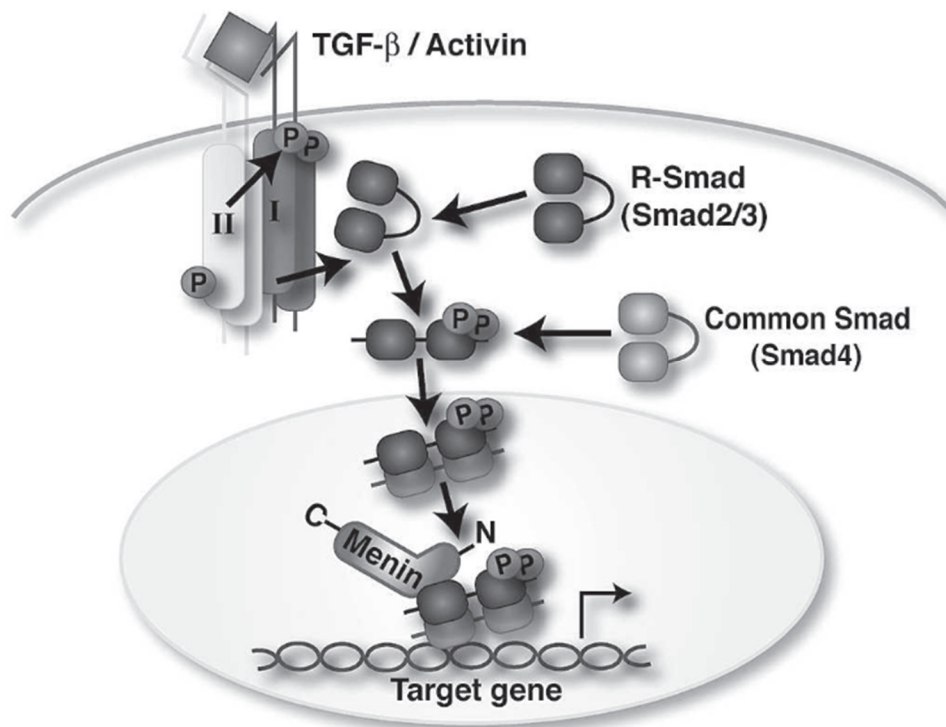


Figure 1.5: Menin and TGFβ/Activin signaling pathway. (Adapted from Hendy *et al.* 2005)¹⁷¹

1.7.4 MEN1 in melanoma

Even if MEN1 syndrome was associated primarily with endocrine tumors of the parathyroid, pancreas and anterior pituitary, cases of melanoma associated with MEN1 were reported in several families¹⁷². It was found that loss-of-heterozygosity (LOH) of MEN1, corresponding to the complete loss of one gene copy and its surrounding chromosomal region on one allele, was detected in a small sub-group of melanoma tumor tissues¹⁷². The same group detected a novel somatic non-sense mutation in exon7 (Q349X) in sporadic melanoma tumor samples¹⁷². A study showed that MEN1 and MLL are recruited to the promoters of BRCA1, RAD51, and RAD51AP1, which are implicated in HR¹⁷³. This complex recruitment necessitates the estrogen receptor 1 and results in increased H3K4me3 transcription, Moreover, ectopic expression of some patient-derived mutants of MEN1 fails to bind to BRCA1 promoters and are unable to perform HR-directed DNA repair¹⁷³. These results highlight the important role of MEN1 in genome integrity of melanoma as well as specific phenotypic outcome in MEN1 mutations. Ectopic overexpression of Menin in melanoma was shown to decrease proliferation, migration and metastasis of melanoma cells through downregulation of protein tyrosine phosphatase (PTN), accompanied by its receptor, and

phosphatidylinositol 3-kinase (pI3K)¹⁷⁴. Moreover, menin overexpression also decreased the phosphorylation of focal adhesion kinase (FAK) and ERK1/2, further highlighting the tumor suppressive role of MEN1 in melanoma¹⁷⁴. A study implicating the comparison of cutaneous manifestations of patients affected by MEN1 with their relatives lacking the mutation revealed a higher prevalence in affected patients than in non-carriers¹⁷⁵. An exome-wide sequencing study on melanoma and two other benign cutaneous lesions, spizoid nevi and conventional nevi, which revealed genetic similarities, including mutations of the MEN1 gene¹⁷⁶. In summary, MEN1 is associated with some cutaneous lesions and could be useful for detecting MEN1 carriers in an affected family.

1.8 Overview of the pancreas

The pancreas is an organ located in the back of the abdomen and has two main roles (Fig 1.6). The first one is the exocrine function, which is responsible for secretion of digestive enzymes and water in the gastrointestinal tract by acinar cells and ions by bicarbonate-secreting ductal cells. These fluids are conveyed through the pancreatic ductal network, which includes centroacinar cells located in the acinus, connecting acinar and ductal cells, as well as an epithelial lining within the branched ductal tubes. Stellate cells are stromal cells that play an important role in the maintenance of the extracellular matrix in the pancreas. The second function of the pancreas is the endocrine function, having an important role in maintaining normal blood glucose level. The hormone-secreting endocrine islets play a crucial role in the regulation of the body's metabolism and are composed of several cell types. Alpha cells boost blood sugar levels by releasing glucagon, while beta cells secrete insulin, lowering blood sugar. Delta cells, on the other hand, release somatostatin to fine-tune the endocrine interplay in the pancreas. The PP cells (Pancreatic Polypeptide cells) release pancreatic polypeptide, which plays a role in regulating appetite and digestion. The pancreatic polypeptide cells are behind appetite control and digestion regulation with their release of pancreatic polypeptide.¹⁷⁷

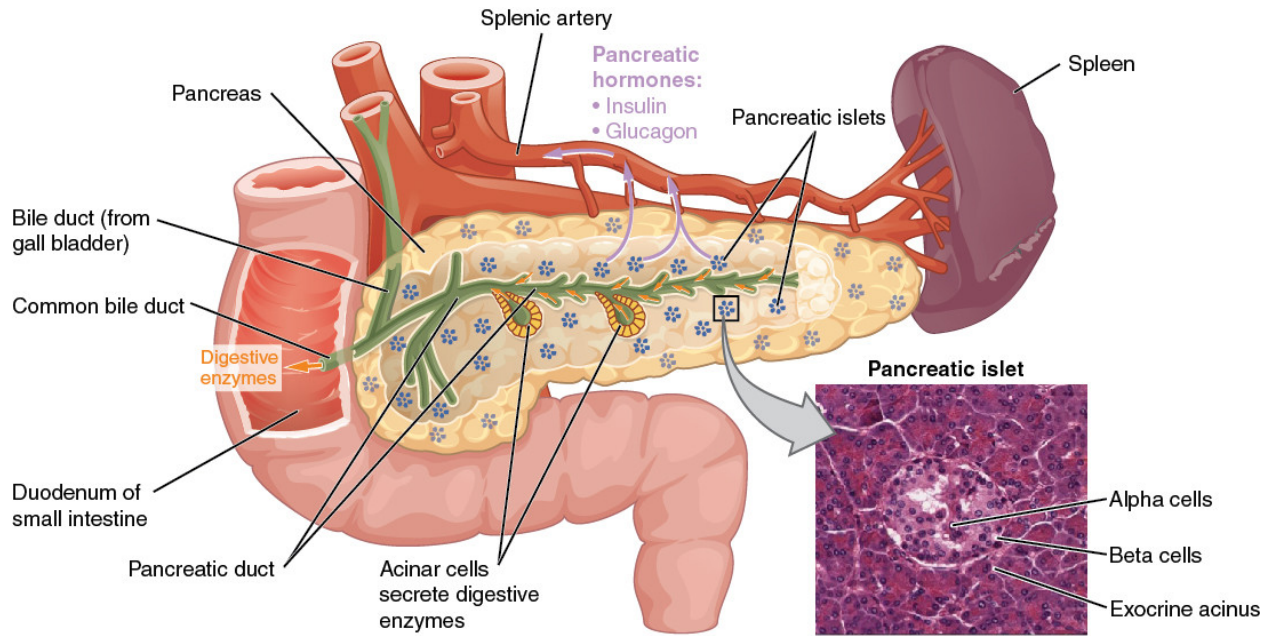


Figure 1.6: Physiology of the pancreas and histology of pancreatic cancer. (Adapted from wiley online library and Kleef *et al.* 2016).¹⁷⁸

1.8.1 Pancreatic Cancer

Pancreatic cancer is the fourth leading cause of cancer death in developed countries and is expected to rise in second rank in within the next decades¹⁷⁹. Several subtypes of pancreatic exist (Fig. 1.7). The poor prognosis of pancreatic cancer is mainly due to late diagnosis since symptoms occurs when the disease is in an advanced stage¹⁷⁸. Pancreatic cancer is known to be aggressive, with neoplastic invasion of nerves, vascular local growth, distant metastases quickly spreading, resistance to conventional chemotherapy, radiotherapy and targeted therapy. Pancreatic cancer occurring in the exocrine gland is the most prevalent (80-90%), which is implicated in secretion of digestive juice. Pancreatic neuroendocrine tumors (NETs), occurring in around 10-15% of pancreatic neoplasms, are from the hormone-producing region, the endocrine gland, including gastrinomas, insulinomas and glucagonomas. Colloid carcinomas represent 2% of all pancreatic cancers and are characterized by the formation of pools of mucin in the stroma. Solid-pseudopapillary pancreatic neoplasms, characterized by poorly cohesive cells, represent merely 2% of all cases in this category. Acinar cell carcinomas, a low-occurring form of pancreatic cancer (1%), are characterized by granular cytoplasm and a single prominent nucleolus rare characterized

by cells. Pancreatoblastomas, which are rarer (0.5%), are characterized by neoplastic cells with acinar differentiation and squamoid nests. Other extremely rare variants exist such as adenosquamous, hepatoid, medullary, signet ring cell and undifferentiated carcinomas (not shown in Fig. 1.7).

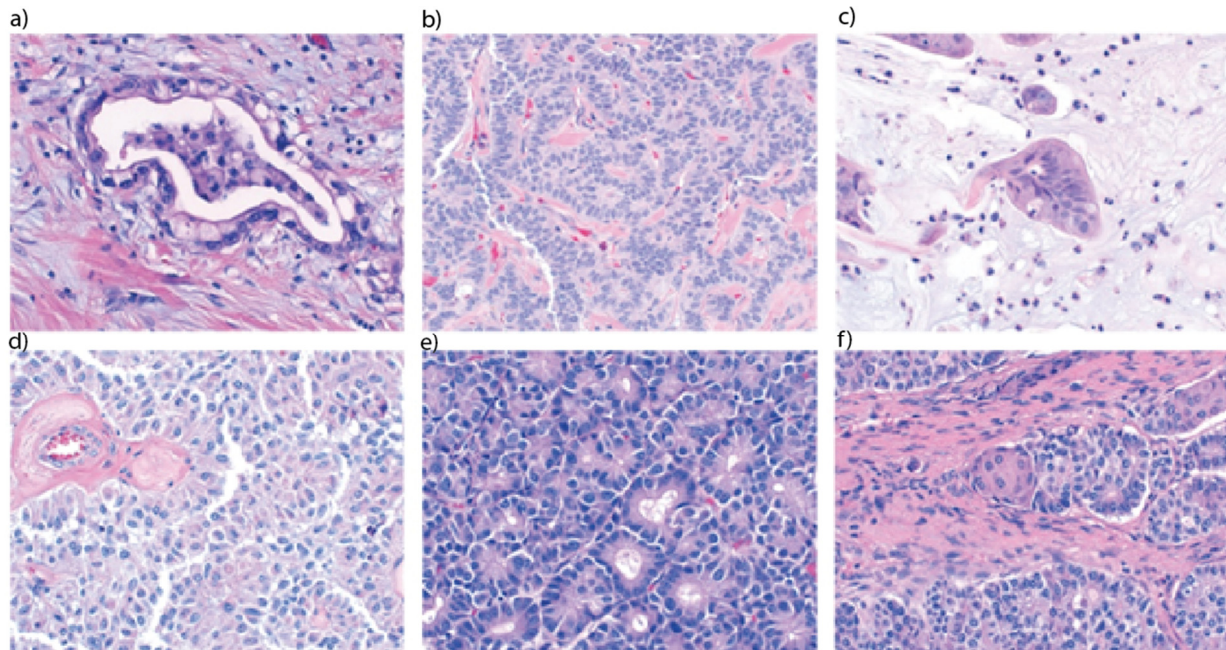


Figure 1.7: Histology of pancreatic cancer different subtypes. (Adapted from Kleef *et al.* 2016)¹⁷⁸

- a) Adenocarcinomas are characterized by atypical neoplastic glands in a dense stroma.
- b) Pancreatic neoplasms are neuroendocrine tumours
- c) Colloid carcinomas
- d) Solid-pseudopapillary tumours
- e) Acinar cell carcinomas
- f) Pancreatoblastomas

1.8.2 Pancreatic Cancer driver mutations

A panoply of genetic alterations is found in pancreatic cancer and implicates many pathways including KRAS, TGF- β , WNT, NOTCH, ROBO/SLIT signaling, G1/S transition, SWI-SNF, chromatin modification, DNA repair and RNA processing (Figure 1.8). Moreover, omics-based approaches enabled the classification of PDAC into 4 subtypes relating with a specific expression profile: squamous, pancreatic progenitor, immunogenic and aberrantly differentiated endocrine

exocrine. All of these subtypes correlate with characteristic histopathological form of PDAC¹⁸⁰. Deep whole- exome sequencing revealed recurrent somatic mutations in KRAS, TP53, CDKN2A, SMAD4, RNF43, ARID1A, TGFβR2, GNAS, RREB1, and PBRM1, among others¹⁸¹. KRAS wild-type tumors harbored alterations in other oncogenic drivers, including GNAS, BRAF, CTNNB1, and additional RAS pathway genes¹⁸¹. Real-time genomic profiling of advanced pancreatic cancer has demonstrated its ability to enhance the decision-making process regarding treatment choices¹⁸².

In figure 1.9, the normal exocrine pancreas cells are represented, transitioning from left to right into increasingly dysplastic PanIN and PDAC. Visible abnormalities including papillary morphology, loss of polarity, nuclear atypia, intraluminal budding, and stromal invasion are shown. PanIN-PDAC progression is associated with increasing accumulation of genetic lesions including activation of KRAS and loss of tumor suppressor genes including CDKN2A, TP53, SMAD4, and BRCA2.

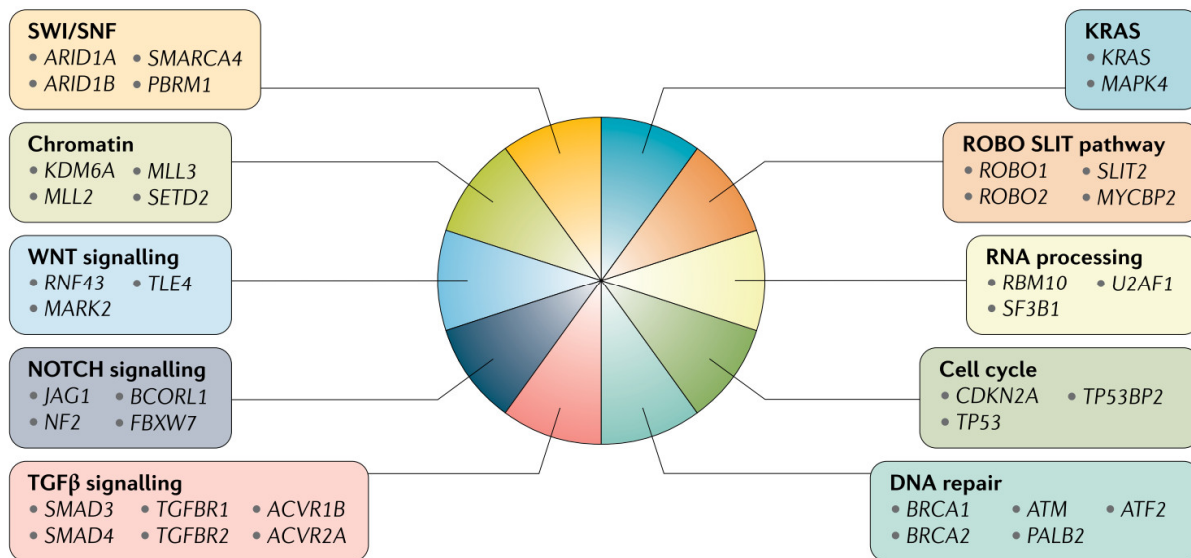


Figure 1.8: Pathways and respective genes mutation burden in pancreatic cancer

(Adapted from Collisson *et al.*, 2019)¹⁸³

1.8.2.1 KRAS

The most prevalent mutation in PDAC is the activation of KRAS, which is present in more than 90% of PDAC tumor samples, confining PDAC as a KRAS-addicted cancer. Indeed, KRAS

mutation is one of the first events happening in the transition of normal pancreatic duct epithelium to advanced stages of noninvasive microscopic ductal lesion, termed as pancreatic intraepithelial neoplasms (PanINs) (Fig 1.9). KRAS is a small GTPase functioning as a ON-OFF molecular switch, cycling between an active state when bound to guanosine triphosphate and inactive guanosine diphosphate-bound state¹⁸⁴. KRAS protein interacts with several effector proteins such as RAFs, activating MEK1/2 kinases that subsequently phosphorylate ERK1/2 and then further phosphorylates nuclear proteins ELK1 and c-JUN. Moreover, KRAS controls the transcription of several genes of mitotic pathways including as PI3K, AKT, mTOR, RAF, MEK/MAPK and have been shown to regulate cancer cell proliferation and survival as well as resistance to chemotherapy¹⁸⁵. The activation of this signaling network results in dysregulation of cellular growth. In cancer, 98% of all KRAS mutations harbor a missense mutation in three mutational hotspots such as Glycine-12 (G12), Glycine-13 (G13) or glutamine-61 (G61). These mutations induce a constitutive GTP-bound active state resulting in overstimulation of mitogenic pathways driving cancer growth¹⁸⁴. KRAS mutations has been long considered as an undruggable target since the affinity of the KRAS GTP-pocket is in the picomolar range while cellular concentration of GTP is around 0.5 μ M. As a result, the competition between the endogenous GTP against a non-covalent small-molecule inhibitor is a foregone conclusion. Recent efforts in targeting the mutation G12C of KRAS with covalent drugs, such as Sotorasib¹⁸⁶ ARS1620¹⁸⁷ and BI-2852¹⁸⁸, showed anticancer activity in clinical trial of solid advanced tumors and led to tumor regression in experimental models. The next challenges towards targeting KRAS will be to find drug resistance mechanisms¹⁸⁹.

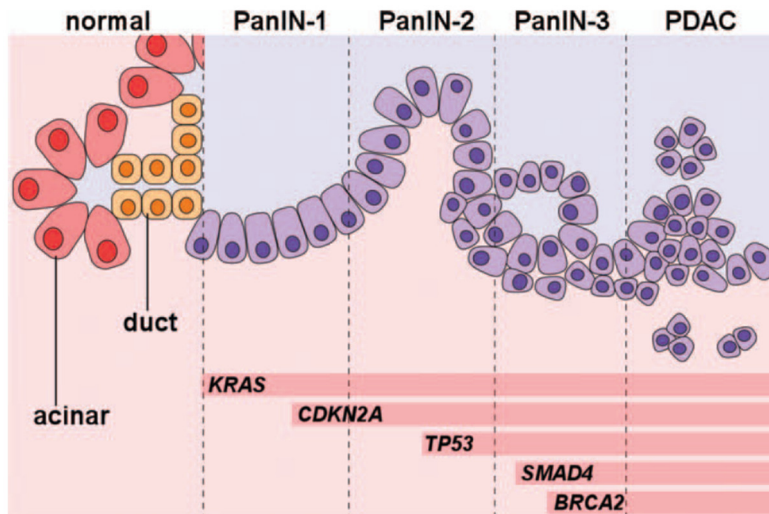


Figure 1.9: Pancreatic cancer progression stages.

1.8.2.2 Other mutations in PDAC

Many other mutations are often found in PDAC. CDKN2A gene, a well-known susceptibility gene for melanoma predisposition, is also mutated at a high rate in PDAC¹⁹⁰. CDKN2A can be inactivated by methylation or homozygous deletion, shutting down its tumor suppressor functions. The tumor suppressor TP53 (also known as p53), activates several genes through transcriptional activation in response to cellular stress such as DNA damage and acts as a ‘guardian of the genome’^{191,192}. TP53 is mutated in 70% of PDAC tumors samples. SMAD4 is also highly mutated in PDAC by homozygous deletion, hindering TGF β tumor suppressive functions, participating in progression of higher grades of paNINs (paNIN-3) (Fig. 1.9)¹⁹³. Another mutation in PDAC is the Ubiquitin E3 ligase ring finger 43 (RNF43), which loss-of-function is found in 5-10% of in PDAC tumours^{178,194}. The role of RNF43 in normal physiological context is to negatively regulate the Wnt/ β -catenin signaling pathway by degrading and internalizing Wnt receptors, including Frizzleds (FZDs) and LRP5/6 at the cell surface, serving as a negative feedback loop. Indeed, inactivation of RNF43, which happens in PDAC, increases the membrane levels of Frizzled receptors, conferring a Wnt-dependency on RNF43 and sustained proliferation¹⁹⁴. Tumors dependent on Wnt signaling for proliferation are sensitive to pharmacological inhibition of Porcupine (PORCN), which has been shown in preclinical models¹⁹⁴ and clinical trials¹⁹⁵.

1.9 Discovery of CRISPR: The rise of CRISPR as the genome-editing technology

CRISPR caught the attention of scientists in the 2010s for its formidable genome editing capacity. The first paper proving its existence was published in 1987, when an unusual repetitive DNA sequence was detected in the locus of *Escherichia coli* genome during the analysis of the gene responsible for isozyme conversion of alkaline phosphatase¹⁹⁶. This system was further discovered in many other types of bacteria^{197,198} and archaea¹⁹⁹. However, the function of this repeated DNA sequence in the genome of bacteria/archaea remained unknown for a decade. In the early 2000s, three independent research team linked the CRISPR system with the immune defense mechanism against bacteriophages²⁰⁰⁻²⁰². They found that these non-repetitive CRISPR spacers are interspaced with repetitive DNA sequences and that a protospacer adjacent motif (PAM), is required for target recognition by Cas9. Indeed, these acquired DNA sequences (spacers) have high homology to viral genes. A major discovery in the CRISPR scientific literature is the discovery of four CRISPR-associated genes (*cas1*, *cas2*, *cas3* and *cas4*), revealed by *in-silico* analysis²⁰³. These *cas* proteins were participating in the mechanism of defense against bacteriophages and plasmids, a system highly similar to RNA interference in eukaryotes²⁰⁴. It was only a year later (in 2007), that CRISPR was defined as an adaptive immune system where an integration of de novo integration of phage DNA in the CRISPR locus allow the bacteria to fight the next wave of attacking phage, a mechanism only requiring Cas9 alone for its function²⁰⁵. More insights about how CRISPR system interfere with invading phages was found where spacer sequences are transcribed into guide RNAs helping Cas9 nuclease to target specific DNA sequence²⁰⁶. It was only two year later that the cleavage pattern was mapped, as Cas9 protein creates double-stranded breaks in target DNA, more precisely 3 nucleotides upstream of the PAM sequence²⁰⁷. The year 2012 was a turning point for the CRISPR scientific community as a major discovery was published in the high impact factor scientific journal *Science*. Emmanuelle Charpentier and Jennifer Doudna co-discovered the sequence-specific and directed genome-editing ability of the CRISPR system²⁰⁸. A pair of RNA structure consisting of a mature CRISPR RNA (crRNA) that is base-paired to trans-activating crRNA (tracrRNA) induce the Cas9 protein to introduce double-stranded breaks in target DNA²⁰⁸. These two women were the first to define the role *in vitro* of the CRISPR/Cas9 system that could both cut viral DNA of bacteriophage and therefore participating in bacteria immunity, and that could be programmed with a guide RNA to cut any DNA at a sequence-specific site. Moreover, they discovered that Cas9 can be guided by a

single chimeric RNA, engineered by the fusion of a tracrRNA and crRNA, therefore called single guide RNA (sgRNA). The impact of this discovery was massive and led to advances in plant and animal engineering, personalized medicine, and promising clinical therapeutics. Both women were awarded with the 2020 Nobel prize of Chemistry. In 2013, Feng Zhang's team successfully adapted the CRISPR/Cas9 system in eukaryote, enabling genome-editing in human cells²⁰⁹, which truly inspired a lot of scientist especially in the field of molecular biology and medicine. In parallel, another research team reported similar findings and was published in the same issue of Science²¹⁰. Moreover, there are two groundbreaking publications showing that CRISPR can be performed in an *in vivo* manner for genome-editing in eukaryotic cells^{211,212}.

1.9.1 The diversity of the CRISPR system

CRISPR-Cas system, which have been worldly validated as an important gene editing tool to study gain/loss-of-function of genes²¹³, function as an adaptive immune defense mechanism to protect phage intrusion in bacteria and archaea in nature. There are many families of CRISPR-Cas systems where each one shows a great diversity of Cas protein sequence, gene composition as well as genomic arrangements. These CRISPR systems are classified according to the structure of Cas genes that are typically adjacent to the CRISPR arrays. In 2015²¹⁴, a total of 2 classes, 5 types and 16 subtypes was discovered. In 2020²¹⁵, the new classification was expanded more than 2 classes, 6 types and 33 subtypes. The Class I system has multi-unit effector modules comprised of many Cas proteins. The class II system distinguishes itself from Class I where single, multidomain crRNA-binding protein combines all functions required for interference. Indeed, the Class II system is preferred because of the advantages of a single-effector protein. Each subdivision of Class II system uses a distinct type of Cas protein. The type II for Cas9 variants and class V for Cas12 variants utilize RNA-guided DNA endonuclease activity and type-VI for Cas13 variants appears to have preferential RNA-targeting and cleavage activity. A recent study²¹⁶ showed for the first time a new RNA-guided DNA endonuclease, Fanzor (Fz), in eukaryotes. The transposon-encoded protein Fz, having a structural similarity to Cas12, has the capacity to be programmed for engineered applications, therefore behaving exactly like Cas9. The diversity of newly identified CRISPR-Cas systems has greatly improved due to the great advances in computational analysis of big data and metagenomics of CRISPR-expressing organisms.

1.9.2 Genome editing with CRISPR, a biotechnology tool

Of all the different Cas proteins, Cas9 enzyme revolutionized the scientific world with its formidable programmable genome-editing capacity²¹⁷. The CRISPR-Cas9 system is composed of an endonuclease protein, the Cas9, whose DNA cutting ability is guided by a sgRNA (Fig. 1.10). Cas9 enzyme has an HNH domain responsible for cleaving the DNA strand complementary to the guide RNA sequence (the target strand) and a RuvC nuclease domain essential for cleaving the noncomplementary strand (the non-target strand). The sequential enzymatic activity of both domains induces double-strand DNA breaks (DSBs)^{218,219}. The sgRNA is comprised of two different parts: The CRISPR RNA (crRNA), a nucleotide sequence of length varying from 17 to 20 base pair complementary to the DNA target and the trans activating RNA (tracrRNA), a binding scaffold for the Cas nuclease. These two key components are joined together artificially by a tetraloop which results in the formation of a chimeric sgRNA. An important part of the sgRNA is the seed sequence, a 10-12 bp sequence having perfect homology with the adjacent site of the PAM sequence of the DNA target sequence. Indeed, the homology is critical for cleavage activity and few mismatches can hinder Cas9 activity²²⁰. In addition to the required seed sequence of the sgRNA, another motif present on the genomic DNA is essential for the sgRNA recognition, the PAM site, serving as a binding signal for the nuclease. However, the PAM site sequence varies according to the origin of the species of the bacteria it has been extracted. For example, the Cas9 from *Streptococcus pyogenes* (Sp) recognizes the NGG PAM-site sequence. CRISPR/Cas9 system can also be used for transcriptional control using dead Cas9^{D10A/H840A} (dCas9) lacking nuclease activity and cannot cleave DNA²¹⁷. When dCas9 is fused to a Krüppel-associated box (KRAB) repressor, the transcription is inhibited. This alternative CRISPR system is known as CRISPR interference (CRISPRi).²²¹ On the other hand, dCas9 can be tethered to transcriptional activators such as VP64 and VP64-p65-Rta to strongly activate transcriptional activity at the promoter.²²¹ This other alternative CRISPR system is known as CRISPR activation (CRISPR_{act}). The dCas9 fused to methylase Tet1 or DNA methyltransferase Dnmt3a enables the editing of DNA methylation. Epigenetic regulation modification such as methylation of targeted gene promoter can result in silencing while demethylation induce gene expression²²².

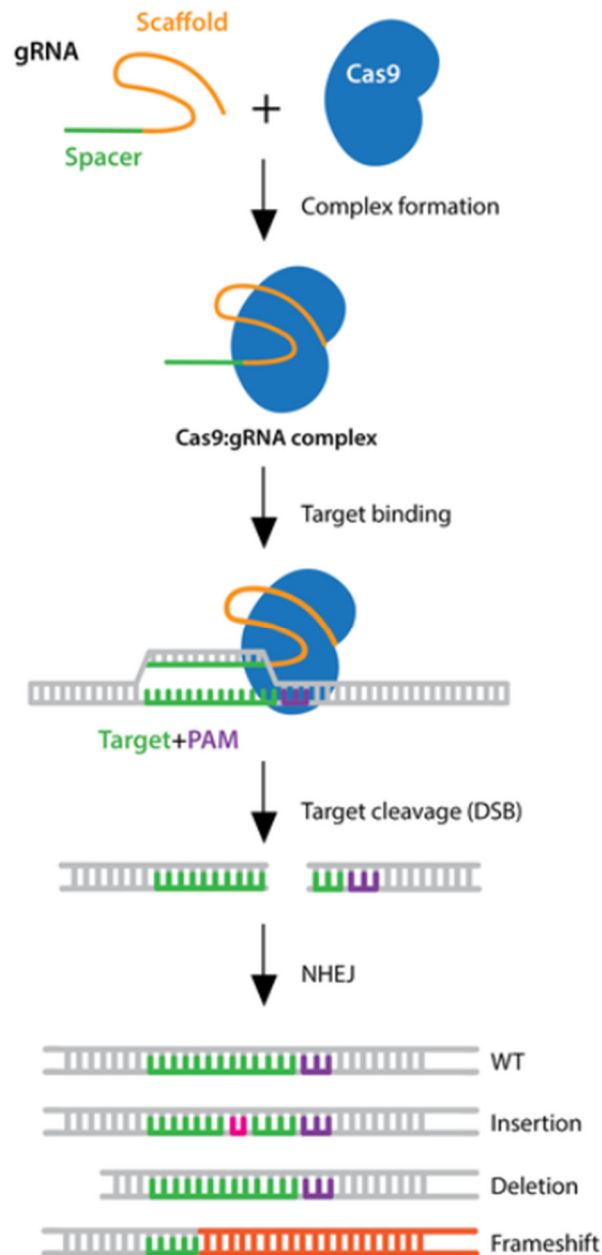


Figure 1.10: CRISPR/Cas9 genome editing mechanism. (Source: Addgene)

1.9.3 DNA repair mechanisms of Cas cleavage

CRISPR-Cas9 initiates double-stranded DNA breaks (DSBs) at DNA target site that are complementary to the sgRNA (Fig. 1.11). This event subsequently activates the DNA repair pathway machinery for genome-editing, therefore creating a variety of DNA repair outcomes²²³. In eukaryotic cells, there are three different mechanisms of DSBs repair: Non-Homologous End-

joining (NHEJ), Homology-directed repair (HDR) and microhomology-mediated end joining (MMEJ) pathways. The NHEJ pathway machinery, including the heterodimer Ku, is the dominant repair pathway when CRISPR-Cas9 cleaves target DNA. NHEJ happens during the cell cycle progression and is known to be error-prone, where small nucleotide insertions and deletions (indels) occur frequently at the cleavage site having DSBs²²⁴. On the other hand, mediation of HR, mostly mediated by BRAC2 and RAD51, has quite high fidelity since DNA donors with homologous sequence are present in the broken spot. However, HR is restricted to undergoing S and G2 phase of the cell cycle, leading to lower frequency of perfect DNA repair upon CRISPR-Cas9 cleavage compared to NHEJ²²⁵. Additionally, it is known that MMEJ, a form of alternative end-joining, uses regions with 5-25 bp of microhomology flanking a DSB to repair DNA. The DNA ends are chewed back to reveal homology, allowing the strands to anneal and DNA polymerases then fill the empty gaps. In the end of this process, there is the retention of a single microhomology sequence and a deletion of the region between the microhomology, the latter participating in creating mutations in the repaired DNA²²⁶.

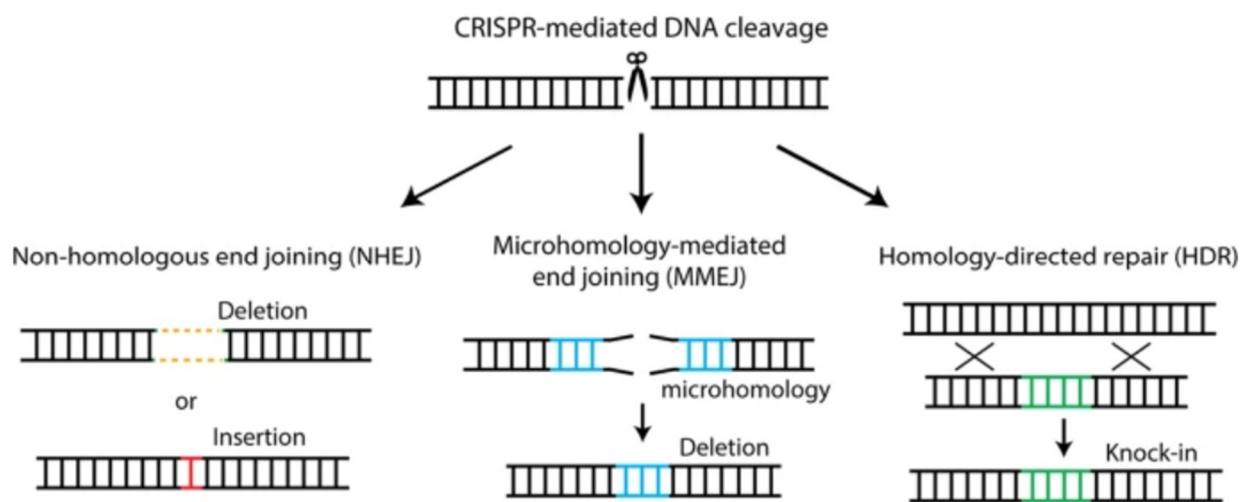


Figure 1.11: DNA repair upon CRISPR/Cas9 cleavage (Adapted from Jang *et al.* 2020)²²⁷

1.9.4 CRISPR off-target effects

The high specificity of the CRISPR system is highly advantageous to target specific locus with the synthesized sgRNA but trade-off with potential off-target effects, namely the deposition of unexpected, unwanted, or even adverse alterations to the genome²²⁸. Indeed, CRISPR systems

evolved as a defense mechanism against viruses having high frequency mutations. As such, a less specific CRISPR system was deemed advantageous for the microorganism's immunity. Even if Cas9 is taught to be strictly guided by the 20-nt sequence of the sgRNA and the adjacent PAM sequence, off-target effect can still happen with three to five base-pair mismatches in the PAM-distal part of the sgRNA sequence²²⁹. A study using genome-wide mapping binding site of catalytically inactive dead-Cas9 (dCas9) emphasized the importance that Cas9 off-target binding sites are enriched at open chromatin regions and that 70% of off-targets are associated with genes²³⁰. Formation of secondary structure and misfolding of sgRNA are likely to induce potential off target effects and can be countered by stabilizing their hairpin structures²³¹. There are many *in silico* tools that can predict off-target sites according to the DNA sequence the sgRNA targets, which are based on data describing the level of sgRNA alignment to the putative off-target sites in the genome or algorithm-based score-model²²⁹. These prediction algorithms of these software mostly rely on sgRNA sequences. For example, one of the algorithms called MIT, weights the position effect of the mismatches between the sgRNA and the targeted DNA and generates a nominal score between 0 and 100 of off-target assessment²³². Also, it is known that Cas9 can cause sgRNA-independent cleavages²²⁸.

1.9.5 Design of sgRNA for genome-editing

Indeed, several tools calculate the off-target efficacy of sgRNA, and others have a bigger focus on the 'on target' activity of the sgRNA. As such, a good sgRNA design relies on the maximal On-target activity and minimal Off-target activity of the Cas9 nuclease. There is an increasing number of computational tools and resources for efficient sgRNA design, therefore maximizing its efficiency and specificity²³³. Big advances in empirical scoring algorithms and machine-learning modeling greatly facilitated researchers to design their sgRNAs used to target and alternate their genes of interest. There are several accessible web-based tools for sgRNA design which are listed in this review²³³.

1.9.6 Alternative CRISPR technologies

In addition to the wild-type nuclease activity of Cas9 enzyme, there are three other types of genome-editing technologies serving to convert a targeted DNA sequence into a new desired sequence: Base editors, transposases/recombinases, and prime editors (Fig. 1.12). While the Cas9

introduces stochastic and heterogenous indels mutations, the base-editors agents install PAM-proximal transition points mutations without the required DSBs or donor DNA templates. Current base-editors contain a bio-engineered Cas9 lacking nuclease activity and is fused to a deaminase enzyme such as cytosine editors, creating the transition mutations C•G to A•T, or adenosine editors, converting A•T to G•C base pair. Interestingly, these two types of base conversion represent around 30% of all human pathogenic variants²³⁴.

Another important partner of the CRISPR system, CRISPR prime editors, possesses the ability to introduce all 12 DNA base-pair combination swaps, consisting of the 4 transition mutations and 8 transversion mutations. Moreover, CRISPR prime editors can perform small insertions and deletion in a precise and targeted manner. The prime editor was created by engineering an impaired Cas9 nuclease fused to a reverse transcriptase. Then, the prime editor is programmed with a prime editing guide RNA (pegRNA) having a dual function that direct the target site and encodes the desired sequence²³⁵. This technology, with high capabilities of genome editing, could correct up to 89% known genetic variants that are associated with human diseases^{234,235}.

The last class is the CRISPR-associated transposons (CASTs), mediating rearrangements of large segments of DNA. CASTs combine transposon machinery, including Tn7-like variants, with an artificial Cargo-DNA to be integrated in the genome by the RNA-guided CRISPR-Cas system. The left-end and right-end motifs flanking the Cargo-DNA of the transposon are recognized by the transposon machinery, which activates the excision of the Cargo-DNA from the donor locus into the host DNA. The main advantage of this technology is that cells are not restricted to the host low-efficacy HDR repair and are therefore not limited to division and mitosis during the genome-editing process. However, this system is restricted to bacteria and incidence of random integration events can still happen²³⁶.

Another alternative genome editing tool is Cas12a, previously known as Cpf1²³⁷, is another protein of the type V-A CRISPR family than can be used for genome-editing purposes by cleaving DNA via a staggered (sticky-end) DNA double-stranded cut²³⁸. Another important effector is the Cas12b, formerly known as C2c1²³⁹, which is in the type V-B CRISPR family. DNA interference by Cas12b is mediated through 5'-PAM site binding, which is located in the direct-repeat region targeted by the crRNA, in a similar fashion to Cpf1. However, unlike Cpf1, which relies on a single crRNA for efficient nuclease activity, C2c1 needs both crRNA and tracrRNA to cleave DNA²³⁹. Another effector of the Cas protein family have the unique capacity of targeting RNA as

a single effector, Cas13, formerly known as C2c2²⁴⁰. Cas13, included in the type VI CRISPR effector family, has an RNA-guided system like Cas9 or Cas12, but uniquely cleaves RNA instead of DNA. A Cas13 recombinant variant from the *Leptotrichia wadei* bacteria (LwaCas13a) expressed in mammalian or plant cells was shown to have guided RNase activity with a similar efficiency and specificity as the shRNAs from the RNAi system²⁴¹. Moreover, an engineered Cas13 ortholog lacking nuclease activity (dCas13) was shown to be able to edit RNA in a guided-manner when fused with ADA12, which can direct the hydrolytic deamination of adenosine-to-inosine²⁴².

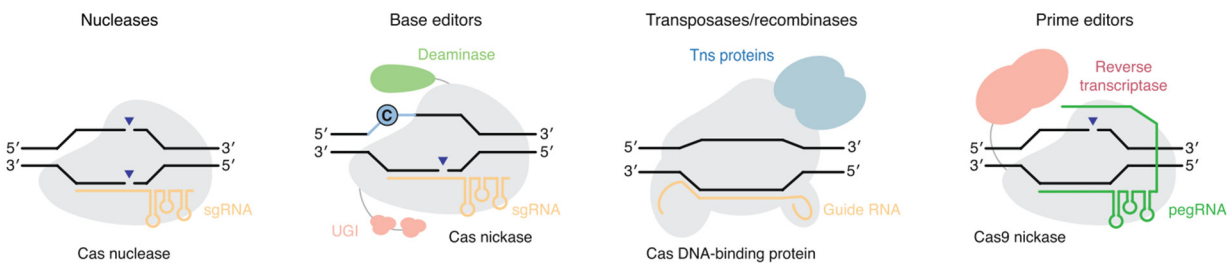


Figure 1.12: Schematic representation of genome editing strategies and agents for CRISPR-based genome editing (Adapted from Anzalone *et al.*)²⁴³

1.9.7 CRISPR/Cas editing strategy

Several factors need to be examined for a proper experimental design in a study utilizing genome-editing. First, the cell type needs to be considered, where bacteria, yeast, mammalian cancer cells or terminally differentiated cells, can be modified by genome-editing. Another factor is the microenvironment, where the selected organism will be investigated. Cells cultures *in vitro* or transplanted *in vivo* or 3D models including organoids will impose different constraints for proper delivery of CRISPR/Cas machinery. The nature of the agent of the CRISPR/Cas machinery (plasmid DNA, ribonucleoprotein complex, mRNA or viral vector) and the delivery method (lipofection, electroporation, nucleofection or viral infection) are primordial in the design of a study, where each of them will have different desired/undesired outcomes (Fig. 1.13). For example, plasmid delivery by viral infection or nucleofection can cause potential problems including insertional mutagenesis since the plasmid is integrated in the host DNA and sustained Cas9 expression, where chances of off targets are increased. Delivery by viral infection can elicit immunologic responses by viral proteins expressed in the viral vectors. These potential problems can be overcome by transfecting the mRNA of Cas9 directly in the host, offering a transient

expression of Cas9 since mRNA is unstable. The recombinant Cas9 protein of bacterial origin can also be delivered in cells, which is the most transient delivery method, but increases the complexity and the price of the experiment. Plasmid integration by either nucleofection or viral delivery have the slowest onset of genome editing because transcription and translation are needed for Cas9 expression in the desired organism. On the other hand, it is the most cost-effective option where basic laboratory techniques are used such as plasmid preparation from bacteria extracts and transfection in HEK293 virus-producing cancer cells. Another advantage of viral or plasmid delivery is the sustained expression of Cas9 and sgRNAs. In the end, each editing strategy will require rigorous optimization to improve the efficiency of genome-editing in cells.^{244,245}

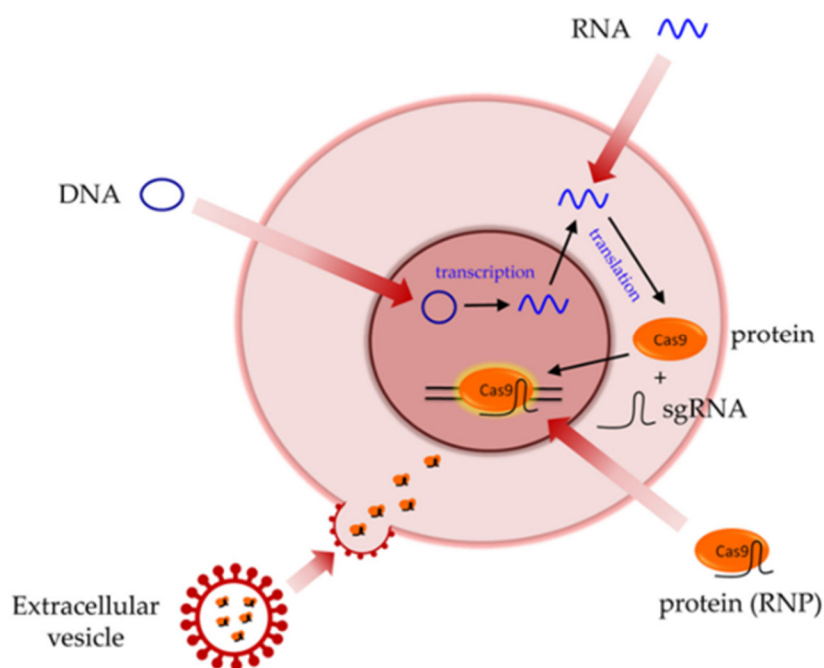


Figure 1.13: Strategies for CRISPR/Cas delivery (Adapted from Yip, 2020)²⁴⁴

1.9.8 CRISPR in cancer research

With the help of data from all levels of biology including genomics, transcriptomic and proteomics among others, the utilization of CRISPR to produce specific mutations can help to recreate cancer-linked events to understand their contribution at each stage of carcinogenesis²⁴⁶. Indeed, a systematic approach to investigate the function of individual genes in experimental cancer models could assess their impact on tumor growth, metastasis and other cancer-related processes^{246,247}. New experimental models can be created more rapidly and efficiently by introducing allele-

specific mutations (homozygous, biallelic, heterozygous or chimeric) by using CRISPR in cancer cell lines, organoids or animal models²⁴⁸. Moreover, establishment of models having genetic mutations associated with hereditary cancer syndromes, such as the MEN1 syndrome^{147,249,250}, by using CRISPR-mediated genome engineering could help in early detection and prevention of cancer in individuals with a high genetic risk²⁵¹.

1.9.9 CRISPR screening in cancer research

The most substantial contribution CRISPR had on cancer research reside in its application in genetic screens^{252–254}. CRISPR screening, a powerful tool for biological discovery, enables the unbiased investigation of a gene function in defined experimental conditions. The screening process is often made in two different formats, either in arrayed or pooled condition (Fig. 1.14)²⁵⁵. CRISPR screens can also be performed *in vitro* or *in vivo*, the latter through direct or indirect delivery of the CRISPR library (Fig. 1.15).

1.9.9.1 Pooled and arrayed CRISPR screens

Pooled CRISPR screening utilizes libraries consisting of thousands of individual plasmids pooled together. In the library, different sgRNAs can target each selected gene, which can result in knock-out, activation or inhibition according to the used CRISPR technology. Libraries can target the whole genome or a partial set of genes such as the nucleome, metabolome, kinome, non-coding regions, pathway-related genes, etc. Moreover, these CRISPR libraries can be custom-made to meet other specific research questions. Delivery of the library by plasmid transfection or viral transduction in the studied cell model will result in a mix of pooled mutants. These mutants will go through a selective pressure, which can be cell proliferation, drug treatment or viral infection among other biological challenges. Phenotypic responses will end in increased resistance or sensitivity of the tested perturbation. After the screening process, the sgRNAs amount of both control and experimental samples are mapped and counted by high-throughput sequencing and subsequent bioinformatic analysis. The depletion of sgRNA count identifies genes whose CRISPR-induced disruption sensitized cells to the perturbation as opposed to sgRNA enrichment which results in increased resistance to the selective pressure²⁵⁵. Indeed, CRISPR screening enabled the discovery genes implicated in drug resistance/sensitivity²⁵⁶, synthetic lethal interactions²⁵⁷, immunotherapy targets such as PD-L1²⁵⁸ and essential genes²⁵⁹. CRISPR screen

can be made with different Cas protein such as Cas12²⁶⁰ and Cas13²⁶¹. One study exploited this experimental setup by combining both Cas9 and Cas12 to optimize the screening process²⁶².

1.9.9.2 Arrayed CRISPR screens

The arrayed CRISPR screening utilized separated samples processed in parallel through separate compartments. Arrayed screenings have the disadvantage of being limited in capacity, more labor-intensive and costly than pooled screenings. However, arrayed screens can provide user-friendly read-outs, including imaging, proteomics and metabolic profiling, which are less expensive than next-generation sequencing.

1.9.9.3 High content CRISPR screens

Many other types of CRISPR screening involve higher content read-outs, such as fluorescence-activated cell sorting (FACS). FACS-based screening involves cells of interest sorting, bypassing the need for a selective survival process. Indeed, cells are marked through a pathway reporter, a cell-permeable dye or by an antibody targeting a specific protein or peptide of interest²⁶³. Another type of CRISPR screening is by single cell RNA sequencing, enabling the simultaneous profiling of the perturbation and the corresponding transcriptomic profile in single cells²⁶⁴. Many subtypes exist such as Perturb-seq²⁶⁵, CRISP-seq²⁶⁴ and CROP-seq²⁶⁶ which involve simultaneous measurement of gene expression combining both RNA and DNA sequencing. Mosaic-seq²⁶⁷, more complex, uses a barcoding system joining the transcriptomic profile with its sgRNA modulator, which quantifies the effects of dCas9-KRAB-mediated enhancer repression in single-cells.

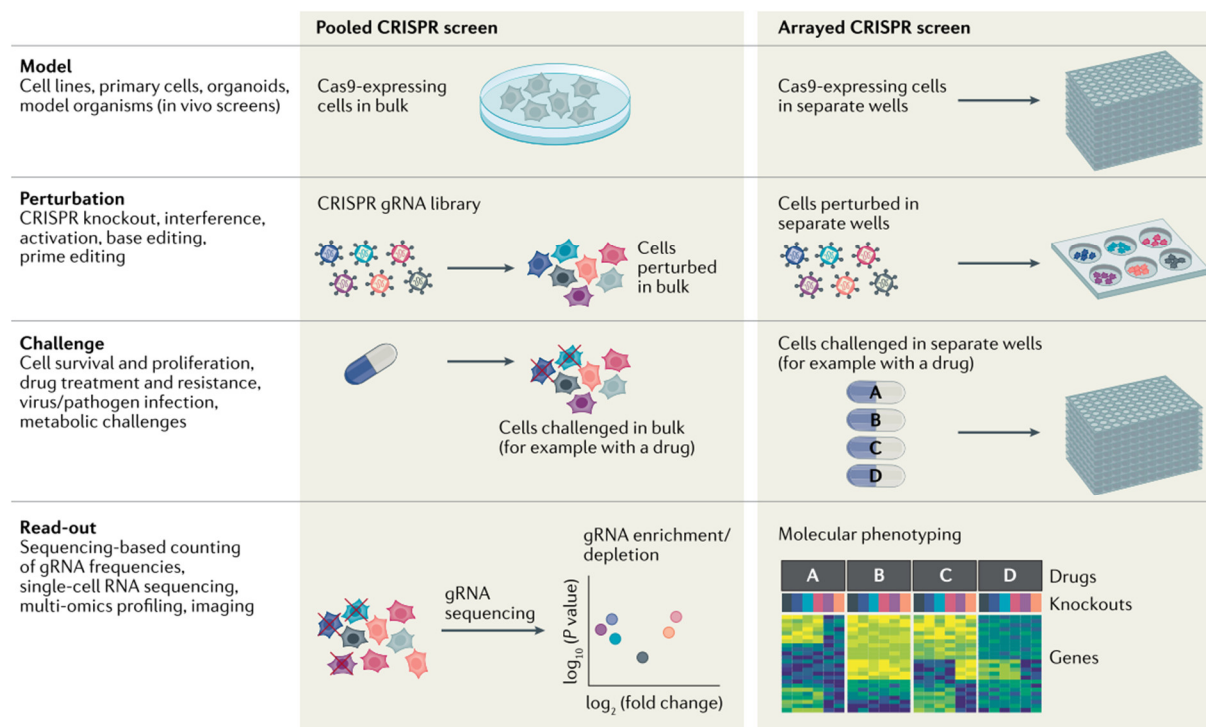


Figure 1.14: Parameters of CRISPR screening. (Adapted from Bock *et al.*, Nature Reviews Methods Primers, 2022²⁵⁵)

1.9.9.4 In vivo CRISPR screening

CRISPR-Cas9 screens conducted in an *in vivo* setting have shown to better recapitulate tumor biology by incorporating the complex microenvironment, extracellular matrix, vascularization as well as autocrine, paracrine and endocrine signaling^{268,269}. Furthermore, these screens have proven to be valuable for the discovery of genes implicated in tumorigenesis and metastasis²⁶⁸. CRISPR screens performed *in vivo* through xenotransplantation (Fig. 1.15) have the same statistical needs such as low M.O.I. to ensure one mutation at a time is performed in each individual cells as well as sufficient cell coverage of the library to ensure each element is represented sufficiently. Scaling-up the coverage is needed particularly when large-scale libraries like genome-wide ones are being used, which necessitates a significantly higher number of cells and mice. Otherwise, the library size will need to be adjusted. Moreover, high cell engraftment in tumors and cell expansion capacity are crucial factors for the choice of experimental model for an *in vivo* CRISPR screening. Another type of *in vivo* CRISPR screening is available, where the library is delivered directly in the animal through lentiviral or adenoviral transduction through intravenous, intracranial or

intratracheal viral injections (Fig. 1.15). As such, animal organs can be directly targeted by the library.

The first published CRISPR-Cas9 knock-out (CRISPR_{ko}) screening was performed in a non-metastatic cell line in which a genome-wide sgRNA library was introduced by viral transfection²⁷⁰. Following subcutaneous transplantation of the CRISPR library-mutagenized cells in mice, tumors were allowed to grow and metastasis in the lung were monitored. The following collection, sequencing and sRNAs statistical analysis from the lung metastases samples enabled the identification, followed by a validation, of several genes in which loss-of-function drove lung metastasis. Several CRISPR screens performed in mice helped the identification of tumor suppressors^{271–274}, oncogenes^{275–277}, pro-metastatic factors²⁷⁸, synthetically lethal genes²⁷⁹ and regulators of cancer immune response and immunotherapy^{280–285}. Moreover, a CRISPR screening performed by our own lab revealed the oncogenic mTOR and tumor-suppressive Hippo signaling pathways as central regulators of tumorigenesis in Triple-negative breast cancer (TNBC)²⁸⁶. We showed that a combinatorial pharmacological inhibition of both mTORC1/2 and oncoprotein YAP efficiently reduced tumorigenesis in TNBC in a synergistic manner. A recent CRISPR screening from our research group enabled the identification of a subset of genes implicated in stemness and paclitaxel resistance of TNBC²⁸⁷.

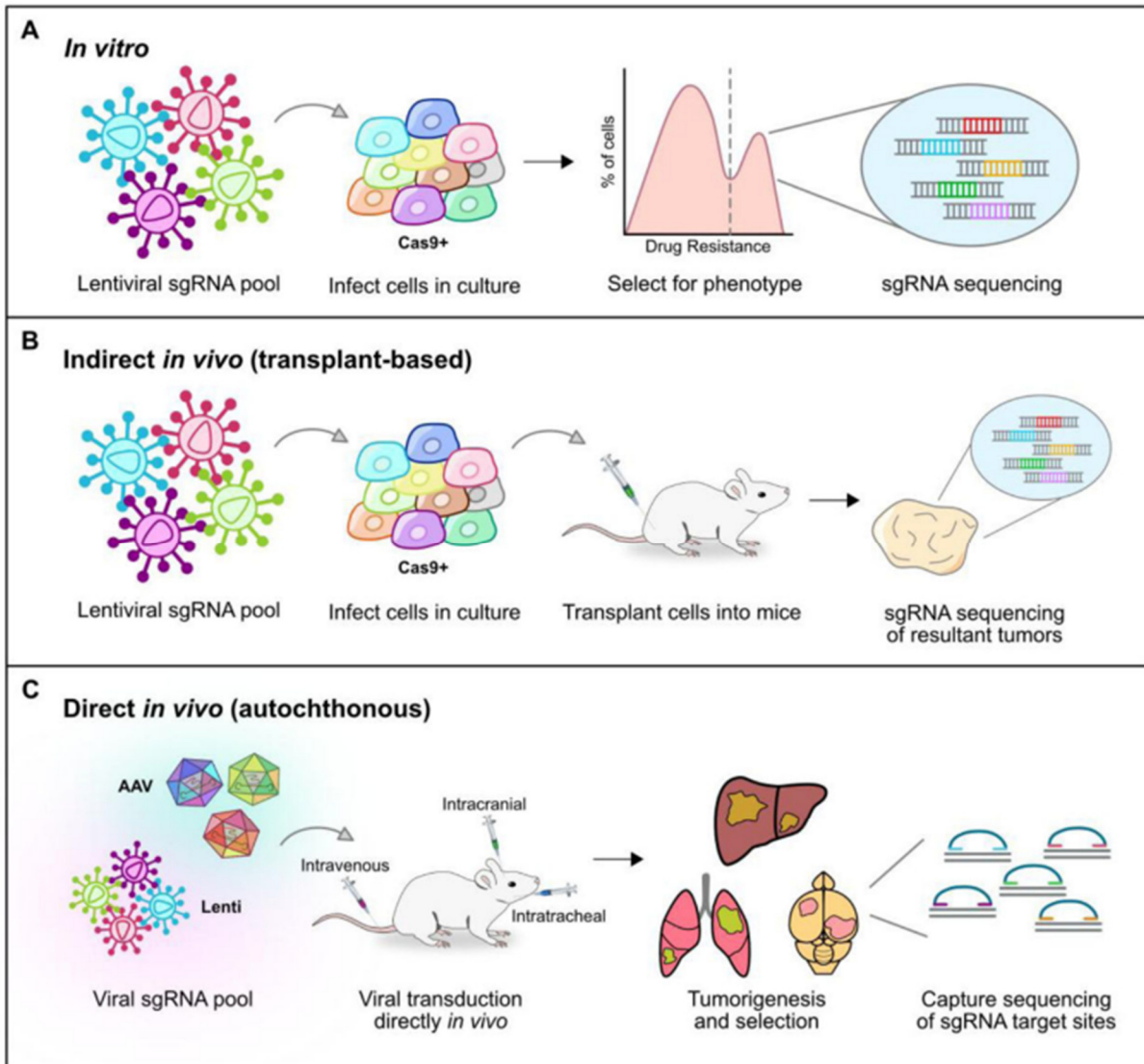


Figure 1.15 Schematic illustration of three distinct modes of CRISPR screening.

(A) CRISPR screening performed *in vitro* (B) CRISPR screen performed *in vivo* through xenotransplantation (indirect) (C) CRISPR screen performed *in vivo* through viral transduction in an animal (direct). (Adapted from Chow et al., Trends in Cancer, 2018)²⁶⁸

1.9.9.5 Large-scale CRISPR screening

The Cancer Dependency Map (DepMap) is a collaboration between the Broad Institute (Project Achilles) and the Wellcome Sanger Institute (Project Score) where 1000 pan-cancer genome-wide CRISPR_{ko} viability screens were performed in 900 cancer cell lines to identify key genomic alterations implicated in cancer to find unique vulnerabilities, termed as dependencies^{259,288–290}.

Such screening effort facilitated the discovery of more than 2103 common-essential genes, demonstrating fitness across multiple cancer types²⁹¹. The DepMap initiative is an ongoing project as new data is released every yearly quartile. The 23Q2 dataset, released at the beginning of 2023, includes an astonishing number of 1864 screened cell lines. A co-jointed published study from both groups found that batch effects, termed as systematic variations or statistical biases not related to the study variable, are driven by two specific parameters: the reagent library and the assay length²⁹². These results indicate a high reproducibility of the thousand conducted CRISPR-Cas9 screens from both institutes²⁹¹. By combining these massive integrated datasets, a better comprehension of heterogeneous cancer types will serve as a basis for precision medicine with novel biomarkers for better patient stratification.

1.10 Heat shock proteins, Heat Shock response, Heat Shock factors and HSPE1 (Hsp10)

In chapter 4, a heat shock protein (HSP) what characterized, namely HSPE1 (Hsp10), which is included in this family of proteins that functions in response to cellular stresses, such as changes in temperatures, exposure to UV light, anoxia, hypoxia, heavy metals, drugs, tissue remodeling and wound healing or any chemical agents where exposure induces stress or protein denaturation. HSPs belong to the molecular chaperone's family, predisposed to participate in protein folding and maintenance of native protein structure. HSPs have a crucial role in protection of cell integrity in normal physiological condition. Proteins need specific three-dimensional configuration to perform their intended biological role, which is maintained by proper folding²⁹³. Molecular chaperones exist in all cellular compartment where they assist ribosomal translation of nascent polypeptide and work thorough prevention of misfolded structure in both normal and stress conditions in an ATP-dependent manner²⁹⁴. Indeed, high temperature can cause protein denaturation and aggregation. Under cellular stress, HSPs expression is upregulated, termed as heat shock response (HSR)²⁹⁵. The transcriptional upregulation is triggered by the heat-shock factors (HSF) consisting of four members, HSF1, HSF2, HSF3 and HSF4²⁹⁶. A critical regulator in HSR is HSF1 protein, where it becomes trimerized and phosphorylated then binds to the Heat Shock Element (HSE) on DNA to initiate the transcriptional machinery²⁹⁷. This molecular response participates in the combat of the negative effects of the cellular stress, such as protein aggregation induced by heat stress, and majorly preventing wrongful conformation of protein and their degradation.

1.10.1 HSPs classification

HSPs are classified according to their molecular weight in kilodalton (kDa) in several subgroups. Small-sized HSPs are HSP27, HSP40, HSP60, HSP70, HSP90 and large-sized HSP are HSP110 and HSP170²⁹⁸. All HSPs below 43 kDa are ATP-independent, whereas their function is majorly by binding to other partners to form functional multi-protein complexes²⁹⁹. HSP60 and HSP10 proteins belongs to a subfamily called the chaperonins, which is subdivided into two classes, class I and II³⁰⁰. The Hsp60 (also called HSPD1) and Hsp10 (also called HSPE1), are both encoded by their respective genes, HSPD and HPSE³⁰¹. HSP60 is included in the type I chaperonin family, which need a co-chaperone (HSP10) acting as a lid the central folding chamber structure³⁰². The type II chaperonin family includes a sole member (TRiC/CCT) found in eukaryotic cytosol and *Archaeobacteria*. Even though HSPs are classified according to their molecular weight, they can have similar role in cancer such as preventing apoptosis^{303,304} and conferring drug resistance³⁰⁵.

1.10.2 HSFs and HSPs in cancer

Depletion of HSF1 in mice counteracts tumorigenesis and cancer progression³⁰⁶. Additionally, elevated levels of HSF1 have been detected in several cancers such as breast and prostate cancer³⁰⁶. Genetic depletion of HSF1 using RNA interference showed a significant reduction in the fitness of cancer cell lines³⁰⁷. HSF1 acts as a protector from oncogene such as *RAS* and *p53*. Despite the HSF1-dependent stress response which evolved to enhance lifespan and survival in a cellular context by protecting disease process such as ischemic injury and neuro-degeneration, theses broadly recognized effect contrast dramatically in the context of cancer³⁰⁷. HSPs can play an important role in proliferation, differentiation, and cancer³⁰³. In fact, many HSP are overexpressed in cancer and are associated with poor outcomes³⁰⁸. In preclinical models of murine, overexpression of HSPs such as HSP27, HSP60, HSP70 and HSP90, increases tumor growth, metastatic dissemination, and resistance to chemotherapy.

1.10.3 HSP60 and HSP10

The tetradecameric Hsp60 protein functions in partnership of his heptameric co-chaperone Hsp10 by forming a ring-complex that catalyze protein folding through the capture of unfolded and misfolded polypeptides in the mitochondria³⁰⁹. The confinement of the polypeptide in the central

cavity of Hsp60/Hsp10 complex is driven by the catalytic activity of Hsp60 using ATP hydrolysis³⁰⁹. GroEL, the bacterial homolog of Hsp60, served as a structural model to understand the mechanism of action of class I chaperonin family. Indeed, high conservation between bacterial and eukaryotic chaperonins such as GroEL/Hsp60 provided an excellent model system to understand their functions³¹⁰. Hsp60 consists of two stacks of 7-fold symmetric rings. The co-chaperone Hsp10, called GroES in *E. coli*, binds to GroEL and acts as a 'lid' to expand the size of the folding chamber therefore preventing substrate withdrawal. Hsp60 and Hsp10 bind together via a dependent-association mechanism. Temperature-sensitive lethal Hsp10 mutants were cloned and tested in yeast which enable the mapping of a functional internal loop, crucial for binding with Hsp60³¹¹. Also, the prevention of the interaction hindered the intramitochondrial sorting of the Rieske Fe/S protein, a known substrate of the Hsp60/Hsp10 complex³¹¹. HSP60 is principally localized within the mitochondria and interacts with numerous proteins other than HSP10, including mortalin (HSPA9), survivin and p53 regulating apoptosis³¹². Moreover, HSP60 can also be found in the cytosol, where it plays different roles, such as protein trafficking and in cellular signaling promoting pro-survival or pro-apoptotic pathways. HSP60 can be found on the cell surface or released in the extracellular space interacting with the immune system³¹³. A recent study showed that HSP10 can induce the proteolytic inactivation of OPA1, a dynamin-related GTPase fusing mitochondrial membranes, independently of HSP60³¹⁴. The inactivation of OPA1 was mediated by a stress-activated metalloprotease, OMA1. The protease OMA1 is known to be a central regulator of cell survival and cell death through mitochondrial stability maintenance³¹⁵. Also, the stress-induced activation of OMA1 to mitochondrial fragmentation, which segregates and remove damaged mitochondria by mitophagy³¹⁶.

1.11 Rationale and objectives

Aggressive cancers such as melanoma and PDAC are often diagnosed at advanced stages and metastasize to distant organs, leading to poor prognosis. Melanoma and PDAC are associated with resistance to most common therapies used to treat patients. Thus, there is an urge to find more specific targeted therapies to increase overall survival of patients. My objectives in my thesis projects were to study a pathway (TGF β), a single gene (MEN1), in melanoma, and the whole genome, in PDAC to better understand cancer cell growth and tumorigenesis. Indeed, these

aggressive cancers were studied by using several techniques to modify gene expression such as CRISPR technology among others.

Aim1:

We previously showed that in melanoma, TGF β has a tumor suppressive role *in vitro*⁸². We recently showed that TGF β plays a central role in breast cancer stem cells, which are proposed as key players in tumorigenesis and cancer progressive. One objective of this thesis is to assess the role of TGF β in melanoma stemness, tumorigenesis and metastasis. Thus, we hypothesized that TGF β could play a negative role in melanoma self-renewal, which could be linked with tumorigenic and metastatic potential, as opposed to breast cancer.

Aim 2:

Previously, we showed that inactivation of *MEN1* can inhibit TGF β signaling mediated by SMAD3, implicating a mechanism of tumor suppression in endocrine tumors of parathyroids, pancreatic islets, and anterior pituitary³¹⁷. These findings led to the second objective of this thesis, which is to evaluate the impact of MEN1 loss-of-function or inactivation in melanoma. We hypothesized that MEN1 inactivation could increase the tumorigenic potential of melanoma cells.

Aim 3:

CRISPR screening are powerful tools to find genes implicated in cancer such as oncogene and tumor suppressors. We recently showed that a CRISPR screening in triple-negative breast cancer model uncovered an intricate interplay between oncogenic and tumor suppressor pathways, highlighting essential roles of the mTOR and Hippo pathways in TNBC regulation. Therefore, our third objective was to find genes or pathway underlying PDAC tumorigenesis. We hypothesized that genome wide CRISPR screening is an efficient tool to find potential candidates driving PDAC formation.

Chapter 2

Transforming growth factor- β /Smad signaling inhibits melanoma cancer stem cell self-renewal, tumor formation and metastasis

Julien Boudreault, Ni Wang, Mostafa Ghozlan, Jean-Jacques Lebrun

Department of Medicine, McGill University Health Center, Cancer Research Program, Montreal, QC, Canada.

2.1 Preface:

Melanoma cancer stem cells are associated with higher tumor-initiating capacity, metastatic potential and resistance to therapies. These cell types express specific cell surface receptors, and their overexpression is linked to elevated tumorigenicity and metastasis. However, the tumor suppressive role of TGF β is not well understood in melanoma. In this chapter, we thus investigated the role of TGF β in melanoma stemness to better understand its role in tumorigenesis and metastasis.

2.2 Abstract:

The secreted protein transforming Growth Factor-beta (TGF β) plays essential roles, ranging from cell growth regulation and cell differentiation in both normal and cancer cells. In melanoma, TGF β acts as a potent tumor suppressor in melanoma by blocking cell cycle progression and inducing apoptosis. In the present study, we found TGF β to regulate cancer stemness in melanoma through the Smad signaling pathway. We discovered that TGF β /Smad signaling inhibits melanosphere formation in multiple melanoma cell lines and reduces expression of the CD133+ cancer stem cell sub-population in a Smad3-dependent manner. Using preclinical models of melanoma, we further showed that preventing Smad3/4 signaling, by means of CRISPR knockouts, promoted both tumorigenesis and lung metastasis in vivo. Collectively, our results define new functions for the TGF β /Smad signaling axis in melanoma stem-cell maintenance and open avenues for new therapeutic approaches to this disease. Keywords: TGF β , Melanoma Stem Cells, Tumor Formation, metastasis

2.3 Introduction:

Melanoma is a malignant tumor of melanocytes which typically arises from the skin. Despite recent progress in targeted therapies, melanoma has the highest death tolls among all skin cancer types³¹⁸. Patients diagnosed with early stage melanoma (I-III) can have their skin tumors removed surgically with high success³¹⁹. However, high plasticity and metastatic capacity in later stages (IV) of aggressive melanoma is linked with poor prognosis³¹. A major challenge in the treatment of melanoma originates from the multiple levels of heterogeneity of this disease³²⁰.

Multiple mutations in the BRAF, NRAS, NF1, PTEN, KIT, TP53 and hTERT genes have been reported in melanoma³²¹. Several other signalling pathways are also often mutated in cutaneous melanoma, including PI3K/AKT³²², Wnt³²³, NF- κ B³²⁴, Jnk³²⁵, JAK/STAT³²⁶ and TGF β ³²⁷. In particular, previous work from our laboratory and others revealed that TGF β act as a strong tumor suppressor and inhibit cell growth, migration and invasion in melanoma^{80,82, 81}. TGF β signalling pathway is activated through ligand binding on its membrane receptors, triggering their serine-threonine protein kinase activity. The subsequent recruitment and phosphorylation of TGF β central downstream effectors, Smads then initiate the signal transduction cascade. Smads act as transcription factors and regulate expression of the multiple TGF β target genes regulating its tumor suppressive effects, including inhibition of cell proliferation, induction of apoptosis and suppression of cell immortalization^{32,328}.

Tumors possess a hierarchical organization of cells and contain stem-like cells, which are responsible for sustaining tumor growth^{329,330}. These cancer stem cells (CSCs) represent a rare sub-population of the bulk of the tumor that possess self-renewal capacities and exhibit high resistance to conventional treatments. Such plastic and resilient cells have propagating functions that are essential for primary tumor growth and metastasis dissemination³³¹. The embryonic origin of melanocytes, from which melanoma arises, comes from the neural crest stem cell³³². Comparable to other types of CSCs, melanoma CSCs can initiate new tumors and regenerate the heterogeneous cancer cell populations of the bulk of the tumor¹²⁵. Several cell-surface markers have been linked to melanoma CSC self-renewal capacity, including ABCG2³³³, ABCB5³³⁴, ALDH^{335,336}, CD133³³³, CD20¹²⁵, CD166³³⁷, CD271³³⁸ and Nestin³³⁷. CSCs reside and interact with the surrounding microenvironment, called the 'niche', via secreted factors and molecular signals maintaining their sustainability and maintenance³³⁹. One of such factors, TGF β has been linked with the regulation of cancer stem-cell maintenance in different types of cancer^{340,341,342}.

However, a role for TGF β in regulating stemness in melanoma has yet to be uncovered and established.

Considering the strong anti-tumorigenic effects of TGF β in melanoma, we hypothesized that TGF β signalling pathway could play a role in regulating melanoma stemness, as part of its tumor suppressive activities. In this study, we found that TGF β inhibits melanoma stem cell maintenance in various cutaneous melanoma cell lines originated from different patients. We showed that TGF β can inhibit melanoma tumorsphere formation and reduce CD133⁺ melanocytic stem cell population. We further show that these effects are mediated through the Smad pathway and that Smad3/4 gene silencing by means of CRISPR/Cas9 knockout (KO) could prevent the TGF β anti-stemness effects in melanoma. Moreover, using preclinical models of melanoma, we showed that orthotopic transplantation of Smad3/4 CRISPR-KO melanoma cells led to significant increase in tumor growth and lung metastatic nodule formation *in vivo*, further highlighting the strong tumor-suppressive role of TGF β in melanoma. Together, these results define a new role for the TGF β /Smad signaling axis in stem-cell maintenance in melanoma and open avenues for the development of new therapeutic approaches to this deadly disease. Indeed, clinical approaches aiming at stimulating TGF β signaling could prove useful to improve melanoma patient outcome, including patients with both primary and secondary metastatic tumors.

2.4 Material and methods Introduction:

Reagents and Chemicals

Recombinant human Transformation Growth Factor beta (TGF β), Epidermal Growth Factor (EGF), Fibroblast Growth Factor-basic (b-FGF) was purchased from Peprotech (Ville-St-Laurent, Quebec, Canada), Puromycin, Tissue culture medium RPMI1640, DMEM, Fetal Bovine Serum, B-27TM Plus Supplement (50X) Catalog were purchased from GIBCO (Waltham, Massachusetts, USA).

Cell lines

Cutaneous melanoma cell line WM793B was isolated from the primary tumors of a 37-year-old male patient and is mutant for BRAF (V600E and W274X), PTEN (homozygous deletion) and CDK4 (K22Q). WM278 cell lines were isolated from a 62-year-old female patient and is mutant for BRAF (V600E) and PTEN (hemizygous deletion). A375m, the metastatic variant of A375, was

isolated from a 54-year-old patient having an amelanotic melanoma cancer and is BRAF (V600E) and CDKN2A (E61X and E69X) mutant. BLM cell line, mutant for NRAS (Q61R) is obtained from lung metastasis of BRO melanoma cell line, which comes from a 34-year-old male. WM793B, WM278, BLM and A375m were kindly provided by Dr Alan Spatz and Mounib Elchebly (McGill University, Montreal, Canada). DAUV (also called LB33-MEL.A) was derived from a subcutaneous metastatic lesion (stage IV) in a 42-year-old female patient (WT for BRAF and NRAS). DAUV cell line was generously provided by Dr. Louise Larose (McGill University, Montreal, Canada). RPMI medium supplemented with 10% FBS is used for 1205Lu, DAUV, MALME-3M, WM278 and WM793 cell line. DMEM medium supplemented with 10% FBS was used for A375m and BLM cell line.

CRISPR Knock-out

LentiCRISPRv2 (Addgene, cat. No. 52961) was digested using Esp3I restriction enzyme (ThermoFisher, cat. No. ER0451), dephosphorylated using FastAP (ThermoFisher, cat. No. EF0654), agarose gel purified and extracted using QIAquick Gel Extraction Kit (QIAGEN, cat. No. 28704). Each single-guide primer sequences below (5'-3') were phosphorylated using T4 PNK (NEB, cat. No. M0201S), annealed by slow cooling from 65°C to room temperature in T4 ligation buffer (NEB, cat. No. B0202S) and ligated in Esp3I digested lentiCRISPRv2 purified plasmid using Quick Ligase (NEB, cat. No. M2200S). Each sgRNA ligated plasmid was transformed in STBL3 chemically competent E. coli (ThermoFisher, cat. No. A10469) and collected from an amplified single bacterial colony using QIAprep Spin Miniprep Kit (QIAGEN, cat. No. 27104).^{253,254}

Each sgRNAs were designed with ChopChop³⁴³. Chromosomal positioning of sgRNA binding site as well as off-target and on-target activity evaluation was performed with CRISPOR³⁴⁴ (Supplementary table 1).

Table 1

Primer name	Single-guide primer sequence
scrs1-F	5' - CACCGACGGAGGCTAAGCGTCGCAA - 3'
scrs1-R	5' - AAACCTTGCGACGCTTAGCCTCCGTC - 3'
scrs2-F	5' - CACCGCGCTTCCGCGGCCCGTTCAA - 3'
scrs2-R	5' - AAACCTTGAACGGGCCGCGGAAGCGC - 3'
scrs3-F	5' - CACCGATCGTTTCCGCTTAACGGCG - 3'
scrs3-R	5' - AAACCGCCGTTAAGCGGAAACGATC - 3'
Smad2sg4-F	5' - CACCGTGGCGGCGTGAATGGCAAGA - 3'
Smad2sg4-R	5' - AAACCTTGCCATTCACGCCGCCAC - 3'
Smad3sg2-F	5' - CACCGTTCACGATCGGGGAGTGAA - 3'
Smad3sg2-R	5' - AAACCTCACTCCCCGATCGTGAAC - 3'
Smad4sg1-F	5' - CACCGAACTCTGTACAAAGACCGCG - 3'
Smad4sg1-R	5' - AAACCGCGGTCTTTGTACAGAGTTC - 3'

qPCR

Total RNAs were extracted using Trizol™ (Invitrogen, ThermoFisher Scientific, ON, Canada) as per the manufacturer's instructions. 2µg of RNA was reverse transcribed using M-MLV reverse transcriptase and random primers (Invitrogen) as per manufacturer's protocol. Amplification of cDNA was performed by quantitative real time PCR (qPCR) SsoFast™ EvaGreen® Supermix (Bio-Rad, ON, Canada) using Rotor-Gene™ 6000 Real-time Analyzer (Corbett Life Sciences, CA, USA) and data were analyzed with its corresponding software. The qPCR conditions were: 30 seconds at 95°C, then 40 cycles of 5 seconds at 95°C, 5 seconds at 60°C and finally 5 seconds at 72°C. Human GAPDH was used as a housekeeping gene. Primer sequences are listed in the table below.

Table 2

Primer	
name	Primer sequence for qPCR
CD133-F	TACCAAGGACAAGGGGTTTAC
CD133-R	CAGTCGTGGTTTGGCGTTGTA
ABCG2-F	GCTCAGGAGGCCTTGGGATA
ABCG2-R	GGCTCTATGATCTCTGTGGCTTT
ALDH1A1-F	CTGTGTTCCAGGAGCCGAAT
ALDH1A1-R	CTGCCTTGTC AACATCCTCCTTA
ALDH1A3-F	GGAAGAAGGAGATAAGCCCGAC
ALDH1A3-R	AGCCCTCCAGGTTCGATGAAA
GAPDH-F	GACAGTCAGCCGCATCTTCT
GAPDH-R	GCGCCCAATACGACCAAATC

Lentivirus production and cell infection

HEK293T cells were cultured to 90% confluence in complete medium and transfected with respective lentiCRISPRv2 scramble (scr), Smad2, Smad3 or Smad4 constructs or shRNAs Non-targeting control (NTC) and SMAD3 (Sigma) lentiviral packaging plasmids pMD2.G (Addgene#12259 and ps.PAX2 (Addgene #35002), Opti-MEM medium (Invitrogen) and bPEI (Sigma Aldrich). Medium enriched in virus particle was collected after 48 hours. Cells were grown to 50% confluence in antibiotic-free medium in 6-well plates, each well was infected with the 100µl of lentiviruses in presence of polybrene (hexadimethrine bromide) at 8 µg/ml. For BLM and WM278, cells were infected by spinfection (2 hours, 1500G and 33°C) and medium was replenished immediately after centrifugation. For a375m cell line, incubation was made overnight and replenished with fresh complete medium for 48 hours. Cells were selected with 1µg/ml puromycin 2 days post-infection. The pool of resistant cells forming the stable CRISPR knockout cells was expanded in complete medium supplemented with 1µg/ml puromycin.

Western blot assays

Cells were lysed in ice-cold full lysate buffer (10mM Tris-HCl, pH 7.5, 5mM EDTA, 150mM NaCl, 30mM sodium pyrophosphate, 50mM sodium fluoride, 1mM sodium orthovanadate, 1%

Triton X-100, 1mM phenylmethanesulfonyl fluoride, 10µg/ml leupeptin hydrochloride, 10µg/ml aprotinin, 10µg/ml pepstatin and 10X Phosstop (Sigma)). Total protein lysates were quantified using Pierce™ BCA Protein Assay Kit (Thermo Scientific). Lysates containing 50µg of total protein were separated by SDS-PAGE, transferred to a nitrocellulose membrane using a wet transfer tank system and probed using specific primary antibodies and HRP-conjugated secondary antibodies. The primary antibodies used for Western blot analysis were rabbit polyclonal Smad2/3 antibody (Santa Cruz Biotechnology, D767), Smad4 antibody (EMD millipore, MAB1132) B-Tubulin (Cell signaling, 2146S)

Flow Cytometry

Monolayer cells were dissociated, washed once in ice-cold PBS, resuspended in FACS buffer (PBS, 2% FBS) and counted using TC20™ Automated Cell Counter (BioRad). Cells were aliquoted at a density of 0.25×10^6 – 1×10^6 cells per tube. R-phycoerythrin (PE) Mouse Anti-Human CD133 antibody (Miltenyi Biotec) were added to the cell suspension in a ratio of 1:20 (v/v), gently mixed with cells by gentle flicking and incubated on ice protected from light using aluminum foil tube covering for 30 minutes. Samples were washed twice with FACS buffer and analyze with BD FACSCanto flow cytometer using excitation 488-nm and emission using a 575/26 bandpass filter. Data was analyzed with FlowJo software (Tree Star Inc.)

The CD133+ population was analyzed using an anti-CD133 antibody (Miltenyi Biotec™) and the ALDH+ population by assessing the enzymatic activity of ALDH with non-immunological ALDEFLUOR™ kit. Unstained cells were used to gate the population of CD133+, while ALDH was gated based with enzymatic ALDH inhibitor, N,N-diethyl-amino-benzaldehyde (DEAB), used to block all ALDH isoenzymes activity.

Melanosphere culture assay

Melanoma cells were seeded at a density from 5000-10,000 cells per well in ultra-low-attachment 24-well plates (Corning) in 1ml of freshly prepared stem cell medium (serum-free RPMI1640 or DMEM medium supplemented with 10 ng/ml EGF, 10 ng/ml bFGF and 1X B-27™ Plus Supplement). Low-attachment plates were incubated continually without handling and disruption for 7 days at 37 °C with 5% CO₂. Spheroids from both passages of a diameter $\geq 50\mu\text{m}$ were counted as melanospheres.

In vivo studies

Mice housing and handling was made in accordance to the approved guidelines of the Canadian Council on Animal Care and the Animal Care Committee of McGill University (AUP # 7497). The immune-deficient non-obese diabetic scid gamma (NSG) mouse breeders were purchased from The Jackson Laboratory.

Human melanoma cancer cell line a375m (1×10^6 /mouse) was inoculated in 7-week-old male NSG mice by subcutaneous injection to generate melanoma tumor. The mice were euthanized at the indicated endpoint time and tumor size was measured with a digital electronic caliper three times per week. To generate a growth curve, tumor volumes were calculated according to the following formula:

$$\frac{4}{3} * \pi * \left(\frac{Length}{2}\right) * \left(\frac{Width}{2}\right)^2$$

Human melanoma cancer cell line a375m (5×10^5 /mouse) was injected by tail vein to allow for lung metastasis development. The mice were euthanized 15 days post-injection. The lung tissues were fixed with Bouin's solution and metastatic nodules were counted using a microscope.

2.5 Results:

TGF β inhibits stem-cell maintenance and CSC self-renewal capacity in melanoma.

The role of TGF β on CSC stemness remains to be fully investigated and appears context dependent, as TGF β can either inhibit or sustain CSC maintenance³⁴¹. TGF β has been reported to regulate CSCs in breast cancer^{342,345-347} glioblastoma³⁴⁸, gastric carcinoma cells³⁴⁹ and squamous carcinoma stem cells³⁵⁰. Despite its potent tumor suppressive role in melanoma, the effect of TGF β cancer stemness has not been addressed yet in these tumors. To first address this, we examined the TGF β effects *in vitro* using a melanoma tumorsphere-forming assay (TFA)¹²⁵. TFAs are standard assays used for tumor-initiating capacity measurement and self-renewal assessment^{342,347}. We investigated a panel of 7 different human cutaneous melanoma cell lines with various clinical backgrounds (WM278, WM793, a375m, BLM, MALME-3M, 1205Lu and DAUV). We found that TGF β 1 significantly reduced melanoma tumorsphere formation at picomolar concentrations in all cell lines tested, except WM278 and 1205Lu (Fig. 1a). These effects were particularly striking

in WM793 cells where TGF β stimulation led to complete inhibition of tumorsphere formation. While the WM278 cell line showed no statistical difference in the reduction of the number of tumorspheres, they exhibited smaller tumorsphere in size (Fig1a). This consistent suppression of non-adhesive sphere formation across various cell lines suggests a mechanism where TGF β inhibits CSC self-renewal capacity in melanoma.

To further investigate the function of TGF β on melanoma cancer stemness we measured its effects on 2 well characterized melanoma CSC markers, expression of the cell-surface marker CD133³³³ and aldehyde dehydrogenase (ALDH) enzymatic activity^{335,336}. Indeed, cells with high CD133 (CD133+) expression³³³ or high ALDH enzymatic activity (ALDH+) exhibit increased tumor burden when transplanted in immunodeficient mice, in correlation with high CSC self-renewal properties³³³. *In silico* TCGA analysis further revealed that melanoma tumors are enriched in ALDH1A1 and ALDH1A3 isoenzymes¹¹⁶. We thus investigated whether TGF β could modulate CD133+ and ALDH+ populations in A375m melanoma cells, using flow-cytometry. A375m melanoma cells are enriched in CD133+ population and exhibit a high metastatic potential, and as such this cell line represents an ideal model to study melanoma stemness. As shown in Figs.1b and 1c, TGF β decreased the percentage of both CD133+ and ALDH+ CSC sub-populations.

To get further insights into the mechanism by TGF β regulates markers implicated in melanoma stemness, we examined TGF β -mediated regulation of specific melanoma CSC markers (ALDH1A1, ALDH1A3, CD133 and ABCG2), at the transcriptional level. As shown in Fig.2a-b, exposure of a375m and BLM cells to picomolar concentrations of TGF β significantly reduced mRNA expression of all four CSC markers, in a time dependent manner. TGF β -mediated decreased in ALDH1A3 expression were also observed in a third melanoma cell line (WM278), as shown in Fig. 2c). We then assessed the TGF β effects on expression of these CSC markers using a more relevant 3D culture model, which better represents the morphology and heterogenous aspects of the tumor biology³⁵¹. Interestingly, TGF β stimulation of the cells also led to significant and strong decrease of the CSC markers in tumorsphere conditions (Fig.2d). Altogether, these results define a new function for TGF β in regulating stem cell maintenance in melanoma and highlight its strong inhibitory effects on CSC self-renewal activity and cell surface CSC marker expression.

The Smad3/4 pathway is required for TGF β -mediated inhibition of melanoma cancer self-renewal.

The main signaling pathway activated downstream of TGF β is the canonical Smad pathway. In particular, Smad2, 3 and 4 play a central role in mediating the TGF β tumor suppressive activities in multiple types of cancer³². To address whether the canonical Smad pathway is involved in the mediation of the TGF β effects on melanoma self-renewal, we generated specific Smad2, Smad3 and Smad4 knockout (KO) in two different melanoma cell lines, A375m and BLM, using CRISPR genomic editing. Specific guide RNAs (gRNAs) were designed for each Smad, as described in the methods. Non-targeting scrambled (scr) gRNAs were used as negative controls. Interestingly, we found that blocking Smad3 and Smad4 gene expression, but not Smad2 significantly increased melanoma tumorsphere formation in both cell lines (Fig.3a-b). Efficiency of the Smad CRISPR KOs were verified by western blot and showed near complete inhibition of their respective targets (Figs.3e and 3f). To further broaden the scope of our findings and further strengthen our results, we also used a parallel shRNA approach to knockdown Smad3 gene expression in BLM cells as well as in a third melanoma cell lines (WM278). A non-targeting (NT) was used as negative control. As shown in Figs.3 and 3d, blocking Smad 3 expression also resulted in a significant increase in tumorsphere formation in both cell lines, consistent with the data obtained with the CRISPR KOs. High efficiency of the Smad3 shRNA knockdown was verified by western blot (Figs. 3g and 3h).

We further analyzed the TGF β effects on CD133 expression in the different Smad-KOs, using flow cytometry. As shown in fig.3i, we also found that blocking Smad3 and Smad4 significantly reversed the TGF β inhibitory effect on CD133 expression. Smad2 gene silencing showed significant effect on the TGF β response, consistent with the result obtained in the tumorsphere assay. These results indicate that TGF β -mediated regulation of CSC self-renewal capacity and possible stemness maintenance is Smad-dependent but also specific to the Smad3/4 pathway.

Blocking TGF β /Smad signaling promotes melanoma tumor growth *in vivo*

Having shown that Smad3/4 gene silencing promote stemness and increases tumorsphere formation, and considering the prominent role played by cancer stem cells in promoting tumor formation, we next assessed the Smad3/4 CRISPR KOs *in vivo*, using preclinical models of

melanoma tumor formation. Orthotopic subcutaneous human tumor xenografts were performed in NOD-SCID IL2R γ null (NSG) mice. A total of 4 groups of NSG mice (7 mice/group) received a subcutaneous injection of non-targeting control, Smad3 and Smad4 CRISPR KOs, generated in the A375m melanoma cell line (Fig.4a). Interestingly, blocking the Smad signaling pathway, by means of Smad3/4 CRISPR KO, significantly increased both tumor volume (Fig.4b) and tumor mass (Fig.4c) compared to non-targeting control (scrambled) and parental cell (A375m) groups. The observed increase in primary melanoma tumor growth upon depletion of Smad proteins demonstrates their crucial role in suppressing tumorigenicity *in vivo*, further highlighting the strong tumor suppressive role played by the TGF β signaling pathway in melanoma. Moreover, while no mice from the parental and scrambled KO groups harbored any secondary metastatic tumors, several mice in both the Smad3 and Smad4 groups developed spontaneous liver metastasis (Fig.4d). These results suggest that the TGF β /Smad signaling axis not only act as a potent tumor suppressor but also as a suppressor of metastasis.

The TGF β /Smad pathway inhibits melanoma lung metastasis *in vivo*

Our previous study demonstrated that TGF β stimulation of melanoma cells suppressed cell migration *in vitro*⁸⁰. Furthermore, as shown in Fig.4d, blocking the Smad pathway in our orthotopic transplantation model led to an increased liver metastatic burden. Thus, these results suggest that blocking TGF β /Smad signalling *in vivo* could also regulate the metastatic dissemination of melanoma cells to distant organs. To address this, we used a preclinical model of melanoma lung colonization^{352–354}. Briefly, as described in Fig5a, Smad3 CRISPR-KO, Smad4 CRISPR-KO and control NT CRISPR-KO a375m melanoma cell were injected intravenously into NSG mice (tail vein injection; 7 mice/group).

Twenty one days post injection, animals were sacrificed and lungs were resected before being stained in Bouin solution, as previously described³⁵³. Interestingly, as shown in Fig.5b, both Smad3 and Smad4 CRISPR-KOs showed a strong increase in numbers of metastatic lung lesions, compared to control animals. Fig.4c shows representative images of the resected tumors. These results indicates that inhibition of TGF β /Smad canonical signalling pathway not only increased primary tumor growth but also significantly increased the metastasis burden. They are also consistent with our results from the spontaneous liver metastasis preclinical model (Fig.5d). Altogether, our data define the TGF β /Smad signaling axis as a potent suppressor of metastasis.

2.6 Discussion:

In this study, we investigated the role of TGF β in stem cell maintenance in melanoma and the relationship with the TGF β /Smads signaling axis in tumorigenesis and metastasis. We found that TGF β inhibits stem cell maintenance in several human cutaneous cell lines. Furthermore, we found that TGF β acts as a potent tumor suppressor, blocking primary tumor formation but also as a strong suppressor of metastasis, preventing the spread and development of secondary liver and lung metastatic nodules *in vivo*. Our data are in agreement with and support our previous *in vitro* work showing that TGF β act as an anti-migratory factor in melanoma^{80,82}. They underscore TGF β and Smad signaling as potent regulators implicated in self-renewal, as well as suppressors of both tumor formation and metastasis in cutaneous melanoma.

Melanoma stem cells have many capabilities compared to differentiated cells, such as self-renewal, differentiation, plasticity, immune evasion, drug resistance and promotion of cell migration and metastasis. A study showed that melanoma CSCs secreted factors can activate neutrophils and support cancer progression, therefore increasing the importance of the interplay between tumor microenvironment and cancer progression³⁵⁵. Indeed, soluble factors such as TGF β can modify the tumor microenvironment. Such mechanisms implicating CSCs are directly associated with melanoma progression, metastasis and tumor heterogeneity⁹⁶. Thus, our data defining TGF β as an inhibitor of CSC self-renewal is consistent with a role of TGF β as an inhibitor of tumor formation, progression, and metastasis. Moreover, in future studies, it will be interesting to further characterize the precise role of TGF β signaling on stemness, using *in vivo* and *in vitro* diluting limiting assay.

In melanoma, several stem cell markers are expressed in sub-populations of CSCs which exhibit increased tumor potential. One of the first identified CSC marker is CD133, an extracellular protein linked to a subset of melanoma cells displaying stem-cell like properties and increased tumorigenicity³³³. Isolated subpopulations of melanoma cells expressing CD133 are more proliferative and more invasive than CD133-negative counterpart^{106,107}. Furthermore, CD133 was also found to be expressed in metastatic extract from melanoma patients, consistent with a role for CSC in promoting metastasis³³³. Another CSCs sub-population is characterized by the ALDH+ melanoma cells. In particular, the ALDH1A1 and ALDH1A3 isoenzymes that were shown to be enriched in melanoma tumors¹¹⁶. In this study, we found that TGF β inhibits CSCs self-renewal capacity in multiple melanoma cell lines. We also show that TGF β efficiently reduces the

percentage of several of the main CSC sub-populations, CD133+, ALDHA1 and ALDHA3. These potent effects inhibiting self-renewal ability likely reflect the strong tumor suppressor role played by TGF β in these tumors. These results are also in line with what observed in other types of solid tumors, such as pancreatic cancer, where Smad4 up-regulation was found inversely correlated with ALDHA1 expression³⁵⁶. They suggest that TGF β /Smad signaling may exert anti-CSC self-renewal activity on a broader range of tumors, than melanoma alone.

Interestingly, while the TGF β effects on melanoma cancer stem cell maintenance require the Smad pathway they also appear to be Smad3/4 specific and Smad2-independent. Such Smad2 or Smad3 specificity downstream of TGF β signaling has been reported in the context of other cancer-related mechanisms^{165,357-360}. For instance, the E1A-like inhibitor of differentiation-2 (EID-2) protein can suppress TGF β signaling by specifically blocking TGF β -induced formation of Smad3-Smad4 complexes³⁵⁸. Another study showed that Smad3 silencing in keratinocytes interfered with growth inhibition while Smad2 silencing had no phenotypic effect³⁶⁰. Our group also previously showed that menin, a potent tumor-suppressor, specifically interacts with Smad3 to mediate TGF β anti-proliferative responses in pituitary adenoma¹⁶⁵. Furthermore, previous work from our laboratory and others also showed that TGF β -mediated inhibition of telomerase activity and cell immortalization relies on Smad3 signaling, independently of Smad2^{357,359}. A previous study showed that constitutive phosphorylation of the Smad3 linker region by MAPK and CDK/GS3 modulates TGF β -mediated resistance to cell cycle arrest, by interfering with p15 and p21³⁶¹. Thus, phosphorylation on distinct specific sites of the Smads can lead to differential regulation of cell cycle. Altogether, these studies are consistent with our present findings in melanoma, suggesting that Smad3 may play a more prominent role in the mediation of the TGF β tumor suppressive effects, compared to Smad2 in various models of solid tumors.

Phenotype switching refers to the switch from a proliferative to an invasive phenotype, conferring plasticity to cancer cells. The switch implicates transcriptional reprogramming involving a panoply of signaling pathways with their respective downstream regulators including TGF β /SMADs, Hippo/TAP/TAZ and Wnt/B-catenin³⁶². Furthermore, MITF (microphthalmia-associated transcription factor) is an important melanocytic lineage-specific transcription factor also associated with phenotype switching. Indeed, MITF low expression is correlated with invasiveness and high expression with more proliferative phenotype³⁶³. TGF β has been shown to inhibit the MITF transcription through repressed protein kinase A activity, therefore correlated with the

invasiveness phenotype of TGF β ³⁶⁴. In parallel, TGF β has been shown to exert a dual role during cancer progression, in some types of cancer^{32,365}. While inducing tumor suppression in normal epithelial cells and early carcinomas, TGF β promotes metastasis in more advanced stages of cancer^{32,366–368}.

However, the TGF β function in melanoma remains controversial. While previous studies showed that overexpression of the TGF β signaling inhibitor SMAD7 reduced the proliferation and metastatic potential of 1205Lu melanoma cell line^{369,370}, other studies suggested that TGF β itself could inhibit tumor cell migration and metastasis^{80,82}. Interestingly, the 1205Lu melanoma cell line used in the former studies^{364,369,370}, was not responding to TGF β in the tumorsphere assays performed in our study, which could explain the differential TGF β outcome observed in other melanoma cell lines. A separate study showed that a recombinant cytotoxin (cytotoxin-II) indirectly inhibited SMAD2/3 mRNA expression, and correlated with increased caspase 8 and 9 *in vitro*³⁷¹. However, these results, using an indirect inhibitory approach were not confirmed *in vivo*. In contrast, our results clearly indicate that direct TGF β silencing, using SMAD KOs significantly reduced proliferation, tumorigenesis and metastasis, both *in vitro* and *in vivo*.

We previously found TGF β to inhibit cell migration and invasion *in vitro* in several model of melanoma⁸⁰. The present study is in accordance with these results and clearly indicate that TGF β /Smad signalling prevent tumor progression *in vivo*, using preclinical models of melanoma metastasis. They are also consistent with a role for TGF β as an inhibitor of CSC self-renewal, further highlighting TGF β as an anti-metastatic factor in melanoma.

2.7 Acknowledgements :

The authors would like to thank Dr. Alan Spatz and Dr. Louise Larose for providing the melanoma cell lines. Figure 3A and 4A were created with BioRender (BioRender.com).

2.8 Figures of chapter 2

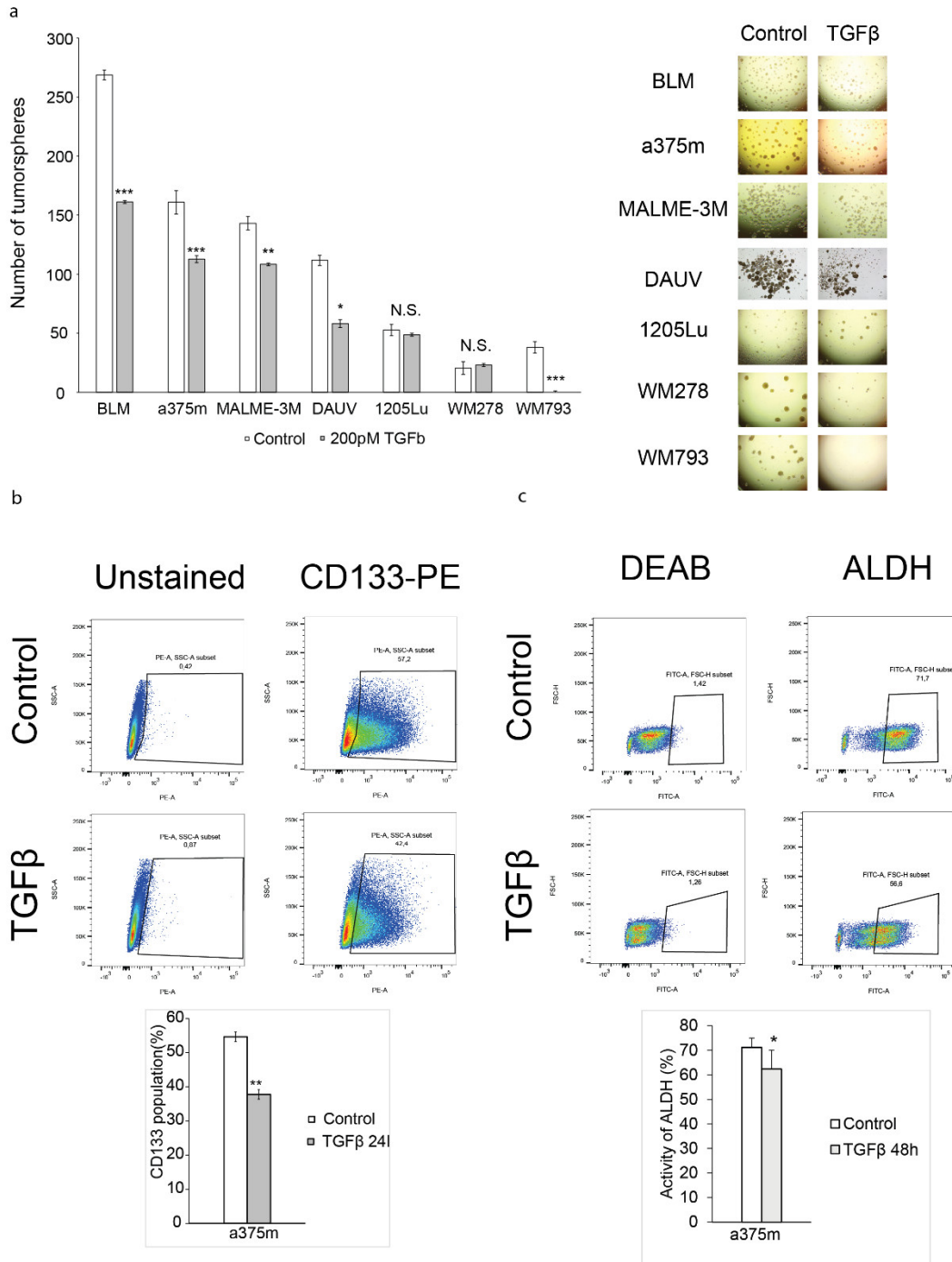
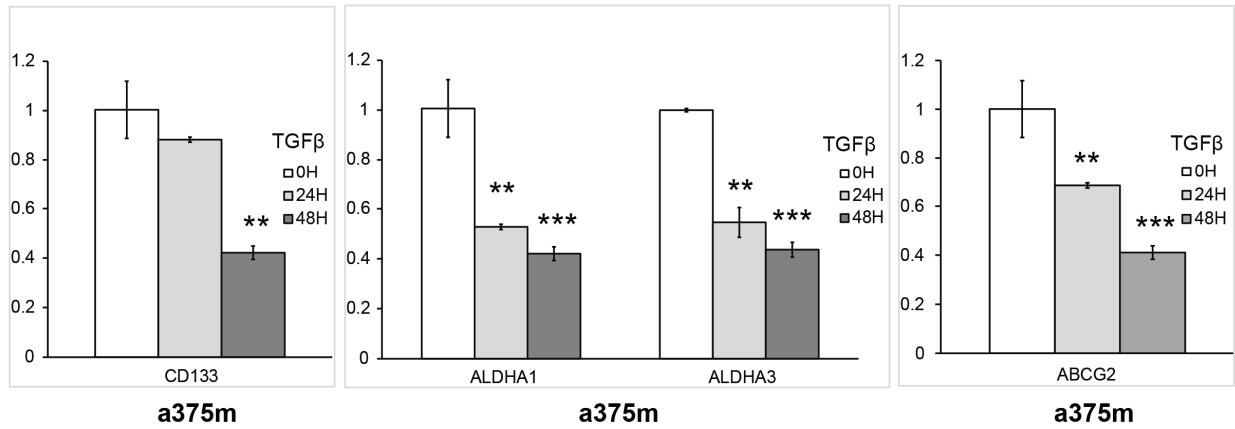
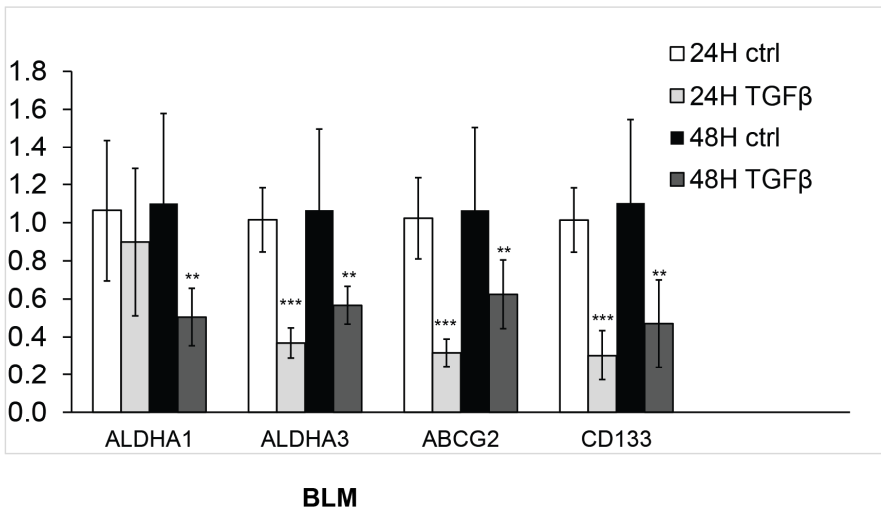


Figure 2.1. TGF β inhibits tumorsphere formation and self-renewal capacity in melanoma. (a) TGF β effects on tumorsphere formation of different melanoma cell lines. Left panel: Histogram showing the number of tumorspheres. Data are expressed as mean \pm standard error. *P \leq 0.05, n.s. not significant. Right Panel: Representative images of tumorspheres of each melanoma cell lines. (b) Histogram of flow cytometry analysis of a375m cells untreated or treated with TGF β (200 pM) for 24h and labeled with an PE-conjugated anti-CD133 antibody. The percentage of CD133-positive/negative populations of a replicate is represented in the dot-plot. Gating was set by unstained samples. (c) Histogram of flow cytometry analysis of a375m cells untreated or treated with TGF β (200 pM) for 48h and evaluated with enzymatic assay ALDEFUOR™ kit.

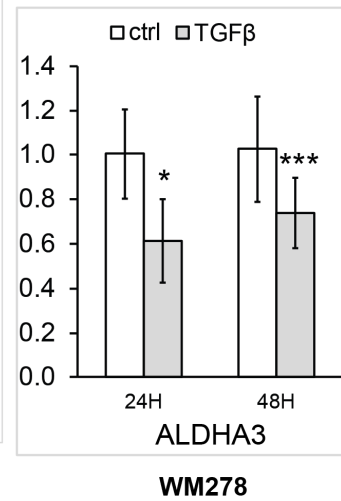
a



b



c



d

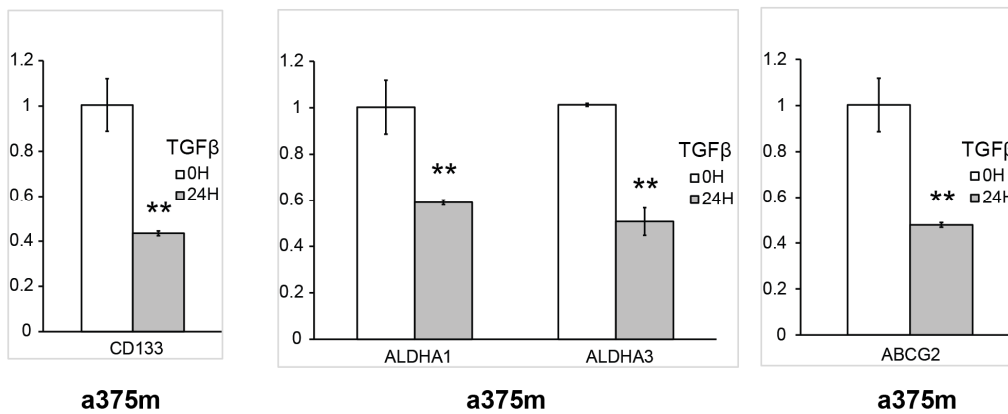


Figure 2.2. Transcriptional downregulation of stemness markers by TGF β in Melanoma (a-c) Histogram of relative mRNA expression measured by qPCR of cells collected from (a) a375m, (b) BLM and (c) WM278 cultured in monolayer condition and a375m in tumorsphere condition (d). Cells were exposed to TGF β (200 pM) for 24h or 48h. Data represents \pm SEM of triplicate experiments.

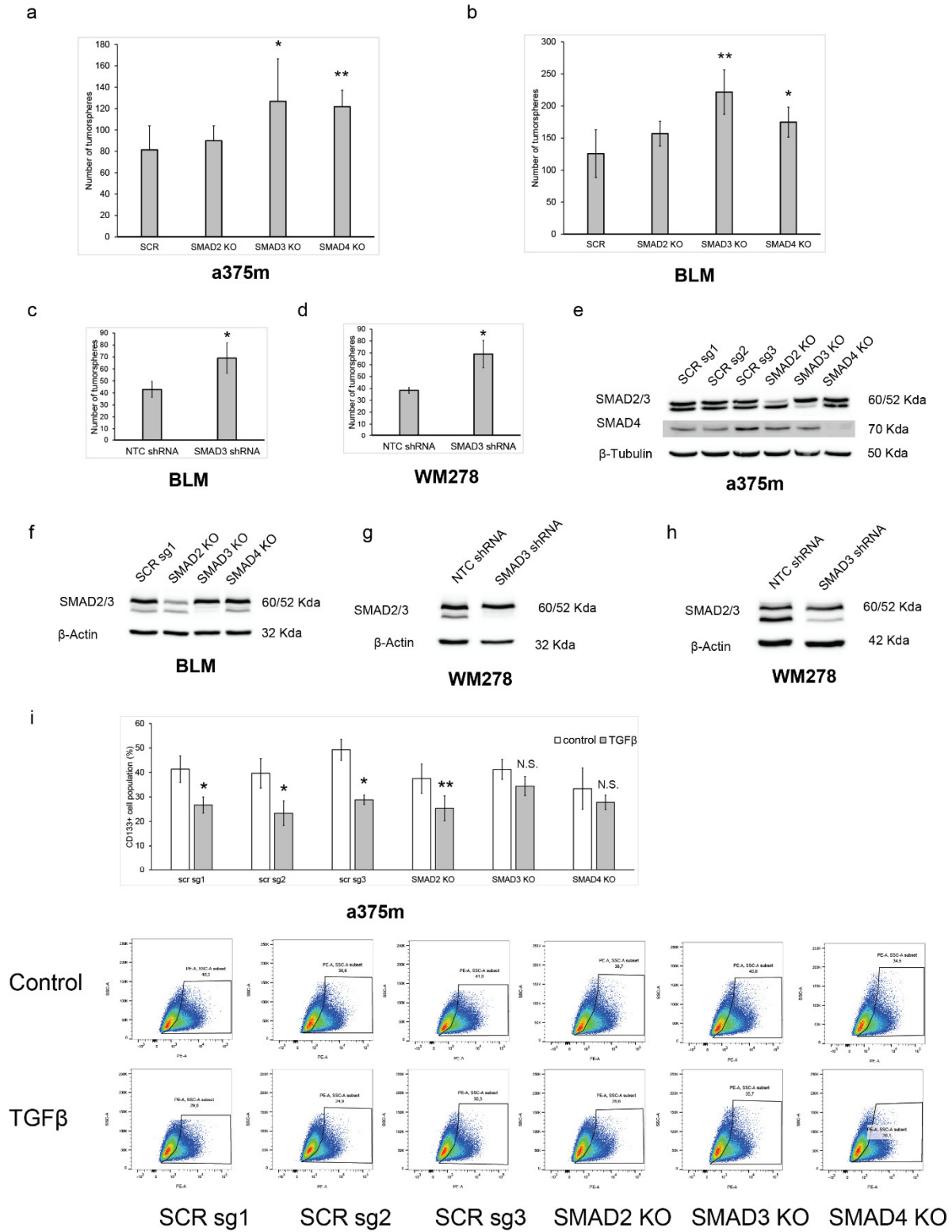
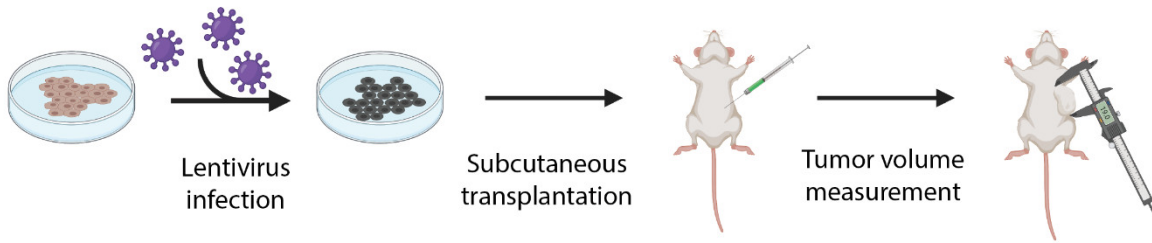
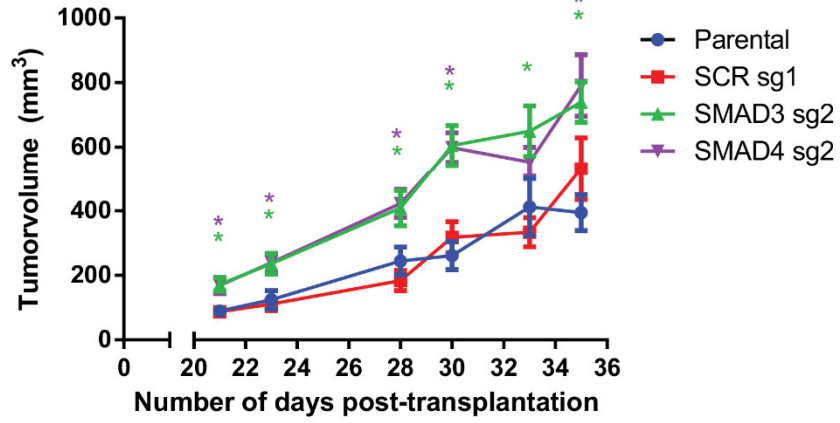


Figure 2.3. The Smad3/4 pathway is required for TGF β -mediated inhibition of melanoma cancer stemness. Histograms showing the number of tumorspheres after 7 days culture under low-attachment conditions with CRISPR-Smad2, 3, 4 KOs in (a) a375m and (b) BLM cell lines or Smad3 shRNA knockdown in (c) BLM and (d) WM278 melanoma cell lines. Efficiency of the (e, f) CRISPR KOs and (g, h) shRNA knockdown was ensured by western blot. Data are expressed as mean \pm standard error. *P \leq 0.05, n.s. (i) Histogram of flow cytometry analysis of different CRISPR KOs produced in a375m cells untreated or treated with TGF β (200 pM) for 24h and labeled with an PE-conjugated anti-CD133 antibody. Gating was set by unstained samples. The percentage of CD133-positive/negative populations is indicated.

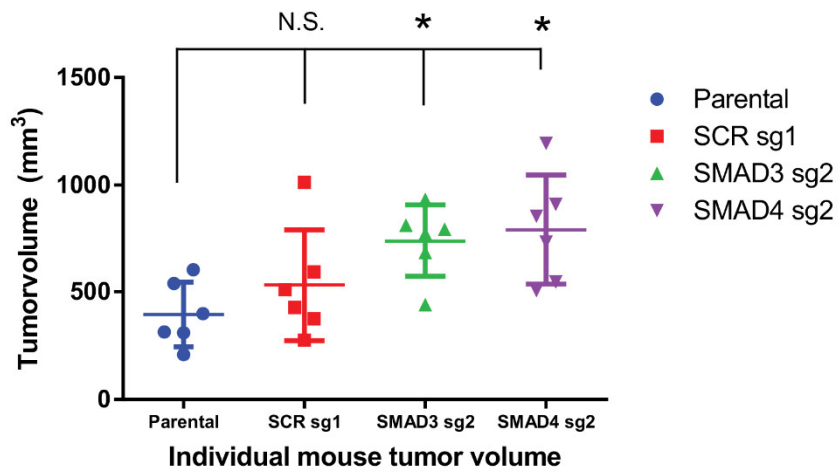
a



b



c



d

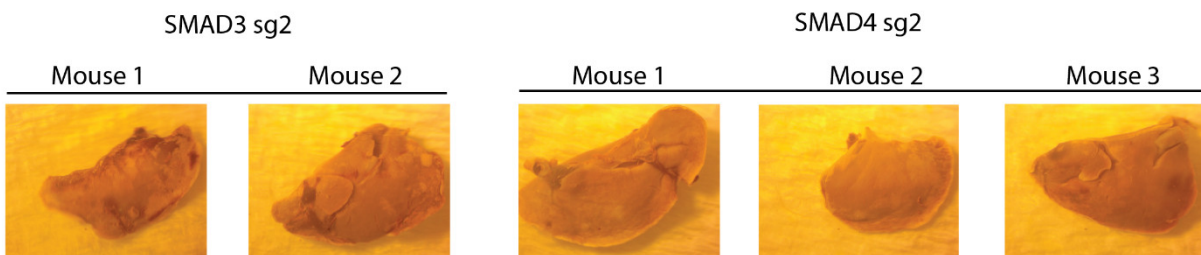


Figure 2.4. Blocking TGF β /Smad signaling promotes melanoma tumor growth in vivo. (a) Graphical abstract of the orthotopic subcutaneous transplantation of melanoma cells in NSG mice (n=6 per group). (b,c) One million CRISPR KO a375m cells were transplanted in NSG mice. Tumor growth was assessed by measuring tumor volume 3 times/week (b) and at endpoint (c). Data are represented as mean \pm SEM. p values are comparing each KO group vs. Scramble control by two-sided unpaired t test at the same day. *P < 0.05, **P < 0.01 or ***P < 0.001. (d) Representative pictures of spontaneous metastasis in resected liver by Blouin staining.

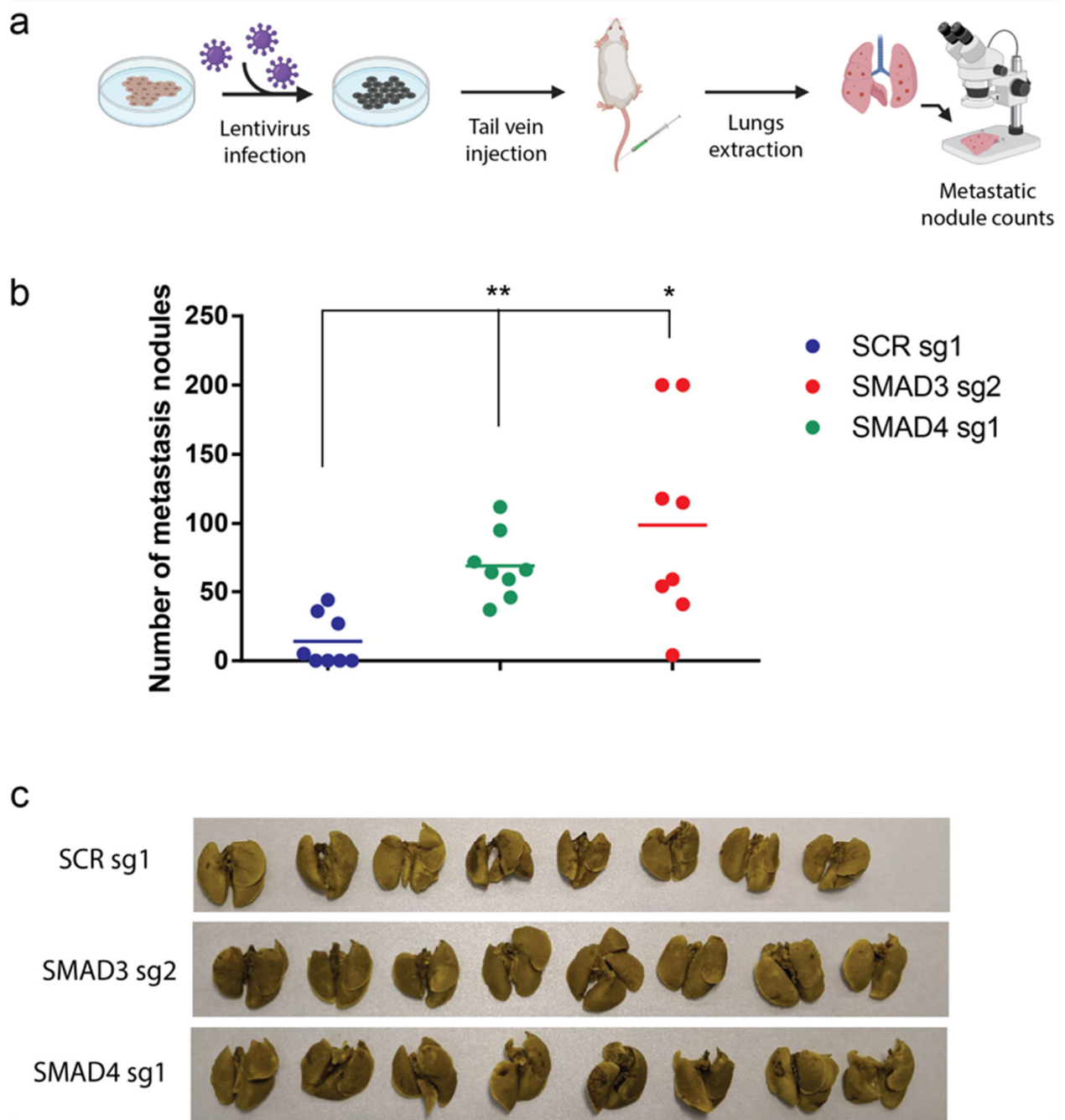


Figure 2.5. The TGF β /Smad pathway inhibits melanoma lung metastasis in vivo (a) Graphical abstract of the tail vein injection of melanoma cells in NSG mice (n=8 per group). (b) SCR, SMAD3 and SMAD4 KO a375m melanoma cells were injected intravenously in the tail vein of NSG mice (n=9 per group) to assess the number metastatic nodules in the lungs. Data are represented as dot plots for individual mice. The midlines show median value. (c) Representative images of metastatic nodules are shown for each mouse's lungs.

Chapter 3:

Multiple endocrine neoplasia type 1 regulates TGF β -mediated suppression of tumor formation and metastasis in melanoma

Julien Boudreault*, Lucie Canaff*, Mostafa Ghozlan*, Ni Wang, Vito Guarnieri, Antonio Stefano Salcuni, Alfredo Scillitani, Geoffrey Hendy, Suhad Ali and Jean-Jacques Lebrun

*These authors contributed equally

3.1 Preface:

Multiple endocrine neoplasia type 1 (MEN1) is a dominant genetic disorder characterized by endocrine tumors formation of parathyroids, pancreatic islets, and anterior pituitary. Many mutations in Multiple endocrine neoplasia type 1 gene (*MEN1*), encoding for menin protein, are inactivating, giving rise to a truncated protein, and are associated with increased cancer occurrence. We thus investigated menin implication in TGF β signaling and inactivation in preclinical models of melanoma. Moreover, we studied novel *MEN1* mutations in patients with melanoma and tested menin stability, protein degradation and outcome on TGF β signaling.

3.1 Abstract

Over the past few decades, the worldwide incidence of cutaneous melanoma has been increasing remarkably, leading to the highest rate of skin cancer-related deaths. While localized tumors are easily removed by excision surgery, late-stage metastatic melanomas are refractory to treatments and exhibit poor prognosis. As such, unfolding the molecular mechanisms underlying melanoma tumorigenesis and metastasis is crucial for developing novel targeted therapy. We found the transforming growth factor beta (TGF β) and multiple endocrine neoplasia type 1 gene (*MEN1*), encoding for menin protein, to induce tumor suppression in vitro and in vivo using melanoma preclinical xenograft models. We further identified point mutations in two MEN1 kindreds affected by melanoma, leading to proteasomal degradation of the *MEN1* gene product and to a loss of TGF β signaling. Interestingly, blocking the proteasome degradation pathway, using FDA-approved drug and RNAi targeting could efficiently restore menin expression and TGF β transcriptional responses. Together these results provide new potential therapeutic strategies and patient stratification for the treatment of cutaneous melanoma.

3.2 Introduction

Cutaneous melanoma is a deadly and aggressive cancer accounting for about 80% of skin cancer-related mortality³⁷². Global statistics ranked melanoma as the fifteenth most common cancer, with 230,000 diagnosed cases per year and 55,000 deaths. Furthermore, melanoma incidence significantly increased during the past fifty years¹⁷⁹. Worldwide, melanoma stands as one of the most prevalent cancers amongst younger adults of the ages between 20-35 years³⁷³. Based on histopathology and prognostic outcome, melanomas conventionally fall into four clinical stages.

While patients with stage I melanoma have localized primary tumors that can be removed by surgical excision³⁷⁴, stage IV patients exhibit secondary metastatic tumors to the lung, liver, bones or brain and are refractory to traditional chemotherapy³⁷⁵. As a result, while 5-year and 15-year survival rates are very good in stage I patients (97% and 85% respectively), they plummet to only 15% and 5%, respectively in patients with stage IV melanoma^{179,372}. Besides UV radiation, the primary environmental factor predisposing to cutaneous melanoma, the other genetic and molecular factors that are involved in the genesis of the disease remain to be fully characterized³⁷⁶. Hence, understanding the molecular and signaling mechanisms leading to melanoma development and progression is essential to help in developing better targeted treatments.

Melanoma tumorigenesis results from mutations in genes implicated in the regulation of various biological processes, such as cell growth and proliferation (BRAF, NRAS, NF1, PTEN and KIT), apoptosis (TP53) and cell immortalization (hTERT)^{377,378}. While mutations in the mitogenic RAS-RAF-MEK-ERK signaling pathway are very frequent, other signaling pathways, such as Jnk/c-Jun, Wnt, NF- κ B, PI3K/AKT, JAK/STAT and TGF β have also been implicated in the tumorigenesis process³⁷⁹⁻³⁸². The TGF β signaling pathway plays an essential role in both normal melanocytes and melanoma. TGF β signals through a complex of 2 serine/threonine kinase receptors and intracellular Smad proteins (Smad2, 3 and 4). In melanoma, the TGF β /Smad3 signaling pathway acts as a strong tumor suppressor by blocking cell growth and immortalization, cancer stem cell self-renewal activities and by inducing cell death and autophagy^{80,82,383,384}.

Multiple endocrine neoplasia type 1 (MEN1) is an autosomal dominant disorder affecting the endocrine system characterized by the concomitant existence of tumors in the pancreas as well as the parathyroid and anterior pituitary glands. The Multiple endocrine neoplasia type 1 gene (*MEN1*) encodes menin, a 610-amino-acid protein which interacts with numerous protein partners including several transcription factors^{148,385}. Menin plays a significant role in cell cycle regulation by inducing cyclin-dependent kinase inhibitor (*CDKI*) gene expression^{386,387}. Interestingly, menin was found to leverage TGF β signaling at a transcriptional level thus facilitating its cytostatic and differentiation functions^{317,388}. Notably, non-endocrine tumors have also been reported in *MEN1* patients. These include skin tumors of mesenchymal origin such as angiofibroma, collagenomas, lipomas, as well as malignant melanomas³⁸⁹⁻³⁹¹. Loss of heterozygosity in 11q13 were detected in six melanoma tumors and deletion in the *MEN1* locus was found in 19 cases of sporadic metastatic melanoma. Another study implied that multiple melanoma tumor suppressors are

localized in chromosome 11q, which incidentally includes the *MEN1* region, thus raising the possibility of an association between *MEN1* and melanoma³⁹².

In this study, we identified TGF β /Smad3/*MEN1* signaling axis as a potent tumor suppressor pathway in cutaneous melanoma. Moreover, genetic analysis of two *MEN1* kindreds affected by melanoma also revealed the presence of specific point mutations within the *MEN1* gene. We found these point mutations to induce *MEN1* gene product degradation, further leading to a loss of TGF β signaling. Moreover, we show that targeting the co-chaperone of the proteasome degradation pathway, CHIP could restore menin expression and TGF β signaling in these melanoma cells. Together, this study defines the TGF β /*MEN1* axis as a potent tumor suppressor pathway in cutaneous melanoma and provides novel perspectives for tailor-made targeted remedies of this highly lethal malignancy.

3.3 Material and methods

Reagents: Recombinant human TGF β (Peprotech, Canada), Tissue culture medium RPMI1640, DMEM (Hyclone Logan, USA), Fetal Bovine Serum and Penicillin/Streptomycin (GIBCO), Branched Polyethyleneimine (Sigma), MMLV reverse transcriptase and random primers (Life Science, USA). Control siRNA sc-37007 and CHIP siRNA, sc-43555 (Santa Cruz, CA, USA). Missense mutations were generated with the Quik Change Site-Directed Mutagenesis kit from Stratagene (La Jolla, CA, USA),

Antibodies:

β -tubulin (3F32G) (Santa Cruz); anti-Flag M2 monoclonal antibody (Sigma); MEN1 (2605) (Abcam); P21 (C-19) (Santa Cruz, Cat#sc-397); SMAD2-3(Santa Cruz, Cat#sc-6032); SMAD4 (Santa Cruz, Cat#sc-7966) Caspase-3 (H-277) (Santa Cruz Cat#sc-7148); c-myc (9E10) (Santa Cruz Cat#sc-40)

Cell Lines: Cell lines were cultured at 37°C, 5% CO₂ in RPMI1640 (BLM, DAUV, WM278, WM1232) or DMEM (HEK293 and a375m) medium supplemented with 10% FBS and 1% penicillin/streptomycin.

TGF β Treatment: Cell monolayers were grown in complete medium to 60% confluence, starved overnight in serum-free medium (0% FBS), and treated with a final concentration of 200pM of human recombinant TGF β 1 for the indicated time periods.

Quantitative real-time PCR

Total RNA was extracted using Trizol™ (Invitrogen, Canada). RNA was reverse transcribed using M-MLV reverse transcriptase and random primers (Invitrogen) as per manufacturer's protocol. Amplification of cDNA was performed by quantitative real-time PCR (qPCR) SsoFast™ EvaGreen® Supermix (Bio-Rad, ON, Canada) using Rotor-Gene™ 6000 Real-time Analyzer (Corbett Life Sciences, USA). Human GAPDH was used as a housekeeping gene. Primer sequences are listed in the table below:

Gene		Sequence
MEN1	forward	5'- GGAAGACGACGAGGAGATCTACA-3'
MEN1	reverse	5'- CAGTAGTTCAGAGGCCTTTGCGCT-3'
GAPDH	forward	5'-GCCTCAAGATCATCAGCAATGCCT-3'
GAPDH	reverse	5'-TGTGGTCATGAGTCCTTCCACGAT-3'

Cell Proliferation Assay: Melanoma cells (WM278) grown in a 6-well plate (1000 cells) in complete RPMI medium (10%FBS). Medium was replenished after 1 week and cells were fixed, stained (0.5% w/v crystal violet, 20% v/v methanol) at endpoint and washed with PBS.

Cell Cycle Analysis: Cells were stimulated or not with TGF-β (200 pM) for 24hrs or 48hrs, in 1% FBS. Cells were washed and resuspended in PBS at 1X10⁶ cells/mL and fixed in ice-cold by drop-wise addition of ethanol 70% while vortexing. Incubation on ice was made for 30 minutes after fixation. When ready for analysis, cells were resuspended in a solution containing 50 µg/ml propidium iodide, 50 µg/ml RNase A, HEPES 10mM pH 7.4, CaCl₂ 2.5mM and NaCl 140mM. An incubation at 15 minutes at room temperature is followed. Cell cycle analysis was measured using BD FACSCanto flow cytometer and analyzed by FACS Diva (BD Biosciences, Canada) and FlowJo V10 Software (FlowJo LLC, USA).

Immunoblotting: Cells were lysed at 4°C for 15 minutes in RIPA buffer (1 mM DTT, 1 mM EDTA, 1 mM EGTA, 150 mM NaCl, 50 mM Tris-HCl pH 7.4, 1% Triton X-100) supplemented with protease inhibitors (10 µg/ml aprotinin and leupeptin, 2 µg/ml of pepstatin A, 1 mM PMSF). Total lysates were immunoblotted via SDS-PAGE using specific antibodies. Immunoreactivity was revealed by chemiluminescence using Clarity™ Western ECL Substrate and detected using ChemiDoc™ Imaging System. Densitometric analysis of protein levels was performed using Image Lab™ Software (Bio-Rad, Canada).

Lentiviral Generation and Infection: HEK293T cells were cultured in T75 flasks to 90% confluence using complete medium, transfected with either scrambled, *MEN1* shRNA and the packaging plasmids pMD2.G and psPAX2 using Opti-MEM® (Invitrogen) and branched polyethyleneimine (Sigma). Melanoma cells were grown in 6-well plates to a confluence of 70–80% confluence and infected with 100 µl lentivirus in presence of hexadimethrine bromide; polybrene (8 µg/ml). Cells were selected with 1 µg/ml puromycin for 3 days post infection.

Generation of *MEN1* CRISPR knockout cells: Guide RNAs (gRNAs) non-targeting control (SCR, scramble) or targeting *MEN1* or *Smad2/3/4* were cloned into a lentiCRISPRv2 plasmid for lentiviral packaging²⁵³. Melanoma cells were grown in 6-well plates to 50% confluence in antibiotic-free medium, infected with 100µl of lentivirus. For a375m and DAUV cell line, viral incubation was made overnight and medium was replenished the next day with fresh complete medium for 2 days. For BLM, WM1232 and WM278, cells were infected by spinfection (2 hours, 1500G and 33°C) and medium was replenished immediately after centrifugation and cells were let grown for 2 days. The pool of resistant cells forming the stable CRISPR knockout cells was expanded in complete medium (supplemented with 10% FBS) and selected with 0.5µg/ml (DAUV) or 1µg/ml (a375m, BLM, WM1232 and WM278) puromycin. Before proceeding with experiments, the knockout efficiency was verified using by Western blotting.

gRNA sequences

Gene		Sequence
MENsg1	forward	5'- CACCGCACCTGCTGCGATTCTACGA -3'
MENsg1	reverse	5'- AAACCTCGTAGAATCGCAGCAGGTGC -3'
MEN2sg2	forward	5'- CACCGACGTCGTCGATGGAGCGCAG -3'
MEN2sg2	reverse	5'- AAACCTGCGCTCCATCGACGACGTC -3'
SMAD2sg1	forward	5'- CACCGTCCCCTGATCTATCGTATT -3'
SMAD2sg1	reverse	5'- AAACAATACGATAGATCAGTGGGAC -3'
SMAD2sg2	forward	5'- CACCGTGGCGGCGTGAATGGCAAGA -3'
SMAD2sg2	reverse	5'- AAACCTTGCCATTCACGCCGCCAC -3'
SMAD3sg1	forward	5'- CACCGCCCATCGTGAAGCGCCTGC -3'
SMAD3sg1	reverse	5'- AAACGCAGGCGCTTCACGATCGGGC -3'
SMAD3sg2	forward	5'- CACCGTTCACGATCGGGGGAGTGAA -3'

SMAD3sg2	reverse	5'- AAACCTTCACTCCCCGATCGTGAAC -3'
SMAD4sg1	forward	5'- CACCGAACTCTGTACAAAGACCGCG -3'
SMAD4sg1	reverse	5'- AAACCGCGGTCTTTGTACAGAGTTC -3'

Luciferase Assay: Cells were transfected with 1.5 µg promotor luciferase reporter construct, 1.5 µg of β-galactosidase (pCMV-lacZ) expression vector and 9 µg of Polyethyleneimine (PEI) 25000. Cells were serum-starved in RPMI overnight and cultured with or without TGFβ (200pM) for 24h. Cells were washed in PBS and lysed in 100 µl of passive lysis buffer (25 mM glycyglycine, 15 mM MgSO₄, 4 mM EGTA, 1 mM DTT and 1% Triton X-100) on ice. Supernatants were collected by centrifugation (14,000 rpm, 10 minutes, 4°C). 45µL of the clear cell lysates were mixed with 5µL of the cocktail buffer (30 mM ATP, 100 mM KH₂PO₄ pH 7.8, 100 mM MgCl₂) and the luciferase activity was measured after injection of 50 µl of 0.25 mM D-luciferin using luminometer where the luminescence levels were expressed as relative light units (RLU). In parallel, 5µL of lysates were mixed with 45µL of ONPG (6 mg/mL) in β-Gal buffer (60 mM Na₂HPO₄, 40 mM NaH₂PO₄, 50 mM βME, 10 mM KCl, 1 mM MgCl₂) and incubated at 37°C for 1 hour. The OD was measured at 420 nm and the normalized luciferase activity of each lysate was calculated by dividing the RLU value of the luciferase activity by the corresponding β-galactosidase activity of the co-transfected β-gal vector.

Subcutaneous Tumor Xenografts: Male NSG mice were bred from mouse breeding pairs that were purchased from The Jackson Laboratory and were used for the experiments at the age of 7 weeks. The mice were housed and handled in accordance with the approved guidelines of the Canadian Council on Animal Care (CCAC) under the conditions and procedures approved by the Animal Care Committee of McGill University (AUP # 7497).

For tumor xenografts, the mice were randomized into two groups that respectively received 1x10⁶ MEN or scrambled knockout stable cells (BLM, WM1232 and WM278) per mouse by subcutaneous route. Tumor volumes were calculated according to the formula below and tumor growth curves were generated.

$$\frac{4}{3} * \pi * \left(\frac{Length}{2}\right) * \left(\frac{Width}{2}\right)^2$$

Sequence Analysis of the *MEN1* Gene—Leukocyte DNA was isolated by standard techniques. Exons 2–10 of the *MEN1* gene were amplified as described previously³⁹³. Gel-purified PCR products were directly sequenced.

Statistics: Data were collected from three or more independent experiments, expressed as the arithmetic means, all error bars are standard errors of means (SEM). Statistical analysis was done using Student *t*-test or ANOVA one way comparing TGFβ-treated to non-treated control (**p* < 0.05, ***p* < 0.01, ****p* < 0.001).

Ethics: Informed consent was obtained from each patient or subject, and the study was conducted according to a protocol that was approved by the IRCCS Casa Sollievo della Sofferenza Hospital, Research Ethics Board.

Animal work: All experimental protocols and procedures were performed in accordance with McGill University regulations. All preclinical experimental protocols and *in vivo* procedures were approved by McGill University (AUP # 7497).

3.4 Results

TGFβ induces *MEN1* gene expression in melanoma cells through Smad3.

MEN1 patients can develop other malignancies than the classical endocrine tumors, including skin tumors³⁹⁴. Previous work from our laboratory and others showed that the TGFβ signaling pathway acts as a potent tumor suppressor in melanoma^{80,82,383,384}. Thus, this prompted us to investigate whether *MEN1* could relay some of the TGFβ tumor suppressive response in melanoma. For this, we first investigated whether TGFβ could regulate *MEN1* gene expression in melanoma. A panel of human cutaneous melanoma cell lines with various pathological backgrounds were stimulated or not with TGFβ before assessing menin mRNA and protein levels by qPCR and Western blot, respectively. As shown in Fig.1A, TGFβ significantly upregulated *MEN1* at both protein (left panel) and mRNA (right panel) levels in all melanoma cell lines.

To then assess whether the Smad pathway was involved in the mediation of the TGFβ effects on *MEN1* gene expression, we next silenced Smad2, 3 and 4 expressions in DAUV, using CRISPR/Cas9 technology. Specific guide RNAs (gRNAs) targeting these genes were selected and efficiency of the Smad2/3/4 (Fig.1B) CRISPR-knockouts (KOs) was verified using Western blot. Interestingly, knocking out Smad3 and Smad4, but not Smad2 impaired TGFβ-mediated menin expression (Fig. 1C), indicating that TGFβ-induced *MEN1* gene expression is Smad3-

specific and Smad2-independent. Together these results highlight MEN1 as a novel TGF β /Smad target in melanoma, further suggesting that MEN1 may be acting downstream of TGF β in melanoma cells.

***MEN1* is essential for inhibiting melanoma cell growth and tumorigenesis.**

The TGF β /Smad signaling pathway exerts potent tumor suppressive activities in melanoma³⁸⁴. We thus investigated the role and contribution of *MEN1* downstream of TGF β -mediated growth inhibition. To this end, we generated *MEN1* CRISPR-KOs in WM278 melanoma cells (Fig. 2A) and assessed their effects on tumor cell growth *in vitro*. As shown in Fig.2B, we found that silencing MEN1 strongly increased cell growth. These results indicate that MEN1 exerts potent tumor suppressive activity in melanoma. We next investigated whether the tumor suppressive effects of the *MEN1* pathway could lead to inhibition of tumor formation *in vivo*, using preclinical models of melanoma. For this, we generated *MEN1* knockout models in three different melanoma cell lines (WM1232, BLM and WM278). The KO efficacies in all cell lines were verified by Western blotting (Fig.2C). Subsequently, MEN1 KOs and scr controls were transplanted subcutaneously in immunocompromised NOD/SCID/IL2R γ ^{-/-} (NSG) mice, as previously described. Interestingly, as shown in Figs. 2D-F, results showed that mice injected with the *MEN1* KO melanoma cells harbored significantly larger tumors than control animals. These results are consistent with our aforementioned *in vitro* data showing that *MEN1* is required for tumor growth inhibition. The significant increases in primary tumor formation observed *in vivo*, upon *MEN1* silencing further emphasize a central role for *MEN1* in mediating tumor suppression in melanoma.

The TGF β /Smad3/*MEN1* axis is essential for inducing cell cycle arrest and apoptosis in human melanoma cells.

TGF β exerts its tumor suppressive effects through regulation of cell cycle, apoptosis, autophagy and cell immortalization³⁹⁵. To gain further insights into MEN1 implication in cell cycle, we performed flow cytometry analysis of propidium iodide-stained scrambled and *MEN1* KO WM278 cells treated or not with picomolar concentrations of TGF β . Beforehand, all KOs efficiency was tested by western blotting (Fig.3A left panel). As shown in Fig.3A (right panel), we found that in control cells (SCR), TGF β significantly increased cell numbers in the G1 phase of the cell cycle, with a concomitant decrease in cell numbers in the S and G2/M phases. However, in MEN1 KO

cells, the TGF β -mediated increase in cells G1 was reduced while no TGF β -mediated decrease in cells in the S phase were observed, compared to scrambled. The Smad3 KO was used as a positive control and showed near complete blockage of the TGF β effects. The TGF β effects on cell cycle arrest are well characterized and involve up-regulation of several cyclin-dependent kinase inhibitors such as p21³⁹⁶ with a concomitant down-regulation of c-myc³⁹⁷. We thus next assessed the TGF β response on p21 expression in MEN1 or SCR KO cells. While we found TGF β to increase p21 gene expression in control (scr) cells, these effects were strongly reduced in the two MEN1 KO cell lines (Fig.3B, right panel). Efficacy of the MEN1 KO was assessed by western blot (Fig.3B, left panel). To further assess the regulatory role played by MEN1 on p21 and c-myc expression in a more clinically relevant system, we also examined p21 and c-myc expression levels in resected tumor samples from the MEN1 KO preclinical experiments (Fig.2). Interestingly, as shown in Fig.3C, MEN1 KO tumors exhibited significantly higher levels of c-myc and no detectable p21, compared to control tumors (scr). These data are consistent with what observed in vitro and collectively indicate that MEN1 is required for TGF β -mediated p21 increase, c-myc down-regulation and cell cycle arrest.

The TGF β tumor suppressor effects in melanoma not only involve cell cycle arrest but also induction of cell death by apoptosis³⁹⁸. To evaluate whether *MEN1* could also play a role in apoptosis, we assessed the TGF β effects on apoptosis, using annexin V staining. As shown in Fig.3D, TGF β treatment of WM278 melanoma cells led to an increase in apoptotic and dead cells, however these effects were partially reversed in the MEN1 KO cells, similar to what observed for the Smad3 KO. Looking at resected tumor samples from our in vivo transplantation experiments (Fig.2), we also found that MEN1 KO tumor samples exhibited lower caspase 3 levels, on average, compared to control tumors (Fig.3E). Taken together, these results strongly suggest that MEN1 acts downstream the TGF β signaling pathway to regulate cell cycle arrest and apoptosis in melanoma.

Identification of *MEN1* mutations in melanoma patients and loss of TGF β responses. To gain further clinical insights into the role and contribution of *MEN1* towards melanoma development, we identified melanoma patients carrying *MEN1* mutations. *Family 1* (Figure 4A, left panel): The proband, a 61-year-old male (individual II-2) was admitted for a follow up of pathologically diagnosed parathyroid carcinoma showing capsular invasion and infiltration into the esophagus.

Proband's serum ionized calcium (iCal, mmol/liter) was at 1.48 (normal range, 1.12-1.31) and PTH levels were at 286 pg/ml (normal range, 10-65). At surgery, a hyperplastic parathyroid gland was removed. Proband was heterozygous for a germline *MEN1* recurrent missense mutation D418N. This patient also developed *in situ* (scapula) melanoma. Assessment of first-degree relatives revealed the presence of hypercalcemia and hypercalciuria with high levels of PTH in the proband's brother (individual II-1) and daughter (individual III-1) and both were also heterozygous for D418N mutation and developed melanoma. Proband's brother was operated for melanoma and lipoma. *Family 2 (figure 4A, right panel)*: The proband (individual II-1), a 34-year-old female presented with serum ionized calcium (iCal, mmol/liter) was at 1.41 (normal range, 1.12-1.31) and PTH levels were at 215 pg/ml (normal range, 10-65). She was operated on for removal of a parathyroid adenoma. Proband was shown to be heterozygous for a novel germline *MEN1* deletion mutation, causing a frameshift leading to a truncated menin protein (c.628_631delACAG (p.D210Afs*18). This change was not found in 100 *MEN1* gene alleles from 50 unrelated normal individuals. The proband also developed melanoma *in situ* (arm) and the father of the proband (individual I-1) deceased from melanoma.

To study the expression and activity of the patients *MEN1* mutations, we reproduced these patient's mutations (D418N, D210A) in the wild type (WT) *MEN1* cDNA, using *in vitro* site-directed mutagenesis. We also reproduced other well-characterized *MEN1* mutations (L22R, I86F, Δ 184-218, A242V) as controls. Of these L22R and I86F mutants were previously shown to be unstable and were used here as positive controls, while mutants (Δ 184-218 and A242) for which expression is stable were used as negative controls^{399,400}. As shown in Fig.4B, while WT *MEN1* and the positive controls (Δ 184-218 and A242V) were all well expressed when transiently transfected in HEK293 cells, missense mutants (D418N and L22R) were expressed at much lower levels while frameshift mutant D210A was not expressed. Previous studies showed that missense *MEN1* mutants can be targeted to degradation via the ubiquitin-proteasome pathway³⁹⁹⁻⁴⁰¹. Thus, our results suggest that the *MEN1* mutation characterized in family 1 (proband individual II-1) may lead to the production of unstable *MEN1* products, further leading to their rapid degradation and further loss of the TGF β transcriptional responses. As for mutant D210A from family 2 (proband individual II-1), the frameshift mutation leads to a truncated menin product lacking more than 50% of the protein, including the nuclear localization signals. As such, that product is predicted to be rapidly degraded and to unstable⁴⁰² and as a result cannot be overexpressed (Fig.4A).

To start addressing this, we first reduced *MEN1* WT expression levels, using a shRNA knockdown (KD) strategy in WM278 melanoma cells. As shown in Fig.4C, the efficiency of the lentiviral infection and *MEN1* shRNA knockdown were ensured at both mRNA and protein levels, using qPCR and Western blotting, respectively. Moreover, as shown in Fig.4C, right top panel), decreasing *MEN1* levels significantly reduced the TGF β transcriptional responses on 2 different luciferase reporter constructs (CAGA and 3TPLux). To then address whether the mutants *MEN1* could rescue the KD phenotype, WT and missense mutant D418N were transiently transfected in the WM278 KD cells. As shown in Fig.4B (right panel, bottom), while overexpression of WT *MEN1* was able to restore TGF β -induced luciferase activity on both promoter constructs, overexpression of the missense mutant D418N failed to do so, presumably due to instability and rapid degradation. Similar results were obtained when knocking down *MEN1* in WM793B cells (Fig.4D). These results indicate that the *MEN1* mutant D418N is functionally inactive in relaying the TGF β transcriptional responses.

Expression and activity of *MEN1* missense mutants can be partially rescued by a proteasome inhibitor. Having shown that the *MEN1* mutant D418N failed to restore TGF β signaling, we next investigated whether blocking its degradation could restore the TGF β responses and tumor suppression. The proteasome inhibitor PS-341 (Velcade, Bortezomib) is in clinical use for relapsed multiple myeloma and exhibits favorable selectivity towards tumor over normal cells⁴⁰³. As shown in Fig.5A, blocking the proteasome with the PS-341 inhibitor (4 hours at 90nM) partially restored menin missense mutant D418N expression as well as mutant L22R, used here as a positive control. As expected, PS-341 showed no effect on WT or stable menin mutants (A242V and Δ 184-218). To then examine whether blocking the proteasome could offer some therapeutic value for those patients harboring *MEN1* mutations, we examined whether expression of the unstable *MEN1* mutants and TGF β transcriptional responses could be rescued using the proteasome inhibitor. For this, we used the melanoma cell lines engineered above (Fig.5C, 5D; cells depleted for endogenous *MEN1*, overexpressing WT or mutant *MEN1*). KD cells were then transfected with the 3TPLux luciferase reporter before being stimulated by TGF β . As shown in Figure 5B (upper panels), in control WM278 *MEN1* KD and WM793B *MEN1* KD melanoma cells, the TGF β transcriptional response was enhanced in cells overexpressing the WT menin, relative to empty vector, whereas no difference was observed in cells overexpressing *MEN1* mutants, confirming that the mutants

fail to relay the TGF β responses. Interestingly, when performed in WM278 *MENI* KD and WM793B *MENI* KD cells treated with PS-341 for 6hrs (Fig.5B, lower panels), the WT and the unstable *MENI* mutants (D418N and L22R) were able to partially restore the TGF β responses, consistent with the partial restoration of *MENI* mutant's expression (Fig.5A). As expected, the negative control (stable mutant (Δ 184-218)) showed no effect. Thus, blocking the proteasome degradation pathway using a specific chemical inhibitor can restore both *MENI* expression and TGF β response.

Expression and activity of *MENI* missense mutants can be rescued by inhibition of the ubiquitin ligase CHIP. In parallel and to more specifically block the proteasome degradation pathway, we knocked-down expression of the C terminal Hsp70 binding protein (CHIP) in melanoma cells. CHIP acts as a co-chaperone that can interact with the molecular chaperones Hsp70 and Hsp90, further leading to unbalancing the folding-refolding machinery towards the degradation pathway⁴⁰⁴. Interestingly, blocking the proteasome through silencing CHIP gene expression using a specific siRNA completely restored expression of the two *MENI* mutants (DN418 and L22R), while showing no effect on WT and stable *MENI* mutants (Fig.6A, left panel). Efficiency of the CHIP siRNA KD was verified by Western blot (Fig.6A, right panel).

We next examined whether missense *MENI* mutant expression and TGF β transcriptional responses could be rescued by silencing CHIP expression. WM278 *MENI* KD and WM793B *MENI* KD were co-transfected with a scrambled (control) or CHIP specific siRNA and the 3TPLux luciferase reporter before being stimulated by TGF β . As shown in Fig.6B (upper panels), only WT *MENI* could induce TGF β -mediated luciferase activity in control WM278 *MENI* KD and WM793B *MENI* KD melanoma cells, consistent with results observed with the proteasome inhibitor. However, as shown in Fig.6B (lower panels), both WT and missense *MENI* mutants (D418N and L22R) were able to almost completely restore the TGF β responses, while the negative control (Δ 184-218) showed no effect.

Altogether, these results indicate that the loss of TGF β tumor suppressive responses in patients harboring *MENI* mutation leading to *MENI* degradation could be circumvented by blocking the proteasome degradation pathway, thereby offering new therapeutic opportunity for these patients with melanoma.

3.5 Discussion

This study highlights *MEN1* as a potent tumor suppressor pathway, efficiently blocking tumorigenesis in cutaneous melanoma. Identification of specific point mutations in *MEN1* kindreds affected by melanoma also revealed increased *MEN1* gene product degradation, further leading to a loss of TGF β signaling. Using pharmacological inhibitors and RNA interference strategies we show that we could efficiently restore both *MEN1* gene expression and TGF β signaling in melanoma cells. Our findings indicate that the use of currently FDA-approved drugs against proteasomal degradation and/or tailor-made therapies mimicking the TGF β /Smad3/*MEN1* signaling pathway would be of great benefit to melanoma patients, efficiently preventing the initial tumor formation/progression and further hindering the spread of metastatic tumors to secondary organs.

Previous work highlighted *MEN1* as a downstream TGF β signaling component, regulating cell growth and proliferation in pituitary adenoma cells and osteoblasts^{317,405,406}. The present study expands on this, highlighting *MEN1* as a potent tumor suppressor, downstream of TGF β in non-endocrine tumors, such as melanoma. Results from our *in vivo* preclinical models clearly indicate that the *MEN1* knockout leads to increased primary melanoma tumor growth. Thus, *MEN1* appears to function as a potent regulator of tumorigenesis process in multiple tissues, of endocrine and non-endocrine origins, further increasing the broad range of biological processes regulated by *MEN1*. While TGF β was found to exert a dual role and promote metastasis in breast cancer⁴⁰⁷⁻⁴¹⁰, TGF β signaling exhibit anti-metastatic properties in uveal melanoma⁴¹¹, retinal Müller glia⁴¹² and cutaneous melanoma. Thus, new therapeutic strategies aiming at activating the TGF β /*MEN1* signaling pathway could prove useful for melanoma patients at different stages of the disease, including primary tumor formation.

It is interesting to note that multiple potential melanoma tumor suppressors are localized in chromatin 11q, which includes the *MEN1* region (located on chromosome 11q13), thus raising the possibility of an association between *MEN1* and melanoma. In confirmation of this, our study clearly highlights menin as being a major determinant in melanoma tumorigenesis. Furthermore, we report here two kindreds with melanoma in which at least two first-degree family members have been tested positive for *MEN1* mutations. Interestingly, in addition to exhibiting the typical *MEN1* set of endocrine tumors, these patients also developed melanoma, thereby highlighting *MEN1* as strong candidate gene for familial malignant melanoma (referring to families in which 2

or more first-degree relatives, such as a parent, sibling, and/or child, exhibit skin cancer)^{141,392}. As such, on the clinical side, we suggest patients to be tested for potential *MEN1* gene mutations, whenever 2 or more family members have developed melanoma. Moreover, melanoma being a deadly disease, our study suggests that patients being tested positive for *MEN1* mutations are at risk and should be monitored for melanoma.

Characterization of the *MEN1* gene in two kindreds bearing melanoma highlighted specific *MEN1* mutations, leading to loss of expression or increased degradation of the *MEN1* gene product, further leading to a loss of TGF β signaling. It is interesting to note that twenty percent of *MEN1* cases are menin missense, small deletion or insertion mutations. Results from this study and work from others revealed that most of these mutants are expressed at markedly reduced levels relative to the wild-type menin. We found that blocking the proteasome degradation pathway, using specific proteasome inhibitor (PS-341, Velcade, bortezomib) or using RNA interference strategy aiming at silencing expression of the molecular cochaperone CHIP, efficiently restored *MEN1* expression and the TGF β transcriptional responses. Specific gene silencing has the potential to provide additional therapies to those currently available for the treatment of melanoma. The use of small chemical inhibitors appears also very promising for melanoma treatment. The proteasome inhibitor PS-341 (Velcade, bortezomib) used in this study is already in clinical use for relapsed multiple myeloma^{403,413}. Although it is appreciated that proteasome inhibitors have multiple effects on apoptosis and cell proliferation, the present study provides proofs of principle that future exploration of their use to treat subsets of *MEN1* cases is warranted.

3.6 Acknowledgements

The authors are grateful to Dr. Alan Spatz and Dr. Louise Larose for kindly providing the melanoma cell lines. This work was supported by grants from the Canadian Institutes for Health Research (CIHR to JJJ).

Authors' contributions

JB and LC performed most of the experiments and analyses, MG performed Western blotting, NW and JB performed the *in vivo* work. VG, ASS and AS characterized the MEN1 mutants and collected the clinical patient data. SA, GH and JJJ supervised and designed the study. JB, MG, LC and JJJ wrote the manuscript.

3.7 Figures of chapter 3

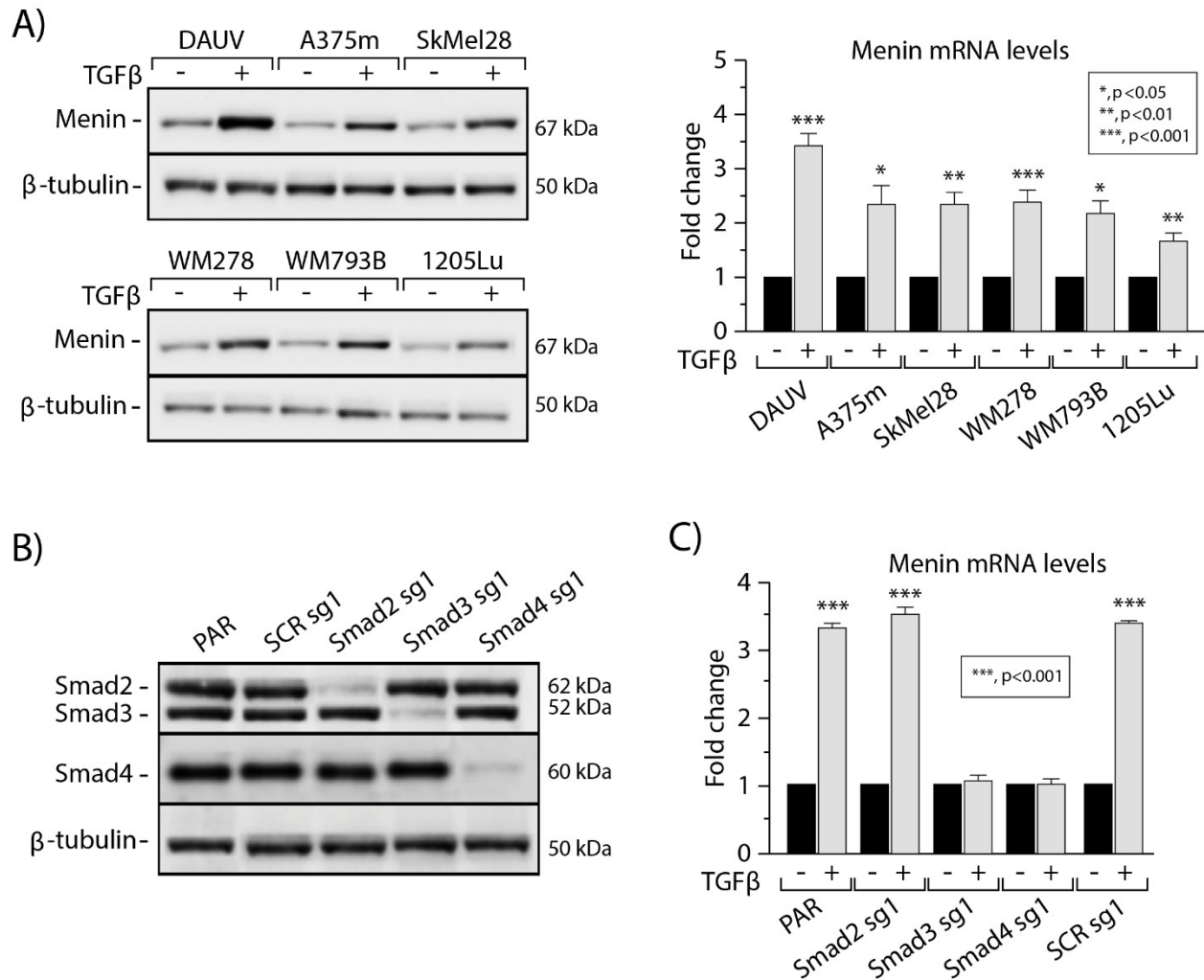


Figure 3.1. TGFβ induces *MEN1* gene expression in melanoma cells through Smad3.

(A) Regulation of Menin Protein (left panel) and mRNA (right panel) in human melanoma cell lines. Changes in Menin protein and mRNA expression following TGFβ treatment at 200pM, for 24h. Menin and β-tubulin protein expression was determined by western blotting. *MEN1* mRNA levels were determined by qPCR with *GAPDH* as reference gene. (B) Generation of DAUV melanoma CRISPR/Cas9 *SMAD2/3/4* and control (SCR, scrambled) knockout (KO) cell line. Efficiency of knockout was assessed using Western blotting. (C) *MEN1* mRNA expression levels of DAUV CRISPR/Cas9 *SMAD2/3/4* and control (SCR, scrambled) KO cells. *MEN1* mRNA levels were determined by qPCR with *GAPDH* as reference gene.

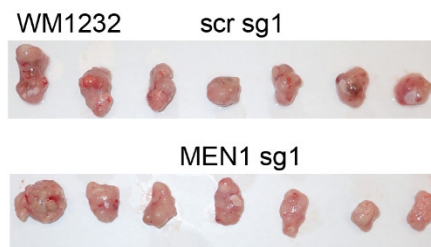
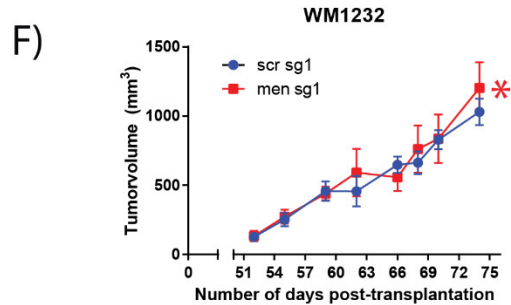
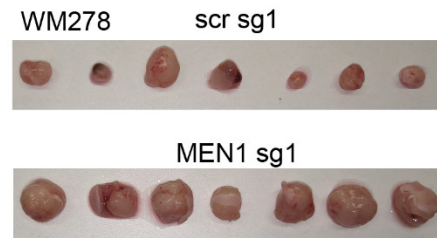
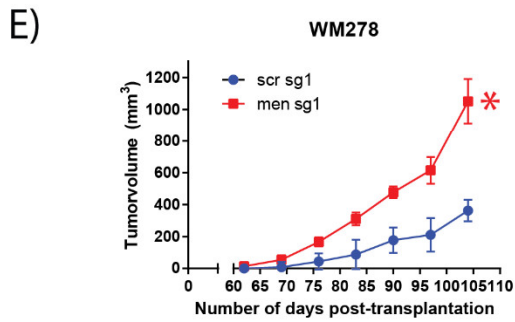
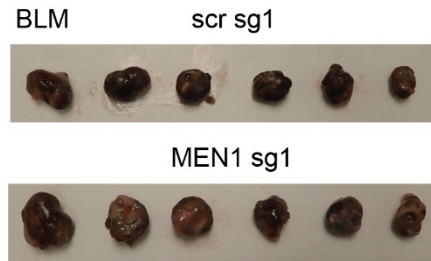
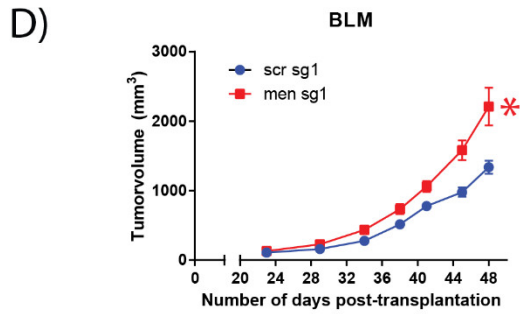
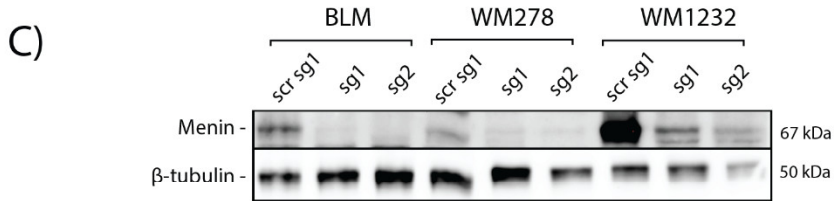
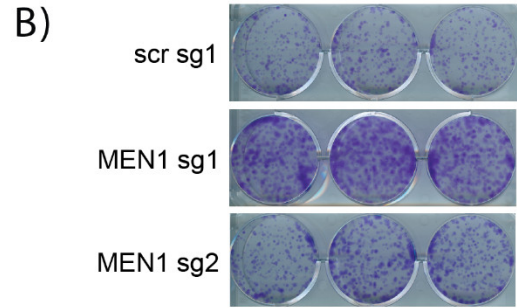
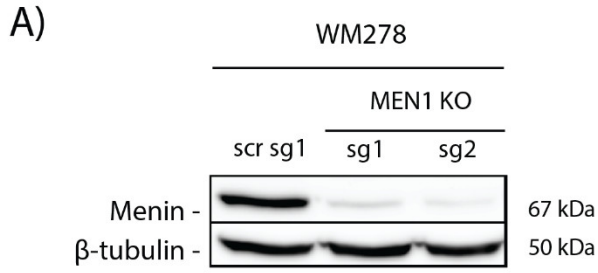


Figure 3.2. The TGF β /Smad3/*MEN1* axis is essential for inhibiting melanoma tumor formation *in vivo*.

(A) Generation of WM278 melanoma *MEN1* KO and control (SCR, scrambled) CRISPR/Cas9 knockout (KO) cell line. KO efficiency of *MEN1* was measured by western blotting. (B) Cell growth assay of WM278 cultured for 2 weeks, seeded at low density (100 cells/well). (C) Generation of BLM, WM278 and WM1232 melanoma CRISPR/Cas9 *MEN1* KO. KO efficiency was measured by western blotting. (D-F) NSG mice were injected subcutaneously with either BLM (Fig.2D) WM278 (Fig.2E) or WM1232 (Fig.2F) scrambled (SCR), or *MEN1* knockout melanoma cells at 1×10^6 cells/mouse. Shown in D, E and F, left panel is mean tumor volumes and right panel is representative images of tumors at the tumor collection endpoint.

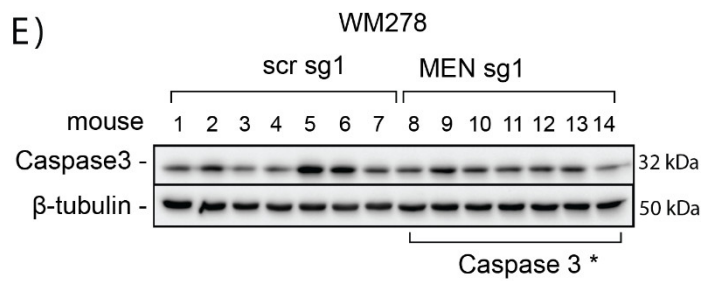
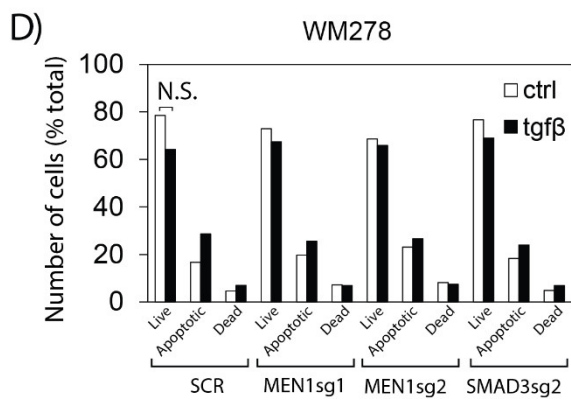
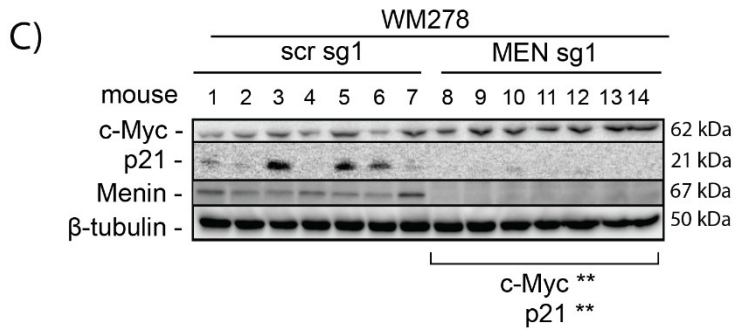
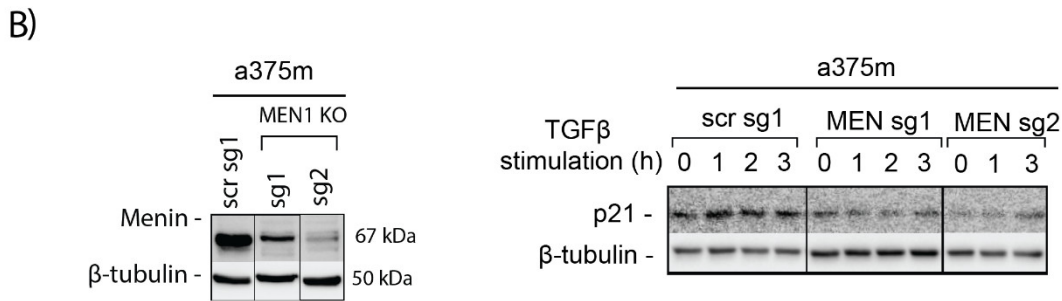
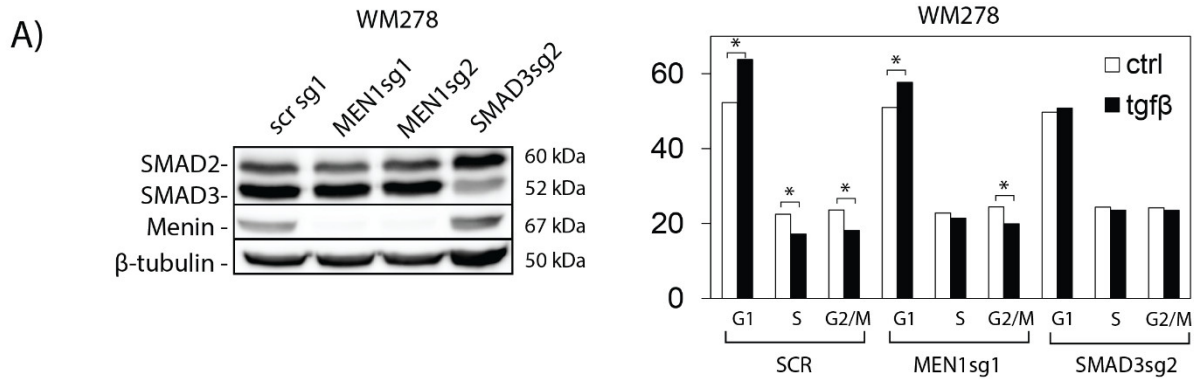


Figure 3.3. The TGF β /Smad3/MEN1 axis is essential for inducing cell cycle arrest in human melanoma cells.

(A). Cell cycle distribution assessed by flow cytometry analysis of propidium iodide stained WM278scrambled, *MEN1* KO and SMAD3 KO cells following TGF β treatment (24 hours). (B) (left Panel) Generation of a375m melanoma CRISPR/Cas9 *MEN1* KO. (Right panel) P21 expression upon TGF β short stimulation in WM278 CRISPR/Cas9 scrambled or *MEN1* KOs (sg10 and sg14). Gene expression was measured by western blotting. (C) Regulation of cell cycle expression in tumor tissues from WM278 CRISPR/Cas9 SCR (scrambled) or *MEN1* KO. Protein levels change was assessed through western blotting. (D) Annexin V assay indicated that the percentages of live, apoptotic and dead cells induced by TGF β treatment. (E) Regulation of Caspase 3 expression in tumor tissues from WM278 CRISPR/Cas9 SCR (scrambled) or *MEN1* KO. Protein levels change was assessed through western blotting.

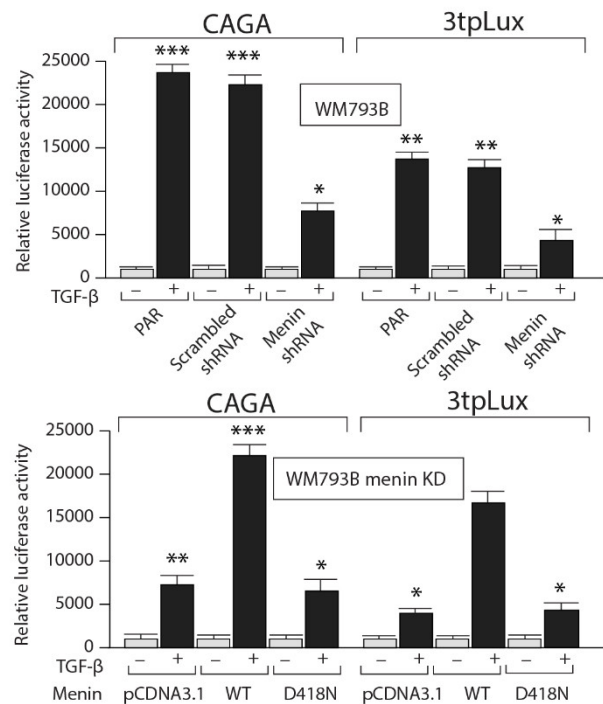
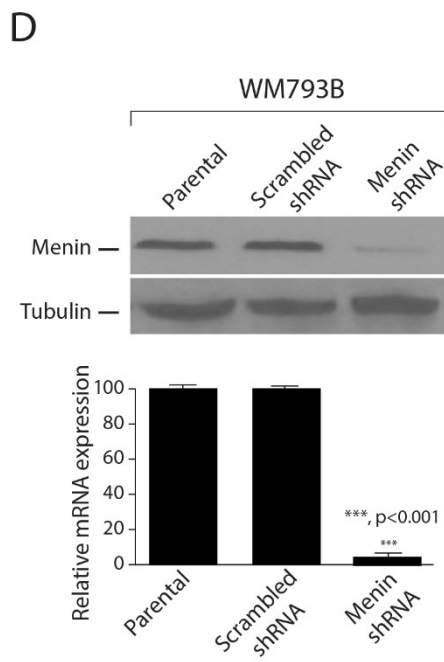
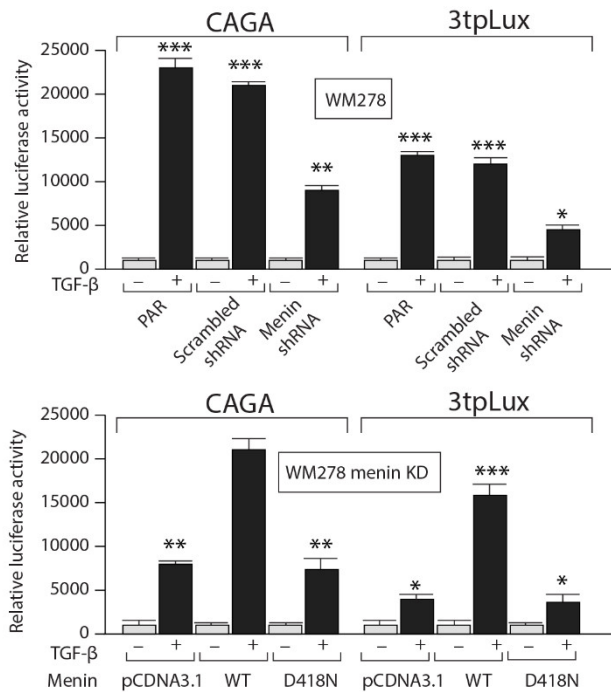
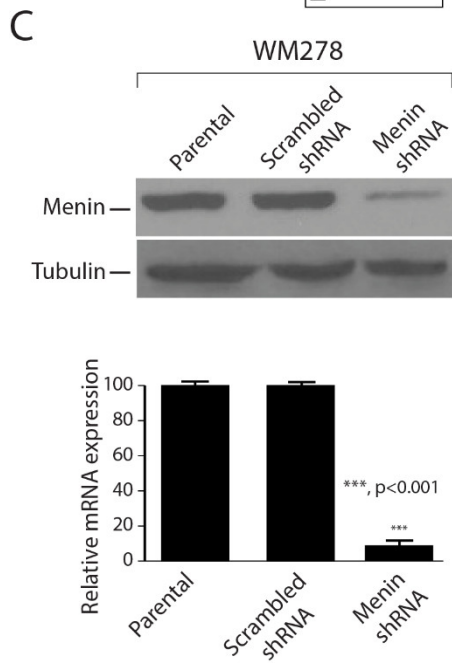
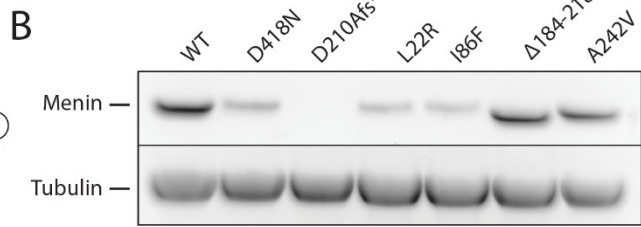
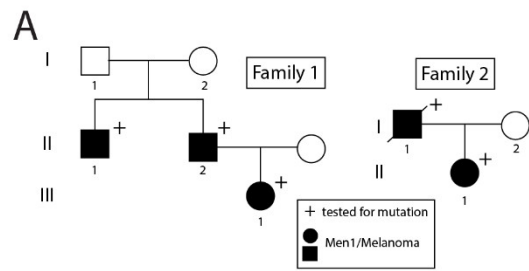
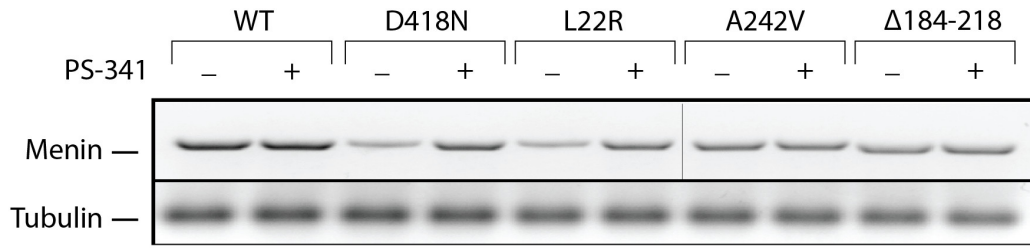


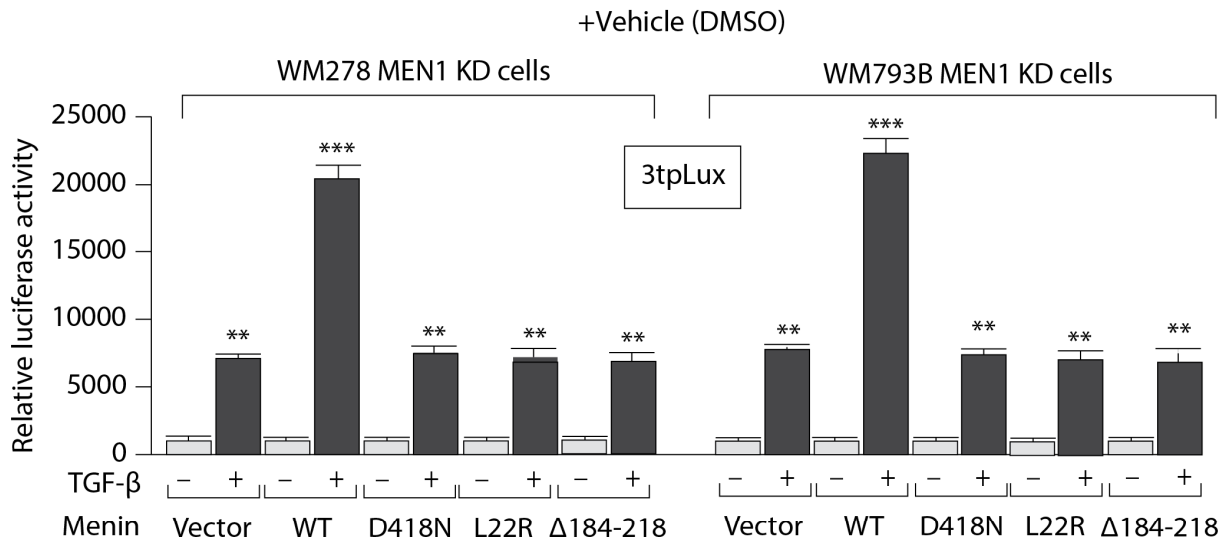
Figure 3.4. Expression of Menin mutants in HEK293 cells and generation of stable Men1 knock out melanoma cell lines

(A). Pedigrees of two MEN1 kindreds. (B). Flag-tagged menin WT and mutant constructs were transfected into HEK293 cells, and after 48 h, cell lysates were subjected to Western blot analysis with anti-Flag and anti- β -tubulin antibodies. (C). Efficiency of menin knockdown in WM278 parental and shRNA infected cells. Menin protein and mRNA (left panel) expression was measured by western blot analysis and qPCR. TGF β responsive CAGA and PAI-1 (3tpLlux) gene promoter activity in WM278 parental cells (right top panel) and WM278 Men1 KD cells (right lower panel). Data is graphed as the arithmetic mean of relative luciferase units normalized to β -galactosidase activity. (D). Efficiency of menin knockdown in WM793B parental and shRNA infected cells. Menin protein and mRNA (left panel) expression was measured by western blot analysis and qPCR. TGF β responsive CAGA and PAI-1 gene promoter activity in WM793B parental cells (right top panel) and WM793B Men1 KD cells (right lower panel). Data is graphed as the arithmetic mean of relative luciferase units normalized to β -galactosidase activity.

A



B



C

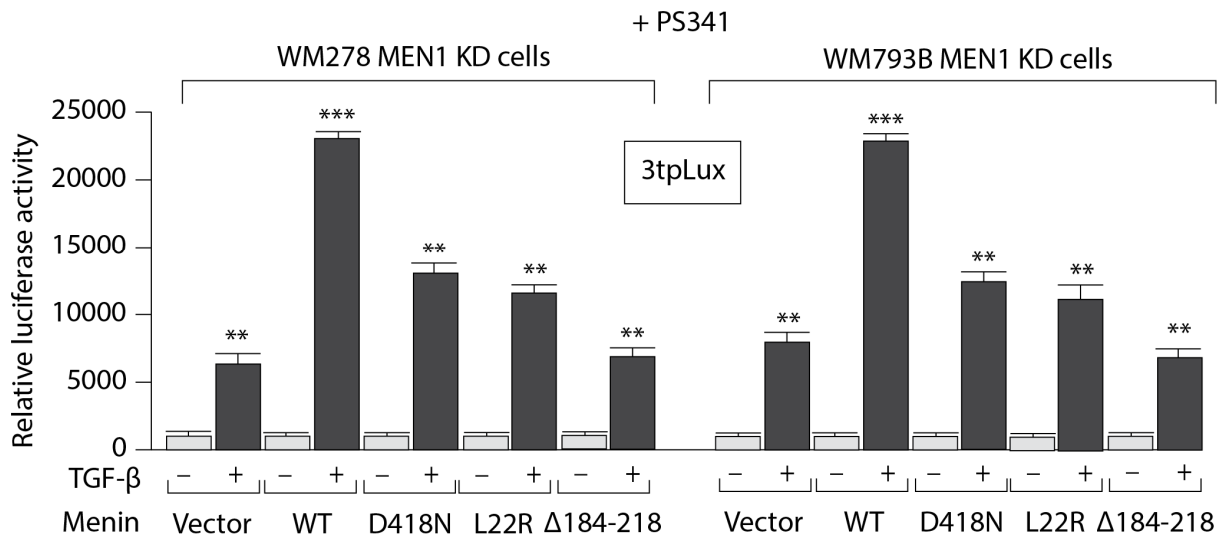


Figure 3.5. Expression and activity of menin missense mutants can be rescued by the proteasome inhibitor PS-341.

(A). Western blot analysis of HEK293 cells transfected with Flag-tagged Menin WT and mutants treated or not with PS-341 (Velcade). (B, C). TGF β responsive PAI-1 (3tpLux) gene promoter activity in WM278 and WM793B MEN1 KD cells treated with either vehicle or PS341. Data is graphed as the arithmetic mean of relative luciferase units normalized to β -galactosidase activity.

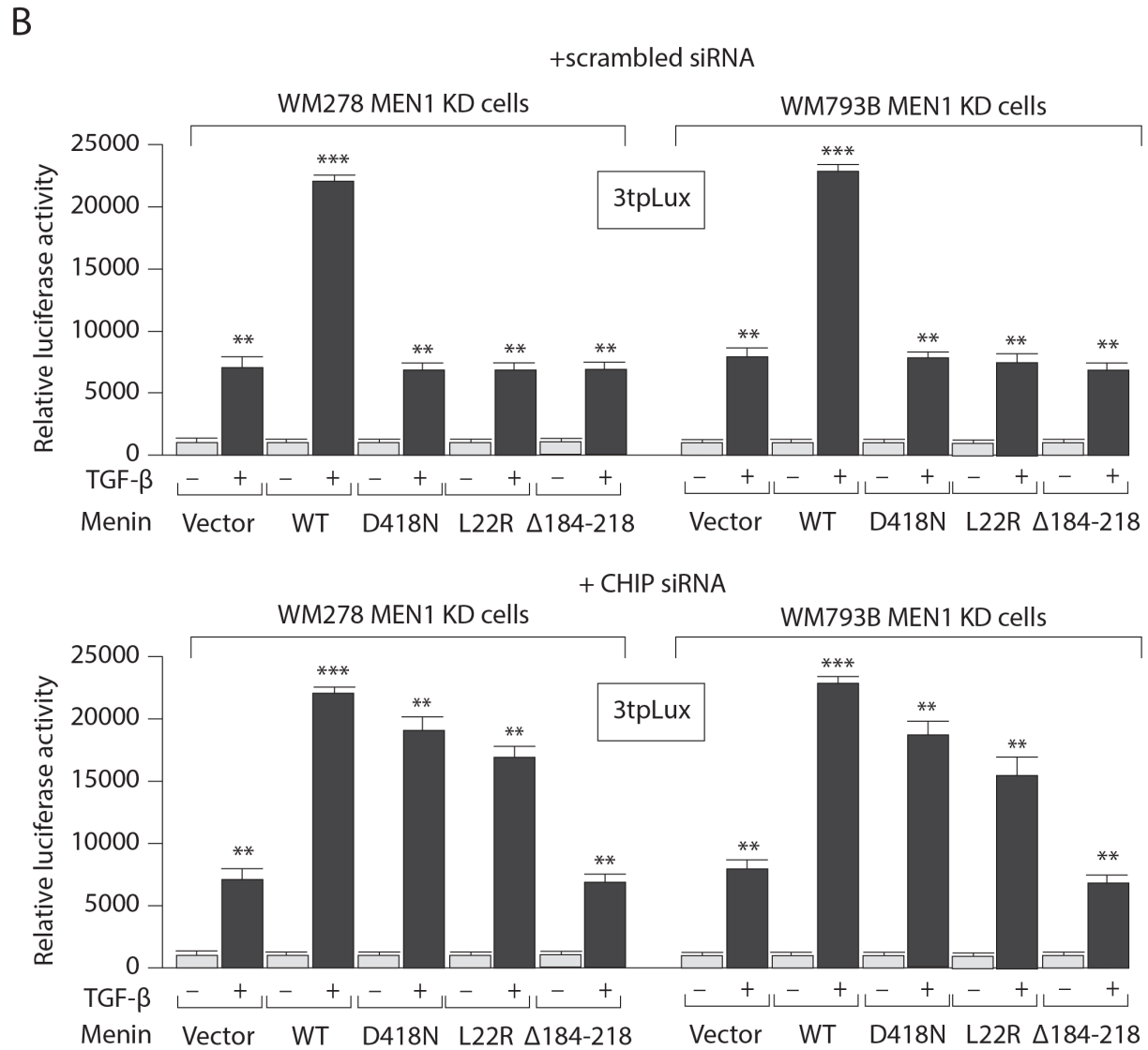
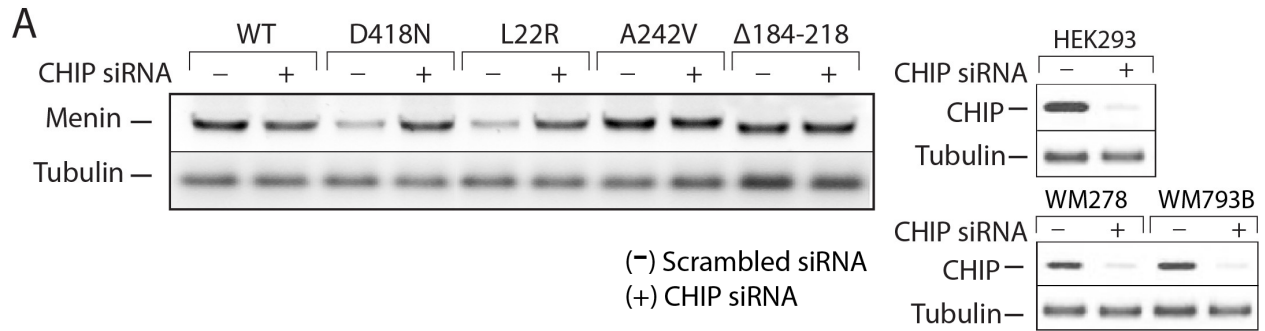


Figure 3.6. Expression and activity of menin missense mutants can be rescued by RNAi targeting of the ubiquitin ligase CHIP.

(A). Western blot analysis of HEK293 cells transfected with Flag-tagged Menin WT and mutants treated with scrambled or specific CHIP siRNA (left panel). Western blot analysis of CHIP in HEK293, WM278 and WM793 cells treated with scrambled or specific CHIP siRNA (right panel).

(B) TGF β responsive PAI-1 (3tpLux) gene promoter activity in WM278 MEN1 KD (upper panel) and WM793B MEN1 KD cells transfected with scrambled siRNA or specific CHIP siRNA. Data is graphed as the arithmetic mean of relative luciferase units normalized to β -galactosidase activity.

Chapter 4

***In vivo* genome wide CRISPR screen defines HSPE1 as a novel actionable cancer vulnerability in pancreatic ductal adenocarcinoma.**

Julien Boudreault, Ni Wang, Gang Yan, Meiou Dai, Sophie Poulet, Jean-Jacques Lebrun
Department of Medicine, McGill University Health Center, Cancer Research Program, Montreal,
QC, Canada.

4.1 Preface

Alongside with metastatic melanoma, which were presented in chapter 2 and 3, PDAC exhibits aggressive phenotypes and is a major cause of death in cancer patients. While advances in combination chemotherapy have improved median survival in treated patients, the long-term survival remains poor which emphasizes the need for novel therapeutic approaches. Thus, it is critical to define novel genes underlying PDAC tumorigenesis. Genetic CRISPR/Cas9 screens have proven to be a powerful tool to identify novel oncogenes, tumor suppressors and pathway implicated in cancer. We thus hypothesized that carrying out a CRISPR/Cas9 screen in an *in vivo* model of PDAC could identify novel regulators of PDAC tumorigenesis. This approach shows the potential for discovering novel targeted therapies, particularly in contrast to melanoma, where successful targeted therapies already target the MAPK/ERK pathway and utilize immune checkpoint therapy.

4.2 Abstract

Superior knowledge of cancer biology has enabled unprecedented innovations in therapies targeting mutated driver genes. Despite the attempt of targeting cancer-inducing genes such as KRAS, the life expectancy of patients diagnosed with pancreatic ductal adenocarcinoma (PDAC) has poorly improved. We performed an unbiased genome wide *in-vivo* loss-of-function CRISPR screen to discover novel oncogenes and identified heat-shock protein HSPE1, whose function is still unknown in PDAC. Depletion of HSPE1 expression reduced in PDAC cell growth in both *in vitro* and *in vivo* manner. We exploited this vulnerability by disrupting HSPE1 function by using KHS101, a validated HSPD1-HSPE1 complex inhibitor. Several PDAC cell lines cultured *in vitro* were sensitive upon KHS101 treatment and *in vivo* administration of KHS101 reduced tumorigenesis. In our PDAC experimental model, exposure to KHS101 or silencing HSPE1 led to reduced expression of several cell cycle regulators. Mechanistically, we found that silencing HSPE1 induced OPA1 cleavage in several PDAC cell lines. Moreover, OPA1 inhibitor MYLS22 significantly reduced PDAC tumor formation. Our findings highlight a new role underlying PDAC tumorigenesis for HSPE1 and could unlock a new area of research towards precision medicine.

4.3 Introduction

Ductal adenocarcinoma represents 90% of all malignant neoplasms of the pancreas and is the fourth highest cause of cancer death and is expected to rise to second place by 2040^{179,414}. Pancreatic ductal adenocarcinoma (PDAC) lacks early detection by advanced imaging or diagnostic biomarker⁴¹⁵, and exhibits resistance to chemotherapy, radiotherapy and immunotherapy⁴¹⁶. To date, complete tumor removal followed by chemotherapy is regarded as the only potential treatment for PDAC, even though only 20% of patients are eligible for initial surgical resection⁴¹⁷. Most patients are diagnosed with advanced metastatic pancreatic cancer and are treated with first-line chemotherapy treatment regimens⁴¹⁸. While various kinase inhibitors have been tested in alone or in combination with chemotherapy, the vast majority failed to yield significant patient survival improvements^{419,420}. Thus, there is an urge to find, develop and improve therapies aiming at efficiently targeting this type of aggressive cancer. The most frequently mutational events occurring in pancreatic cancer are the oncogenic activation of KRAS (over 90% of PDAC patients) and the loss-of-function of CDKN2A (encoding p16), TP53, and SMAD4, each of which is mutated in more than 50-80% of genotyped patients¹⁸³. Apart from these four common mutations, which are currently undruggable, other mutations have low prevalence, raising doubt about their clinical relevance¹⁷⁸. To thus overcome the lack of targeted therapies for treating PDAC patients, druggable key signaling hubs and cancer vulnerabilities must first be identified.

CRISPR/Cas9 (Clustered Regularly Interspaced Short Palindromic Repeats) emerged as a powerful tool to identify essential and context-dependent fitness genes in cancer cell lines²⁵⁹, as well as to uncover new cancer vulnerabilities^{253,270,286,421}. Large-scale CRISPR screens revealed networks of core and context-specific fitness genes in PDAC cell lines²⁸⁸. They also defined drug-resistance mechanisms to MEK^{422,423}, Wnt⁴²⁴ inhibition and chemotherapy^{425,426} and revealed several synthetic lethal interactions implicating known pharmacological inhibitors (MEK^{423,427}, PORCN⁴²⁸, PI3K⁴²⁹, Ras⁴³⁰, CDKs⁴³¹ and chemotherapy⁴³²⁻⁴³⁴).

Here, we performed an *in vivo* genome wide CRISPR screen, using a preclinical model of PDAC and uncovered novel pancreatic cancer vulnerabilities, underlying PDAC formation. In particular, we found HSPE1 (also known as Hsp10) as a potent tumor-promoter in PDAC. HSPE1 is a co-chaperone protein from the highly conserved heat-shock family proteins (HSPs) which binds HSPD1 (also called Hsp60) through a double-ring complex⁴³⁵. We showed that blocking expression of HSPE1 by means of CRISPR knockouts (KOs) strongly inhibited cell growth and

colony formation in pancreatic cancer cell lines. Using *in vivo* preclinical models of PDAC, we further showed that HSPE1 CRISPR-KO significantly impeded tumorigenesis *in vivo*. From the mechanistic angle, we showed that PDAC cells lacking HPSE1 expression exhibit decreased cell cycle regulators, particularly from the G2/M phase, further leading to increased cell cycle arrest and apoptosis. To further transition this discovery to clinical and patient-oriented settings, we investigated the therapeutic potential of KHS101, a small synthetic molecule, that targets the HSPD1-HSPE1 complex and impairs mitochondrial HSPD1 activity⁴³⁶. Interestingly, we found that KHS101 could induce cell cycle arrest and inhibit tumorigenesis in preclinical models of PDAC. At the molecular level, we found that OPA1 is a direct target of HSPE1, but not HSPD1 and that pharmacological inhibition of OPA1 significantly reduced tumor growth in PDAC. Therefore, pharmacological inhibition of HSPE1/HSPD1 complex and OPA1 highlights a potential new efficient targeted therapy for pancreatic cancer.

4.4 Material and methods

Cell lines: Cell lines were cultured at 37°C, 5% CO₂ in RPMI (BxPC3 and Mia-PaCa2), EMEM (HPAF-II) medium supplemented with 10% FBS (Gibco) and the human embryonic kidney cell line HEK293T was cultured in Dulbecco's Modified Eagle Medium (DMEM) supplemented with 10% FBS (Gibco).

Library preparation and sequencing. All PCR reactions were performed using Herculase II Fusion DNA Polymerase (Agilent) and the total number of reactions were based on extracted gDNA yields. PCR1 reactions were prepared by mixing 20 µL Herculase 5× Buffer, 1 µL of 100mM dNTP, 2.5 µL of Adapter Primer F, 2.5 µL of Adapter Primer R, 1 µL Herculase II Fusion Enzyme, 10 µg of the gDNA extracted and PCR grade water to a final 100 µL volume. PCR1 reactions were performed using a thermocycler (98 °C for 2 min, 98 °C for 10 s, 60 °C for 20 s, 72 °C for 30 s, and 72 °C for 2 min for 18 cycles). All PCR1 reactions were then pooled and kept at -20 °C. For PCR2, 8 reactions were performed for each sample in a total 100 µL volume (20 µL Herculase 5× Buffer, 1 µL of 100 mM dNTP, 2.5 µL of Adapter Primer F, 2.5 µL of Adapter Primer R, 1 µL Herculase II Fusion Enzyme, 5 µL of PCR1 amplicon and 68 µL of PCR grade water). PCR2 reactions were performed as described for PCR1. Final PCR products were run on a 2% gel and extracted and purified using the QIAquick PCR & Gel Cleanup Kit (Qiagen) and

subjected to next generation sequencing by Quebec Genome Center. 80 cycle and 20 million reads for each sample were performed by Hiseq 2500.

Genome-wide library lentiviral production and infection. Human genome-wide CRISPR/cas9 knockout pooled library GeCKOv2 was a gift from Feng Zhang (Addgene#1000000048). The amplification and virus production of GeCKOv2 library A were performed as described in the Addgene protocol²⁵³, cells were plated at a density of 3×10^6 cells per well in 12 well plates and polybrene was added to a final concentration of 8 $\mu\text{g}/\text{mL}$. Viruses were titered and optimal virus concentrations allowing for 30% cell survival were used. Following spinfection at $1000 \times g$ for 2 h at 32 °C, cells were incubated overnight, trypsinized, pooled, and transferred in T225 flasks at a density of 3×10^6 cells per flask. After 24 h, puromycin (1 $\mu\text{g}/\text{mL}$) was added for selection for 8 days. After 8 days, 30 million cells were frozen at -80 °C for genomic DNA extraction, referring as cell representation control (cell rep) and deep-sequencing. The remaining cells were prepared for transplantation in an animal model.

Bioinformatics. MAGeCK-VISPR (0.5.3)⁴³⁷ was used for mapping back the reads to sgRNA CRISPR library. Log₂ fold change (LogFC) was calculated to determine the change in abundance of each guide in each sample. Robust Rank Aggregation values (p values) were determined using the MAGeCK algorithm (version 0.5.3), as described in Li et al⁴³⁷.

Genomic DNA Extraction. Genomic DNA extraction for genome-wide knockout cells and tumor samples were performed as described in the study²⁷⁰. 30 million cells or 200 mg grinded tumor tissues from each sample were lysed in 6 mL of NK Lysis Buffer (50 mM Tris, 50 mM EDTA, 1% SDS, pH 8) and 30 μL of 20 mg/mL Proteinase K (Qiagen). Cell lysates were incubated at 55 °C for 1 h (cell pellet) and overnight for tumor tissues. RNase A (Qiagen) was added at a final concentration of 0.05 mg/mL and incubated at 37 °C for 30 min. The samples were then cooled on ice for 10 min prior to adding 2 mL of ice-cold 7.5 M ammonium acetate (Sigma). The samples were vortexed at high speed for 20 s and centrifuged at $4000 \times g$ for 10 min and supernatants were collected and mixed with isopropanol for DNA precipitation. Following centrifugation at $4000 \times g$ for 10 min, supernatants were carefully decanted, and pellets washed in 70% cold ethanol, air-dried and resuspended in 500 μL 1 \times TE Buffer at 65 °C for 1 h. The gDNA concentration was measured using the Epoch Microplate Spectrometer (ThermoFisher).

CRISPR knockout plasmid cloning. For knockout genes, LentiCRISPR v2 backbone vector was a gift from Feng Zhang (Addgene plasmid #52961). Cloning was performed as described in the

Addgene protocol²⁵⁴. Oligo sequences for sgRNAs KO targeting each gene listed in Supplementary Table 2. 5 µg LentiCRISPRv2 vector was digested and dephosphorylated by for 30 min at 37 °C with FastAP enzyme (ThermoFischer scientific). The digested plasmid was then gel-purified by QIAquick Gel Extraction Kit (Qiagen). The pair of oligos for each gene were phosphorylated and annealed using T4 PNK enzyme in a thermocycler by incubating 30 min at 37 °C and 5 min at 95 °C and slow-cooled to 25°C at 0.1°C/sec. Annealed oligos were diluted at 1:200 and ligated together with digested vector using Quick ligase (NEB) for 20 min at room temperature.

Lentiviral Generation and Infection: HEK293T cells were cultured in T75 flasks to 90% confluence using complete medium, transfected with either shRNA or CRIPSR constructs and the packaging plasmids pMD2.G and psPAX2 using Opti-MEM® (Invitrogen) and branched polyethyleneimine (Sigma). Cell culture medium with lentiviruses particles in cell culture medium was collected. Cells were grown in 6-well plates to a confluence of 70–80% confluence and infected with 100µl (SUM159, PC3) or 1mL (HPAF-II, BxPC3, Mia-PaCa2 or PANC-1) lentivirus in presence of hexadimethrine bromide; polybrene (8 µg/ml). Cells were selected and grown in medium supplemented with 1 µg/ml puromycin.

SURVEYOR assay. The genomic DNA cleavage assays for gene knockouts were performed using GeneArt Genomic Cleavage Detection Kit (Invitrogen) according to the manufacturer's protocol. Briefly, genomic DNA was extracted from 5 × 10⁵ lentiCRISPRv2-knockout bulk cells. Primers were designed to amplify the specific Cas9/sgRNA genetically modified region by PCR. The primer sequences are listed in Supplementary Table 3. The modifications (the insertion, deletion, or mismatched DNA) of the interested region from the PCR products were then cleaved and detected by the Detection Enzyme from GeneArt Genomic Cleavage Detection Kit.

Western Blot. At collection, cells were washed twice with ice-cold PBS (Wisent Bio), collected, and lysed in ice-cold cell lysis buffer (50 mM Tris-HCl, 150 mM NaCl, 1% Triton X-100, 1 mM EDTA, 100 mM Na₃VO₄, and 1× protease inhibitors, phosphatase inhibitor cocktails). The protein concentration of the supernatant was determined using the BCA Kit (ThermoFisher). Samples were boiled at 95 °C for 5 min in loading buffer (10% SDS, 0.313 M Tris-HCl, pH 6.8, 50% glycerol, 0.5% Bromophenol Blue, and 0.5 M DL-Dithiothreitol) prior to loading on gel. Following electrophoresis, proteins were transferred onto nitrocellulose (0.22µm for blots implicating low molecular weight HSPE1 protein and 0.45µm for all other blots) and blocked for

1 h (5% non-fat dry milk) at room temperature. Incubation with primary antibodies, listed below, was performed overnight at 4 °C. Following 1 h incubation with specific secondary antibodies, membranes were washed, revealed by ECL, and data analyzed using the ChemiDoc Touch Instrument (Bio-Rad). The antibodies used in the studies are β -tubulin, β -Actin, CDC25C, CDK2, CDK4 and CDK6 from Santa Cruz, HSPE1, HSPD1 from sigma and PLK1, CDK1 (*cdc2*), CyclinB1 from cell signaling.

Flow cytometry. Cell cycle analysis by PI staining: HPAF-II cells were starved in EMEM serum-free medium for 24h and replenished with medium supplemented with 1% FBS for 24h. Cells were washed and resuspended in PBS at 1×10^6 cells/mL and fixed in ice-cold by drop-wise addition of ethanol 70% while vortexing. Incubation on ice was made for 30 minutes after fixation. When ready for analysis, cells were resuspended in a solution containing 50 μ g/ml propidium iodide, 50 μ g/ml RNase A, HEPES 10mM pH 7.4, CaCl₂ 2.5mM and NaCl 140mM. An incubation at 15 minutes at room temperature is followed. Cell cycle analysis was measured using BD FACSCanto flow cytometer and analyzed by FACS Diva (BD Biosciences, Canada) and FlowJo V10 Software (FlowJo LLC, USA).

Apoptosis assay. HPAF-II cells were starved overnight in serum-free medium and replenished the next morning with EMEM-medium supplemented with 1% FBS and subjected to stain with Annexin V FITC and PI using Annexin V Apoptosis Detection Kit (Santa Cruz) for 15 min at room temperature according to the manufacturer's protocol. Percentage of Annexin V-/PI- (live cells), Annexin V+/PI- (apoptotic cells) or Annexin V+/PI+ (dead cells) was measured by flow cytometry FACSCanto II and quantified by FlowJo v10 software. Gating was performed with single-stained conditions (PI or Annexin V alone)

Xenograft transplantations. Genome-wide library infected HPAF-II cells (30×10^6 /mouse) were subcutaneously injected into the right flank of NSG mice. For individual gene knockout or activation validation, transduced HPAF-II knockout or activation cells (1×10^6 /mouse) were resuspended in serum-free EMEM medium and then inoculated in the right flank through subcutaneous injection, in 9-week old, male NSG mice to generate tumors. Tumor sizes were measured with a digital electronic caliper three times per week and allowed to reach maximum volume of 1000 mm³ prior to euthanasia. Tumor volumes were calculated according to the following formula: $[4/3 \times \pi \times (\text{length}/2) \times (\text{width}/2)^2]$ to generate a growth curve. For *in vivo* experiment, KHS101 was dissolved in a solution 2-Hydroxypropyl- β -cyclodextrin⁴³⁸ (15%) in

sterile saline solution. MYLS22 was dissolved in a solution of DMSO (10%), PEG300 (40%), Tween-80 (5%) and saline (45%).

Animal work (Ethics and housing): All experimental protocols and procedures were performed in accordance with McGill University regulations. All preclinical experimental protocols and *in vivo* procedures were approved by McGill University (AUP # 7497). Housing condition for mice: Temperature = 21°C; Humidity = 40–60%, Lighting = 12 h. ON / 12 h, OFF daily cycle.

Statistics: Data were collected from three or more independent experiments, expressed as the arithmetic means, all error bars are standard errors of means (SEM). Statistical analysis was done using Student t-test two way comparing control or experimental condition (* $p < 0.05$, ** $p < 0.01$, *** $p < 0.001$).

4.5 Results

In vivo genome-wide loss-of-function CRISPR screen in pancreatic cancer.

To identify new cancer vulnerabilities in pancreatic cancer, we performed an *in vivo* pooled CRISPR screen at the genome scale. For this, we used HPAF-II, a well-differentiated and highly tumorigenic human pancreatic carcinoma cell line. HPAF-II is known to maintain junctional complexes and apical basal polarity under cell culture conditions and thus, well reflects the epithelium of the pancreas *in vivo*^{439–441}. HPAF-II is also a good model to represent pancreatic cancer patients' populations. Even though WT for Smad4, HPAF-II cells carry an in-frame deletion of the tumor-suppressor CDKN2A/p16, a P151S mutation in the tumor-suppressor TP53 and a G12D mutation of the oncogenic KRAS gene⁴⁴².

As illustrated in Fig.1a, HPAF-II cells (3 independent biological replicates) were transduced with a pooled loss-of-function CRISPR library (GeckoV2 library A²⁵⁴), containing a total of 57,140 sgRNAs targeting 19,050 genes (3 sgRNAs per gene), 7,456 sgRNAs targeting 1,864 miRNAs (4 sgRNA per miRNA) and 1000 non-targeting-control (NTC). HPAF-II cells were infected with a multiplicity of infection of 0.3 so that cells will receive a single viral integration. For each biological replicate, 200 million cells were transduced to ensure a minimum library coverage of 300x. Puromycin selection (at 1µg/ml) carried on for 8 days before cells were subcutaneous transplanted in NOD scid gamma (NSG) mice. Tumor growth was allowed for a subsequent 30 days before resecting the tumors. An additional 30 million cells were used as the initial and unperturbed sgRNA distribution (referred to as Cell Rep1/2/3). Following tumor resection and

weight measurement (Fig.1b) genomic DNA was extracted for PCR amplification and next-generation sequencing. The sgRNAs were mapped (Supplemental Fig.1a) and their abundance and distribution were quantified using MaGeCK Robust Rank Aggregation algorithm, as previously shown^{286,443}. The sgRNA counts from tumors collected following the *in vivo* selection pressure (PDAC tumor samples) were compared to the cell representation (Cell Rep1/2/3) and normalized to the sum of all NTCs (Fig.1c). Notably, more than 99.9% of sgRNAs from Cell Rep1/2/3 samples and around 88% of sgRNAs from tumor samples were detected, indicative of both very good library representation and sufficient coverage (Fig.1d and Supplemental Fig.1b). The Gini Index, a measure of statistical dispersion, was less than 0.1 for the Cell Rep1/2/3 (Fig.1e), indicating an even distribution of the sgRNAs before applying the selection pressure. The Gini index in the tumor samples increased to 0.4, reflecting a successful *in vivo* selection pressure in the tumors (Fig.1e). The proper sgRNA distribution is also reflected in the shift observed in the log₁₀(read counts) cumulative distribution frequency curve of the sequenced sgRNAs, for both Cell Rep and tumor samples (Fig. 1f). Finally, as shown in Fig.1g, a high correlation was also observed between the Cell Rep samples, indicative of a strong similarity between biological replicates and highlighting the high consistency of the CRISPR screen.

In vivo CRISPR screen identifies tumor-promoting genes in pancreatic cancer.

The depletion and enrichment of specific sgRNAs enable robust identification of context-dependent tumor-promoting genes and tumor suppressors, respectively. As shown in Fig.2a (blue insert), we found 276 genes to be significantly depleted (FDR < 0.25). Loss of function for these genes negatively affected tumorigenesis, suggesting they exert potential oncogenic functions in PDAC tumor formation. Enriched sgRNAs, on the other hand correspond to candidate genes with tumor suppressive like activity. While we only found two genes (SMRC7 and NF2) in this category, this validated our screen and provided a proof-of concept (Fig.2a, red insert). Indeed, NF2 is a well characterized tumor suppressor and its inactivation is known to be tumorigenic in many cancer models⁴⁴⁴, including PDAC⁴⁴⁵. Interestingly, none of the 1000 NTC was ranked in either positive or negative selection, confirming that the perturbation is not caused by randomness.

The stringency of the CRISPR screen was further assessed by overlapping both common essential and non-essential reference genes from the Achilles dataset 20Q1 from DepMap database with our dataset. Common essential genes are required for cell survival and proliferation as opposed to non-essential genes, for which loss-of-function leads to unperturbed fitness^{259,446}. As further proof of concept, a total of 77 common essential genes were found in our 276 gene list, indicative of a strong selection pressure against inactivation of genes displaying reduced survivability phenotype (Fig.2b). As expected, only a few non-essential genes (7 genes) were found in our dataset. Using EnrichR⁴⁴⁷, a pathway enrichment analysis tool, we further found our 276 candidate genes to cluster in several crucial cellular processes such as RNA degradation/transcription, protein synthesis/export and cell cycle (Fig.2c). Among the top-ranking, we found the Wnt signaling pathway, highlighting the Wnt/ β -catenin dependency of HPAF-II cells for survivability. HPAF-II cells exhibit an inactivating mutation in the Ubiquitin E3 ligase ring finger 43 gene (RNF43) and are known to be dependent on ligand-induced Wnt/ β -catenin signaling and sensitive to PORCN inhibition¹⁹⁴. Indeed, RNF43 acts as a negative regulator of Wnt signaling and RNF43 mutations are found in 5-10% of pancreatic cancer tumors. Moreover, we found FZD5, a Frizzled receptor implicated in driving Wnt pathway, as a top candidate of our CRISPR screen. FZD5 was previously identified as a context-dependent fitness gene in RNF43-mutants cell lines⁴⁴⁸. These results highlight the robustness and consistency of the CRISPR screen and further define a 192 gene shortlist of potential tumor-promoting cancer vulnerabilities in PDAC tumors, after removing the 77 common essential and 7 non-essential genes (Fig.2b). For the validation process, we employed an unbiased 3-way parallel approach by selecting genes with the highest statistical ranking (Fig.2b; RSL24D1, PFN1, DDI2, RAB40B, CCR5), genes clustered in the Wnt pathway (Fig.2c; FZD5, SKP1, CSNK1E and PRICKLE4) and pancreatic cancer essential genes, intersecting with the DepMap database (Fig.2d; MED30, LSM2, LSM7, HSPE1, MYL12A and RABGAP1).

We generated populations of CRISPR-KO for each single gene to validate, as opposed to single cell derived clones, to avoid inter-clonal heterogeneity. We used SURVEYOR, an enzyme mismatch cleavage assay, to analyze and verify proper Indel mutation insertions for each CRISPR-KO (Supplementary Fig.2). We then assessed the impact of the specific CRISPR loss-of-function on tumor cell growth, using *in vitro* colony formation assays⁴⁴⁹. Colony formation was assessed by Crystal violet staining and quantified with ImageJ software and the ColonyArea plugin⁴⁵⁰. As

shown in Figs.2e-g, all individual KOs, except one (PFN1) led to significant cell growth inhibition, validating not only our CRISPR screen but also candidate genes selection processes. Importantly, of all 15 candidate genes, we found the HSPE1-KO to exert the strongest and highly significant growth inhibitory effects (Fig.2g). As such, HSPE1 was further selected for the rest of the study as our top pancreatic cancer vulnerability candidate.

Understanding the role of HSPE1 as a tumor-promoter in PDAC tumor formation

While a role for HSPE1 in pancreatic cancer has yet to be defined, its overexpression was reported in oral squamous cell carcinoma⁴⁵¹, invasive ductal breast carcinoma⁴⁵², astrocytoma⁴⁵³, prostate⁴⁵⁴, lung⁴⁵⁵, liver⁴⁵⁶, colorectal⁴⁵⁷, nasopharyngeal⁴⁵³, large bowel and uterine exocervix⁴⁵⁸ cancer. In ovarian cancer, HSPE1 was proposed as a potential biomarker⁴⁵⁹. HSPE1 is a co-chaperone that can form a ring-complex with the heat shock protein D1 (HSPD1) to catalyze protein folding through the capture of unfolded and misfolded polypeptides in the mitochondria³⁰⁹. We investigated the depletion of HSPE1 by means of CRISPR KO through different assays measuring cell growth, including colony formation assay, SRB assay and PrestoBlue assay. Moreover, to avoid the limitation of a single-cell line, we generated HSPE1-KO in different PDAC cell lines. We validated the KOs efficiency by western blot prior to the experimentation (Fig. 3a). Different PDAC cancer cell lines exhibited significant decrease in cell growth. Indeed, colony formation (Fig. 3b), cell density (Fig.3c upper panel) and cell viability (Fig.3c bottom panel) were negatively affected.

HSPD1 plays a role in tumorigenesis and stemness in metastatic head and neck cancer through interaction with β -catenin^{460,461}. Moreover, HSPD1 deficiency in the intestine leads to mitochondrial dysfunction and inhibition of epithelial stem cell maintenance⁴⁶². Hence, we hypothesized that HSPE1, being an HSPD1 interactor could also play a role in stemness and tumor-initiation. To address this, we generated a CRISPR HSPE1-KO cell line in HPAF-II to assess the HSPE1 effect on PDAC tumor initiating capacity, using tumorsphere assay. Expression of HSPE1 was assessed by western blot (Fig. 3d). As shown in Fig.3e, HSPE1-KO cells exhibited significantly lower numbers in stem/progenitor cells, compared to NTC control cells, indicative of a role for HSPE1 in PDAC stemness regulation.

To further investigate the role of HSPE1 in pancreatic cancer tumorigenesis *in vivo*, we used a preclinical xenograft model of PDAC. Control scrambled-KO or HSPE1-KO HPAF-II cells were

injected subcutaneously in NSG mice and tumors were allowed to grow and expand for 1 month. Tumor volume was measured through caliper measurements at regular intervals. As shown in Fig.3f, tumor growth from the HSPE1-KO animal group was significantly reduced compared to control animals. At experimental endpoint, animals were sacrificed, and tumor resected. Interestingly, we found that HSPE1 gene silencing also led to a significant decrease in tumor weight, compared to the control group (Fig.3g). Collectively these results indicate that HSPE1 regulates cancer stem cells self-renewal activity and tumor growth in PDAC, highlighting a novel pro-oncogenic function for HSPE1 in PDAC.

HSPE1 silencing induces cell cycle arrest and apoptosis.

HSPD1 and HSPE1 have a coordinated co-expression pattern in various tissues^{463,464}. To then better understand the downstream molecular mechanisms by which HSPE1 regulates tumor growth in relation with HSPD1, we analyzed their respective effects on cell cycle progression, using HSPE1 and HSPD1 CRISPR-KOs and RNA interference (shRNA) knock-down (KD) models in HPAF-II.

To further understand the cell transduction pathway of the complex HSPE1/HSPD1, we generated individual knock-down for both HSPE1 and HSPD1 gene in HPAF-II cell line and investigated their impact on cell cycle with propidium iodide (PI) staining, therefore quantifying the quantity of G₀/G₁, S and G₂/M phase cell population. We showed that HSPE1-KD cells displayed a significantly higher population percentage of G₀/G₁-arrested cells (Fig.4b). This result highlights to role of HSPE1 in the deregulated cell cycle progression in PDAC. Then, we performed western blotting on several cancer-related proteins and found that several cell cycle proteins from the G₂/M, including the phosphatases PLK1 and CDC25C as well as CDK1 and Cyclin B1 in HSPE1 knockdown. Interestingly, HSPD1-KD did not induce the same cell cycle regulators downregulation, implicating a HSPE1-specific effect. In contrast, proteins from the G/S phase, including CDK2, CDK4 and CDK6 expression was not changed in both HSPE1 and HSPD1 knockdowns (Fig.4b). Since PLK1 is known to play a major role in G₁/S and G₂/M cell cycle⁴⁶⁵, we explored the top co-dependencies of PLK1 on the CRISPR screening DEMETER DepMep dataset (Supplementary Table 1). Genes with similar CRISPR screen DepMap scores, also called dependency scores, are said to be co-dependent. We found that HSPE1 is significantly correlated

with PLK1, where both genes have negative fitness score in the same cancer cellular lineages (Supplemental Table 1).

Silencing of HSPD1 has been demonstrated to destabilize the mitochondrial survivin pool, leading to mitochondrial dysfunction, initiation caspase-dependent apoptosis and activation and release of p53³¹². We then hypothesized that HSPE1 could play a role in apoptosis. We performed an apoptosis assay by Annexin V, a common method to detect dead cells. After quantification by flow cytometry analysis, we detected a significant increased number of pre-apoptotic and dead cells in both HSPD1 and HSPE1 (fig.3c) knock-down and (fig.3d) knock-out cells. Interestingly, we found that HSPE1-silenced cells have a greater number of apoptotic cells, highlighting the importance of this co-chaperone in the HSPD1/HSPE1 complex as a tumor promoter. Finally, our data demonstrates that HSPD1/HSPE1 might have a crucial role in regulating the cell cycle and apoptosis in PDAC, which could be pharmaceutically exploited.

HSPE1 as a therapeutic target in PDAC

We sought to explore the therapeutic value of HSPE1 and take advantage of its vulnerability in PDAC. Since HSPE1 is not druggable, we opted for KHS101, a small-molecule inhibitor disrupting the whole HSPD1-HSPE1 complex enzymatic activity. KHS101 was found to be cytotoxic and showed *in vivo* antitumor activity in glioblastoma⁴³⁶ and non-small cell lung cancer⁴⁶⁶. KHS101 has been shown to interact directly with the mitochondrial chaperone HSPD1 by disrupting its enzymatic activity and impairing mitochondria integrity⁴³⁶. To gain further insights about the outcome of KHS101 in PDAC, we assessed the *in vitro* cytotoxicity by Sulforhodamine B colorimetric assay⁴⁶⁷ and cell viability by PrestoBlue™ fluorescent assay. Exposure of micromolar doses of KHS101 induced cell death in different PDAC cell lines (Fig.5a-b). Moreover, as proof of principle, we generated CRISPR KO to repress the expression of both HSPE1 and HSPD1 (Supplemental Fig.3). Genetic repression by CRISPR resulted in reduction of cell growth in both genes, confirming the tumor-promoting network of HSPE1 and HSPD1, which is similar to KHS101 treatment.

Based on our findings, we assessed the effect of KHS101 in tumor growth in a xenograft mice model of PDAC. Following subcutaneous transplantation of two different PDAC cell lines, tumors were allowed to grow until they reached 100mm³. Mice bearing similar tumors volumes were

selected and separated into three different groups (10 mice for control group and 5 mice for experimental group) for subsequent drug treatment: vehicle or KHS101 (1mg/kg and 3mg/kg doses). The injection was achieved by intraperitoneal injection for 2 weeks at 3 times/week intervals. KHS101 treatment significantly slowed the tumor growth (Fig.5c). Moreover, we observed a trend in the reduction of tumor weight (Fig.5d) in both PDAC experimental models. These findings demonstrate the importance of the HSPE1-HSPD1 complex in tumor-promotion of PDAC and that pharmacological inhibition through KHS101 administration can effectively slow tumor growth while showing no indication of negative welfare or damage to internal organs, such as the liver, for all experimental mice.

OPA1 is implicated in oncogenic activities of HSPE1 in PDAC

A recent study³¹⁴ revealed a unique mechanism involving HSPE1 in the cleavage of OPA1, a dynamin related GTPase responsible for fusing the mitochondrial membrane. This cleavage is carried out by the metalloprotease OMA1^{468,469} and was shown to occur independently of HSPD1³¹⁴. Moreover, the loss of OPA1 was correlated with induction of apoptosis through cytochrome C release, suggesting OPA1 as an antiapoptotic gene^{470,471}. Thus, we hypothesized that HSPE1 downregulation could downregulate or inactivate OPA1. We found that HSPE1 downregulation by means of shRNA knockdown or CRISPR knockout decreased the long forms isoforms (L1 and L2) of OPA1 in all cell lines. Interestingly, no change between the expression of OPA1 or the ratio between the short and long isoforms in the knockdown of HSPD1. Our results are in line with a previous study³¹⁴, where HSPE1 invoke a specific mechanism independently of HSPD1.

OPA1 regulates the equilibrium between mitochondrial fusion and fission. Disruptions to this balance, frequently observed during stress and under pathological conditions, lead to mitochondrial fragmentation and induce apoptosis and cell death⁴⁷². We sought to exploit this vulnerability by using an OPA1 inhibitor, MYLS22, to target PDAC cells. To this end, we preformed HPAF-II tumors in mice by xenograft. We treated those mice by intraperitoneal injection with vehicle or MYLS22 (10 or 20mg/kg). The drug was administered by intraperitoneal injection performed 3 times/week. Remarkably, mice treated with MYLS22 had significantly reduced tumor volume compared to vehicle control. This result highlights the importance of OPA1 in cancer progression in PDAC, a direct target downstream HSPE1. We then performed a similar

xenograft assay by combining both KHS101 and MYLS22 in mice and found a reduced tumor weight in the drug-combination. Thus, pharmacological targeting of HSPE1 and OPA1 seems to be an effective strategy for PDAC treatment.

4.6 Discussion

One challenge to treat pancreatic cancer and improve patient survival outcome relies on finding novel actionable targets in order to generate efficient targeted therapies, rather than relying on standard chemotherapy treatment with limited efficacy. In this study, we opted for a genome wide CRISPR-based screening in aggressive PDAC cells to identify specific and contextual genetic pancreatic cancer vulnerabilities. Our findings provide unvaluable novel information towards a better understanding of pancreatic cancer tumorigenesis with the long-term goal of translating these basic research discoveries into the clinic through the development of new therapeutic approaches to pancreatic cancer. In this study, we identified HSPE1 as a central and critical regulator of tumor growth formation in pancreatic cancer, exerting its effects through parallel signaling pathways. We found on one hand HSPE1 can regulate tumor growth through its interaction with its partner heat shock protein HSPD1 but also found HSPE1-specific effects that do not rely on HSPD1 but instead involve regulation of the OPA1 antiapoptotic protein.

Several members of the HSPs family, including HSP27, HSP40, HSP60, HSP70, HSP90, and other large HSPs, have been found to play a significant role in many molecular mechanisms related to cancer. The HSPD1-HSPE1 complex, which we assessed in our study, import and fold proteins inside the mitochondria³¹¹. More specifically, the confinement of the polypeptide to be folded in the central cavity of HSPD1/HSPE1 complex is driven by the catalytic activity of HSPD1 using ATP hydrolysis³⁰⁹. Additionally, it is known that the ATP-dependent chaperone function of HSPD1 is dependent on HSPE1 binding to the complex⁴⁷³. Proper protein folding by HSPs therefore maintain proteostasis and guard cells from different types of cellular stress³¹¹. In spite of that, cancer cells are known to hijack the protective roles of HSPs during tumor progression³⁰⁵. Among these HSPs, HSPD1 oncogenic role has been largely characterized in the literature⁴⁷⁴. However, few studies assessed the role of HSPE1 alone in cancer.

Our study highlights the strong regulatory role played by HSPE1, exerting strong and pronounced effects on the decrease in the expression of several G2/M cell cycle regulators, particularly evident

in the case of PLK1 when compared to HSPD1. Indeed, PLK1 is a major actor in both G2/M and S phase checkpoints and is involved in restarting the cell cycle after a G2 arrest upon DNA damage or DNA repair at stalled replication forks⁴⁷⁵. Elevated amounts and active mutants of PLK1 can overcome a DNA damage-induced arrest in G2⁴⁷⁶. Additionally, a stronger effect on induction of apoptosis was observed in HSPE1-depleted condition, highlighting the potential differential role that HSPE1 could have in PDAC progression over HSPD1.

Several HSPD1 inhibitors and modulators are commercially available and are being actively evaluated as novel anti-cancer agents in the scientific literature⁴⁷³. Based on the oncogenic role of the druggable HSPD1, we exploited the complex of HSPD1/HSPE1 as a potential therapeutic target to treat pancreatic cancer with a small molecule inhibitor, KHS101. We found that KHS101 successfully inhibited cell proliferation in many PDAC cell lines and hindered tumorigenesis. A research group showed by in-vitro pull-down assay, that HSPD1 can directly interact with KHS101⁴³⁶. The same group also found that KHS101 did not alter the mRNA and protein levels of HSPD1, suggesting that cytotoxicity is independent of genetic expression. Therefore, we propose that there are two different independent mechanisms where HSPD1/HSPE1 could increase proliferation and tumorigenesis in PDAC regarding to either enzymatic activity or protein expression.

The small-molecule KHS101 used in our study was first suggested as a TACC3 inhibitor, demonstrating suppression of cell growth, motility, epithelial-mesenchymal transition (EMT), and breast cancer cell stemness, along with the induction of apoptotic cell death⁴⁷⁷. However, Polson *et al.* discovered a rapid autophagic response in KHS101-treated GBM cells before the downregulation of TACC3 induced by the compound, suggesting an early HSPD1/HSPE1-dependent activity of KHS101⁴⁷⁸. Moreover, KHS101 induced cell death in glioblastoma tumors, which is associated with compromised metabolism and disruption of mitochondrial integrity⁴³⁶. This mechanism is known to be involved in HSPD1/HSPE1 depletion⁴⁷⁹. Hence, the use of KHS101 is justified to target the HSPD1/HSPE1 complex.

The crystal structure of the mitochondrial chaperonin complex HSPE1/HSPD1 was described in a previous study⁴⁸⁰. The complex consists of a double-ring structure of HSPD1 (tetradecamers) bound to HSPE1 (heptamers) through its apical domain, forming an “American football”-shaped complex⁴⁸⁰. Another study showed the nucleotide dependence for HSPD1 ring assembly where

both single- and double-ring complexes coexists in the HSPD1/HSPE1 chaperonin reaction cycle⁴³⁵. Such molecular structure-function studies are tremendously important to improve pharmacological properties of drugs. Indeed, several synthetic drugs, natural compounds and bioactive molecules were shown to inhibit HSPD1/HSPE1 chaperonin system⁴⁸¹, including the small-molecule inhibitor KHS101 used in our study. Additionally, Several other HSPs inhibitors are been tested in pre-clinical studies such as Hsp90^{482,483}. Still, many preclinical studies must be made to ensure the lowest therapeutic index and maximal on-target activity.

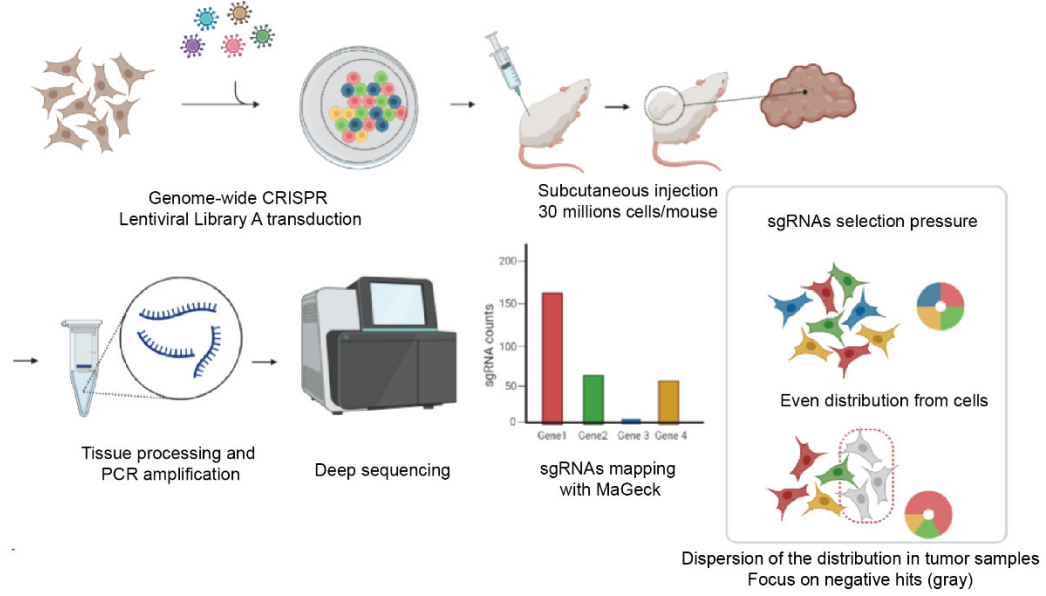
A recent study showed that HSPE1 depletion, but not HSPD1, led to proteolytic inactivation of OPA1, a dynamin-related GTPase that fuses the mitochondrial membrane mediated through stress-activated metalloprotease OMA1³¹⁴. This is the sole study showing a unique role of HSPE1 in the HSPE1/HSPD1 complex, where HSPE1 plays a protective role from mitochondrial stress independently of HSPD1. Therefore, OPA1 emerges as a promising targets in cancer therapy⁴⁸⁴. We exploited this vulnerability by using a first-in-class OPA1 inhibitor MYLS22, which showed great efficacy our PDAC model as well as a preclinical model of breast cancer⁴⁸⁵. We also showed at the molecular level that HSPE1 depletion modulates the expression of the long form of OPA1 (L-OPA1). The uncleaved L-OPA1 plays a role in mediating mitochondrial fusion, a process restricted during OPA1 processing whereas S-OPA1, produced through the proteolysis of L-OPA1, promotes mitochondrial fission⁴⁸⁶. Therefore, it could be interesting to assess the role of HSPE1 in the equilibrium of the mitochondrial fission and fusion as well as the implication of the proteins OMA1 and YME1L1 implicated in OPA1 proteolytic cleavage⁴⁷².

4.7 Acknowledgements

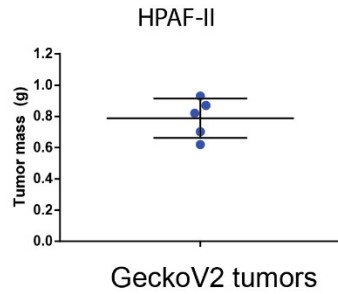
We would like to thank Dr. George Zogopoulos for Mia-PaCa2 cell line and Dr. Zu-Hua Gao for PANC-1 cell line. Girija Deliah provided technical assistance. This work was supported by grants from the Canadian Institutes for Health Research (CIHR to JJL). We would like to thank Dr. Ivan Litvinov for western blot antibodies.

4.7 Figures of chapter 4

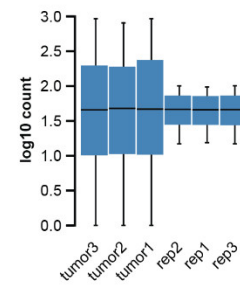
a



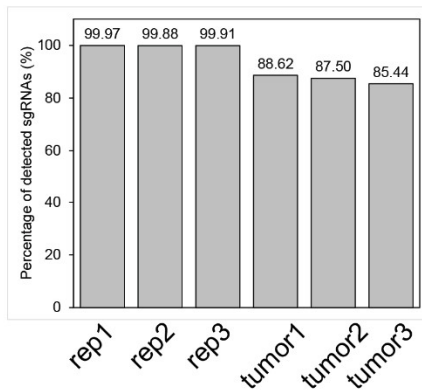
b



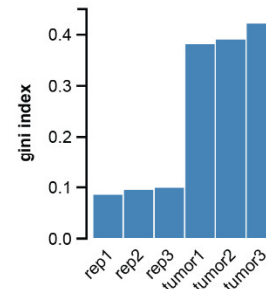
c



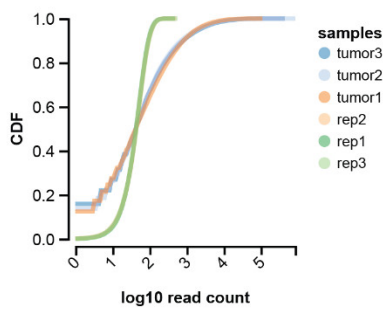
d



e



f



g

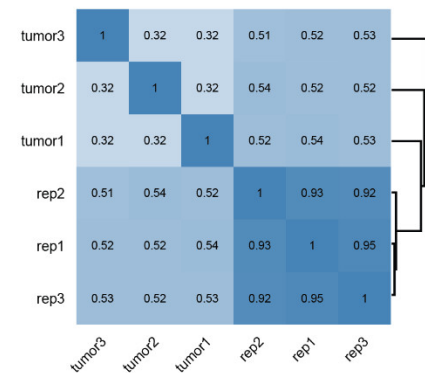


Fig. 4.1: In vivo genome-wide CRISPR screening in PDAC. (a) Schematic representation of the loss-of-function genome-wide screen using the human lentiviral CRISPR/Cas9 library (GeCKOv2) library A in pancreatic ductal adenocarcinoma cell line (HPAF-II). (b) Average mass of extracted tumor from NSG mice subcutaneous transplanted with 30 millions cells and grown for 28 days. Mean of three independent infection replicate experiments ($n = 5$, 1 mouse per biological replicate was randomly selected for deep sequencing). Data are represented as $\text{mean} \pm \text{SEM}$. (c) Normalized read count distribution from sequenced amplicons. (d) The unmapped percentage of sgRNAs in the library in cells before transplantation ($n = 3$), and tumor samples ($n = 3$) at day 28. (e) Statistical dispersion graphic (Gini index) of the sgRNA distribution within samples from cells and tumor replicates. (f) Cumulative distribution function of library sgRNAs in the three transduced cell replicates and six tumor replicates. Shift in tumor samples indicate the altered read counts in a subset of sgRNAs. (g) Pearson correlation of the sgRNA reads between all samples from in vitro and in vivo.

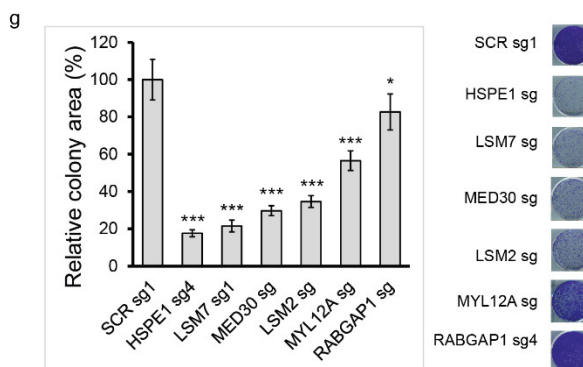
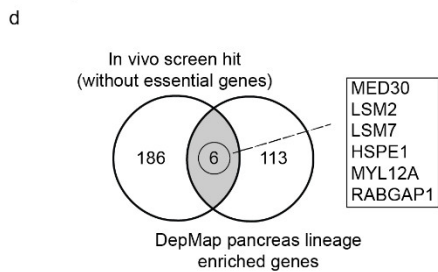
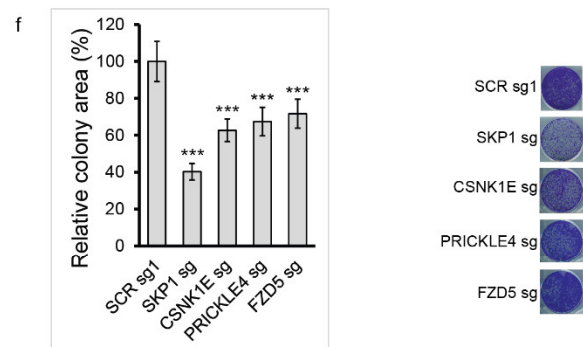
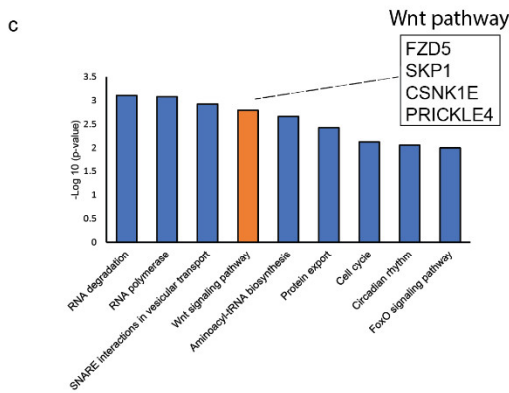
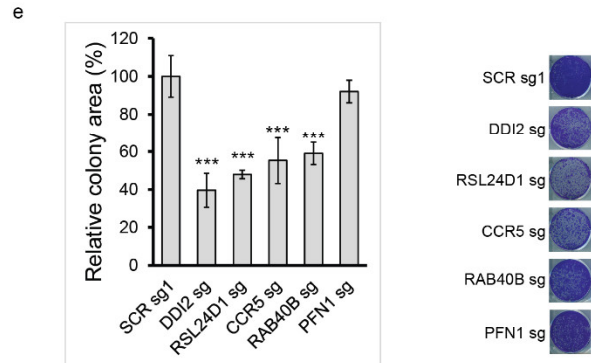
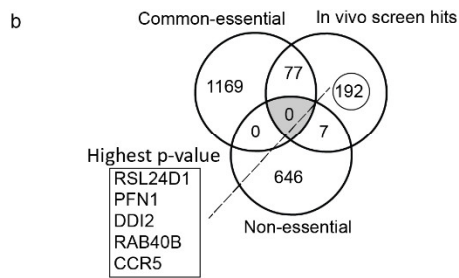
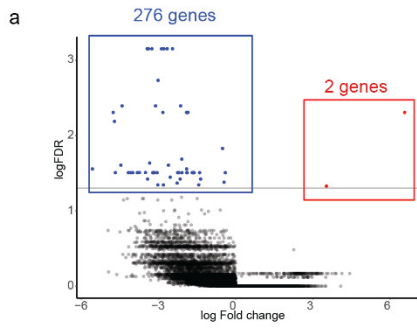


Fig. 4.2: Validation of depleted genes from CRISPR screen. (a) Scatter plot representing the Log₂ (fold change) of top ranked genes in both positive (red) and negative (blue) selection profiles (false discovery rate (FDR) < 0.25) in tumor samples normalized by non-targeting control. (b-d) Three different strategies for the selection of the genes for the validation process. (b) Venn diagram comparing common-essential, non-essential and genes with highest statistical value from in vivo screening depleted list (negative selection). Validated genes with the highest p-value are shown in the black box (SNRNP25 is omitted from the list). (c) Histogram showing the gene set pathway enrichment analysis from EnrichR. Validated genes from Wnt pathway are shown in the black box (d) Venn diagram comparing the highest statistical value from in vivo screening depleted list (negative selection) with the DepMap pancreas lineage enriched genes. (e-g bottom panel) Histogram displaying the relative colony formation area from (e) Highest p-values gene list (f) Wnt pathway gene list (g) DepMap pancreas enriched lineage gene list. (e-g bottom panel) Representative images of colony formation assay

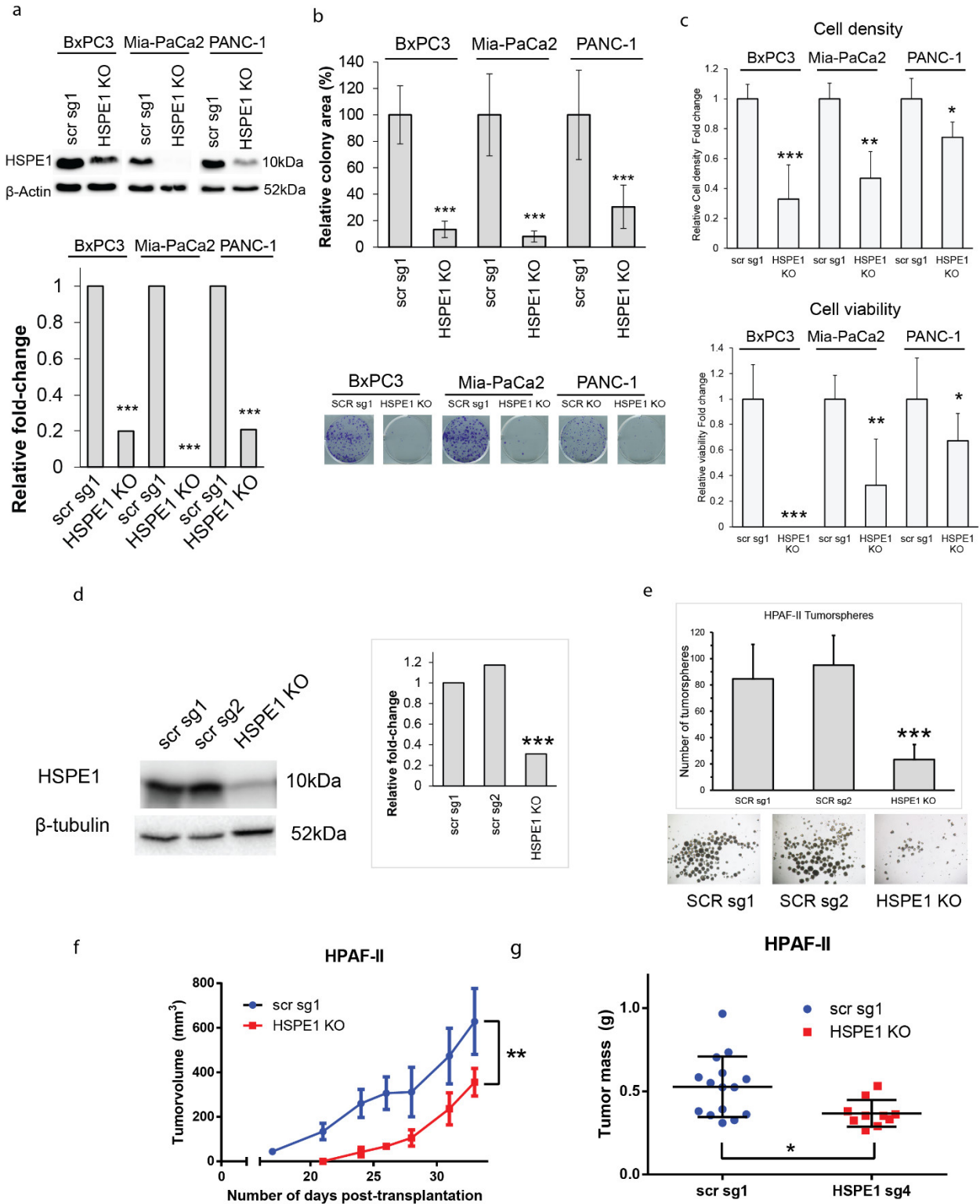


Fig.4.3: HSPE1 promotes cell proliferation, tumorigenesis and increases higher tumor-initiating capacity in PDAC. (a) Relative expression of HSPE1 measured in monolayer-cultured PDAC cell lines (BxPC3, Mia-PaCa2 and PANC-1) by immunoblotting and histogram showing the quantification by densitometry for each band. β -Actin was used as a loading control. (b) Upper panel: Histogram showing the percentage of relative colony area of three different PDAC cell lines (n=3) having either a Non-Targeting control scramble (scr) or HPSE1-induced KO by CRISPR 7 days post-transfection. Bottom panel: Representative images of cells stained with Crystal Violet (c) Histogram showing cell density assay measured by SRB assay (upper panel) and cell viability measured by PrestoBlue® assay (bottom panel). (d) Relative expression of HSPE1 measured in monolayer-cultured HPAF-II cell line by immunoblotting and histogram showing the quantification by densitometry for each band. β -tubulin was used as a loading control. (e) Histogram representing the number of tumorspheres (>50 μ m diameter) that were counted for assessing tumor-initiating capacity. Representative tumorsphere image (f-g) An amount of 1 million HPAF-II cells either transduced with a non-Targeting control (scr) or HSPE1-KO construct were transplanted subcutaneously in individual NSG mice (9-week-old). Tumors volumes (f) were measured 3 times/week with a caliper. Data are represented as mean \pm SD. Significance was calculated using two-sided, unpaired t-test, p-value * <0.05, *** <0.01. (g) Tumor mass was weighted at the endpoint (34 days post-transplantation).

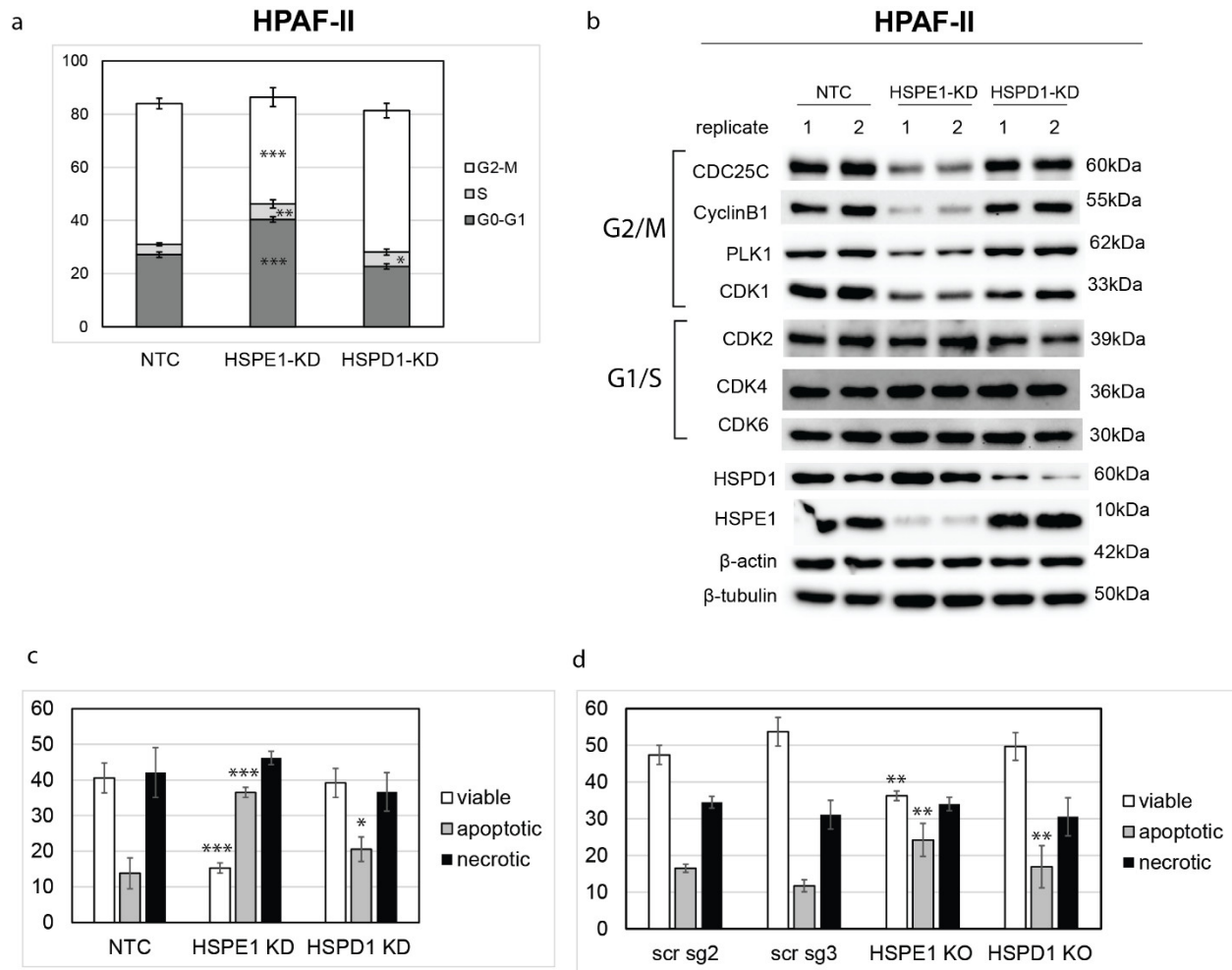
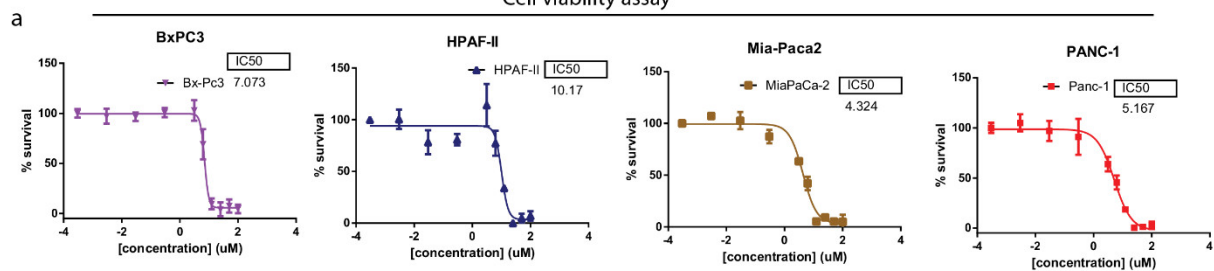


Fig.4.4: Depletion of HSPE1 induces cell cycle arrest and increase apoptosis. (a) Flow cytometry analysis of cell cycle in NTC, HSPE1 or HSPD1 knockdown HPAF-II cells stained with Propidium Iodide. (b) Relative expression of cell cycle regulators in HPAF-II cell line. Non-targeting control (NTC), HSPE1 or HSPD1 shRNA-knockdown were measured in by immunoblotting in replicates. β -Actin and β -tubulin were used as loading control. (c-d) Flow cytometry analysis of apoptosis in (c) NTC, HSPE1 or HSPD1 shRNA-knockdown (KD) or (d) SCR, HSPE1 or HSPD1 CRISPR-Knockout (KO) on live HPAF-II cells stained with Propidium Iodide and Annexin V. For flow cytometry experiment, all cells were starved for 24h in starvation medium (serum-free) followed by 24h in full-medium (10% FBS) prior to fixation.

Cell viability assay



b Cell density assay

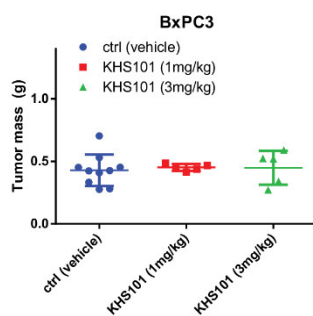
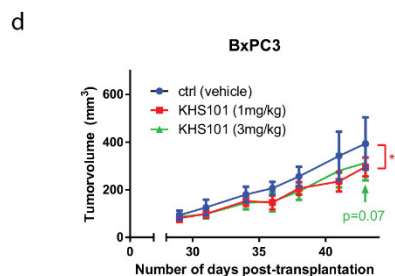
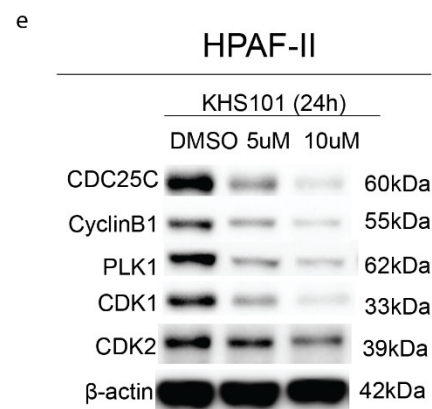
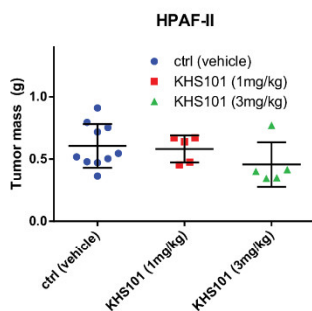
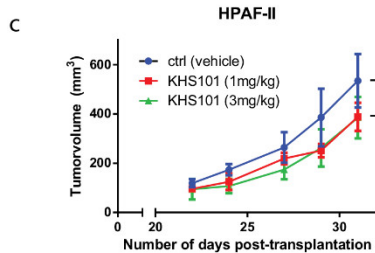
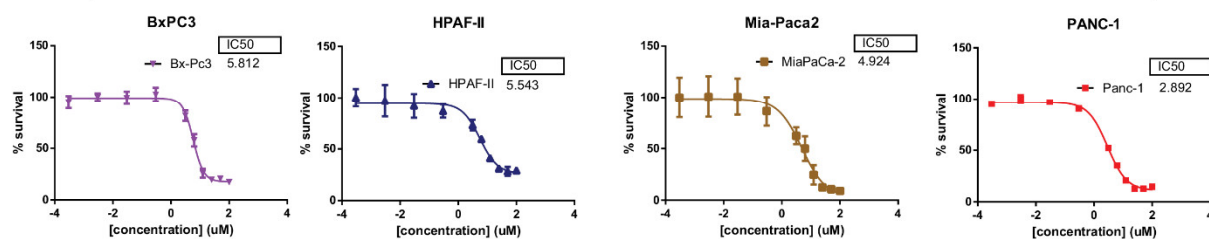


Fig.4.5: KHS101 small-molecule curtails PDAC tumor formation (a) Dose-response curves (normalized to the DMSO control) and the corresponding IC₅₀ (half-maximal inhibitory concentration) values (log₁₀ micromolar) are shown for the indicated cell models and KHS101 concentrations after a 4-day treatment period. Data are means ± SD of three biological replicates. (c-d) An amount of 1 million (c) HPAF-II or (d) BxPC3 cells were transplanted subcutaneously in individual NSG mice (9-week-old). Tumors were let grown up to 100mm³ and randomized into three groups (vehicle, 1 or 3mg/kg KHS101). Tumors volumes (left panel) were measured 3 times/week with a caliper. (right panel) Tumor mass was weighted at the endpoint (34 days post-transplantation). (e) Relative expression of cell cycle regulators in HPAF-II cell line treated with KHS101. β-Actin was used as loading control.

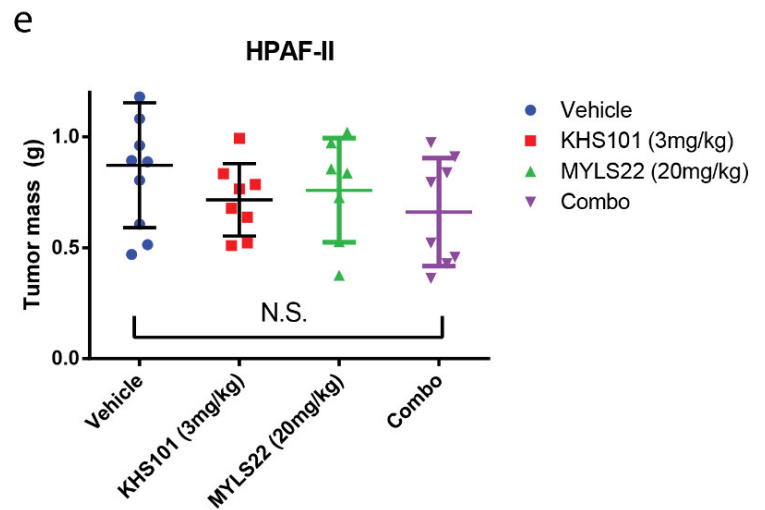
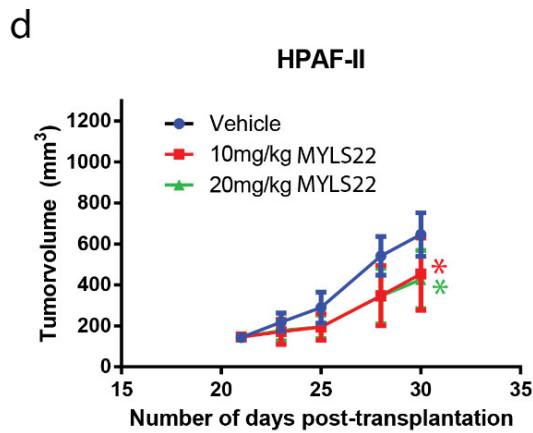
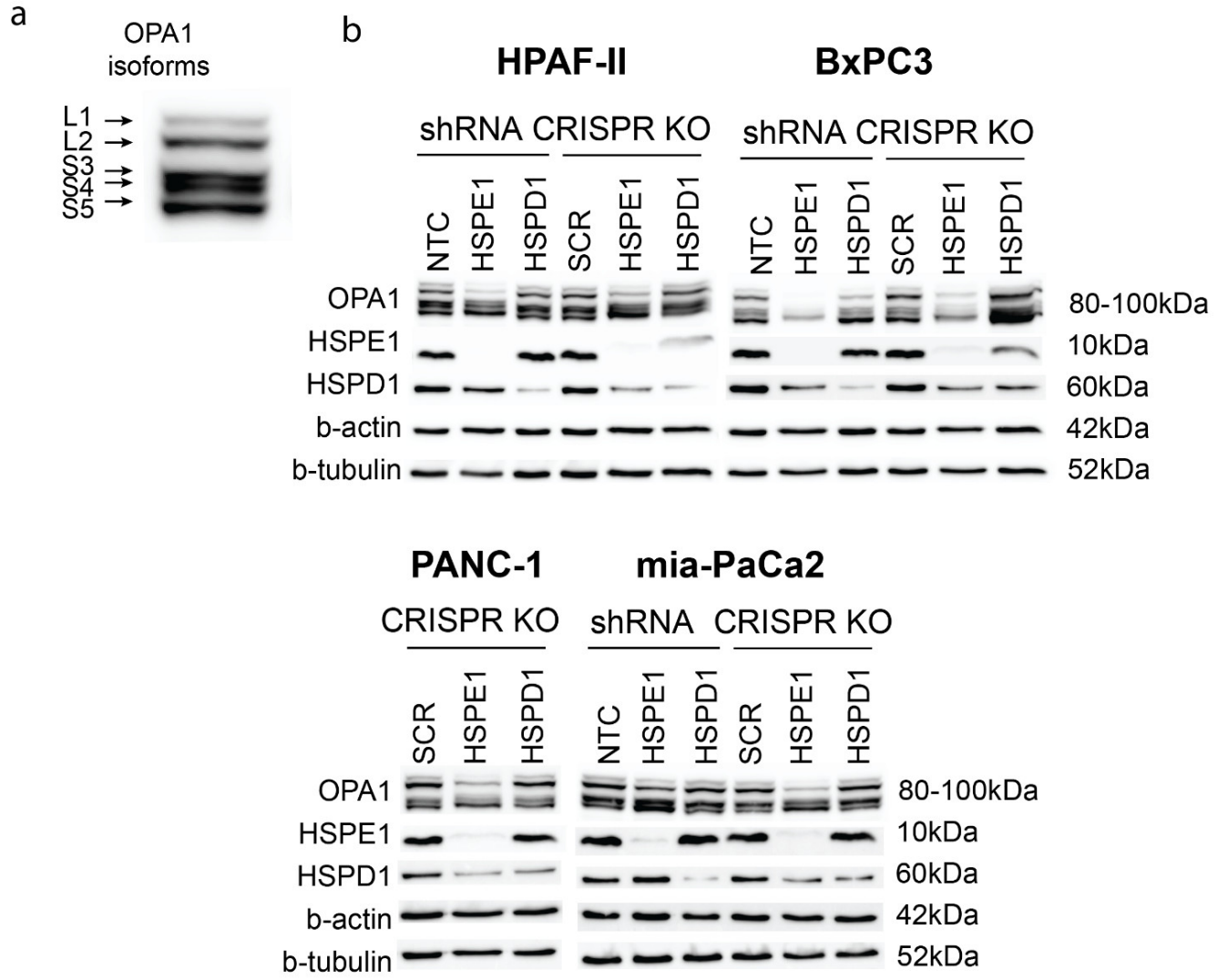
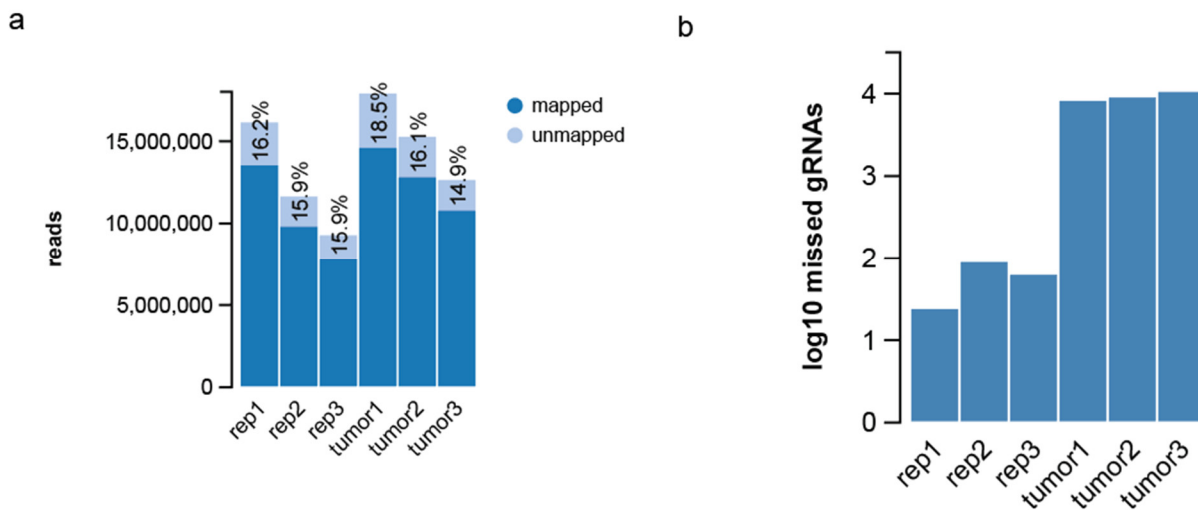
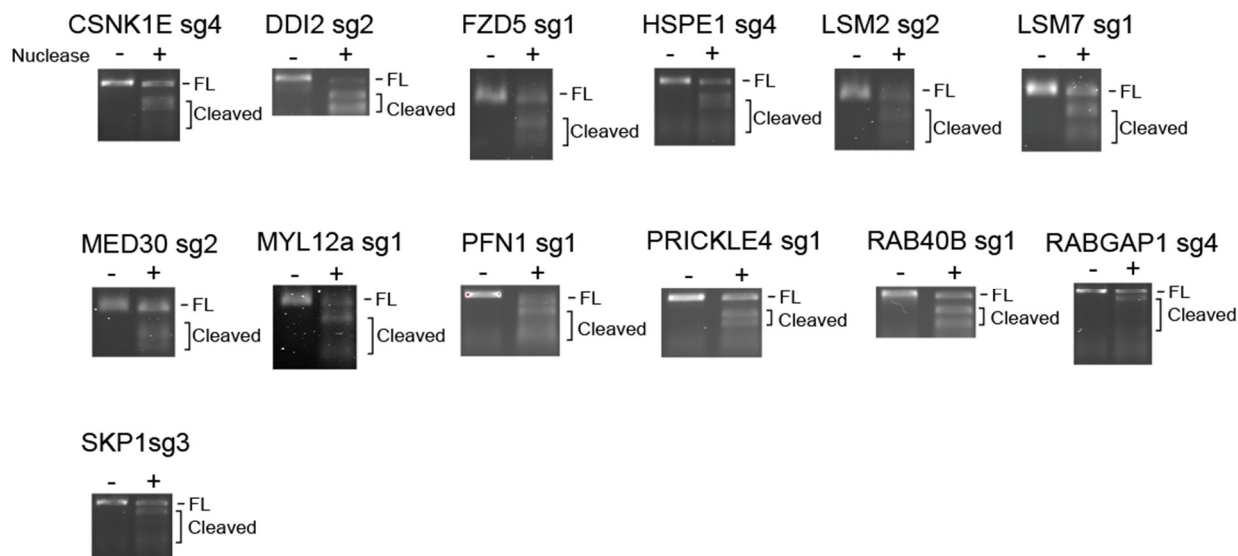


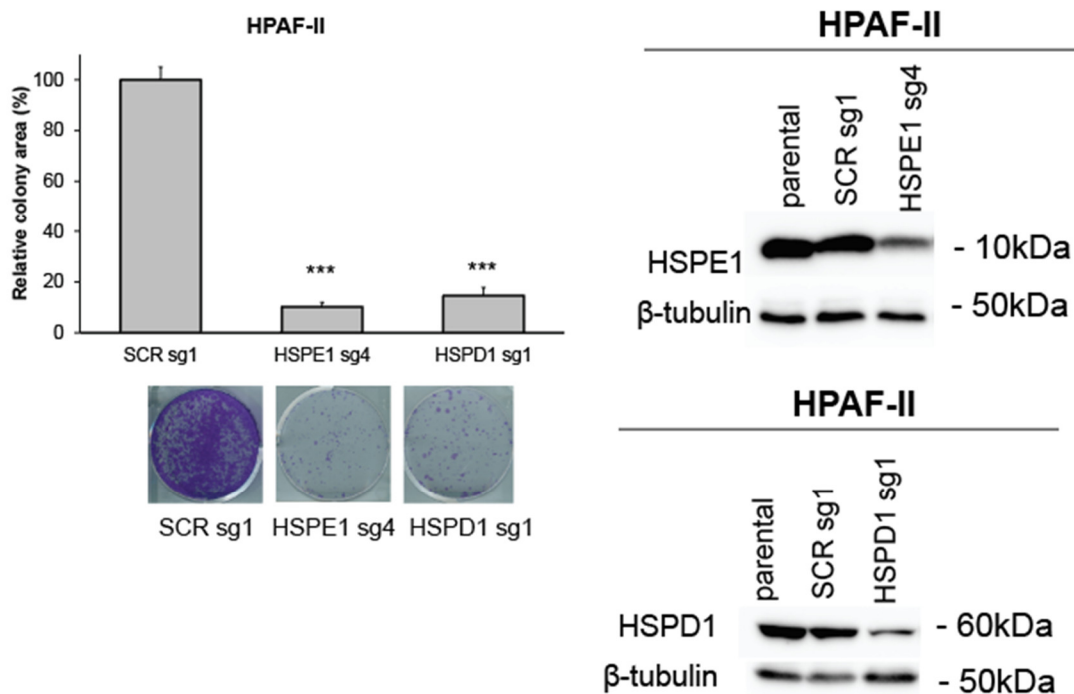
Fig.4.6: Role of OPA1 antiapoptotic protein in HSPE1-Induced oncogenic activities. (a) Representation of OPA1 isoforms by immunoblotting (HPAF-II Non-Targeting Control condition). (b) Immunoblotting of non-targeting control (NTC), HSPE1 or HSPD1 shRNA-knockdown or SCR, HSPE1 or HSPD1 CRISPR-Knockout (KO) of shown genes in HPAF-II, BxPC3, PANC-1 and mia-PaCa2 cell lines. β -Actin and β -tubulin were used as loading control. (c) An amount of 1 million HPAF-II cells were transplanted subcutaneously in individual NSG mice (9-week-old). Tumors were let grown up to 100mm³ and randomized into three groups (vehicle, 10 or 20mg/kg MYLS22). Tumors volumes were measured 3 times/week with a caliper. (d) An amount of 1 million HPAF-II cells were transplanted subcutaneously in individual NSG mice (9-week-old). Tumors were let grown up to 100mm³ and randomized into four groups (vehicle, 3mg/kg KHS101, 20mg/kg MYLS22 or combination of both 3mg/kg KHS101 and 20mg/kg MYLS22). Tumor mass was weighted at the endpoint (34 days post-transplantation). Data are represented as mean \pm SD. Significance was calculated using two-sided, unpaired t-test, p-value * <0.05. (e) Tumor mass was weighted at the endpoint (34 days post-transplantation).



Supplemental Fig.4.1: Mageck bioinformatic analysis of read counts of lof10 of missed gRNAs (a) Histograms showing mapped and unmapped sgRNAs read counts (b) Log10 fold-change of missed sgRNAs in HPAF-II cell representation control, before injection in mice, and collected tumor samples of HPAF-II GeckoV2.



Supplemental Fig.4.2: SURVEYOR Assay. Gene modification detection (INDELs) of individual pooled CRISPR-mediated knockouts of top candidate genes using SURVEYOR assay prior to colony formation growth assay. Full length (FL) and cleaved bands are shown under control (-) and nuclease enzymatic reaction (+) condition.



Supplemental Fig.4.3: Colony formation assay of CRISPR-KO SCR, HSPE1 or HSPD1 HPAF-II cell line. Histogram showing relative area. Immunoblot of HSPE1 and HSPD1 expression in HPAF-II cell line.

Supplemental Table 1: Table showing the statistical correlation (r) and Z-Score values of the gene dependency of PLK1 provided by the 20q3 DepMap database

Correlated gene dependency	Correlation (r)	Z_score
SPC24	0.63	5.2
NUF2	0.6	4.9
RPLP2	0.58	4.8
SPC25	0.58	4.8
POLR2C	0.56	4.7
RPL24	0.56	4.7
SRSF3	0.56	4.6
NUTF2	0.55	4.6
HSPE1	0.56	4.6
UBL5	0.55	4.6

Supplemental Table 2: Sequence of sgRNA used for molecular cloning

Prime Name	sgRNA primer sequence
Scramble_sg1	CACCGACGGAGGCTAAGCGTCGCAA
Scramble_sg2	CACCGCGCTTCCGCGGCCCGTTCAA
Scramble_sg1	AAACTTGCGACGCTTAGCCTCCGTC
Scramble_sg2	AAACTTGAACGGGCCGCGGAAGCGC
CCR5_sg_F	CACCGAGTTTACACCCGATCCACTG
CCR5_sg_R	AAACCAGTGGATCGGGTGTAAGTTC
CSNK1E_sg_F	CACCGCGGGCTTGTCGTCAAACCGC
CSNK1E_sg_R	AAACGCGGTTTGACGACAAGCCCGC
DDI2_sg_F	CACCGGCTCGAAGTCGGCGTCGACC
DDI2_sg_R	AAACGGTCGACCGGACTTCGAGCC

FZD5_sg_F	CACCGGGTGGGCACGCTCTTCCTGC
FZD5_sg_R	AAACGCAGGAAGAGCGTGCCACCC
HSPE1_sg_F	CACCGTAAACGCTTGTCCTGCCTGT
HSPE1_sg_R	AAACACAGGCAGGACAAGCGTTTAC
LSM2_sg_F	CACCGTGTGTGTCGACCTCATCTGC
LSM2_sg_R	AAACGCAGATGAGGTCGACACACAC
LSM7_sg_F	CACCGCGTGGTGCTAATCTGCCCGC
LSM7_sg_R	AAACGCGGGCAGATTAGCACCCACGC
MED30_sg_F	CACCGACGGCGTCGCTGTGCCGCAT
MED30_sg_R	AAACATGCGGCACAGCGACGCCGTC
MYL12A_sg_F	CACCGGGAACATGGTGAAATTGATG
MYL12A_sg_R	AAACCATCAATTTACCATGTTCCC
PFN1_sg_F	CACCGTTTATACTTAGCCCCACGG
PFN1_sg_R	AAACCCGTGGGGGCTAAGTATAAAC
PRICKLE4_sg_F	CACCGTCTGCAGGAGCGCTACTGCC
PRICKLE4_sg_R	AAACGGCAGTAGCGCTCCTGCAGAC
RAB40B_sg_F	CACCGCGAATGCACGGGCCGCCCGG
RAB40B_sg_R	AAACCCGGGCGGCCCGTGCATTCGC
RABGAP1_sg_F	CACCGCGTATGTTATTACGGGGAGC
RABGAP1_sg_R	AAACGCTCCCCGTAATAACATACGC
RSL24D1_sg_F	CACCGATGTAGTACTCACCTGCAAG
RSL24D1_sg_R	AAACCTTGCAGGTGAGTACTACATC
SKP1_sg_F	CACCGACTATTAAGACCATGTTGGA
SKP1_sg_R	AAACTCCAACATGGTCTTAATAGTC

Supplemental Table 3: primers for PCR amplification used for SURVEYOR assay.

Primer name	PCR primer sequence
CCR5_surveyor_F	TAAAAAAGACCTCTCCCACCCAC
CCR5_surveyor_R	GTCCTTCTCCTGAACACCTTCC
CSNK1E_surveyor_F	TGTTGCCTCCTTTTCTTGCTCTC

CSNK1E_surveyor_R	AGCTCGTACCTCCCCTGTGT
DDI2_surveyor_F	CAGTAGCAAAGGGAGGGAGTG
DDI2_surveyor_R	GAGGGAGTGACTCACTGAGC
FZD5_surveyor_F	AGGTAGCAGGCCACCACAATG
FZD5_surveyor_R	TGTCGCTCACCTGGTTCCTG
HSPE1_surveyor_F	CAACAGCGACTACTGTTGCTTGC
HSPE1_surveyor_R	CCTAACAGACGTAAGGAATCGGG
LSM2_surveyor_F	CCCTGGGTGGTTAGAGGACA
LSM2_surveyor_R	CTCAAGAGAGGATAGCTGTTCCC
LSM7_surveyor_F	TTCCTGGAGGTCCCTCAGTC
LSM7_surveyor_R	GAATCCAGGTTTCCTCAGAAGGTC
MED30_surveyor_F	ATCCACGGGCCCCACGTAAA
MED30_surveyor_R	GCGGCCGCTGTTTTGAAATCG
MYL12A_surveyor_F	CCTCTCACTTACCAGTTGCTTCTTCATC
MYL12A_surveyor_R	GGTTCGTGTGTGTGTGTGTGTG
PFN1_surveyor_F	CCGGTCTTTGCCAACCAGGA
PFN1_surveyor_R	GCTTCTGCTTTTCCTGAAGGAGAG
PRICKLE4_surveyor_F	GAAGGGGAATTTGGGGGGGAG
PRICKLE4_surveyor_R	GCCTGTCAGGACCTGATTGATG
RAB40B_surveyor_F	ATTTTCTCGTAGCTCTGGAAGCCG
RAB40B_surveyor_R	AGAAACCCACGTTGAGGGGC
RABGAP1_surveyor_F	GGGGGTAACTGTTGTTCACTCAC
RABGAP1_surveyor_R	GTGGTAGACTCACTTCCCCC
RSL24D1_surveyor_F	CCCATCTGTGGGGCTAACTTAAG
RSL24D1_surveyor_R	GCATAACTTGGGGGGATATGGAAC
SKP1_surveyor_F	CTCTCAAGCACCTTATGACAGGC
SKP1_surveyor_R	GCAGGCCTTAAAAGCTTCTGTTCC
hU6-F primer	GAGGGCCTATTCCCATGATT

Supplemental Table 4: List of validated genes and their known function.

DDI2	Aspartic protease mediating the cleavage of NFE2L1/NRF1 at 'Leu-104', promoting the release of NFE2L1/NRF1 from the endoplasmic reticulum membrane.
RSL24D1	Uses alternative polyadenylation signals. Unknown function.
CCR5	Member of the beta chemokine receptor family. Expressed on the surface of T-cells and macrophages and acts as a receptor for chemokines.
RAB40B	Member RAS Oncogene Family. Unknown function.
PFN1	Member of the profilin family of small actin-binding proteins. Plays an important role in actin dynamics by regulating actin polymerization in response to extracellular signals.
SKP1	Essential component of the SCF (SKP1-CUL1-F-box protein) ubiquitin ligase complex. Implicated in ubiquitination and proteosomal degradation.
CSNK1E	Serine/threonine protein kinase and a member of the casein kinase I protein family. Implicated in cytoplasmic and nuclear processes, DNA replication and repair
PRICKL4	Member of the LIM domain protein family. REST/NRSF-interacting LIM domain protein, which is a putative nuclear translocation receptor.
FZD5	Member of the 'frizzled' gene family. Receptor for the Wnt5A ligand.
HSPE1	Heat shock protein which functions as a co-chaperonin with HSPD1. Implicated in mitochondrial protein important and macromolecular assembly.
LSM2 and LSM7	Key members in the LSml-7 complex. Sm-like proteins are thought to form a stable heteromeric complex present in tri-snRNP particles, which are important for pre-mRNA splicing.
MED30	Member of the mediator complex. Implicated in regulating mitochondrial functions and integrity.
MYL12A	Encodes a nonsarcomeric myosin regulatory light chain. Activated by phosphorylation and regulates smooth muscle and non-muscle cell contraction.
RABGAP1	Involved in regulation of GTPase activity. Implicated in lysosomal positioning.

Source: GeneCards.org

Chapter 5: Integrative discussion

Discussion of the experimental work

The purpose of this thesis was to further investigate the role of specific pathways, such as TGF β , specific genes, including *MEN1* and the whole genome itself in the tumor development and progression of aggressive and hard to treat cancers such as melanoma and PDAC. I had specific aims in my thesis which were to (1) investigate the role of TGF β signaling pathway in melanoma stemness, (2) define the role of the tumor suppressor *MEN1* in melanoma and (3) use a genome wide CRISPR screen approach to find novel oncogenes in PDAC. These findings will be summarized and discussed in this chapter.

Stemness and melanoma

Over the last decade, an increased number of scientific publications integrated the concept of stemness into their experimental frameworks, with a particular emphasis on cancer stem cells. Stemness, a biological trait associated with pluripotency and self-renewal capacity, assumes a critical role in the context of cancer progression, especially in melanoma. In chapter 2 of this thesis, we demonstrated that TGF β signaling pathway inhibits tumorsphere formation in several melanoma cancer cell lines as well as reducing the population and expression of stem cell markers such as ALDH, CD133 and ABCG2. The experiments implemented in my research allowed the investigation of several aspects implicated in stemness, self-renewal and tumor-initiating capacities of melanoma cancer stem cells. However, this research field is still in its early stages and is subject to many debates in the scientific community, particularly in melanoma. For example, some studies showed that ALDH⁺ melanoma cells have increased tumorigenic potential^{115,487} while another one found ALDH expression to be unspecific to distinguish tumor-initiating and therapy-resistant cells, suggesting that ALDH population is not associated with more-aggressive subpopulations⁴⁸⁸. Melanoma cancer stem cell depletion by pharmacological targeting (combination of BCL-2 inhibitor with Fenretinide⁴⁸⁹; Lunasin^{490,491}) differentiating ALDH⁺ to ALDH⁻ phenotype, decreased tumorigenesis and reduced melanoma formation efficiency. These studies implicating small-molecule inhibitors targeting melanoma stem cells are in line with our finding, linking reduced self-renewal capacity with decreased tumor initiating capacities.

A study showed that⁴⁹² high ALDH1 mRNA expression correlates with better overall survival in melanoma patients. Another study¹¹³ demonstrated that ALDH1A1 isoform suppression through shRNA silencing reduced melanoma cell viability, tumorigenesis, and chemoresistance. These

conflicting findings highlight the importance and significance of the investigated ALDH1 isoform. In our study, we used an ADELFLUOR assay to measure the ALDH enzymatic activity. It was shown that 9 of the 19 ALDH isoforms could be implicated in the enzymatic reaction of ALDEFLUOR assay, including ALDH1A1, ALDH1A2, ALDH1A3, ALDH1B1, ALDH2, ALDH3A1, ALDH3A2, ALDH3B1, and ALDH5A1⁴⁹³. Thus, the ADELFLUOR assay is limited as cannot distinguish which isoform catalyzes the reaction, which is used to quantify the number of cancer stem cells in the population of a tested cell line. As different ALDH isoforms have different prognostic in melanoma, it could be interesting to test which specific isoform is affected by TGF β ^{113,116,492}.

Silencing CD133 in FEMX-I metastatic melanoma cell lines was shown to reduce cell growth rate, cell motility and their ability to form tumorsphere⁴⁹⁴. Moreover, this study showed that mice treated with monoclonal antibody decreased metastatic burden. A study showed that andrographolide, an anticancer agent, reduced the tumorigenic and metastatic potential of CD133+ cells by targeting Notch1/MAPK pathway⁴⁹⁵. Similarly, a combination of the chemotherapeutic agents, Etoposide and Bevacizumab, showed a reduction in melanoma tumorsphere formation and increased apoptosis in CD133+ MSCs⁴⁹⁶. These findings are consistent with our study, revealing a correlation between the TGF β -induced reduction of CD133+ population and decreased tumorigenesis and metastasis. However, two research teams found that expression of cell surface marker CD133 have different phenotype, where CD133+ are more proliferative and CD133- are more invasive^{106,107}. It has been shown that CD133 expression is tightly regulated with cell cycle expression, where CD133 antibody reactivity is reduced when cells are in the G1/G0 arrest compared to the mitotic G2/M phase in melanoma cell lines¹⁰⁵. Again, the role of CD133 could be contextual and more research should be done to understand its role in melanoma stemness and self-renewal.

ABCB5, another stem cell marker in melanoma, was shown to be enriched in subpopulation of human malignant-melanoma-initiating cells¹²¹. Indeed, inhibition of ABCB5+ melanoma stem cells through treatment of anti-ABCB5 monoclonal antibody resulted in reduction of tumorigenesis in preclinical mouse model of melanoma¹²¹. Another study showed that ABCB5 is a direct target of MITF and β -catenin and that its expression is associated with melanoma differentiated cells, raising the significance of both differentiated and undifferentiated cells to induce tumorigenesis⁴⁹⁷. Alongside with ABCB5 marker, the TGF β outcome in the expression of

other markers could be assessed in melanoma cell lines, including CD20¹²⁶, CD166³³⁷, CD271¹⁰⁸, BMI-1⁴⁹⁸, CXCR6⁴⁹⁹ and JARID1B⁵⁰⁰. Overall, many reports are in line with our study, as we demonstrated that TGF β could possibly reduce the ALDH+ and CD133+ MSC subpopulations. The protective role of TGF β could be exploited by targeting and differentiating MSC subpopulation responsible for tumor heterogeneity and relapse in melanoma.

Addressing the dual role of TGF β

The TGF β signaling pathway has a multitude of roles in the regulation of cell growth, apoptosis, differentiation and migration, which was described in chapter 1. TGF β can have a dual role through cancer progression, such as in breast cancer. In the early stages of breast cancer tumor growth, TGF β works as a tumor suppressor by inducing apoptosis and cell cycle arrest as well as the prevention of immortalization³⁹⁵. However, deletions or mutations in the key parts of the TGF β signaling pathway leads to resistance of tumor-suppressive properties of TGF β in later stages. TGF β also favors tumor progression by contributing to the invasion and migration of tumor cells to distant organs and paracrine signaling in the tumor microenvironment, enabling the evasion of the immune system. Moreover, TGF β is secreted in large quantities by tumor cells, remodeling the extracellular matrix by activating MMP proteins and plasmin generation, which contribute to angiogenesis^{501,502}. Therefore, how TGF β responds, and its impact strongly depends on the context, including the type of cell, tissue, and cancer. This is not the case for all cell types: in colon cancer for instance, as TGF β was shown to inhibit cell migration and invasion, as it reverses the mesenchymal-like phenotype to a polarized epithelial phenotype⁵⁰³. In diffuse-type gastric carcinoma, TGF β was shown to reduce tumorsphere formation, which was associated with a downregulation of ABCG2 transporters, and also reduce the tumorigenic and stemness potential through ALDH1 and REG4^{349,504}. Therefore, the dual function of TGF β does not occur in all tissue types, such as melanoma. TGF β also exhibits a dual role on breast cancer stemness. Data from our own group demonstrated that TGF β promotes stemness in TBNC³⁴². In contrast, TGF β has an inhibitory role toward less aggressive luminal subtypes of breast cancer⁵⁰⁵. Having shown that TGF β has a negative role on self-renewal abilities of melanoma cancer stem cells, it could be interesting to mimic the TGF β effects in melanoma tumors to decrease the tumor-initiating potential of these low-occurring types of cancer cells. Furthermore, a clinical trial with metastatic melanoma patients found that fresolimumab, an anti-TGF β monoclonal antibody, did not produce

favorable results. This finding supports our aim of blocking the metastasis-promoting effect of TGF β in melanoma patients⁵⁰⁶.

Still, there are some other contexts where melanoma cell lines can respond differently to TGF β ⁷⁶. Specifically, those with transcriptional signatures associated with more invasive phenotypes showed decreased tumor-initiating capacity compared to cells with proliferative transcriptomic profile⁸⁹. The growth-inhibitory effect of TGF β is mediated by MITF, as demonstrated by siRNA knockdown in proliferative signature melanoma cells, making them less susceptible to TGF β -mediated growth inhibition⁸⁹. Furthermore, melanoma cells with a proliferative transcriptomic signature are more susceptible to the TGF β -mediated growth inhibition than cells with invasive signature⁸⁷. Another study showed that long term exposing of TGF β slow down cell cycle progression, induce an invasive EMT-like phenotype in melanoma cells *in vitro* and has been shown to be dependent on PI3K signaling⁵⁰⁷. CD271, a melanoma stemness marker, has been shown to regulates phenotype switching in melanoma from a high-proliferative/low-invasive to a low-proliferative/high-invasive state¹⁰⁹. Moreover, SALL4 stem-cell epigenetic factor appears to regulate phenotype switching in melanoma through an HDAC2- mediated mechanism⁵⁰⁸. These results imply that melanoma cells, depending on their transcriptomic profile or the expression levels of specific stemness-related markers, may exhibit a dual function, transitioning between proliferative and invasive states. However, this thesis contributes to define TGF β as a tumor and a metastasis suppressor since it inhibits self-renewal ability of melanoma cancer stem cells. Still, in the cellular contexts case where TGF β acts as a tumor-promoter, it could be beneficial to block TGF β pathway. There are several agents targeting the TGF β that are currently assessed in clinical trials. AVID200, a highly effective and specific TGF β 1/3 inhibitor, was shown to reduce the proliferation of human mesenchymal stromal cells normally induced by TGF β 1⁵⁰⁹. Dalantercept, a soluble ALK1 inhibitor receptor fusion protein, was safe and displayed modest dose-dependent activity in recurrent or metastatic squamous cell carcinoma of the head and neck⁵¹⁰ and ovarian cancer⁵¹¹. Luspatercept, a recombinant fusion protein that binds TGF β superfamily ligands to reduce SMAD2/3 phosphorylation, showed anti-tumor response in a phase 2 study in lower-risk myelodysplastic syndromes patients⁵¹². Bintrafusp alfa is a bifunctional fusion protein able to both trap TGF β 1 ligand and block PD-L1 activity that showed positive clinical activity and safety profile⁵¹³. Testing these new drugs could be helpful in situations where TGF β suppresses the

immune system, as blocking TGF β in the tumor microenvironment could keep the immune cells potential to kill cancer cells.

SMAD2, SMAD3 and SMAD4 differential signaling in oncogenesis

In our study, we showed that SMAD2 and SMAD3 have a differential role on self-renewal capacity of melanoma cancer stem cells. Structurally, SMAD2 and SMAD3 have two domain separated by a linker region, where MH1 have strong affinity for DNA and the other domain, MH2, interacts with other partners such as SMADs, different LDTFs, chromatin readers, co-activators or co-repressor⁵¹⁴. SMAD2 structure is different from SMAD3, where two additional stretches of amino acids in the N-terminal MH1 domain are lacking in SMAD3⁵¹⁵. This unique MH1 domain in SMAD3 protein confers its DNA binding capacity and transcriptional activity in CAGA box-containing promoters⁵¹⁵. At the biochemistry level, both SMAD2 and SMAD3 are found mostly as monomer in unstimulated conditions but SMAD3 existing in multiple oligomeric states upon TGF β stimulation⁵¹⁶. Since the structure/function relationship between SMAD2 and SMAD3 is different, it could explain why the outcome of SMAD2 and SMAD3 in the context of melanoma is different as well.

Another study³⁶⁰ showed that silencing either SMAD2, SMAD3 or SMAD4 in keratinocyte cells had different outcome, where SMAD3 antisense molecules interfered the induction of TGF β -mediated cell cycle arrest by blocking the increase of p21 and blocking also the decrease of phosphorylated Rb and MYC protein levels. In the same study, silencing of SMAD2 had no phenotypic effect and silencing SMAD4 only exhibited a partial response³⁶⁰. This result is also in agreement with the reduced TGF β -mediated response on growth inhibition of primary keratinocytes from Smad3-null mice⁵¹⁷. This indicates that the SMAD complexes can be responsible for the regulation of different genes within one cell type, such as the SMAD3 protein in melanoma model used in our study having a critical role in tumor suppressive TGF β mediation. SMAD3 loss is a common mechanism in cancer which impairs the inhibitory effect of TGF β . In leukemia cells, SMAD3 inactivation is synergistic with p27 inactivation, preventing the TGF β -induced cell cycle arrest⁵¹⁸. An altered cell line (EpRas) with an oncogenic H-Ras, showed less SMAD3 expression correlated with higher cell growth compared to the normal cell line (EpH4), which tends to be more quiescent⁵¹⁹. When epithelial cells resist the growth-arresting effects of TGF β in the G1 phase, it coincides with a gradual decrease in SMAD3 expression. Cell cycle

progression resumes when SMAD3 levels are restored to their initial state. Notably, this recovery occurs without reverting the cells to an epithelial phenotype or affecting the MAPK pathway⁵²⁰. As such, by using CRISPR to abrogate the expression of SMAD3 in our study, we reproduce this SMAD3-loss phenotype inducing oncogenesis in cancer cell lines and tumor progression.

In the context of SMAD4 deficiency, such as pancreatic ductal adenocarcinoma where SMAD4 is mutated in more than 30% of tumor samples¹⁹³, the outcome is different. The activation of an invasive migratory transcriptional program is triggered by SMAD2 and SMAD3 in SMAD4-deficiency context⁵²¹. Still, in SMAD4-deficient tumors of PDAC patients samples, high levels of phospho-SMAD2 is linked with aggressive and poorer prognosis⁵²¹. Again, this result highlights the different response between SMAD2 and SMAD3 where gain of function of SMAD2 has stronger oncogenic effect than SMAD3. This finding is in accordance with our findings as SMAD3 depletion increased self-renewal but not SMAD2.

Discussion of MEN1 and melanoma

Previous work from our research group showed that Menin can directly interact with Smad3, which is implicated in the canonical pathway of TGF β ^{317,405,406}. By silencing Menin using siRNA, we showed that Menin depletion hindered several TGF β -mediated actions, such as the inhibition of proliferation and transcriptional activity of SMAD3 in pituitary adenomas. Of note, depletion of Menin did not affect TGF β -induced SMAD3/4 oligomerization and nuclear translocation. In Osteoblasts, Menin was also shown to interact with BMP-related proteins, SMAD1, SMAD5 and Runx2⁵²². Our previous finding highlights Menin as a tumor suppressor acting downstream of TGF β /Smad3 signaling axis in pituitary adenoma cells. In this thesis, the implication of Menin in the TGF β pathway was investigated through several experimental procedures in melanoma. In the chapter 3 in of thesis, we showed that TGF β stimulation in DAUV melanoma cell line increased Menin expression in control and SMAD2-KO condition but not SMAD3/4-KO condition. These results are in accordance with our previous finding as the SMAD3/4 axis seems to be important in the regulation of menin. Also, we showed that shRNA-silencing of *MEN1* in melanoma significantly reduced the TGF β transcriptional responses, highlighting the important role of menin in the transcriptional activity of the SMADs. Still, further mechanistic characterization at the molecular level should be performed to better understand the signaling cascade of menin in the canonical and non-canonical pathway of TGF β in melanoma.

The nuclear protein menin was also demonstrated to influence the cell cycle progression of cancer cells. It was shown that both JunD and menin expression increased in cells entering in the S Phase^{523,524}. Cells synchronized in G2/M phase expressed lower levels of Menin. A mutant MEN1 induces cells stalled in G0/G1 phase to a rapid progression in S phase, aligning with the findings discussed earlier⁵²⁵. Also, another study showed that menin overexpression induced apoptosis through Bak/Bax dependent pathway in mouse embryonic fibroblasts⁵²⁶. A similar study showed that reconstitution of Menin expression in a Men1-deficient Leydig cell tumor mouse cell-line blocked the G0/G1 to S phase cell cycle transition as well as an increase in apoptosis⁵²⁷. Moreover, this cell cycle arrest was mediated by an increased expression in the CDK inhibitors p18 and p27. Menin was also shown to induce cell cycle arrest by epigenetic regulation by interacting and modulating the activity of histone-methyltransferase. For example, Menin binds to the promoter of p18 and p27 CDKIs and increases methylation of lysine-4 in histone H3, inducing a strong tumor suppression in PNETs³⁸⁷. A recent study showed that genetic depletion of Menin or pharmacological inhibition of Menin/MLL complex led to defect in mitosis cell cycle checkpoints such as spindle assembly⁵²⁸. In melanoma, menin was shown to play tumor-suppressive role through genomic stability by activating the transcription of several genes implicated in HR¹⁷³. These findings align with the research presented in Chapter 3, demonstrating the strong tumor suppressive role of menin.

Some controversial studies showed that MEN1 can be oncogenic in specific cellular contexts^{529–533}. For example, menin was shown to directly interact with the TAD domain of MYC and binds to E-boxes, which leads to transcription activation of MYC target genes and increased proliferation⁵³¹. A study showed that MEN1 overexpression, in a renal fibrosis model, is preventing the TGF β -induced EMT⁵³⁴. Indeed, renal tubular epithelial cells transdifferentiate into myofibroblasts in the progression of renal fibrosis⁵³⁴. This study also showed that a conditional knockout of MEN1 increased EMT, G2/M cell cycle arrest and JNK signaling. In normal pancreatic beta cells, decreases of MLL-menin interactions and TGF β signaling by small molecules inhibitors downregulated the cell cycle inhibitors CDKN1A, CDKN1B and CDKN1C and increased their proliferation⁵³⁵. This study, since it has been done in normal cells, could be beneficial for patients having diabetes but its applicability in cancer patients remains uncertain. Finally, the tissue-specific nature of MEN1 function, whether oncogenic in hematopoietic lineage

or tumor suppressor in the endocrine lineage, suggests the possibility of manifesting contrasting effects across various tissue types, whether cancerous or non-cancerous.

Over the years, more reports show that MEN1 patients develop non-endocrine tumors such as prostate cancer¹⁶⁴, gastrointestinal stromal tumors⁵³⁶, lung cancer⁵³⁷, melanomas¹⁷², lipomas⁵³⁸, collagenomas⁵³⁸ and angiofibromas⁵³⁸. The occurrence of cutaneous melanoma in a MEN1 patient is atypical and it is probable that other genetic contexts are responsible for this association. A study showed that MEN1 gene alterations such as deletion or mutations were not found in primary and metastatic melanoma samples⁵³⁹. Also, the same group claim that MEN1 genomic alterations are not associated with tumorigenesis of malignant melanoma and that MEN1 tumor suppressor gene involve only MEN1-associated diseases such as parathyroid, pancreatic islets and anterior pituitary tumors⁵³⁹. Whether a subgroup of MEN1 individuals is prone to develop dermatological tumors is still an open issue⁵⁴⁰.

We identified a germline mutation of MEN1 (D210A) in a family that developed melanoma. This mutation was found to induce a reading-frame shift (D210A) leading to a truncated menin protein. By reproducing these mutations in melanoma cell lines, we found that the frameshift mutation (D210A) induced a drastic degradation of menin at the protein level when compared to wild-type menin, positive controls menin that are known to be stable (Δ 184-218 and A242V) or other missense mutations that are partially degraded (D418N and L22R). Moreover, we showed that we could restore the frameshift mutants menin expression through inhibition of the proteasome machinery by pharmacological inhibition with PS-341 (Bortezomib) or inhibition of ubiquitin ligase CHIP. Finally, specific gene silencing through gene therapy or small-molecule inhibitors targeting the proteasome could be beneficial for melanoma patients having *MEN1* germline mutations. This study provides evidence that further investigation into their application for treating specific subsets having of *MEN1* cases is justified.

Discussion of PDAC and CRISPR screening

In the chapter 4 of this thesis, we employed a CRISPR-based approach to analyze the entire genome of an aggressive PDAC cell line, aiming to identify genetic vulnerabilities. Our findings reveal that HSPE1 exhibits specific oncogenic properties in PDAC, acting as a regulator of cell cycle and apoptosis through the OPA1 antiapoptotic protein. This demonstrates that CRISPR screen is a powerful tool that can be used to find potential vulnerabilities in cancer. Indeed, several

CRISPR screenings have been performed in PDAC, each of them with unique experimental design and research questions, which will be discussed in the next sections.

CRISPR screening for cancer driver genes discovery in PDAC

The first PDAC CRISPR screen was performed in RNF43-mutant PDAC cell lines, which are dependent in WNT-signaling for substantial growth⁴⁴⁸. FZD5, a member of the ten different Frizzled receptors from the WNT family, is essential for WNT-driven PDAC proliferation. Moreover, antibodies targeting FZD5 strongly inhibited cellular growth of RNF43-mutant PDAC and colorectal cells, highlighting a common vulnerability that can be exploited therapeutically. Our study was performed in HPAF-II cell line, which is also RNF43 mutant. We found FZD5 as a validated target in our CRISPR screening and used it as a positive control. Another study, using a negative selection of a CRISPR_{ko} screen performed in a panel of PDAC cell lines, identified PSMA6, a proteosomal subunit of the 20S core complex, as a critical gene for survival⁵⁴¹. Additionally, proteasomal inhibition was shown to induce a cytotoxic response in PANC-1 cell line. Another study employed CRISPR screening to uncover significant regulators of invasion in PANC-1 cell line⁵⁴². Two genes, MBNL3 and KANSL2, were validated, as their inhibition by a doxycycline-inducible shRNA system revealed them to be powerful drivers of invasive potential without affecting proliferation. A CRISPR_{ko} screening using a small library focused on genes implicated in metabolism enabled the identification of essential genes required for PDAC tumor progression in immunocompetent mice⁵⁴³. The *in vivo* susceptibility of heme synthesis was identified as a liability, which was attributed to the upregulation of the heme-degrading enzyme Hmox1, an effect independent of the tissue origin or immune system. Moreover, they performed an identical screening process in immunocompetent mice. They found that autophagy, typically serving as a protective mechanism for cancer cells against CD8+ T cell killing through TNF α -induced cell death, is a primary metabolic requirement for pancreatic immune escape mechanism. In conclusion, these unbiased CRISPR screens provide some crucial insights about novel genes that can drive PDAC proliferation, tumorigenesis or metastasis, such as HSPE1 mentioned in our study.

Elucidation of drug resistance/sensitivity mechanisms of chemotherapy/radiotherapy in PDAC

A research group performed a CRISPR screening in PDAC to identify genes involved in resistance or sensitivity of NUC-1031, an analog of the gemcitabine chemotherapy agent currently used as a single-agent to treat PDAC patient⁴³². They identified two genes, DCK and DCTPP1, which typically play roles in the pyrimidine metabolic pathway by regulating dCMP/dCTP levels. These genes were found to modulate sensitivity to NUC-1031. Moreover, a parallel screen from the same research team, carried out with gemcitabine, produced no consistent hits, highlighting a unique mechanism of the pyrimidine pathway related with NUC-1031 sensitivity. Another study with similar experimental design showed that SH3D21, a nuclear protein with unknown functions, acts as a gemcitabine sensitizer in highly resistant to chemotherapy PANC-1 cell line⁴³³. Another CRISPR screening in an orthotopic patient-derived xenograft (PDX) model was performed to identify gene targets whose inhibition sensitize cells to gemcitabine treatment⁴³⁴. The protein arginine methyltransferase gene 5 (PRMT5) was recognized as a promising target as its inhibition created a synergistic cytotoxic effect in PDAC cells exposed to gemcitabine through the depletion of replication protein A (RPA) and impaired HDR activity. A CRISPR_{act} screening identified MTA3, a component of the nucleosome remodeling deacetylase transcriptional repression complex, as a mediator of gemcitabine resistance acting through CRIP2 transcriptional repression⁵⁴⁴. Pharmacologically targeting of MTA3 by Colchicine effectively sensitized PDAC cells to gemcitabine treatment, emphasizing the therapeutic potential of MTA3. A dual CRISPR_{ko} and endogenous CRISPR_{act} screening combined with RNA-seq and CHIP-seq was performed to assess the resistance mechanisms of four common chemotherapy agents currently used to treat PDAC patients (gemcitabine, 5-fluorouracil, irinotecan, and oxaliplatin)⁴²⁶. The screens facilitated the identification of two genes whose loss or gain-of-function modulated the sensitivity of chemotherapy drugs: ABCG2, a well-described efflux pump and served as a positive control and HDAC1, upon up-regulation, an increased promoter occupancy and expression of key EMT genes, as well as migration and invasion, highlighting its role in metastasis. A CRISPR screening using a library targeting the kinome identified CDK7 as a candidate for gemcitabine and paclitaxel sensitization in pancreatic cancer by analysis of depleted genes from a CRISPR_{ko} screen⁴³¹. CRISPR-induced genetic depletion of CDK7 and pharmacological inhibition with THZ1, a CDK7 inhibitor, induced both apoptosis and DNA damage upon chemotherapy treatment, through signal transduction decrease of STAT3-MCL1-CHEK1 pathway. Furthermore, THZ1 synergized with gemcitabine and paclitaxel in preclinical models, showing promising therapeutic effects. A

CRISPR_{ko} Screen using a library targeting the kinome identified DYRK1A whose loss-of-function sensitized PDAC cell to radiotherapy⁵⁴⁵. This mechanism was therapeutically exploited through pharmacological suppression of DYRK1A by harmine which increased DSBs, impaired homologous repair and resulted in significant increased cell death. In conclusion, these CRISPR screenings were conducted to identify potential synthetic lethal targets in chemotherapy. These findings hold the potential for developing targeted therapies directed at specific chemotherapy resistance genes in PDAC.

Screening of drug resistance/sensitivity factors of targeted therapy in PDAC

A CRISPR_{ko} synthetic lethality screen was performed to identify genes implicated in sensitization of Farnesyl thiosalicylic acid (FTS), also known as Salirasib, which is a RAS inhibitor that demonstrated poor efficacy in PDAC patients⁴³⁰. In this context, the genetic inhibition of several genes implicated in endoplasmic reticulum-associated protein degradation (ERAD) pathway, such as HRD1 and SEL1L, was found to potentiate the cytotoxic effect of FTS. This mechanism of action was validated with the pharmacological inhibition of ERAD with Eeyarestatin I treatment, which induced the unfolded protein response and apoptosis in several human and mouse PDAC cell lines. CDK4/6 inhibition in PDAC, which restores CDKN2A activity, has shown limited efficacy in clinical trials of PDAC⁵⁴⁶. A CRISPR_{ko} screen with CDK4/6 inhibition (CDK4/6i) with palbociclib as a selection pressure was performed to identify drug-sensitivity mechanisms⁵⁴⁶. CDK2, a gene implicated in the progression of G₁ cell cycle phase, was found to have the strongest synergistic shift in CDK4/6i EC₅₀ value when silenced. Moreover, they found that treatment of PDAC by using as selective CDK2/4/6 inhibitor PF- 06873600⁵⁴⁷ led to an increased amount of apoptotic cells blocked in S-phase with increased DNA damage when compared to the dual CDK4/6i. Moreover, they observed an increase in ERK activation in triple CDK inhibition, which is also a well-known compensatory mechanism for CDK4/6i. This compensatory mechanism was exploited by combining CDK2/4/6i with ERKi which blocked pERK activation and further reduced cell viability in PDAC cell lines. These results support the clinical evaluation of combinatorial and pharmacological CDK2i and CDK4/6i for KRAS-mutant PDAC, which are also supported by two other research teams^{547,548}. A CRISPR_{ko} screen using RNF43-mutant PDAC model demonstrated that the combined pharmacological inhibition of both PI3K/mTOR and WNT pathway resulted in a synergistic effect, suppressing cell proliferation and glucose metabolism⁴²⁸.

As such, dual inhibition of both pathway with PORCN inhibitor ETC-159 and the pan-PI3K inhibitor GDC-0941 have therapeutic potential in the treatment of WNT-driven PDAC cancers. Another *in vivo* CRISPR screen performed from the same research team, utilizing PORCN inhibition to shutdown WNT pathways, identified drug resistance genes implicated in the regulation of β -Catenin levels, including APC, AXIN1, CTNNBIP1. Furthermore, their finding demonstrated that the depletion of histone acetyltransferase EP300 (p300) reduced GATA6 expression, effectively suppressing the GATA6-regulated differentiation program. This signaling shift led to a phenotypic transition from the classical subtype to the dedifferentiated basal-like/squamous subtype of pancreatic cancer. EP300 mutation and loss of GATA6 function bypassed the antidifferentiation activity of Wnt signaling, rendering these cancer cells resistant to Wnt inhibition⁴²⁴. Two different CRISPR screen performed in PDAC enabled the identification of mediators of sensitivity or resistance to MEK pharmacological inhibition^{422,423}. A genome-wide CRISPR screen revealed that combining ERBB or mTOR inhibition with PI3K pharmacological inhibition by alpelisib and pictilisib in pancreatic cancer can drive drug-sensitivity⁵⁴⁹. Moreover, the ribosomal S6 phosphorylation, a key step in PI3K signaling⁵⁵⁰, was correlated with PI3K inhibition sensitivity increase. This study highlights the therapeutic potential of a combinatorial therapy, even in the presence of KRAS, as PI3K pathway activity is a requirement for KRAS-induced tumorigenesis. A study using high throughput genomic such as RNA-seq and chromatin immunoprecipitation (ChIP) sequencing complemented with CRISPR screening showed molecular dependencies of pancreatic cancer stem cells⁵⁵¹. These included the nuclear hormone receptor retinoic-acid-receptor-related orphan receptor gamma (ROR γ), which is implicated in inflammatory cytokine production and T-cell differentiation. ROR γ upregulation was shown to increase pancreatic cell proliferation and ROR γ pharmacological inhibition led to a significant reduction in cell fitness. This study suggests that pharmacological agents shutting down immune-regulatory signals in pancreatic cancer could be exploited to treat this aggressive and untreatable cancer.

All these CRISPR screenings exploit potential vulnerabilities to treat PDAC in a similar fashion as our study, which highlighted both HSPE1, through the dual complex HSPD1/HSPE1, as well as OPA1, as actionable targets to treat PDAC. In conclusion, the findings revealed in this thesis could be potentially applicated directly from the bench to the clinic, paving the way for new therapies in aggressive cancer such as metastatic melanoma and PDAC.

Conclusion and perspectives

Chapter 2 of this thesis showed that TGF β has a negative role in the self-renewal ability of melanoma cancer stem cells through SMAD3/4 signaling. Therefore, exploring the differential molecular mechanisms through which SMAD2 and SMAD3 contribute to stem cell maintenance in melanoma could be an intriguing avenue of investigation. Transcriptional profiling could be performed in experimental models expressing differential levels of SMAD2 and SMAD3 which could reveal specific stem cell-related genes implicated in melanoma progression. Moreover, differentiation therapy could be beneficial to remove the high tumor-initiating and metastatic potential of melanoma cancer stem cell through the activation of the TGF β pathway in a SMAD3/4 manner.

Chapter 3 of this thesis demonstrated that MEN1 acts as a tumor suppressor in melanoma. Also, it was shown that novel mutations inactivating MEN1 can be reversed using either pharmacological approaches or gene-silencing techniques targeting proteasomal inhibition. Even if melanoma is a low-occurrence dysplasia in MEN1 patients, targeting the proteasomal machinery in those patients who exhibit aggressive melanoma phenotype could be beneficial for their treatment. Nevertheless, it may be meaningful to improve the specificity of proteasomal pharmacological agents, as their current clinical use often results in various side effects. This highlights the possibility of avoiding unintended targeting of multiple proteins or undesirable targets by employing pharmacological proteasome inhibition.

Chapter 4 of this thesis revealed that HSPE1 is a novel and actionable oncogene in PDAC. Indeed, pharmacological inhibition of the HSPD1/HSPE1 complex or the direct downstream target of HSPE1, OPA1, demonstrated high anti-tumor response in our pre-clinical models. Thus, it could be interesting in evaluating a dual inhibition as a potential combining therapy to enhance its therapeutic efficacy. Moreover, the mechanism where HSPE1 enhances the cleavage of OPA1 by OMA1 is still unknown. It could be relevant to assess if other mitochondria proteins are implicated in this mechanism.

References

1. DeVita, V. T. & Rosenberg, S. A. Two Hundred Years of Cancer Research. *N. Engl. J. Med.* **366**, 2207–2214 (2012).
2. Avery, O. T., MacLeod, C. M. & McCarty, M. STUDIES ON THE CHEMICAL

- NATURE OF THE SUBSTANCE INDUCING TRANSFORMATION OF PNEUMOCOCCAL TYPES. *J. Exp. Med.* **79**, 137–158 (1944).
3. WATSON, J. D. & CRICK, F. H. C. Molecular Structure of Nucleic Acids: A Structure for Deoxyribose Nucleic Acid. *Nature* **171**, 737–738 (1953).
 4. Loenen, W. A. M., Dryden, D. T. F., Raleigh, E. A., Wilson, G. G. & Murray, N. E. Highlights of the DNA cutters: A short history of the restriction enzymes. *Nucleic Acids Res.* **42**, 3–19 (2014).
 5. Garraway, L. A., Verweij, J. & Ballman, K. V. Precision oncology: An overview. *J. Clin. Oncol.* **31**, 1803–1805 (2013).
 6. Park, H. Y., Kosmadaki, M., Yaar, M. & Gilchrist, B. A. Cellular mechanisms regulating human melanogenesis. *Cell. Mol. Life Sci.* **66**, 1493–1506 (2009).
 7. Casalou, C., Moreiras, H., Mayatra, J. M., Fabre, A. & Tobin, D. J. Loss of ‘Epidermal Melanin Unit’ Integrity in Human Skin During Melanoma-Genesis. *Front. Oncol.* **12**, 1–14 (2022).
 8. D’Mello, S. A. N., Finlay, G. J., Baguley, B. C. & Askarian-Amiri, M. E. Signaling pathways in melanogenesis. *Int. J. Mol. Sci.* **17**, 1–18 (2016).
 9. Greene, M. H. *et al.* A study of tumor progression: The precursor lesions of superficial spreading and nodular melanoma. *Hum. Pathol.* **15**, 1147–1165 (1984).
 10. Miller, A. J. & Mihm, M. C. Melanoma. *N. Engl. J. Med.* **355**, 51–65 (2006).
 11. Proietti, I. *et al.* Mechanisms of acquired BRAF inhibitor resistance in melanoma: A systematic review. *Cancers (Basel)*. **12**, 1–29 (2020).
 12. Poynter, J. N. *et al.* BRAF and NRAS mutations in melanoma and melanocytic nevi. *Melanoma Res.* **16**, 267–273 (2006).
 13. Muñoz-Couselo, E., Adelantado, E. Z., Ortiz, C., García, J. S. & Perez-Garcia, J. NRAS-mutant melanoma: Current challenges and future prospect. *Onco. Targets. Ther.* **10**, 3941–3947 (2017).
 14. Wang, A.-X. & Qi, X.-Y. Targeting RAS/RAF/MEK/ERK signaling in metastatic melanoma. *IUBMB Life* **65**, 748–758 (2013).
 15. Flaherty, K. T. *et al.* Combined BRAF and MEK inhibition in melanoma with BRAF V600 mutations. *N. Engl. J. Med.* **367**, 1694–1703 (2012).
 16. Michaloglou, C. *et al.* BRAFE600-associated senescence-like cell cycle arrest of human

- naevi. *Nature* **436**, 720–724 (2005).
17. Patton, E. E. *et al.* BRAF Mutations Are Sufficient to Promote Nevi Formation and Cooperate with p53 in the Genesis of Melanoma. *Curr. Biol.* **15**, 249–254 (2005).
 18. Cabrita, R. *et al.* The Role of PTEN Loss in Immune Escape, Melanoma Prognosis and Therapy Response. *Cancers (Basel)*. **12**, 742 (2020).
 19. Ince, F. A., Shariev, A. & Dixon, K. PTEN as a target in melanoma. *J. Clin. Pathol.* **75**, 581–584 (2022).
 20. Cantley, L. C. & Neel, B. G. New insights into tumor suppression: PTEN suppresses tumor formation by restraining the phosphoinositide 3-kinase/AKT pathway. *Proc. Natl. Acad. Sci. U. S. A.* **96**, 4240–4245 (1999).
 21. Levy, C., Khaled, M. & Fisher, D. E. MITF: master regulator of melanocyte development and melanoma oncogene. *Trends Mol. Med.* **12**, 406–414 (2006).
 22. Hsiao, J. J. & Fisher, D. E. The roles of microphthalmia-associated transcription factor and pigmentation in melanoma. *Arch. Biochem. Biophys.* **563**, 28–34 (2014).
 23. McGill, G. G. *et al.* Bcl2 regulation by the melanocyte master regulator Mitf modulates lineage survival and melanoma cell viability. *Cell* **109**, 707–718 (2002).
 24. Du, J. *et al.* Critical role of CDK2 for melanoma growth linked to its melanocyte-specific transcriptional regulation by MITF. *Cancer Cell* **6**, 565–576 (2004).
 25. Garraway, L. A. & Sellers, W. R. From integrated genomics to tumor lineage dependency. *Cancer Res.* **66**, 2506–2508 (2006).
 26. Rambow, F., Marine, J. C. & Goding, C. R. Melanoma plasticity and phenotypic diversity: Therapeutic barriers and opportunities. *Genes Dev.* **33**, 1295–1318 (2019).
 27. Rambow, F. *et al.* Toward Minimal Residual Disease-Directed Therapy in Melanoma. *Cell* **174**, 843-855.e19 (2018).
 28. Miller, A. J. *et al.* Transcriptional Regulation of the Melanoma Prognostic Marker Melastatin (TRPM1) by MITF in Melanocytes and Melanoma. *Cancer Res.* **64**, 509–516 (2004).
 29. Duncan, L. M. *et al.* Down-regulation of the novel gene melastatin correlates with potential for melanoma metastasis. *Cancer Res.* **58**, 1515–1520 (1998).
 30. Switzer, B., Puzanov, I., Skitzki, J. J., Hamad, L. & Ernstoff, M. S. Managing Metastatic Melanoma in 2022: A Clinical Review. *JCO Oncol. Pract.* **18**, 335–351 (2022).

31. Damsky, W. E., Theodosakis, N. & Bosenberg, M. Melanoma metastasis: New concepts and evolving paradigms. *Oncogene* **33**, 2413–2422 (2014).
32. Neel, J.-C., Humbert, L. & Lebrun, J.-J. The Dual Role of TGF β in Human Cancer: From Tumor Suppression to Cancer Metastasis. *ISRN Mol. Biol.* **2012**, 1–28 (2012).
33. Sun, P. D. & Davies, D. R. The Cystine-Knot Growth-Factor Superfamily. *Annu. Rev. Biophys. Biomol. Struct.* **24**, 269–292 (1995).
34. Miyazono, K., Ichijo, H. & Heldin, C. H. Transforming growth factor- β : Latent forms, binding proteins and receptors. *Growth Factors* **8**, 11–22 (1993).
35. Chen, W. & Ten Dijke, P. Immunoregulation by members of the TGF β superfamily. *Nat. Rev. Immunol.* **16**, 723–740 (2016).
36. Cheifetz, S. *et al.* Distinct transforming growth factor-beta (TGF-beta) receptor subsets as determinants of cellular responsiveness to three TGF-beta isoforms. *J. Biol. Chem.* **265**, 20533–20538 (1990).
37. Yang, Y. *et al.* The Role of TGF- β Signaling Pathways in Cancer and Its Potential as a Therapeutic Target. *Evidence-based Complement. Altern. Med.* **2021**, (2021).
38. Guo, X. & Wang, X. F. Signaling cross-talk between TGF- β /BMP and other pathways. *Cell Res.* **19**, 71–88 (2009).
39. Ishida, W. *et al.* Smad6 is a Smad1/5-induced Smad inhibitor. Characterization of bone morphogenetic protein-responsive element in the mouse Smad6 promoter. *J. Biol. Chem.* **275**, 6075–6079 (2000).
40. Yan, X., Liu, Z. & Chen, Y. Regulation of TGF- β signaling by Smad7. *Acta Biochim. Biophys. Sin. (Shanghai)*. **41**, 263–272 (2009).
41. Zhang, Y. E. Non-Smad pathways in TGF- β signaling. *Cell Res.* **19**, 128–139 (2009).
42. Zhang, Y. E. Non-Smad signaling pathways of the TGF- β family. *Cold Spring Harb. Perspect. Biol.* **9**, (2017).
43. Davis-Dusenbery, B. N. & Hata, A. Smad-mediated miRNA processing: A critical role for a conserved RNA sequence. *RNA Biol.* **8**, 71–76 (2011).
44. Davis, B. N., Hilyard, A. C., Lagna, G. & Hata, A. SMAD proteins control DROSHA-mediated microRNA maturation. *Nature* **454**, 56–61 (2008).
45. Akhurst, R. J. & Hata, A. Targeting the TGF β signalling pathway in disease. *Nat. Rev. Drug Discov.* **11**, 790–811 (2012).

46. Chen, C. R., Kang, Y., Siegel, P. M. & Massagué, J. E2F4/5 and p107 as Smad cofactors linking the TGF β receptor to c-myc repression. *Cell* **110**, 19–32 (2002).
47. Petritsch, C., Beug, H., Baimain, A. & Oft, M. TGF- β inhibits p70 S6 kinase via protein phosphatase 2A to induce G1 arrest. *Genes Dev.* **14**, 3093–3101 (2000).
48. Chalaux, E. *et al.* A zinc-finger transcription factor induced by TGF- β promotes apoptotic cell death in epithelial Mv1Lu cells. *FEBS Lett.* **457**, 478–482 (1999).
49. Jang, C. W. *et al.* TGF- β induces apoptosis through Smad-mediated expression of DAP-kinase. *Nat. Cell Biol.* **4**, 51–58 (2002).
50. Yoo, J. *et al.* Transforming Growth Factor- β -induced Apoptosis Is Mediated by Smad-dependent Expression of GADD45b through p38 Activation. *J. Biol. Chem.* **278**, 43001–43007 (2003).
51. Ramjaun, A. R., Tomlinson, S., Eddaoudi, A. & Downward, J. Upregulation of two BH3-only proteins, Bmf and Bim, during TGF β -induced apoptosis. *Oncogene* **26**, 970–981 (2007).
52. Ohgushi, M. *et al.* Transforming Growth Factor β -Dependent Sequential Activation of Smad, Bim, and Caspase-9 Mediates Physiological Apoptosis in Gastric Epithelial Cells. *Mol. Cell. Biol.* **25**, 10017–10028 (2005).
53. Zhang, H. *et al.* Involvement of programmed cell death 4 in transforming growth factor- β 1-induced apoptosis in human hepatocellular carcinoma. *Oncogene* **25**, 6101–6112 (2006).
54. David, C. J. *et al.* TGF- β Tumor Suppression through a Lethal EMT. *Cell* **164**, 1015–1030 (2016).
55. Gottfried, Y., Rotem, A., Lotan, R., Steller, H. & Larisch, S. The mitochondrial ARTS protein promotes apoptosis through targeting XIAP. *EMBO J.* **23**, 1627–1635 (2004).
56. Valderrama-Carvajal, H. *et al.* Activin/TGF- β induce apoptosis through Smad-dependent expression of the lipid phosphatase SHIP. *Nat. Cell Biol.* **4**, 963–969 (2002).
57. Yang, J. *et al.* Guidelines and definitions for research on epithelial–mesenchymal transition. *Nat. Rev. Mol. Cell Biol.* **21**, 341–352 (2020).
58. Hao, Y., Baker, D. & Dijke, P. Ten. TGF- β -mediated epithelial-mesenchymal transition and cancer metastasis. *Int. J. Mol. Sci.* **20**, (2019).
59. Lamouille, S., Xu, J. & Derynck, R. Molecular mechanisms of epithelial-mesenchymal

- transition. *Nat. Rev. Mol. Cell Biol.* **15**, 178–196 (2014).
60. Vincent, T. *et al.* A SNAIL1-SMAD3/4 transcriptional repressor complex promotes TGF- β mediated epithelial-mesenchymal transition. *Nat. Cell Biol.* **11**, 943–950 (2009).
 61. Hoot, K. E. *et al.* Keratinocyte-specific Smad2 ablation results in increased epithelial-mesenchymal transition during skin cancer formation and progression. *J. Clin. Invest.* **118**, 2722–2732 (2008).
 62. Yu, J. *et al.* MicroRNA-182 targets SMAD7 to potentiate TGF β -induced epithelial-mesenchymal transition and metastasis of cancer cells. *Nat. Commun.* **7**, 1–12 (2016).
 63. Goumans, M. J. *et al.* Balancing the activation state of the endothelium via two distinct TGF- β type I receptors. *EMBO J.* **21**, 1743–1753 (2002).
 64. Breier, G. *et al.* Transforming growth factor- β and RAS regulate the VEGF/VEGF-receptor system during tumor angiogenesis. *Int. J. Cancer* **97**, 142–148 (2002).
 65. Sun, H. *et al.* TGF- β 1/T β RII/Smad3 signaling pathway promotes VEGF expression in oral squamous cell carcinoma tumor-associated macrophages. *Biochem. Biophys. Res. Commun.* **497**, 583–590 (2018).
 66. Gorelik, L. & Flavell, R. A. Abrogation of TGF β signaling in T cells leads to spontaneous T cell differentiation and autoimmune disease. *Immunity* **12**, 171–181 (2000).
 67. Gorelik, L. & Flavell, R. A. Immune-mediated eradication of tumors through the blockade of transforming growth factor- β signaling in T cells. *Nat. Med.* **7**, 1118–1122 (2001).
 68. Tauriello, D. V. F. *et al.* TGF β drives immune evasion in genetically reconstituted colon cancer metastasis. *Nature* **554**, 538–543 (2018).
 69. Mariathasan, S. *et al.* TGF β attenuates tumour response to PD-L1 blockade by contributing to exclusion of T cells. *Nature* **554**, 544–548 (2018).
 70. Albino, A. P., Davis, B. M. & Nanus, D. M. Induction of Growth Factor RNA Expression in Human Malignant Melanoma: Markers of Transformation. *Cancer Res.* **51**, 4815–4820 (1991).
 71. Krasagakis, K., Garbe, C., Schrier, P. I. & Orfanos, C. E. Paracrine and autocrine regulation of human melanocyte and melanoma cell growth by transforming growth factor beta in vitro. *Anticancer Res.* **14**, 2565–2571 (1994).
 72. Mattei, S. *et al.* Expression of cytokine/growth factors and their receptors in human

- melanoma and melanocytes. *Int. J. Cancer* (1994). doi:10.1002/ijc.2910560617
73. Gold, L. I. & Korc, M. Expression of transforming growth factor- β 1, 2, and 3 mRNA and protein in human cancers. *Dig. Surg.* (1994). doi:10.1159/000172246
 74. Rodeck, U. *et al.* Constitutive expression of multiple growth factor genes by melanoma cells but not normal melanocytes. *J. Invest. Dermatol.* (1991). doi:10.1111/1523-1747.ep12477822
 75. Van Belle, P., Rodeck, U., Nuamah, I., Halpern, A. C. & Elder, D. E. Melanoma-associated expression of transforming growth factor- β isoforms. *Am. J. Pathol.* **148**, 1887–1894 (1996).
 76. Krasagakis, K. *et al.* Desensitization of melanoma cells to autocrine TGF-beta isoforms. *J. Cell. Physiol.* **178**, 179–187 (1999).
 77. Rodeck, U. *et al.* Transforming growth factor beta production and responsiveness in normal human melanocytes and melanoma cells. *Cancer Res.* **54**, 575–581 (1994).
 78. Rodeck, U., Nishiyama, T. & Mauviel, A. Independent regulation of growth and SMAD-mediated transcription by transforming growth factor β in human melanoma cells. *Cancer Res.* **59**, 547–550 (1999).
 79. Heredia, A., Villena, J., Romarís, M., Molist, A. & Bassols, A. The effect of TGF-beta 1 on cell proliferation and proteoglycan production in human melanoma cells depends on the degree of cell differentiation. *Cancer Lett.* **109**, 39–47 (1996).
 80. Humbert, L. & Lebrun, J. J. TGF-beta inhibits human cutaneous melanoma cell migration and invasion through regulation of the plasminogen activator system. *Cell. Signal.* **25**, 490–500 (2013).
 81. Ramont, L., Pasco, S., Hornebeck, W., Maquart, F. X. & Monboisse, J. C. Transforming growth factor- β 1 inhibits tumor growth in a mouse melanoma model by down-regulating the plasminogen activation system. *Exp. Cell Res.* **291**, 1–10 (2003).
 82. Humbert, L., Ghozlan, M., Canaff, L., Tian, J. & Lebrun, J. J. The leukemia inhibitory factor (LIF) and p21 mediate the TGF β tumor suppressive effects in human cutaneous melanoma. *BMC Cancer* **15**, 1–16 (2015).
 83. Ritsma, L. *et al.* Integrin β 1 activation induces an antimelanoma host response. *PLoS One* **12**, 1–24 (2017).
 84. Kodama, S. *et al.* Progression of melanoma is suppressed by targeting all transforming

- growth factor- β isoforms with an Fc chimeric receptor. *Oncol. Rep.* **46**, 1–13 (2021).
85. Penafuerte, C. *et al.* Novel TGF- β Antagonist Inhibits Tumor Growth and Angiogenesis by Inducing IL-2 Receptor-Driven STAT1 Activation. *J. Immunol.* **186**, 6933–6944 (2011).
 86. Nelson, B. H., Martyak, T. P., Thompson, L. J., Moon, J. J. & Wang, T. Uncoupling of Promitogenic and Antiapoptotic Functions of IL-2 by Smad-Dependent TGF- β Signaling. *J. Immunol.* **170**, 5563–5570 (2003).
 87. Hoek, K. S. *et al.* Metastatic potential of melanomas defined by specific gene expression profiles with no BRAF signature. *Pigment Cell Res.* **19**, 290–302 (2006).
 88. Bittner, M. *et al.* Molecular classification of cutaneous malignant melanoma by gene expression profiling. *Nature* **406**, 536–540 (2000).
 89. Hoek, K. S. *et al.* In vivo switching of human melanoma cells between proliferative and invasive states. *Cancer Res.* **68**, 650–656 (2008).
 90. Kemper, K., de Goeje, P. L., Peeper, D. S. & van Amerongen, R. Phenotype Switching: Tumor Cell Plasticity as a Resistance Mechanism and Target for Therapy. *Cancer Res.* **74**, 5937–5941 (2014).
 91. Sun, C. *et al.* Reversible and adaptive resistance to BRAF(V600E) inhibition in melanoma. *Nature* **508**, 118–122 (2014).
 92. Tuncer, E. *et al.* SMAD signaling promotes melanoma metastasis independently of phenotype switching. *J. Clin. Invest.* **129**, 2702–2716 (2019).
 93. Caramel, J. *et al.* A Switch in the Expression of Embryonic EMT-Inducers Drives the Development of Malignant Melanoma. *Cancer Cell* **24**, 466–480 (2013).
 94. Heppt, M. V. *et al.* MSX1-Induced Neural Crest-Like Reprogramming Promotes Melanoma Progression. *J. Invest. Dermatol.* **138**, 141–149 (2018).
 95. Fuchs, E. & Chen, T. A matter of life and death: Self-renewal in stem cells. *EMBO Rep.* **14**, 39–48 (2013).
 96. Yin, Q., Shi, X., Lan, S., Jin, H. & Wu, D. Effect of melanoma stem cells on melanoma metastasis (Review). *Oncol. Lett.* **22**, 566 (2021).
 97. Nowell, P. C. The clonal evolution of tumor cell populations. *Science (80-.)*. **194**, 23–28 (1976).
 98. Dick, J. E. & Bonnet, D. Human Acute Myeloid Leukaemia is organised as a heirarchy

- that originates from a primitive hematopoietic cell. *Nat. Med.* **3**, 730–737 (1997).
99. La Porta, C. A. M. & Zapperi, S. Complexity in cancer stem cells and tumor evolution: Toward precision medicine. *Semin. Cancer Biol.* **44**, 3–9 (2017).
 100. Quintana, E. *et al.* Phenotypic heterogeneity among tumorigenic melanoma cells from patients that is reversible and not hierarchically organized. *Cancer Cell* **18**, 510–523 (2010).
 101. Quintana, E. *et al.* Efficient tumour formation by single human melanoma cells. *Nature* **456**, 593–598 (2008).
 102. Glumac, P. M. & LeBeau, A. M. The role of CD133 in cancer: a concise review. *Clin. Transl. Med.* **7**, 18 (2018).
 103. Monzani, E. *et al.* Melanoma contains CD133 and ABCG2 positive cells with enhanced tumourigenic potential. *Eur. J. Cancer* **43**, 935–946 (2007).
 104. Gazzaniga, P. *et al.* CD133 and ABCB5 as stem cell markers on sentinel lymph node from melanoma patients. *Eur. J. Surg. Oncol.* **36**, 1211–1214 (2010).
 105. Jaksch, M., Múnera, J., Bajpai, R., Terskikh, A. & Oshima, R. G. Cell cycle-dependent variation of a CD133 epitope in human embryonic stem cell, colon cancer, and melanoma cell lines. *Cancer Res.* **68**, 7882–7886 (2008).
 106. Grasso, C. *et al.* Iterative sorting reveals CD133+ and CD133- melanoma cells as phenotypically distinct populations. *BMC Cancer* **16**, 1–11 (2016).
 107. Simbulan-Rosenthal, C. M. *et al.* CRISPR-Cas9 knockdown and induced expression of CD133 reveal essential roles in melanoma invasion and metastasis. *Cancers (Basel)*. **11**, 1–23 (2019).
 108. Boiko, A. D. *et al.* Human melanoma-initiating cells express neural crest nerve growth factor receptor CD271. *Nature* **466**, 133–137 (2010).
 109. Restivo, G. *et al.* Low Neurotrophin receptor CD271 regulates phenotype switching in Melanoma. *Nat. Commun.* **8**, (2017).
 110. Filipp, F. V., Li, C. & Boiko, A. D. CD271 is a molecular switch with divergent roles in melanoma and melanocyte development. *Sci. Rep.* **9**, 1–11 (2019).
 111. Radke, J., Roßner, F. & Redmer, T. CD271 determines migratory properties of melanoma cells. *Sci. Rep.* **7**, 1–14 (2017).
 112. Amann, P. M. *et al.* Expression and activity of alcohol and aldehyde dehydrogenases in

- melanoma cells and in melanocytes. *J. Cell. Biochem.* **113**, 792–799 (2012).
113. Luo, Y. *et al.* ALDH1A isozymes are markers of human melanoma stem cells and potential therapeutic targets. *Stem Cells* **30**, 2100–2113 (2012).
 114. Zhang, S., Yang, Z. & Qi, F. Aldehyde dehydrogenase-positive melanoma stem cells in tumorigenesis, drug resistance and anti-neoplastic immunotherapy. *Mol. Biol. Rep.* **47**, 1435–1443 (2020).
 115. Jim B. Boonyaratanakornkit *et al.* Selection of Tumorigenic Melanoma Cells Using ALDH. *J Autism Dev Disord J Invest Dermatol.* **47**, 549–562 (2010).
 116. Samson, J. M. *et al.* Clinical implications of ALDH1A1 and ALDH1A3 mRNA expression in melanoma subtypes. *Chem. Biol. Interact.* **314**, 108822 (2019).
 117. Ravindran Menon, D. *et al.* A stress-induced early innate response causes multidrug tolerance in melanoma. *Oncogene* **34**, 4448–4459 (2015).
 118. Sarvi, S. *et al.* ALDH1 Bio-activates Nifuroxazide to Eradicate ALDH High Melanoma-Initiating Cells. *Cell Chem. Biol.* **25**, 1456-1469.e6 (2018).
 119. Zhu, Y. *et al.* Nifuroxazide exerts potent anti-tumor and anti-metastasis activity in melanoma. *Sci. Rep.* **6**, 1–13 (2016).
 120. Petrachi, T. *et al.* Therapeutic potential of the metabolic modulator phenformin in targeting the stem cell compartment in melanoma. *Oncotarget* **8**, 6914–6928 (2017).
 121. Schatton, T. *et al.* Identification of cells initiating human melanomas. *Nature* **451**, 345–349 (2008).
 122. Wilson, B. J. *et al.* ABCB5 Maintains Melanoma-Initiating Cells through a Proinflammatory Cytokine Signaling Circuit. *Cancer Res.* **74**, 4196–4207 (2014).
 123. Xiao, J., Egger, M. E., McMasters, K. M. & Hao, H. Differential expression of ABCB5 in BRAF inhibitor-resistant melanoma cell lines. *BMC Cancer* **18**, 1–10 (2018).
 124. Sana, G. *et al.* Exome Sequencing of ABCB5 Identifies Recurrent Melanoma Mutations that Result in Increased Proliferative and Invasive Capacities. *J. Invest. Dermatol.* **139**, 1985-1992.e10 (2019).
 125. Fang, D. *et al.* A tumorigenic subpopulation with stem cell properties in melanomas. *Cancer Res.* **65**, 9328–9337 (2005).
 126. Schmidt, P. *et al.* Eradication of melanomas by targeted elimination of a minor subset of tumor cells. *Proc. Natl. Acad. Sci. U. S. A.* **108**, 2474–2479 (2011).

127. Brandenberger, R. *et al.* Transcriptome characterization elucidates signaling networks that control human ES cell growth and differentiation. *Nat. Biotechnol.* **22**, 707–716 (2004).
128. Beattie, G. M. *et al.* Activin A Maintains Pluripotency of Human Embryonic Stem Cells in the Absence of Feeder Layers. *Stem Cells* **23**, 489–495 (2005).
129. Xiao, L., Yuan, X. & Sharkis, S. J. Activin A Maintains Self-Renewal and Regulates Fibroblast Growth Factor, Wnt, and Bone Morphogenic Protein Pathways in Human Embryonic Stem Cells. *Stem Cells* **24**, 1476–1486 (2006).
130. Sirard, C. *et al.* The tumor suppressor gene Smad4/Dpc4 is required for gastrulation and later for anterior development of the mouse embryo. *Genes Dev.* **12**, 107–119 (1998).
131. James, D., Levine, A. J., Besser, D. & Hemmati-Brivanlou, A. TGF β /activin/nodal signaling is necessary for the maintenance of pluripotency in human embryonic stem cells. *Development* **132**, 1273–1282 (2005).
132. Lavker, R. M. *et al.* Hair Follicle Stem Cells: Their Location, Role in Hair Cycle, and Involvement in Skin Tumor Formation. *J. Invest. Dermatol.* **101**, 16S-26S (1993).
133. Nishimura, E. K. *et al.* Key Roles for Transforming Growth Factor β in Melanocyte Stem Cell Maintenance. *Cell Stem Cell* **6**, 130–140 (2010).
134. Kulesza, D. W., Przanowski, P. & Kaminska, B. Knockdown of STAT3 targets a subpopulation of invasive melanoma stem-like cells. *Cell Biol. Int.* **43**, 613–622 (2019).
135. Singh, A. M. *et al.* Signaling network crosstalk in human pluripotent cells: A Smad2/3-regulated switch that controls the balance between self-renewal and differentiation. *Cell Stem Cell* **10**, 312–326 (2012).
136. Qian, X., Jin, L., Grande, J. P. & Lloyd, R. V. Transforming growth factor-beta and p27 expression in pituitary cells. *Endocrinology* **137**, 3051–3060 (1996).
137. Cheli, Y. *et al.* Mitf is the key molecular switch between mouse or human melanoma initiating cells and their differentiated progeny. *Oncogene* **30**, 2307–2318 (2011).
138. Damasceno, P. K. F. *et al.* Genetic Engineering as a Strategy to Improve the Therapeutic Efficacy of Mesenchymal Stem/Stromal Cells in Regenerative Medicine. *Front. Cell Dev. Biol.* **8**, 1–24 (2020).
139. Wainwright, E. N. & Scaffidi, P. Epigenetics and Cancer Stem Cells: Unleashing, Hijacking, and Restricting Cellular Plasticity. *Trends in Cancer* **3**, 372–386 (2017).
140. Carney, J. A. Familial multiple endocrine neoplasia: the first 100 years. *Am. J. Surg.*

- Pathol.* **29**, 254–274 (2005).
141. Chandrasekharappa, S. C. *et al.* Positional cloning of the gene for multiple endocrine neoplasia-type 1. *Science* (80-.). **276**, 404–406 (1997).
 142. Lemos, M. C. & Thakker, R. V. Multiple endocrine neoplasia type 1 (MEN1): analysis of 1336 mutations reported in the first decade following identification of the gene. *Hum. Mutat.* **29**, 22–32 (2008).
 143. Zhuang, Z. *et al.* Mutations of the MEN1 tumor suppressor gene in pituitary tumors. *Cancer Res.* **57**, 5446–5451 (1997).
 144. Harding, B. *et al.* Multiple endocrine neoplasia type 1 knockout mice develop parathyroid, pancreatic, pituitary and adrenal tumours with hypercalcaemia, hypophosphataemia and hypercorticozonaemia. *Endocr. Relat. Cancer* **16**, 1313–1327 (2009).
 145. Dreijerink, K. M. A., Timmers, H. T. M. & Brown, M. Twenty years of menin: emerging opportunities for restoration of transcriptional regulation in MEN1. *Endocr. Relat. Cancer* **24**, T135–T145 (2017).
 146. Scacheri, P. C. *et al.* Genome-wide analysis of menin binding provides insights into MEN1 tumorigenesis. *PLoS Genet.* **2**, 406–419 (2006).
 147. Monazzam, A. *et al.* Generation and characterization of CRISPR/Cas9-mediated MEN1 knockout BON1 cells: a human pancreatic neuroendocrine cell line. *Sci. Rep.* **10**, 1–10 (2020).
 148. Hendy, G. N., Kaji, H. & Canaff, L. Cellular functions of menin. *Adv. Exp. Med. Biol.* **668**, 37–50 (2009).
 149. Marx, S. J. *et al.* Multiple endocrine neoplasia type 1: clinical and genetic features of the hereditary endocrine neoplasias. *Recent Prog. Horm. Res.* **54**, 397–399 (1999).
 150. Agarwal, S. K. *et al.* Menin Interacts with the AP1 Transcription Factor JunD and Represses JunD-Activated Transcription. *Cell* **96**, 143–152 (1999).
 151. Gallo, A. *et al.* Menin uncouples Elk-1, JunD and c-Jun phosphorylation from MAP kinase activation. *Oncogene* **21**, 6434–6445 (2002).
 152. Huang, J. *et al.* The same pocket in menin binds both MLL and JUND but has opposite effects on transcription. *Nature* **482**, 542–546 (2012).
 153. Canaff, L., Vanbellinthen, J. F., Kaji, H., Goltzman, D. & Hendy, G. N. Impaired transforming growth factor- β (TGF- β) transcriptional activity and cell proliferation control

- of a menin in-frame deletion mutant associated with Multiple Endocrine Neoplasia type 1 (MEN1). *J. Biol. Chem.* **287**, 8584–8597 (2012).
154. Hughes, C. M. *et al.* Menin Associates with a Trithorax Family Histone Methyltransferase Complex and with the Hoxc8 Locus. *Mol. Cell* **13**, 587–597 (2004).
 155. Shi, Q., Xu, M., Kang, Z., Zhang, M. & Luo, Y. Menin–MLL1 Interaction Small Molecule Inhibitors: A Potential Therapeutic Strategy for Leukemia and Cancers. *Molecules* **28**, 1–15 (2023).
 156. Brès, V., Yoshida, T., Pickle, L. & Jones, K. A. SKIP Interacts with c-Myc and Menin to Promote HIV-1 Tat Transactivation. *Mol. Cell* **36**, 75–87 (2009).
 157. Heppner, C. *et al.* The tumor suppressor protein menin interacts with NF- κ b proteins and inhibits NF- κ b-mediated transactivation. *Oncogene* **20**, 4917–4925 (2001).
 158. Wang, Y. *et al.* The Tumor Suppressor Protein Menin Inhibits AKT Activation by Regulating Its Cellular Localization. *Cancer Res.* **71**, 371–382 (2011).
 159. Razmara, M., Monazzam, A. & Skogseid, B. Reduced menin expression impairs rapamycin effects as evidenced by an increase in mTORC2 signaling and cell migration. *Cell Commun. Signal.* **16**, 64 (2018).
 160. Dreijerink, K. M. A. *et al.* Menin links estrogen receptor activation to histone H3K4 trimethylation. *Cancer Res.* **66**, 4929–4935 (2006).
 161. Dreijerink, K. M. A. *et al.* The Multiple Endocrine Neoplasia Type 1 (MEN1) Tumor Suppressor Regulates Peroxisome Proliferator-Activated Receptor γ -Dependent Adipocyte Differentiation. *Mol. Cell. Biol.* **29**, 5060–5069 (2009).
 162. Cheng, P. *et al.* Menin prevents liver steatosis through co-activation of peroxisome proliferator-activated receptor alpha. *FEBS Lett.* **585**, 3403–3408 (2011).
 163. Cheng, P. *et al.* Tumor suppressor Menin acts as a corepressor of LXR α to inhibit hepatic lipogenesis. *FEBS Lett.* **589**, 3079–3084 (2015).
 164. Malik, R. *et al.* Targeting the MLL complex in castration-resistant prostate cancer. *Nat. Med.* **21**, 344–352 (2015).
 165. Kaji, H., Canaff, L., Lebrun, J.-J., Goltzman, D. & Hendy, G. N. Inactivation of menin, a Smad3-interacting protein, blocks transforming growth factor type β signaling. *Proc. Natl. Acad. Sci.* **98**, 3837–3842 (2001).
 166. Lacerte, A. *et al.* Activin inhibits pituitary prolactin expression and cell growth through

- Smads, Pit-1 and menin. *Mol. Endocrinol.* **18**, 1558–1569 (2004).
167. Sowa, H. *et al.* Inactivation of menin, the product of the multiple endocrine neoplasia type 1 gene, inhibits the commitment of multipotential mesenchymal stem cells into the osteoblast lineage. *J. Biol. Chem.* **278**, 21058–21069 (2003).
168. Sowa, H. *et al.* Menin Inactivation Leads to Loss of Transforming Growth Factor β Inhibition of Parathyroid Cell Proliferation and Parathyroid Hormone Secretion. *Cancer Res.* **64**, 2222–2228 (2004).
169. Zhang, H., Liu, Z. guo & Hua, X. xin. Menin expression is regulated by transforming growth factor beta signaling in leukemia cells. *Chin. Med. J. (Engl).* **124**, 1556–1562 (2011).
170. Cheng, P. *et al.* Menin Coordinates C/EBP β -Mediated TGF- β Signaling for Epithelial-Mesenchymal Transition and Growth Inhibition in Pancreatic Cancer. *Mol. Ther. - Nucleic Acids* **18**, 155–165 (2019).
171. Hendy, C. N., Kaji, H., Sowa, H., Lebrun, J. J. & Canaff, L. Menin and TGF- β superfamily member signaling via the Smad pathway in pituitary, parathyroid and osteoblast. *Horm. Metab. Res.* **37**, 375–379 (2005).
172. Nord, B. *et al.* Malignant melanoma in patients with multiple endocrine neoplasia type 1 and involvement of the MEN1 gene in sporadic melanoma. *Int. J. cancer* **87**, 463–7 (2000).
173. Fang, M. *et al.* MEN1 Is a Melanoma Tumor Suppressor That Preserves Genomic Integrity by Stimulating Transcription of Genes That Promote Homologous Recombination-Directed DNA Repair. *Mol. Cell. Biol.* **33**, 2635–2647 (2013).
174. Gao, S. Bin *et al.* Menin represses malignant phenotypes of melanoma through regulating multiple pathways. *J. Cell. Mol. Med.* **15**, 2353–2363 (2011).
175. Vidal, A., Iglesias, M. J., Fernández, B., Fonseca, E. & Cordido, F. Cutaneous lesions associated to multiple endocrine neoplasia syndrome type 1. *J. Eur. Acad. Dermatology Venereol.* **22**, 835–838 (2008).
176. Lazova, R. *et al.* Spitz nevi and Spitzoid melanomas: exome sequencing and comparison with conventional melanocytic nevi and melanomas. *Mod. Pathol.* **30**, 640–649 (2017).
177. Physiology of the pancreas. *Adv. Exp. Med. Biol.* **690**, 13–27 (2010).
178. Kleeff, J. *et al.* Pancreatic cancer. *Nat. Rev. Dis. Prim.* **2**, 16022 (2016).

179. Siegel, R. L., Miller, K. D., Fuchs, H. E. & Jemal, A. Cancer statistics, 2022. *CA. Cancer J. Clin.* **72**, 7–33 (2022).
180. Bailey, P. *et al.* Genomic analyses identify molecular subtypes of pancreatic cancer. *Nature* **531**, 47–52 (2016).
181. Raphael, B. J. *et al.* Integrated Genomic Characterization of Pancreatic Ductal Adenocarcinoma. *Cancer Cell* **32**, 185–203.e13 (2017).
182. Aguirre, A. J. *et al.* Real-time genomic characterization of advanced pancreatic cancer to enable precision medicine. *Cancer Discov.* **8**, 1096–1111 (2018).
183. Collisson, E. A., Bailey, P., Chang, D. K. & Biankin, A. V. Molecular subtypes of pancreatic cancer. *Nat. Rev. Gastroenterol. Hepatol.* (2019). doi:10.1038/s41575-019-0109-y
184. Waters, A. M. & Der, C. J. KRAS: The critical driver and therapeutic target for pancreatic cancer. *Cold Spring Harb. Perspect. Med.* **8**, 1–17 (2018).
185. Mann, K. M., Ying, H., Juan, J., Jenkins, N. A. & Copeland, N. G. KRAS-related proteins in pancreatic cancer. *Pharmacol. Ther.* **168**, 29–42 (2016).
186. Hong, D. S. *et al.* KRAS G12C Inhibition with Sotorasib in Advanced Solid Tumors. *N. Engl. J. Med.* **383**, 1207–1217 (2020).
187. Janes, M. R. *et al.* Targeting KRAS Mutant Cancers with a Covalent G12C-Specific Inhibitor. *Cell* **172**, 578–589.e17 (2018).
188. Kessler, D. *et al.* Drugging an undruggable pocket on KRAS. *Proc. Natl. Acad. Sci. U. S. A.* **116**, 15823–15829 (2019).
189. Zhu, C. *et al.* Targeting KRAS mutant cancers: from druggable therapy to drug resistance. *Mol. Cancer* **21**, 1–19 (2022).
190. McWilliams, R. R. *et al.* Prevalence of CDKN2A mutations in pancreatic cancer patients: Implications for genetic counseling. *Eur. J. Hum. Genet.* **19**, 472–478 (2011).
191. Lane, D. P. Cancer. p53, guardian of the genome. *Nature* **358**, 15–16 (1992).
192. Ford, J. M. & Kastan, M. B. *DNA Damage Response Pathways and Cancer. Abeloff's Clinical Oncology* (Elsevier Inc., 2019). doi:10.1016/B978-0-323-47674-4.00011-6
193. Xia, X. *et al.* SMAD4 and its role in pancreatic cancer. *Tumor Biol.* **36**, 111–119 (2015).
194. Jiang, X. *et al.* Inactivating mutations of RNF43 confer Wnt dependency in pancreatic ductal adenocarcinoma. *Proc. Natl. Acad. Sci. U. S. A.* **110**, 12649–12654 (2013).

195. Zhong, Z. & Virshup, D. M. Wnt signaling and drug resistance in cancer. *Mol. Pharmacol.* **97**, 72–89 (2020).
196. Ishino, Y., Shinagawa, H., Makino, K., Amemura, M. & Nakamura, A. Nucleotide sequence of the *iap* gene, responsible for alkaline phosphatase isoenzyme conversion in *Escherichia coli*, and identification of the gene product. *J. Bacteriol.* **169**, 5429–5433 (1987).
197. Hermans, P. W. M. *et al.* Insertion element IS987 from *Mycobacterium bovis* BCG is located in a hot-spot integration region for insertion elements in *Mycobacterium tuberculosis* complex strains. *Infect. Immun.* **59**, 2695–2705 (1991).
198. Nakata, A., Amemura, M. & Makino, K. Unusual nucleotide arrangement with repeated sequences in the *Escherichia coli* K-12 chromosome. *J. Bacteriol.* **171**, 3553–3556 (1989).
199. Mojica, F. J. M., Juez, G. & Rodriguez-Valera, F. Transcription at different salinities of *Haloferax mediterranei* sequences adjacent to partially modified PstI sites. *Mol. Microbiol.* **9**, 613–621 (1993).
200. Bolotin, A., Quinquis, B., Sorokin, A. & Dusko Ehrlich, S. Clustered regularly interspaced short palindrome repeats (CRISPRs) have spacers of extrachromosomal origin. *Microbiology* **151**, 2551–2561 (2005).
201. Pourcel, C., Salvignol, G. & Vergnaud, G. CRISPR elements in *Yersinia pestis* acquire new repeats by preferential uptake of bacteriophage DNA, and provide additional tools for evolutionary studies. *Microbiology* **151**, 653–663 (2005).
202. Mojica, F. J. M., Díez-Villaseñor, C., García-Martínez, J. & Soria, E. Intervening sequences of regularly spaced prokaryotic repeats derive from foreign genetic elements. *J. Mol. Evol.* **60**, 174–182 (2005).
203. Jansen, R., Van Embden, J. D. A., Gaastra, W. & Schouls, L. M. Identification of genes that are associated with DNA repeats in prokaryotes. *Mol. Microbiol.* **43**, 1565–1575 (2002).
204. Makarova, K. S., Grishin, N. V., Shabalina, S. A., Wolf, Y. I. & Koonin, E. V. A putative RNA-interference-based immune system in prokaryotes: Computational analysis of the predicted enzymatic machinery, functional analogies with eukaryotic RNAi, and hypothetical mechanisms of action. *Biol. Direct* **1**, 1–26 (2006).
205. Barrangou, R. *et al.* CRISPR provides acquired resistance against viruses in prokaryotes.

- Science* **315**, 1709–12 (2007).
206. Brouns, S. J. J. *et al.* Small CRISPR RNAs guide antiviral defense in prokaryotes. *Science* (80-.). **321**, 960–964 (2008).
 207. Garneau, J. E. *et al.* The CRISPR/cas bacterial immune system cleaves bacteriophage and plasmid DNA. *Nature* **468**, 67–71 (2010).
 208. Jinek, M. *et al.* A Programmable Dual-RNA–Guided DNA Endonuclease in Adaptive Bacterial Immunity. *Science* (80-.). **337**, 816–821 (2012).
 209. Cong, L. *et al.* Multiplex Genome Engineering Using CRISPR/Cas Systems. *Science* (80-.). **339**, 819–823 (2013).
 210. Mali, P. *et al.* RNA-Guided Human Genome Engineering via Cas9. *Science* (80-.). **339**, 823–826 (2013).
 211. Cong, L. *et al.* Multiplex genome engineering using CRISPR/Cas systems. *Science* (80-.). **339**, 819–823 (2013).
 212. Jinek, M. *et al.* RNA-programmed genome editing in human cells. *Elife* **2013**, 1–9 (2013).
 213. Pickar-Oliver, A. & Gersbach, C. A. The next generation of CRISPR–Cas technologies and applications. *Nat. Rev. Mol. Cell Biol.* **20**, 490–507 (2019).
 214. Makarova, K. S. *et al.* An updated evolutionary classification of CRISPR-Cas systems. *Nat. Rev. Microbiol.* **13**, 722–736 (2015).
 215. Makarova, K. S. *et al.* Evolutionary classification of CRISPR–Cas systems: a burst of class 2 and derived variants. *Nat. Rev. Microbiol.* **18**, 67–83 (2020).
 216. Saito, M. *et al.* Fanzor is a eukaryotic programmable RNA-guided endonuclease. *Nature* **620**, (2023).
 217. Adli, M. The CRISPR tool kit for genome editing and beyond. *Nat. Commun.* **9**, (2018).
 218. Nishimasu, H. *et al.* Crystal structure of Cas9 in complex with guide RNA and target DNA. *Cell* **156**, 935–949 (2014).
 219. Jinek, M. *et al.* Structures of Cas9 endonucleases reveal RNA-mediated conformational activation. *Science* (80-.). **343**, (2014).
 220. Wu, X., Kriz, A. J. & Sharp, P. A. Target specificity of the CRISPR-Cas9 system. *Quant. Biol.* **2**, 59–70 (2014).
 221. Gilbert, L. A. *et al.* CRISPR-Mediated Modular RNA-Guided Regulation of Transcription in Eukaryotes. *Cell* **154**, 442–451 (2013).

222. Liu, X. S. *et al.* Editing DNA Methylation in the Mammalian Genome. *Cell* **167**, 233–247.e17 (2016).
223. Liu, M. *et al.* Global detection of DNA repair outcomes induced by CRISPR-Cas9. *Nucleic Acids Res.* **49**, 8732–8742 (2021).
224. Song, B., Yang, S., Hwang, G.-H., Yu, J. & Bae, S. Analysis of NHEJ-Based DNA Repair after CRISPR-Mediated DNA Cleavage. *Int. J. Mol. Sci.* **22**, 6397 (2021).
225. Lin, S., Staahl, B. T., Alla, R. K. & Doudna, J. A. Enhanced homology-directed human genome engineering by controlled timing of CRISPR/Cas9 delivery. *Elife* **3**, e04766 (2014).
226. Van Vu, T. *et al.* CRISPR/Cas-based precision genome editing via microhomology-mediated end joining. *Plant Biotechnol. J.* **19**, 230–239 (2021).
227. Jang, H. K., Song, B., Hwang, G. H. & Bae, S. Current trends in gene recovery mediated by the CRISPR-Cas system. *Exp. Mol. Med.* **52**, 1016–1027 (2020).
228. Zhang, X.-H., Tee, L. Y., Wang, X.-G., Huang, Q.-S. & Yang, S.-H. Off-target Effects in CRISPR/Cas9-mediated Genome Engineering. *Mol. Ther. Nucleic Acids* **4**, e264 (2015).
229. Guo, C., Ma, X., Gao, F. & Guo, Y. Off-target effects in CRISPR/Cas9 gene editing. *Front. Bioeng. Biotechnol.* **11**, 1–11 (2023).
230. Wu, X. *et al.* Genome-wide binding of the CRISPR endonuclease Cas9 in mammalian cells. *Nat. Biotechnol.* **32**, 670–6 (2014).
231. Riesenbergs, S., Helmbrecht, N., Kanis, P., Maricic, T. & Pääbo, S. Improved gRNA secondary structures allow editing of target sites resistant to CRISPR-Cas9 cleavage. *Nat. Commun.* **13**, 1–8 (2022).
232. Hsu, P. D. *et al.* DNA targeting specificity of RNA-guided Cas9 nucleases. *Nat. Biotechnol.* **31**, 827–832 (2013).
233. Li, C. *et al.* Computational Tools and Resources for CRISPR/Cas Genome Editing. *Genomics, Proteomics Bioinforma.* **21**, 108–126 (2023).
234. Landrum, M. J. *et al.* ClinVar: Public archive of interpretations of clinically relevant variants. *Nucleic Acids Res.* **44**, D862–D868 (2016).
235. Sansbury, B. M. *et al.* CRISPR-Directed Gene Editing Catalyzes Precise Gene Segment Replacement In Vitro Enabling a Novel Method for Multiplex Site-Directed Mutagenesis. *Cris. J.* **2**, 121–132 (2019).

236. Ma, W., Xu, Y. S., Sun, X. M. & Huang, H. Transposon-Associated CRISPR-Cas System: A Powerful DNA Insertion Tool. *Trends Microbiol.* **29**, 565–568 (2021).
237. Zetsche, B. *et al.* Cpf1 Is a Single RNA-Guided Endonuclease of a Class 2 CRISPR-Cas System. *Cell* **163**, 759–771 (2015).
238. Paul, B. & Montoya, G. CRISPR-Cas12a: Functional overview and applications. *Biomed. J.* **43**, 8–17 (2020).
239. Shmakov, S. *et al.* Discovery and Functional Characterization of Diverse Class 2 CRISPR-Cas Systems. *Mol. Cell* **60**, 385–397 (2015).
240. Abudayyeh, O. O. *et al.* C2c2 is a single-component programmable RNA-guided RNA-targeting CRISPR effector. *Science (80-.)*. **353**, (2016).
241. Abudayyeh, O. O. *et al.* RNA targeting with CRISPR-Cas13. *Nature* **550**, 280–284 (2017).
242. Cox, D. B. T. *et al.* RNA editing with CRISPR-Cas13. *Science (80-.)*. **358**, 1019–1027 (2017).
243. Anzalone, A. V., Koblan, L. W. & Liu, D. R. Genome editing with CRISPR–Cas nucleases, base editors, transposases and prime editors. *Nat. Biotechnol.* **38**, 824–844 (2020).
244. Yip, B. H. Recent advances in CRISPR/Cas9 delivery strategies. *Biomolecules* **10**, (2020).
245. Lino, C. A., Harper, J. C., Carney, J. P. & Timlin, J. A. Delivering crispr: A review of the challenges and approaches. *Drug Deliv.* **25**, 1234–1257 (2018).
246. Ford, K., McDonald, D. & Mali, P. Functional Genomics via CRISPR–Cas. *J. Mol. Biol.* **431**, 48–65 (2019).
247. Shalem, O., Sanjana, N. E. & Zhang, F. High-throughput functional genomics using CRISPR-Cas9. *Nat. Rev. Genet.* **16**, 299–311 (2015).
248. Shrock, E. & Güell, M. *CRISPR in Animals and Animal Models. Progress in Molecular Biology and Translational Science* **152**, (Elsevier Inc., 2017).
249. Klementieva, N. *et al.* A Novel Isogenic Human Cell-Based System for MEN1 Syndrome Generated by CRISPR/Cas9 Genome Editing. *Int. J. Mol. Sci.* **22**, 12054 (2021).
250. Even-Zohar, N., Metin-Armagan, D., Ben-Shlomo, A., Sareen, D. & Melmed, S. Generation of isogenic and homozygous MEN1 mutant cell lines from patient-derived iPSCs using CRISPR/Cas9. *Stem Cell Res.* **69**, 103124 (2023).

251. Draper, G. M., Panken, D. J. & Largaespada, D. A. Modeling human cancer predisposition syndromes using CRISPR/Cas9 in human cell line models. *Genes Chromosom. Cancer* **62**, 493–500 (2023).
252. Wang, T., Wei, J., Sabatini, D. & Lander, E. Genetic screens in human cells using the CRISPR/Cas9 system. *Science (80-.)*. **343**, 80–84 (2014).
253. Shalem, O. *et al.* Genome-scale CRISPR-Cas9 knockout screening in human cells. *Science (80-.)*. **343**, 84–87 (2014).
254. Sanjana, N. E., Shalem, O. & Zhang, F. Improved vectors and genome-wide libraries for CRISPR screening. *Nat. Methods* **11**, 783–784 (2014).
255. Bock, C. *et al.* High-content CRISPR screening. *Nature Reviews Methods Primers* **2**, (2022).
256. Shirani-Bidabadi, S. *et al.* CRISPR technology: A versatile tool to model, screen, and reverse drug resistance in cancer. *Eur. J. Cell Biol.* **102**, 151299 (2023).
257. O’Neil, N. J., Bailey, M. L. & Hieter, P. Synthetic lethality and cancer. *Nat. Rev. Genet.* **18**, 613–623 (2017).
258. Xu, Y., Chen, C., Guo, Y., Hu, S. & Sun, Z. Effect of CRISPR/Cas9-Edited PD-1/PD-L1 on Tumor Immunity and Immunotherapy. *Front. Immunol.* **13**, 1–14 (2022).
259. Hart, T. *et al.* High-Resolution CRISPR Screens Reveal Fitness Genes and Genotype-Specific Cancer Liabilities. *Cell* **163**, 1515–1526 (2015).
260. Petiwala, S. *et al.* Optimization of Genomewide CRISPR Screens Using AsCas12a and Multi-Guide Arrays. *Cris. J.* **6**, 75–82 (2023).
261. Wessels, H. H. *et al.* Massively parallel Cas13 screens reveal principles for guide RNA design. *Nat. Biotechnol.* **38**, 722–727 (2020).
262. Li, R. *et al.* Comparative optimization of combinatorial CRISPR screens. *Nat. Commun.* **13**, 1–10 (2022).
263. Przybyła, L. & Gilbert, L. A. A new era in functional genomics screens. *Nat. Rev. Genet.* **23**, 89–103 (2022).
264. Jaitin, D. A. *et al.* Dissecting Immune Circuits by Linking CRISPR-Pooled Screens with Single-Cell RNA-Seq. *Cell* **167**, 1883-1896.e15 (2016).
265. Dixit, A. *et al.* Perturb-Seq: Dissecting Molecular Circuits with Scalable Single-Cell RNA Profiling of Pooled Genetic Screens. *Cell* **167**, 1853-1866.e17 (2016).

266. Datlinger, P. *et al.* Pooled CRISPR screening with single-cell transcriptome readout. *Nat. Methods* **14**, 297–301 (2017).
267. Xie, S., Duan, J., Li, B., Zhou, P. & Hon, G. C. Multiplexed Engineering and Analysis of Combinatorial Enhancer Activity in Single Cells. *Mol. Cell* **66**, 285-299.e5 (2017).
268. Chow, R. D. & Chen, S. Cancer CRISPR Screens In Vivo. *Trends in Cancer* **4**, 349–358 (2018).
269. Kuhn, M., Santinha, A. J. & Platt, R. J. Moving from in vitro to in vivo CRISPR screens. *Gene Genome Ed.* **2**, 100008 (2021).
270. Chen, S. *et al.* Genome-wide CRISPR Screen in a Mouse Model of Tumor Growth and Metastasis. *Cell* **160**, 1246–1260 (2015).
271. Katigbak, A. *et al.* A CRISPR/Cas9 Functional Screen Identifies Rare Tumor Suppressors. *Sci. Rep.* **6**, 1–8 (2016).
272. Song, C. Q. *et al.* Genome-Wide CRISPR Screen Identifies Regulators of Mitogen-Activated Protein Kinase as Suppressors of Liver Tumors in Mice. *Gastroenterology* **152**, 1161-1173.e1 (2017).
273. Kodama, M. *et al.* In vivo loss-of-function screens identify KPNB1 as a new druggable oncogene in epithelial ovarian cancer. *Proc. Natl. Acad. Sci. U. S. A.* **114**, E7301–E7310 (2017).
274. Michels, B. E. *et al.* Pooled In Vitro and In Vivo CRISPR-Cas9 Screening Identifies Tumor Suppressors in Human Colon Organoids. *Cell Stem Cell* **26**, 782-792.e7 (2020).
275. Brauna, C. J. *et al.* Versatile in vivo regulation of tumor phenotypes by dCas9-mediated transcriptional perturbation. *Proc. Natl. Acad. Sci. U. S. A.* **113**, E3892–E3900 (2016).
276. Bajaj, J. *et al.* An in vivo genome-wide CRISPR screen identifies the RNA-binding protein Stauf2 as a key regulator of myeloid leukemia. *Nat. cancer* **1**, 410–422 (2020).
277. Lin, S. *et al.* An In Vivo CRISPR Screening Platform for Prioritizing Therapeutic Targets in AML. *Cancer Discov.* **12**, 432–449 (2022).
278. Jin, M. L., Gong, Y., Ji, P., Hu, X. & Shao, Z. M. In vivo CRISPR screens identify RhoV as a pro-metastasis factor of triple-negative breast cancer. *Cancer Sci.* **114**, 2375–2385 (2023).
279. Yau, E. H. *et al.* Genome-wide CRISPR screen for essential cell growth mediators in mutant KRAS colorectal cancers. *Cancer Res.* **77**, 6330–6339 (2017).

280. Patel, S. J. *et al.* Identification of essential genes for cancer immunotherapy. *Nature* **548**, 537–542 (2017).
281. Ye, L. *et al.* In vivo CRISPR screening in CD8 T cells with AAV–Sleeping Beauty hybrid vectors identifies membrane targets for improving immunotherapy for glioblastoma. *Nat. Biotechnol.* **37**, 1302–1313 (2019).
282. Li, F. *et al.* In Vivo Epigenetic CRISPR Screen Identifies Asf1a as an Immunotherapeutic Target in Kras -Mutant Lung Adenocarcinoma. *Cancer Discov.* **10**, 270–287 (2020).
283. Manguso, R. T. *et al.* In vivo CRISPR screening identifies Ptpn2 as a cancer immunotherapy target. *Nature* **547**, 413–418 (2017).
284. Chen, Z. *et al.* In vivo CD8+ T cell CRISPR screening reveals control by Fli1 in infection and cancer. *Cell* **184**, 1262-1280.e22 (2021).
285. Wang, X. *et al.* In vivo CRISPR screens identify the E3 ligase Cop1 as a modulator of macrophage infiltration and cancer immunotherapy target. *Cell* **184**, 5357-5374.e22 (2021).
286. Dai, M. *et al.* In vivo genome-wide CRISPR screen reveals breast cancer vulnerabilities and synergistic mTOR/Hippo targeted combination therapy. *Nat. Commun.* **12**, 3055 (2021).
287. Yan, G. *et al.* Combined in vitro/in vivo genome-wide CRISPR screens in triple negative breast cancer identify cancer stemness regulators in paclitaxel resistance. *Oncogenesis* **12**, 51 (2023).
288. Behan, F. M. *et al.* Prioritization of cancer therapeutic targets using CRISPR–Cas9 screens. *Nature* **568**, 511–516 (2019).
289. Tsherniak, A. *et al.* Defining a Cancer Dependency Map. *Cell* **170**, 564-576.e16 (2017).
290. Meyers, R. M. *et al.* Computational correction of copy number effect improves specificity of CRISPR–Cas9 essentiality screens in cancer cells. *Nat. Genet.* **49**, 1779–1784 (2017).
291. Pacini, C. *et al.* Integrated cross-study datasets of genetic dependencies in cancer. *Nat. Commun.* **12**, 1–14 (2021).
292. Dempster, J. M. *et al.* Agreement between two large pan-cancer CRISPR-Cas9 gene dependency data sets. *Nat. Commun.* **10**, 5817 (2019).
293. Balchin, D., Hayer-Hartl, M. & Hartl, F. U. In vivo aspects of protein folding and quality control. *Science (80-.).* **353**, (2016).

294. Hartl, F. U. Molecular chaperones in cellular protein folding. *Nature* **381**, 571–580 (1996).
295. Richter, K., Haslbeck, M. & Buchner, J. The Heat Shock Response: Life on the Verge of Death. *Mol. Cell* **40**, 253–266 (2010).
296. Morimoto, R. I. Cells in stress: Transcriptional activation of heat shock genes. *Science (80-.)*. **259**, 1409–1410 (1993).
297. Barna, J., Csermely, P. & Tibor Vellai, . Roles of heat shock factor 1 beyond the heat shock response. *Cell. Mol. Life Sci.* **75**, 2897–2916 (2018).
298. Kampinga, H. H. *et al.* Guidelines for the nomenclature of the human heat shock proteins. *Cell Stress Chaperones* **14**, 105–111 (2009).
299. Bepperling, A. *et al.* Alternative bacterial two-component small heat shock protein systems. *Proc. Natl. Acad. Sci. U. S. A.* **109**, 20407–20412 (2012).
300. Cappello, F. *et al.* Hsp60 chaperonopathies and chaperonotherapy: Targets and agents. *Expert Opin. Ther. Targets* **18**, 185–208 (2014).
301. Slavotinek, A. M. & Biesecker, L. G. Unfolding the role of chaperones and chaperonins in human disease. *Trends Genet.* **17**, 528–535 (2001).
302. Ray, A. M. *et al.* Exploiting the HSP60/10 chaperonin system as a chemotherapeutic target for colorectal cancer. *Bioorganic Med. Chem.* **40**, 116129 (2021).
303. Samali, A. & Orrenius, S. Heat shock proteins: regulators of stress response and apoptosis. *Cell Stress & Chaperones* **3**, 228–236 (1998).
304. Samali, A., Cai, J., Zhivotovsky, B., Jones, D. P. & Orrenius, S. Presence of a pre-apoptotic complex of pro-caspase-3, Hsp60 and Hsp10 in the mitochondrial fraction of Jurkat cells. *EMBO J.* **18**, 2040–2048 (1999).
305. Yun, C. W., Kim, H. J., Lim, J. H. & Lee, S. H. Heat Shock Proteins: Agents of Cancer Development and Therapeutic Targets in Anti-Cancer Therapy. *Cells* **9**, 1–30 (2019).
306. Åkerfelt, M., Morimoto, R. I. & Sistonen, L. Heat shock factors: Integrators of cell stress, development and lifespan. *Nature Reviews Molecular Cell Biology* **11**, 545–555 (2010).
307. Dai, C., Whitesell, L., Rogers, A. B. & Lindquist, S. Heat Shock Factor 1 Is a Powerful Multifaceted Modifier of Carcinogenesis. *Cell* **130**, 1005–1018 (2007).
308. Calderwood, S. K., Khaleque, M. A., Sawyer, D. B. & Ciocca, D. R. Heat shock proteins in cancer: Chaperones of tumorigenesis. *Trends Biochem. Sci.* **31**, 164–172 (2006).

309. Horwich, A. L., Fenton, W. A., Chapman, E. & Farr, G. W. Two families of chaperonin: Physiology and mechanism. *Annual Review of Cell and Developmental Biology* **23**, 115–145 (2007).
310. Levy-Rimler, G., Bell, R. E., Ben-Tal, N. & Azem, A. Type I chaperonins: Not all are created equal. *FEBS Letters* **529**, 1–5 (2002).
311. Höhfeld, J. & Hartl, F. U. Role of the chaperonin cofactor Hsp10 in protein folding and sorting in yeast mitochondria. *J. Cell Biol.* **126**, 305–315 (1994).
312. Ghosh, J. C., Dohi, T., Byoung, H. K. & Altieri, D. C. Hsp60 regulation of tumor cell apoptosis. *J. Biol. Chem.* **283**, 5188–5194 (2008).
313. Cappello, F., De Macario, E. C., Marasà, L., Zummo, G. & Macario, A. J. L. Hsp60 expression, new locations, functions and perspectives for cancer diagnosis and therapy. *Cancer Biol. Ther.* **7**, 801–809 (2008).
314. Yeung, N., Murata, D., Iijima, M. & Sesaki, H. Role of human HSPE1 for OPA1 processing independent of HSPD1. *iScience* **26**, 106067 (2023).
315. Rivera-Mejías, P. *et al.* The mitochondrial protease OMA1 acts as a metabolic safeguard upon nuclear DNA damage. *Cell Rep.* **42**, (2023).
316. Shirihai, O. S., Song, M. & Dorn, G. W. How Mitochondrial Dynamism Orchestrates Mitophagy. *Circ. Res.* **116**, 1835–1849 (2015).
317. Kaji, H., Canaff, L., Lebrun, J. J., Goltzman, D. & Hendy, G. N. Inactivation of menin, a Smad3-interacting protein, blocks transforming growth factor type β signaling. *Proc. Natl. Acad. Sci. U. S. A.* **98**, 3837–3842 (2001).
318. Siegel, R. L., Miller, K. D. & Jemal, A. Cancer statistics, 2019. *CA. Cancer J. Clin.* **69**, 7–34 (2019).
319. Domingues, B., Lopes, J., Soares, P. & Populo, H. Melanoma treatment in review. *ImmunoTargets Ther.* **7**, 35–49 (2018).
320. Shannan, B., Perego, M., Somasundaram, R. & Herlyn, M. Heterogeneity in melanoma. in *Cancer Treatment and Research* **167**, 1–15 (2016).
321. Leonardi, G. C. *et al.* Cutaneous melanoma: From pathogenesis to therapy (Review). *Int. J. Oncol.* **52**, 1071–1080 (2018).
322. Kwong, L. N. & Davies, M. A. Navigating the Therapeutic Complexity of PI3K Pathway Inhibition in Melanoma. *Clin. Cancer Res.* **19**, 5310–5319 (2013).

323. Xue, G., Romano, E., Massi, D. & Mandalà, M. Wnt/ β -catenin signaling in melanoma: Preclinical rationale and novel therapeutic insights. *Cancer Treatment Reviews* **49**, 1–12 (2016).
324. Ueda, Y. & Richmond, A. NF- κ B activation in melanoma. *Pigment Cell Res.* **19**, 112–124 (2006).
325. Hammouda, M. B., Ford, A. E., Liu, Y. & Zhang, J. Y. The JNK Signaling Pathway in Inflammatory Skin Disorders and Cancer. *Cells* **9**, 857 (2020).
326. Thomas, S. J., Snowden, J. A., Zeidler, M. P. & Danson, S. J. The role of JAK/STAT signalling in the pathogenesis, prognosis and treatment of solid tumours. *Br. J. Cancer* **113**, 365–371 (2015).
327. Javelaud, D., Alexaki, V. I. & Mauviel, A. Transforming growth factor- β in cutaneous melanoma. *Pigment Cell Melanoma Res.* **21**, 123–132 (2008).
328. Wu, F., Weigel, K. J., Zhou, H. & Wang, X. J. Paradoxical roles of TGF- β signaling in suppressing and promoting squamous cell carcinoma. *Acta Biochim. Biophys. Sin. (Shanghai)*. **50**, 98–105 (2018).
329. Stingl, J. & Caldas, C. Molecular heterogeneity of breast carcinomas and the cancer stem cell hypothesis. *Nat. Rev. Cancer* **7**, 791–799 (2007).
330. Visvader, J. E. & Lindeman, G. J. Cancer stem cells in solid tumours: Accumulating evidence and unresolved questions. *Nat. Rev. Cancer* **8**, 755–768 (2008).
331. Bellomo, C., Caja, L. & Moustakas, A. Transforming growth factor β as regulator of cancer stemness and metastasis. *Br. J. Cancer* **115**, 761–769 (2016).
332. Dupin, E. & Sommer, L. Neural crest progenitors and stem cells: From early development to adulthood. *Dev. Biol.* **366**, 83–95 (2012).
333. Monzani, E. *et al.* Melanoma contains CD133 and ABCG2 positive cells with enhanced tumorigenic potential. *Eur. J. Cancer* **43**, 935–946 (2007).
334. Frank, N. Y. *et al.* ABCB5-mediated doxorubicin transport and chemoresistance in human malignant melanoma. *Cancer Res.* **65**, 4320–4333 (2005).
335. Luo, Y., Nguyen, N. & Fujita, M. Isolation of human melanoma stem cells UNIT 3.8 using ALDH as a marker. *Curr. Protoc. Stem Cell Biol.* **1**, (2013).
336. Boonyaratanakornkit, J. B. *et al.* Selection of tumorigenic melanoma cells using ALDH. *J. Invest. Dermatol.* **130**, 2799–2808 (2010).

337. Klein, W. M. *et al.* Increased expression of stem cell markers in malignant melanoma. *Mod. Pathol.* **20**, 102–107 (2007).
338. Redmer, T. *et al.* The role of the cancer stem cell marker CD271 in DNA damage response and drug resistance of melanoma cells. *Oncogenesis* **6**, 1–13 (2017).
339. Iwasaki, H. & Suda, T. Cancer stem cells and their niche. *Cancer Science* **100**, 1166–1172 (2009).
340. Sakaki-Yumoto, M., Katsuno, Y. & Derynck, R. TGF- β family signaling in stem cells. *Biochim. Biophys. Acta - Gen. Subj.* **1830**, 2280–2296 (2013).
341. Bellomo, C., Caja, L. & Moustakas, A. Transforming growth factor β as regulator of cancer stemness and metastasis. *Br. J. Cancer* **115**, 761–769 (2016).
342. Tian, J. *et al.* Cyclooxygenase-2 regulates TGF β -induced cancer stemness in triple-negative breast cancer. *Sci. Rep.* **7**, 1–16 (2017).
343. Montague, T. G., Cruz, J. M., Gagnon, J. A., Church, G. M. & Valen, E. CHOPCHOP: A CRISPR/Cas9 and TALEN web tool for genome editing. *Nucleic Acids Res.* **42**, 401–407 (2014).
344. Concordet, J.-P. & Haeussler, M. CRISPOR: intuitive guide selection for CRISPR/Cas9 genome editing experiments and screens. *Nucleic Acids Res.* **46**, W242–W245 (2018).
345. Tang, B. *et al.* Transforming growth factor- β can suppress tumorigenesis through effects on the putative cancer stem or early progenitor cell and committed progeny in a breast cancer xenograft model. *Cancer Res.* **67**, 8643–8652 (2007).
346. Bhola, N. E. *et al.* TGF- β inhibition enhances chemotherapy action against triple-negative breast cancer. *J. Clin. Invest.* **123**, 1348–1358 (2013).
347. Dai, M. *et al.* CDK4 regulates cancer stemness and is a novel therapeutic target for triple-negative breast cancer. *Sci. Rep.* **6**, 35383 (2016).
348. Peñuelas, S. *et al.* TGF- β Increases Glioma-Initiating Cell Self-Renewal through the Induction of LIF in Human Glioblastoma. *Cancer Cell* **15**, 315–327 (2009).
349. Ehata, S. *et al.* Transforming growth factor-B decreases the cancer-initiating cell population within diffuse-type gastric carcinoma cells. *Oncogene* **30**, 1693–1705 (2011).
350. Oshimori, N., Oristian, D. & Fuchs, E. TGF- β Promotes Heterogeneity and Drug Resistance in Squamous Cell Carcinoma. *Cell* **160**, 963–976 (2015).
351. Lee, C., Yu, C., Wang, B. & Chang, W. Tumorsphere as an effective in vitro platform for

- screening anti-cancer stem cell drugs. *Oncotarget* **7**, 1215–1226 (2016).
352. Shams, A. *et al.* Prolactin receptor-driven combined luminal and epithelial differentiation in breast cancer restricts plasticity, stemness, tumorigenesis and metastasis. *Oncogenesis* **10**, (2021).
353. Dai, M. *et al.* Differential regulation of cancer progression by CDK4/6 plays a central role in DNA replication and repair pathways. *Cancer Res.* **81**, 1332–1346 (2021).
354. Yan, G. *et al.* TGF β /cyclin D1/Smad-mediated inhibition of BMP4 promotes breast cancer stem cell self-renewal activity. *Oncogenesis* **10**, (2021).
355. Anselmi, M. *et al.* Melanoma Stem Cells Educate Neutrophils to Support Cancer Progression. *Cancers (Basel)*. **14**, (2022).
356. Hoshino, Y. *et al.* Smad4 decreases the population of pancreatic cancer - Initiating cells through transcriptional repression of ALDH1A1. *Am. J. Pathol.* **185**, 1457–1470 (2015).
357. Lacerte, A. *et al.* Transforming growth factor- β inhibits telomerase through SMAD3 and E2F transcription factors. *Cell. Signal.* **20**, 50–59 (2008).
358. Lee, H. J., Lee, J. K., Miyake, S. & Kim, S. J. A Novel E1A-like Inhibitor of Differentiation (EID) Family Member, EID-2, Suppresses Transforming Growth Factor (TGF)- β Signaling by Blocking TGF- β -induced Formation of Smad3-Smad4 Complexes. *J. Biol. Chem.* **279**, 2666–2672 (2004).
359. Li, H., Xu, D., Li, J., Berndt, M. C. & Liu, J. P. Transforming growth factor β suppresses human telomerase reverse transcriptase (hTERT) by Smad3 interactions with c-Myc and the hTERT gene. *J. Biol. Chem.* **281**, 25588–25600 (2006).
360. Kretschmer, A. *et al.* Differential regulation of TGF- β signaling through Smad2, Smad3 and Smad4. *Oncogene* **22**, 6748–6763 (2003).
361. Cohen-Solal, K. A. *et al.* Constitutive Smad linker phosphorylation in melanoma: A mechanism of resistance to transforming growth factor- β -mediated growth inhibition. *Pigment Cell Melanoma Res.* **24**, 512–524 (2011).
362. Lüönd, F. *et al.* Hierarchy of TGF β /SMAD, Hippo/YAP/TAZ, and Wnt/ β -catenin signaling in melanoma phenotype switching. *Life Sci. Alliance* **5**, 1–14 (2022).
363. Goding, C. R. A picture of Mitf in melanoma immortality. *Oncogene* **30**, 2304–2306 (2011).
364. Pierrat, M. J., Marsaud, V., Mauviel, A. & Javelaud, D. Expression of microphthalmia-

- associated transcription factor (MITF), which is critical for melanoma progression, is inhibited by both transcription factor GLI2 and transforming growth factor- β . *J. Biol. Chem.* **287**, 17996–18004 (2012).
365. Yeh, H. W., Lee, S. S., Chang, C. Y., Lang, Y. D. & Jou, Y. S. A new switch for TGF β in cancer. *Cancer Res.* **79**, 3797–3805 (2019).
 366. Bierie, B. & Moses, H. L. TGF- β and cancer. *Cytokine Growth Factor Rev.* **17**, 29–40 (2006).
 367. Roberts, A. B. & Wakefield, L. M. The two faces of transforming growth factor β in carcinogenesis. *Proc. Natl. Acad. Sci. U. S. A.* **100**, 8621–8623 (2003).
 368. Scheel, C. & Weinberg, R. A. Cancer stem cells and epithelial-mesenchymal transition: Concepts and molecular links. *Semin. Cancer Biol.* **22**, 396–403 (2012).
 369. Javelaud, D. *et al.* Stable overexpression of Smad7 in human melanoma cells impairs bone metastasis. *Cancer Res.* **67**, 2317–2324 (2007).
 370. Javelaud, D. *et al.* Stable overexpression of Smad7 in human melanoma cells inhibits their tumorigenicity in vitro and in vivo. *Oncogene* **24**, 7624–7629 (2005).
 371. Derakhshani, A. *et al.* Targeting TGF- β -Mediated SMAD Signaling pathway via novel recombinant cytotoxin II: A potent protein from naja naja oxiana venom in Melanoma. *Molecules* **25**, (2020).
 372. Balch, C. M. & Mihm, M. C. Reply to the article ‘The AJCC staging proposal for cutaneous melanoma: Comments by the EORTC Melanoma Group’, by D. J. Ruiter *et al.* (Ann Oncol 2001; 12: 9-11). *Ann. Oncol.* **13**, 175–176 (2002).
 373. Ferlay, J. *et al.* Cancer incidence and mortality worldwide: Sources, methods and major patterns in GLOBOCAN 2012. *Int. J. Cancer* **136**, E359–E386 (2015).
 374. Ross, M. I. & Gershenwald, J. E. Evidence-based treatment of early-stage melanoma. *J. Surg. Oncol.* **104**, 341–353 (2011).
 375. Houghton, A. N. & Polsky, D. Focus on melanoma. *Cancer Cell* **2**, 275–278 (2002).
 376. Enninga, E. A. L. *et al.* Survival of cutaneous melanoma based on sex, age, and stage in the United States, 1992–2011. *Cancer Med.* **6**, 2203–2212 (2017).
 377. Krauthammer, M. *et al.* Exome sequencing identifies recurrent somatic RAC1 mutations in melanoma. *Nat. Genet.* **44**, 1006–1014 (2012).
 378. Hodis, E. *et al.* A landscape of driver mutations in melanoma. *Cell* **150**, 251–263 (2012).

379. Davies, H. *et al.* Mutations of the BRAF gene in human cancer. *Nature* **417**, 949–954 (2002).
380. Leonardi, G. C. *et al.* Cutaneous melanoma: From pathogenesis to therapy (Review). *Int. J. Oncol.* **52**, 1071–1080 (2018).
381. Lopez-Bergami, P., Fitchman, B. & Ronai, Z. Understanding signaling cascades in melanoma. *Photochem. Photobiol.* **84**, 289–306 (2008).
382. Humbert, L., Ghozlan, M., Canaff, L., Tian, J. & Lebrun, J. J. The leukemia inhibitory factor (LIF) and p21 mediate the TGF β tumor suppressive effects in human cutaneous melanoma. *BMC Cancer* **15**, 200 (2015).
383. Ramont, L., Pasco, S., Hornebeck, W., Maquart, F. X. & Monboisse, J. C. Transforming growth factor- β 1 inhibits tumor growth in a mouse melanoma model by down-regulating the plasminogen activation system. *Exp. Cell Res.* **291**, 1–10 (2003).
384. Boudreault, J., Wang, N., Ghozlan, M. & Lebrun, J.-J. Transforming Growth Factor- β /Smad Signaling Inhibits Melanoma Cancer Stem Cell Self-Renewal, Tumor Formation and Metastasis. *Cancers (Basel)*. **16**, 224 (2024).
385. Balogh, K., Rácz, K., Patócs, A. & Hunyady, L. Menin and its interacting proteins: elucidation of menin function. *Trends Endocrinol. Metab.* **17**, 357–364 (2006).
386. Milne, T. A. *et al.* Menin and MLL cooperatively regulate expression of cyclin-dependent kinase inhibitors. *Proc. Natl. Acad. Sci. U. S. A.* **102**, 749–754 (2005).
387. Karnik, S. K. *et al.* Menin regulates pancreatic islet growth by promoting histone methylation and expression of genes encoding p27Kip1 and p18INK4c. *Proc. Natl. Acad. Sci. U. S. A.* **102**, 14659–14664 (2005).
388. Sowa, H. *et al.* Menin Inactivation Leads to Loss of Transforming Growth Factor β Inhibition of Parathyroid Cell Proliferation and Parathyroid Hormone Secretion. *Cancer Res.* **64**, 2222–2228 (2004).
389. Thakker, R. V. Multiple endocrine neoplasia type 1. *Endocrinol. Metab. Clin. North Am.* **29**, 541–567 (2000).
390. Baldauf, C., Vortmeyer, A. O., Koch, C. A. & Sticherling, M. Combination of multiple skin malignancies with multiple endocrine neoplasia type 1: Coincidental or pathogenetically related? *Dermatology* **219**, 365–367 (2009).
391. Nord, B. *et al.* Malignant melanoma in patients with multiple endocrine neoplasia type 1

- and involvement of the MEN1 gene in sporadic melanoma. *Int. J. Cancer* **87**, 463–467 (2000).
392. Gray-Schopfer, V., Wellbrock, C. & Marais, R. Melanoma biology and new targeted therapy. *Nature* **445**, 851–857 (2007).
393. Poncin, J. *et al.* Mutation analysis of the MEN1 gene in Belgian patients with multiple endocrine neoplasia type 1 and related diseases. *Hum. Mutat.* **13**, 54–60 (1999).
394. Ito, T., Igarashi, H., Uehara, H., Berna, M. J. & Jensen, R. T. Causes of death and prognostic factors in multiple endocrine neoplasia type 1: A prospective study: Comparison of 106 men1/zollinger-ellison syndrome patients with 1613 literature men1 patients with or without pancreatic endocrine tumors. *Med. (United States)* **92**, 135–181 (2013).
395. Neel, J.-C., Humbert, L. & Lebrun, J.-J. The Dual Role of TGF β in Human Cancer: From Tumor Suppression to Cancer Metastasis. *ISRN Mol. Biol.* **2012**, 1–28 (2012).
396. Datto, M. B. *et al.* Transforming growth factor beta induces the cyclin-dependent kinase inhibitor p21 through a p53-independent mechanism. *Proc. Natl. Acad. Sci.* **92**, 5545–5549 (1995).
397. Warner, B. J., Blain, S. W., Seoane, J. & Massagué, J. Myc Downregulation by Transforming Growth Factor β Required for Activation of the p15 Ink4b G 1 Arrest Pathway. *Mol. Cell. Biol.* **19**, 5913–5922 (1999).
398. Schuster, N. & Krieglstein, K. Mechanisms of TGF- β -mediated apoptosis. *Cell Tissue Res.* **307**, 1–14 (2002).
399. Canaff, L., Vanbellin ghen, J. F., Kaji, H., Goltzman, D. & Hendy, G. N. Impaired transforming growth factor- β (TGF- β) transcriptional activity and cell proliferation control of a menin in-frame deletion mutant associated with Multiple Endocrine Neoplasia type 1 (MEN1). *J. Biol. Chem.* **287**, 8584–8597 (2012).
400. Canaff, L. *et al.* Menin missense mutants encoded by the MEN1 gene that are targeted to the proteasome: Restoration of expression and activity by CHIP siRNA. *J. Clin. Endocrinol. Metab.* **97**, E282-91 (2012).
401. Yaguchi, H. *et al.* Menin Missense Mutants Associated with Multiple Endocrine Neoplasia Type 1 Are Rapidly Degraded via the Ubiquitin-Proteasome Pathway. *Mol. Cell. Biol.* **24**, 6569–6580 (2004).

402. Guru, S. C. *et al.* Menin, the product of the MEN1 gene, is a nuclear protein. *Proc. Natl. Acad. Sci. U. S. A.* **95**, 1630–1634 (1998).
403. Buac, D. *et al.* From Bortezomib to other Inhibitors of the Proteasome and Beyond. *Curr. Pharm. Des.* **19**, 4025–4038 (2013).
404. McDonough, H. & Patterson, C. CHIP: A link between the chaperone and proteasome systems. *Cell Stress Chaperones* **8**, 303–308 (2003).
405. Lebrun, J. J. Activin, TGF- β and menin in pituitary tumorigenesis. *Adv. Exp. Med. Biol.* **668**, 69–78 (2009).
406. Hendy, G. N., Kaji, H., Sowa, H., Lebrun, J.-J. & Canaff, L. Menin and TGF- β Superfamily Member Signaling via the Smad Pathway in Pituitary, Parathyroid and Osteoblast. *Horm. Metab. Res.* **37**, 375–379 (2005).
407. Dai, M. *et al.* A novel function for p21Cip1 and acetyltransferase p/CAF as critical transcriptional regulators of TGF β -mediated breast cancer cell migration and invasion. *Breast Cancer Res.* **14**, R127 (2012).
408. Derynck, R. & Akhurst, R. J. Differentiation plasticity regulated by TGF- β family proteins in development and disease. *Nat. Cell Biol.* **9**, 1000–1004 (2007).
409. Thiery, J. P. Epithelial-mesenchymal transitions in development and pathologies. *Curr. Opin. Cell Biol.* **15**, 740–746 (2003).
410. Moustakas, A. & Heldin, C. H. Signaling networks guiding epithelial-mesenchymal transitions during embryogenesis and cancer progression. *Cancer Sci.* **98**, 1512–1520 (2007).
411. Woodward, J. K. L. *et al.* Stimulation and inhibition of uveal melanoma invasion by HGF, GRO, IL-1 α and TGF- β . *Investig. Ophthalmol. Vis. Sci.* **43**, 3144–3152 (2002).
412. Romo, P., Madigan, M. C., Provis, J. M. & Cullen, K. M. Differential effects of TGF- β and FGF-2 on in vitro proliferation and migration of primate retinal endothelial and Müller cells. *Acta Ophthalmol.* **89**, e263-8 (2011).
413. Mohan, M., Matin, A. & Davies, F. E. Update on the optimal use of Bortezomib in the treatment of multiple myeloma. *Cancer Manag. Res.* **9**, 51–63 (2017).
414. Rahib, L., Wehner, M. R., Matrisian, L. M. & Nead, K. T. Estimated Projection of US Cancer Incidence and Death to 2040. *JAMA Netw. Open* **4**, 1–14 (2021).
415. Pereira, S. P. *et al.* Early detection of pancreatic cancer. *Lancet Gastroenterol. Hepatol.* **5**,

- 698–710 (2020).
416. Kamisawa, T., Wood, L. D., Itoi, T. & Takaori, K. Pancreatic cancer. *Lancet* **388**, 73–85 (2016).
 417. Klaiber, U., Hackert, T. & Neoptolemos, J. P. Adjuvant treatment for pancreatic cancer. *Transl. Gastroenterol. Hepatol.* **4**, (2019).
 418. Saung, M. T. & Zheng, L. Current Standards of Chemotherapy for Pancreatic Cancer. *Clin. Ther.* **39**, 2125–2134 (2017).
 419. Leroux, C. & Konstantinidou, G. Targeted therapies for pancreatic cancer: Overview of current treatments and new opportunities for personalized oncology. *Cancers (Basel)*. **13**, 1–28 (2021).
 420. Rudloff, U. Emerging kinase inhibitors for the treatment of pancreatic ductal adenocarcinoma. *Expert Opin. Emerg. Drugs* **27**, 345–368 (2022).
 421. Wang, T., Wei, J. J., Sabatini, D. M. & Lander, E. S. Genetic Screens in Human Cells Using the CRISPR-Cas9 System. *Science (80-.)*. **343**, 80–84 (2014).
 422. Wang, B. *et al.* ATXN1L, CIC, and ETS Transcription Factors Modulate Sensitivity to MAPK Pathway Inhibition. *Cell Rep.* **18**, 1543–1557 (2017).
 423. Szlachta, K. *et al.* CRISPR knockout screening identifies combinatorial drug targets in pancreatic cancer and models cellular drug response. *Nat. Commun.* **9**, 4275 (2018).
 424. Zhong, Z., Harmston, N., Wood, K. C., Madan, B. & Virshup, D. M. A p300/GATA6 axis determines differentiation and Wnt dependency in pancreatic cancer models. *J. Clin. Invest.* **132**, (2022).
 425. Thummuri, D. *et al.* Overcoming Gemcitabine Resistance in Pancreatic Cancer Using the BCL-XL-Specific Degradable DT2216. *Mol. Cancer Ther.* **21**, 184–192 (2022).
 426. Ramaker, R. C. *et al.* Pooled CRISPR screening in pancreatic cancer cells implicates co-repressor complexes as a cause of multiple drug resistance via regulation of epithelial-to-mesenchymal transition. *BMC Cancer* **21**, 632 (2021).
 427. Falcomatà, C. *et al.* Selective multi-kinase inhibition sensitizes mesenchymal pancreatic cancer to immune checkpoint blockade by remodeling the tumor microenvironment. *Nat. Cancer* **3**, 318–336 (2022).
 428. Zhong, Z. *et al.* PORCN inhibition synergizes with PI3K/mTOR inhibition in Wnt-addicted cancers. *Oncogene* **38**, 6662–6677 (2019).

429. Milton, C. K. *et al.* A genome-scale CRISPR screen identifies the ERBB and mTOR signaling networks as key determinants of response to PI3K inhibition in pancreatic cancer. *Mol. Cancer Ther.* **19**, 1423–1435 (2020).
430. Du, R., Sullivan, D. K., Azizian, N. G., Liu, Y. & Li, Y. Inhibition of ERAD synergizes with FTS to eradicate pancreatic cancer cells. *BMC Cancer* **21**, 1–13 (2021).
431. Zeng, S. *et al.* CDK7 inhibition augments response to multidrug chemotherapy in pancreatic cancer. *J. Exp. Clin. Cancer Res.* **41**, 241 (2022).
432. Sarr, A. *et al.* Genome-scale CRISPR/Cas9 screen determines factors modulating sensitivity to ProTide NUC-1031. *Sci. Rep.* **9**, 1–13 (2019).
433. Masoudi, M., Seki, M., Yazdanparast, R., Yachie, N. & Aburatani, H. A genome-scale CRISPR/Cas9 knockout screening reveals SH3D21 as a sensitizer for gemcitabine. *Sci. Rep.* **9**, 1–9 (2019).
434. Wei, X. *et al.* Targeted CRISPR screening identifies PRMT5 as synthetic lethality combinatorial target with gemcitabine in pancreatic cancer cells. *Proc. Natl. Acad. Sci. U. S. A.* **117**, 28068–28079 (2020).
435. Gomez-Llorente, Y. *et al.* Structural basis for active single and double ring complexes in human mitochondrial Hsp60-Hsp10 chaperonin. *Nat. Commun.* **11**, (2020).
436. Polson, E. S. *et al.* KHS101 disrupts energy metabolism in human glioblastoma cells and reduces tumor growth in mice. *Sci. Transl. Med.* **10**, (2018).
437. Wang, B. *et al.* Integrative analysis of pooled CRISPR genetic screens using MAGeCKFlute. *Nat. Protoc.* **14**, 756–780 (2019).
438. Gould, S. & Scott, R. C. 2-Hydroxypropyl- β -cyclodextrin (HP- β -CD): A toxicology review. *Food Chem. Toxicol.* **43**, 1451–1459 (2005).
439. Kyuno, D. *et al.* Targeting tight junctions during epithelial to mesenchymal transition in human pancreatic cancer. *World J. Gastroenterol.* **20**, 10813–10824 (2014).
440. Rajasekaran, S. A. *et al.* HPAF-II, a cell culture model to study pancreatic epithelial cell structure and function. *Pancreas* **29**, 77–83 (2004).
441. Loukopoulos, P. *et al.* Orthotopic transplantation models of pancreatic adenocarcinoma derived from cell lines and primary tumors and displaying varying metastatic activity. *Pancreas* **29**, 193–203 (2004).
442. Emily L. Deer, M. *et al.* Phenotype and Genotype of pancreatic cancer. *Pancreas* **39**, 425–

- 435 (2010).
443. Liu, X. S. *et al.* MAGeCK enables robust identification of essential genes from genome-scale CRISPR/Cas9 knockout screens. *Genome Biol.* **15**, 1–12 (2014).
444. Petrilli, A. M. & Fernández-Valle, C. Role of Merlin/NF2 inactivation in tumor biology. *Oncogene* **35**, 537–548 (2016).
445. Quan, M. *et al.* Merlin/NF2 suppresses pancreatic tumor growth and metastasis by attenuating the FOXM1-mediated Wnt/ β -catenin signaling. *Cancer Res.* **75**, 4778–4789 (2015).
446. Wang, T. *et al.* Identification and characterization of essential genes in the human genome. *Science (80-.)*. **350**, 1096–1101 (2015).
447. Kuleshov, M. V. *et al.* Enrichr: a comprehensive gene set enrichment analysis web server 2016 update. *Nucleic Acids Res.* **44**, W90–W97 (2016).
448. Steinhart, Z. *et al.* Genome-wide CRISPR screens reveal a Wnt-FZD5 signaling circuit as a druggable vulnerability of RNF43-mutant pancreatic tumors. *Nat. Med.* **23**, 60–68 (2017).
449. Rafahi, H. *et al.* Clonogenic Assay: Adherent Cells. *J. Vis. Exp.* 15–17 (2011).
doi:10.3791/2573
450. Guzmán, C., Bagga, M., Kaur, A., Westermarck, J. & Abankwa, D. ColonyArea: An ImageJ plugin to automatically quantify colony formation in clonogenic assays. *PLoS One* **9**, 14–17 (2014).
451. Feng, J. *et al.* High expression of heat shock protein 10 (Hsp10) is associated with poor prognosis in oral squamous cell carcinoma. *Int. J. Clin. Exp. Pathol.* **10**, 7784–7791 (2017).
452. Chu, S. *et al.* High expression of heat shock protein 10 correlates negatively with estrogen/progesterone receptor status and predicts poor prognosis in invasive ductal breast carcinoma. *Hum. Pathol.* **61**, 173–180 (2017).
453. Feng, J. *et al.* Increased expression of heat shock protein (HSP) 10 and HSP70 correlates with poor prognosis of nasopharyngeal carcinoma. *Cancer Manag. Res.* **11**, 8219–8227 (2019).
454. Cappello, F., Rappa, F., David, S., Anzalone, R. & Zummo, G. Immunohistochemical evaluation of PCNA, p53, HSP60, HSP10 and MUC-2 presence and expression in prostate

- carcinogenesis. *Anticancer Res.* **23**, 1325–1331 (2003).
455. Tang, Y. *et al.* Overexpression of HSP10 correlates with HSP60 and Mcl-1 levels and predicts poor prognosis in non-small cell lung cancer patients. *Cancer Biomarkers* **30**, 85–94 (2021).
456. Ye, Y. *et al.* Comparative mitochondrial proteomic analysis of hepatocellular carcinoma from patients. *Proteomics - Clinical Applications* **7**, (2013).
457. Melle, C. *et al.* Detection and identification of heat shock protein 10 as a biomarker in colorectal cancer by protein profiling. *Proteomics* **6**, 2600–2608 (2006).
458. Cappello, F., Bellafiore, M., David, S., Anzalone, R. & Zummo, G. Ten kilodalton heat shock protein (HSP10) is overexpressed during carcinogenesis of large bowel and uterine exocervix. *Cancer Lett.* **196**, 35–41 (2003).
459. Akyol, S., Gercel-Taylor, C., Reynolds, L. C. & Taylor, D. D. HSP-10 in ovarian cancer: Expression and suppression of T-cell signaling. *Gynecol. Oncol.* **101**, 481–486 (2006).
460. Tsai, Y. P. *et al.* Interaction between HSP60 and β -catenin promotes metastasis. *Carcinogenesis* **30**, 1049–1057 (2009).
461. Fodde, R. & Brabletz, T. Wnt/ β -catenin signaling in cancer stemness and malignant behavior. *Curr. Opin. Cell Biol.* **19**, 150–158 (2007).
462. Berger, E. *et al.* Mitochondrial function controls intestinal epithelial stemness and proliferation. *Nat. Commun.* **7**, 13171 (2016).
463. Cappello, F. *et al.* Hsp60 and Hsp10 down-regulation predicts bronchial epithelial carcinogenesis in smokers with chronic obstructive pulmonary disease. *Cancer* **107**, 2417–2424 (2006).
464. Cappello, F. *et al.* The expression of Hsp60 and Hsp10 in large bowel carcinomas with lymph node metastases. *BMC Cancer* **5**, 1–10 (2005).
465. Liu, X. Targeting polo-like kinases: A promising therapeutic approach for cancer treatment. *Transl. Oncol.* **8**, 185–195 (2015).
466. Parma, B. *et al.* Metabolic impairment of non-small cell lung cancers by mitochondrial HSPD1 targeting. *J. Exp. Clin. Cancer Res.* **40**, 1–20 (2021).
467. Orellana, E. & Kasinski, A. Sulforhodamine B (SRB) Assay in Cell Culture to Investigate Cell Proliferation. *Bio-Protocol* **6**, (2016).
468. Head, B., Griparic, L., Amiri, M., Gandre-Babbe, S. & Van Der Bliek, A. M. Inducible

- proteolytic inactivation of OPA1 mediated by the OMA1 protease in mammalian cells. *J. Cell Biol.* **187**, 959–966 (2009).
469. Ehses, S. *et al.* Regulation of OPA1 processing and mitochondrial fusion by m-AAA protease isoenzymes and OMA1. *J. Cell Biol.* **187**, 1023–1036 (2009).
470. Olichon, A. *et al.* Loss of OPA1 perturbs the mitochondrial inner membrane structure and integrity, leading to cytochrome c release and apoptosis. *J. Biol. Chem.* **278**, 7743–7746 (2003).
471. Olichon, A. *et al.* OPA1 alternate splicing uncouples an evolutionary conserved function in mitochondrial fusion from a vertebrate restricted function in apoptosis. *Cell Death Differ.* **14**, 682–692 (2007).
472. MacVicar, T. & Langer, T. OPA1 processing in cell death and disease - the long and short of it. *J. Cell Sci.* **129**, 2297–2306 (2016).
473. Meng, Q., Li, B. X. & Xiao, X. Toward developing chemical modulators of Hsp60 as potential therapeutics. *Front. Mol. Biosci.* **5**, 1–11 (2018).
474. Tang, Y., Zhou, Y., Fan, S. & Wen, Q. The multiple roles and therapeutic potential of HSP60 in cancer. *Biochem. Pharmacol.* **201**, 115096 (2022).
475. van Vugt, M. A. T. M., Brás, A. & Medema, R. H. Polo-like Kinase-1 Controls Recovery from a G2 DNA Damage-Induced Arrest in Mammalian Cells. *Mol. Cell* **15**, 799–811 (2004).
476. Smits, V. A. J. *et al.* Polo-like kinase-1 is a target of the DNA damage checkpoint. *Nat. Cell Biol.* **2**, 672–676 (2000).
477. Wurdak, H. *et al.* A small molecule accelerates neuronal differentiation in the adult rat. *Proc. Natl. Acad. Sci. U. S. A.* **107**, 16542–16547 (2010).
478. Polson, E. *et al.* The small molecule KHS101 induces bioenergetic dysfunction in glioblastoma cells through inhibition of mitochondrial HSPD1. *bioRxiv* (2017).
479. Bie, A. S. *et al.* An inventory of interactors of the human HSP60/HSP10 chaperonin in the mitochondrial matrix space. *Cell Stress Chaperones* **25**, 407–416 (2020).
480. Nisemblat, S., Yaniv, O., Parnas, A., Frolow, F. & Azem, A. Crystal structure of the human mitochondrial chaperonin symmetrical football complex. *Proc. Natl. Acad. Sci. U. S. A.* **112**, 6044–6049 (2015).
481. Stevens, M. *et al.* HSP60/10 chaperonin systems are inhibited by a variety of approved

- drugs, natural products, and known bioactive molecules. *Bioorganic Med. Chem. Lett.* **29**, 1106–1112 (2019).
482. Zhang, L. *et al.* Concomitant inhibition of HSP90, its mitochondrial localized homologue TRAP1 and HSP27 by green tea in pancreatic cancer HPAF-II cells. *Proteomics* **11**, 4638–4647 (2011).
483. Daunys, S., Matulis, D. & Petrikaitė, V. Synergistic activity of Hsp90 inhibitors and anticancer agents in pancreatic cancer cell cultures. *Sci. Rep.* **9**, 1–8 (2019).
484. Herkenne, S. & Scorrano, L. OPA1, a new mitochondrial target in cancer therapy. *Aging (Albany, NY)*. **12**, 20931–20933 (2020).
485. Zamberlan, M. *et al.* Inhibition of the mitochondrial protein Opa1 curtails breast cancer growth. *J. Exp. Clin. Cancer Res.* **41**, 1–18 (2022).
486. Mishra, P., Carelli, V., Manfredi, G. & Chan, D. C. Proteolytic Cleavage of Opa1 Stimulates Mitochondrial Inner Membrane Fusion and Couples Fusion to Oxidative Phosphorylation. *Cell Metab.* **19**, 630–641 (2014).
487. Santini, R. *et al.* HEDGEHOG-GLI signaling drives self-renewal and tumorigenicity of human melanoma-initiating cells. *Stem Cells* **30**, 1808–1818 (2012).
488. Prasmickaite, L. *et al.* Aldehyde dehydrogenase (ALDH) activity does not select for cells with enhanced aggressive properties in malignant melanoma. *PLoS One* **5**, (2010).
489. Mukherjee, N. *et al.* Combining a BCL2 inhibitor with the retinoid derivative fenretinide targets melanoma cells including melanoma initiating cells. *J. Invest. Dermatol.* **135**, 842–850 (2015).
490. Shidal, C., Al-Rayyan, N., Yaddanapudi, K. & Davis, K. R. Lunasin is a novel therapeutic agent for targeting melanoma cancer stem cells. *Oncotarget* **7**, 84128–84141 (2016).
491. Shidal, C., Inaba, J. I., Yaddanapudi, K. & Davis, K. R. The soy-derived peptide Lunasin inhibits invasive potential of melanoma initiating cells. *Oncotarget* **8**, 25525–25541 (2017).
492. Taylor, L. A. *et al.* High ALDH1 expression correlates with better prognosis in tumorigenic malignant melanoma. *Mod. Pathol.* **30**, 634–639 (2017).
493. Zhou, L. *et al.* Identification of cancer-type specific expression patterns for active aldehyde dehydrogenase (ALDH) isoforms in ALDEFLUOR assay. *Cell Biol. Toxicol.* **35**, 161–177 (2019).

494. Rappa, G., Fodstad, O. & Lorico, A. The Stem Cell-Associated Antigen CD133 (Prominin-1) Is a Molecular Therapeutic Target for Metastatic Melanoma. *Stem Cells* **26**, 3008–3017 (2008).
495. Kumar, D. *et al.* Notch1-MAPK Signaling Axis Regulates CD133+ Cancer Stem Cell-Mediated Melanoma Growth and Angiogenesis. *J. Invest. Dermatol.* **136**, 2462–2474 (2016).
496. Calvani, M. *et al.* Etoposide-Bevacizumab a new strategy against human melanoma cells expressing stem-like traits. *Oncotarget* **7**, 51138–51149 (2016).
497. Louphrasitthiphol, P., Chauhan, J. & Goding, C. R. ABCB5 is activated by MITF and β -catenin and is associated with melanoma differentiation. *Pigment Cell Melanoma Res.* **33**, 112–118 (2020).
498. Mihic-Probst, D. *et al.* Consistent expression of the stem cell renewal factor BMI-1 in primary and metastatic melanoma. *Int. J. Cancer* **121**, 1764–1770 (2007).
499. Taghizadeh, R. *et al.* Cxcr6, a newly defined biomarker of tissue-specific stem cell asymmetric self-renewal, identifies more aggressive human melanoma cancer stem cells. *PLoS One* **5**, (2010).
500. Roesch, A. *et al.* A Temporarily Distinct Subpopulation of Slow-Cycling Melanoma Cells Is Required for Continuous Tumor Growth. *Cell* **141**, 583–594 (2010).
501. Hinz, B. The extracellular matrix and transforming growth factor- β 1: Tale of a strained relationship. *Matrix Biol.* **47**, 54–65 (2015).
502. Merwin, J. R., Anderson, J. M., Kocher, O., Van Itallie, C. M. & Madri, J. A. Transforming growth factor beta 1 modulates extracellular matrix organization and cell-cell junctional complex formation during in vitro angiogenesis. *J. Cell. Physiol.* **142**, 117–128 (1990).
503. Pohl, M. *et al.* SMAD4 mediates mesenchymal-epithelial reversion in SW480 colon carcinoma cells. *Anticancer Res.* **30**, 2603–13 (2010).
504. Katsuno, Y. *et al.* Coordinated expression of REG4 and aldehyde dehydrogenase 1 regulating tumorigenic capacity of diffuse-type gastric carcinoma-initiating cells is inhibited by TGF- β . *J. Pathol.* **228**, 391–404 (2012).
505. Dou, J. *et al.* Isolation and identification of cancer stem-like cells from murine melanoma cell lines. *Cell. Mol. Immunol.* **4**, 467–472 (2007).

506. Morris, J. C. *et al.* Phase I study of GC1008 (Fresolimumab): A human anti-transforming growth factor-beta (TGF β) monoclonal antibody in patients with advanced malignant melanoma or renal cell carcinoma. *PLoS One* **9**, (2014).
507. Schlegel, N. C., von Planta, A., Widmer, D. S., Dummer, R. & Christofori, G. PI3K signalling is required for a TGF β -induced epithelial-mesenchymal-like transition (EMT-like) in human melanoma cells. *Exp. Dermatol.* **24**, 22–28 (2015).
508. Diener, J. *et al.* Epigenetic control of melanoma cell invasiveness by the stem cell factor SALL4. *Nat. Commun.* **12**, 1–18 (2021).
509. Mascarenhas, J. *et al.* A Phase Ib Trial of AVID200, a TGF β 1/3 Trap, in Patients with Myelofibrosis. *Clin. Cancer Res.* **29**, 3622–3632 (2023).
510. Jimeno, A. *et al.* A phase 2 study of dalantercept, an activin receptor-like kinase-1 ligand trap, in patients with recurrent or metastatic squamous cell carcinoma of the head and neck. *Cancer* **122**, 3641–3649 (2016).
511. Burger, R. A. *et al.* Phase II evaluation of dalantercept in the treatment of persistent or recurrent epithelial ovarian cancer: An NRG Oncology/Gynecologic Oncology Group study. *Gynecol. Oncol.* **150**, 466–470 (2018).
512. Fenaux, P. *et al.* Luspatercept in Patients with Lower-Risk Myelodysplastic Syndromes. *N. Engl. J. Med.* **382**, 140–151 (2020).
513. Barlesi, F. *et al.* Bintrafusp Alfa, a Bifunctional Fusion Protein Targeting TGF- β and PD-L1, in Patients With Non-Small Cell Lung Cancer Resistant or Refractory to Immune Checkpoint Inhibitors. *Oncologist* **28**, 258–267 (2023).
514. David, C. J. & Massagué, J. Contextual determinants of TGF β action in development, immunity and cancer. *Nature Reviews Molecular Cell Biology* **19**, 419–435 (2018).
515. Dennler, S., Huet, S. & Gauthier, J. M. A short amino-acid sequence in MH1 domain is responsible for functional differences between Smad2 and Smad3. *Oncogene* **18**, 1643–1648 (1999).
516. Jayaraman, L. & Massagué, J. Distinct oligomeric states of SMAD proteins in the transforming growth factor- β pathway. *J. Biol. Chem.* **275**, 40710–40717 (2000).
517. Ashcroft, G. S. *et al.* Mice lacking Smad3 show accelerated wound healing and an impaired local inflammatory response. *Nat. Cell Biol.* **1**, 260–266 (1999).
518. Wolfrain, L. A. *et al.* Loss of Smad3 in Acute T-Cell Lymphoblastic Leukemia. *N. Engl.*

- J. Med.* **351**, 552–559 (2004).
519. Daly, A. C., Vizán, P. & Hill, C. S. Smad3 protein levels are modulated by ras activity and during the cell cycle to dictate transforming growth factor- β responses. *J. Biol. Chem.* **285**, 6489–6497 (2010).
 520. Nicolás, F. J., Lehmann, K., Warne, P. H., Hill, C. S. & Downward, J. Epithelial to mesenchymal transition in madin-darby canine kidney cells is accompanied by down-regulation of Smad3 expression, leading to resistance to transforming growth factor- β -induced growth arrest. *J. Biol. Chem.* **278**, 3251–3256 (2003).
 521. Bertrand-Chapel, A. *et al.* SMAD2/3 mediate oncogenic effects of TGF- β in the absence of SMAD4. *Commun. Biol.* **5**, 1–13 (2022).
 522. Sowa, H. *et al.* Menin is required for bone morphogenetic protein 2- and transforming growth factor β -regulated osteoblastic differentiation through interaction with Smads and Runx2. *J. Biol. Chem.* **279**, 40267–40275 (2004).
 523. Kaji, H., Canaff, L., Goltzman, D. & Hendy, G. N. Cell cycle regulation of menin expression. *Cancer Res.* **59**, 5097–5101 (1999).
 524. Ikeo, Y. *et al.* Proliferation-Associated Expression of the MEN1 Gene as Revealed by In Situ Hybridization: Possible Role of the Menin as a Negative Regulator of Cell Proliferation Under DNA Damage. *Lab. Investig.* **80**, 797–804 (2000).
 525. Schnepf, R. W. *et al.* Mutation of tumor suppressor gene Men1 acutely enhances proliferation of pancreatic islet cells. *Cancer Res.* **66**, 5707–5715 (2006).
 526. Schnepf, R. W. *et al.* Menin Induces Apoptosis in Murine Embryonic Fibroblasts. *J. Biol. Chem.* **279**, 10685–10691 (2004).
 527. Hussein, N. *et al.* Reconstituted expression of menin in Men1-deficient mouse Leydig tumour cells induces cell cycle arrest and apoptosis. *Eur. J. Cancer* **43**, 402–414 (2007).
 528. Sawicki, M. P., Gholkar, A. A. & Torres, J. Z. Menin Associates With the Mitotic Spindle and Is Important for Cell Division. *Endocrinology* **160**, 1926–1936 (2019).
 529. Zindy, P. J. *et al.* Upregulation of the tumor suppressor gene menin in hepatocellular carcinomas and its significance in fibrogenesis. *Hepatology* **44**, 1296–1307 (2006).
 530. Xu, B. *et al.* Menin promotes hepatocellular carcinogenesis and epigenetically up-regulates Yap1 transcription. *Proc. Natl. Acad. Sci. U. S. A.* **110**, 17480–17485 (2013).
 531. Wu, G. *et al.* Menin enhances c-Myc-mediated transcription to promote cancer

- progression. *Nat. Commun.* **8**, 1–14 (2017).
532. Yokoyama, A. *et al.* The menin tumor suppressor protein is an essential oncogenic cofactor for MLL-associated leukemogenesis. *Cell* **123**, 207–218 (2005).
533. Yokoyama, A. & Cleary, M. L. Menin Critically Links MLL Proteins with LEDGF on Cancer-Associated Target Genes. *Cancer Cell* **14**, 36–46 (2008).
534. Jin, B. *et al.* Loss of MEN1 leads to renal fibrosis and decreases HGF-Adamts5 pathway activity via an epigenetic mechanism. *Clin. Transl. Med.* **12**, (2022).
535. Pahlavanneshan, S. *et al.* Combined inhibition of menin-MLL interaction and TGF- β signaling induces replication of human pancreatic beta cells. *Eur. J. Cell Biol.* **99**, 151094 (2020).
536. Pantaleo, M. A. *et al.* Genome-wide analysis identifies MEN1 and MAX mutations and a neuroendocrine-like molecular heterogeneity in Quadruple WT GIST. *Mol. Cancer Res.* **15**, 553–562 (2017).
537. Fernandez-Cuesta, L. *et al.* Frequent mutations in chromatin-remodelling genes in pulmonary carcinoids. *Nat. Commun.* **5**, 3518 (2014).
538. Ito, T., Igarashi, H., Uehara, H., Berna, M. J. & Jensen, R. T. Causes of Death and Prognostic Factors in Multiple Endocrine Neoplasia Type 1. *Medicine (Baltimore)*. **92**, 135–181 (2013).
539. ABóni, R. *et al.* Mutation analysis of the MEN1 tumour suppressor gene in malignant melanoma. *Melanoma Res.* **9**, 249–252 (1999).
540. Băicoianu-Nițescu, L.-C., Gheorghe, A.-M., Carsote, M., Dumitrascu, M. C. & Sandru, F. Approach of Multiple Endocrine Neoplasia Type 1 (MEN1) Syndrome–Related Skin Tumors. *Diagnostics* **12**, 2768 (2022).
541. Bakke, J. *et al.* Genome-wide CRISPR screen reveals PSMA6 to be an essential gene in pancreatic cancer cells. *BMC Cancer* **19**, 1–12 (2019).
542. Oladimeji, P. O., Bakke, J., Wright, W. C. & Chen, T. KANSL2 and MBNL3 are regulators of pancreatic ductal adenocarcinoma invasion. *Sci. Rep.* **10**, 1–8 (2020).
543. Zhu, X. G. *et al.* Functional Genomics In Vivo Reveal Metabolic Dependencies of Pancreatic Cancer Cells. *Cell Metab.* **33**, 211–221.e6 (2021).
544. Wu, L. *et al.* Genome-wide CRISPR screen identifies MTA3 as an inducer of gemcitabine resistance in pancreatic ductal adenocarcinoma. *Cancer Lett.* **548**, (2022).

545. Lan, B. *et al.* CRISPR-Cas9 Screen Identifies DYRK1A as a Target for Radiotherapy Sensitization in Pancreatic Cancer. *Cancers (Basel)*. **14**, 326 (2022).
546. Goodwin, C. M. *et al.* Combination Therapies with CDK4/6 Inhibitors to Treat KRAS-Mutant Pancreatic Cancer. *Cancer Res.* **83**, 141–157 (2023).
547. Freeman-Cook, K. *et al.* Expanding control of the tumor cell cycle with a CDK2/4/6 inhibitor. *Cancer Cell* **39**, 1404-1421.e11 (2021).
548. Kumarasamy, V., Vail, P., Nambiar, R., Witkiewicz, A. K. & Knudsen, E. S. Functional determinants of cell cycle plasticity and sensitivity to CDK4/6 inhibition. *Cancer Res.* **81**, 1347–1360 (2021).
549. Milton, C. K. *et al.* A Genome-scale CRISPR Screen Identifies the ERBB and mTOR Signaling Networks as Key Determinants of Response to PI3K Inhibition in Pancreatic Cancer. *Mol. Cancer Ther.* **19**, 1423–1435 (2020).
550. Dufner, A. & Thomas, G. Ribosomal S6 kinase signaling and the control of translation. *Exp. Cell Res.* **253**, 100–109 (1999).
551. Lytle, N. K. *et al.* A Multiscale Map of the Stem Cell State in Pancreatic Adenocarcinoma. *Cell* **177**, 572-586.e22 (2019).